Improving spatial reuse in future dense high efficiency Wireless Local Area Networks

Imad Jamil

Thèse

THESE INSA Rennes
sous le sceau de l'Université européenne de Bretagne
pour obtenir le titre de
DOCTEUR DE L'INSA DE RENNES
Spécialité : Electronique et Télécommunications

présentée par
Imad Jamil
ECOLE DOCTORALE : *MATISSE*
LABORATOIRE : *IETR*

Improving spatial reuse in future dense high efficiency Wireless Local Area Networks

Sandrine DESTOUET ROBLOT
Docteur-Ingénieur à Orange Labs Rennes / Membre invité

Thèse soutenue le 17.12.2015
devant le jury composé de :

Hikmet SARI
Professeur à Centrale-Supelec à Gif sur Yvette / Président
André-Luc BEYLOT
Professeur à l'ENSEEIHT de Toulouse / Rapporteur
Didier LE RUYET
Professeur au CNAM de Paris / Rapporteur
Ramesh PYNDIAH
Professeur à Télécom Bretagne / Examinateur
Laurent CARIOU
Docteur-Ingénieur à INTEL à Hilsboro, USA / Co-encadrant
Jean-François HELARD
Professeur à l'INSA de Rennes / Directeur de thèse

Thèse

THESE INSA Rennes
sous le sceau de l'Université européenne de Bretagne
pour obtenir le titre de
DOCTEUR DE L'INSA DE RENNES
Spécialité : Electronique et Télécommunications

présentée par
Imad Jamil
ECOLE DOCTORALE : *MATISSE*
LABORATOIRE : *IETR*

Improving spatial reuse in future dense high efficiency Wireless Local Area Networks

Sandrine DESTOUET ROBLOT
Docteur-Ingénieur à Orange Labs Rennes / Membre invité

Thèse soutenue le 17.12.2015
devant le jury composé de :

Hikmet SARI
Professeur à Centrale-Supelec à Gif sur Yvette / Président
André-Luc BEYLOT
Professeur à l'ENSEEIHT de Toulouse / Rapporteur
Didier LE RUYET
Professeur au CNAM de Paris / Rapporteur
Ramesh PYNDIAH
Professeur à Télécom Bretagne / Examinateur
Laurent CARIOU
Docteur-Ingénieur à INTEL à Hilsboro, USA / Co-encadrant
Jean-François HELARD
Professeur à l'INSA de Rennes / Directeur de thèse

Improving spatial reuse in future dense high efficiency Wireless Local Area Networks

Imad Jamil

En partenariat avec

There is no honor like knowledge,
— Nahj al-Balagha

Dedicated to my beloved parents . . .

Acknowledgements

First and foremost, I would like to thank God, whose many blessings have made me who I am today.

I wish to express my sincere gratitude to the persons who helped to make my three-year's PhD a valuable experience and a pleasing journey that I will never forget.

I am truly grateful to my thesis advisor, Prof. Jean-François Hélard, and to my supervisor, Dr. Laurent Cariou, for all their help throughout my PhD studies. Their guidance helped me in all the time of research and writing of this dissertation.

I would like to thank the jury members, Prof. André-Luc Beylot, Prof. Didier Le Ruyet, Prof. Hikmet Sari, Prof. Ramesh Pyndiah, Dr. Sandrine Destouet Roblot, for reviewing and discussing my dissertation.

Thanks to M. Jean-Christophe Rault for having welcomed me within the CREM's team at Orange and for his continuous support. My thanks also goes to all my colleagues at Orange, where I passed three years of daily enriching interaction with each one of them. I mention Pierrick Louin and Philippe Christin for their help and support. A very special thanks goes to David Bernard, my office mate, who taught me many things through our discussions. I also thank my colleagues and friends at IETR (INSA de Rennes).

Last but not least, I would like to thank all my great friends especially Gunther, Amin, Hanane, Irvin, Malla, Hassan, Kartik, Hussein, Hadi, Mohammad and Marwa for all their support.

Finally, my sincere feelings of gratitude to my parents, Hassan and Khadija, my brother, Ali, and my sisters, Sahar, Youssra and Nagham for their love, patience and encouragement throughout my life.

Rennes, 17 December 2015 Imad

Abstract

Despite their remarkable success, the first widely spread versions of the Institute of Electrical and Electronics Engineers (IEEE) 802.11 Wireless Local Area Network (WLAN) standard, IEEE 802.11a/b/g, featured low spectral efficiencies that are becoming insufficient to satisfy the explosive growth in capacity and coverage demands. Thanks to the advances in the communication theory and the use of the 5 GHz frequency band, the IEEE 802.11n and recently the IEEE 802.11ac amendments improved the Physical Layer (PHY) data rates by introducing Multiple-Input Multiple-Output (MIMO) techniques, higher Modulation and Coding Scheme (MCS), etc. Today, after almost two decades of its first appearance, Wi-Fi is presented as a gigabit wireless technology. However, the full potential of the latest PHY layer advances cannot be enabled in all real world deployment scenarios. With the rapidly increasing density of WLAN deployments and the huge popularity of Wi-Fi enabled devices, spatial reuse must be optimized. On another hand, the new challenging use case environments and the integration of mobile networks mainly for cellular offloading are limiting the opportunity of the current Wi-Fi generations to provide better quality at lower cost.

In this thesis, we contribute to the current standardization efforts aiming to leverage the Wi-Fi efficiency in high density environments. At the time of writing this document, the IEEE 802.11ax Task Group (TG) is developing the specifications for the High Efficiency WLAN (HEW) standard (next Wi-Fi evolution). Rather than continuing to target increased theoretical peak throughputs, we focus in the context of HEW on improving the throughput experienced by users in real life conditions where many other devices, belonging to neighboring overlapping networks, simultaneously contend to gain access.

To enhance this performance, we propose a dynamic adaptation of the carrier sensing mechanism. Compared to controlling the transmission power, the proposed mechanism has more incentives because it benefits directly the concerned user. Extensive simulation results show important throughput gains in dense scenarios. Then, we study the impact of the new adaptation on the current rate control algorithms. We find that our adaptation mechanism operates efficiently without substantially modifying these algorithms that are widely used in today's operating WLANs.

Furthermore, after analyzing the fairness performance of the proposed adaptation, we

devise a new approach to jointly adapt the carrier sensing and the transmission power in order to preserve higher fairness degrees while improving the spatial reuse. This approach is evaluated in different dense deployment scenarios where it proves its capability to resolve the unfairness issues especially in the presence of legacy nodes in the network, while improving the achieved throughput by 4 times compared to the standard performance.
Finally, we design and implement a centralized learning-based solution that uses also an approach based on joint adaptation of transmission power and carrier sensing. This new solution takes benefit from the capability of artificial neural networks to model complex nonlinear functions to optimize the spatial reuse in dense WLANs while preserving fairness among contending nodes.
The different contributions of this work have helped bring efficient solutions for future Wi-Fi networks. We have presented these solutions to the IEEE 802.11ax TG where they were identified as important potential technical improvements for the next WLAN standard.

Key words: High Efficiency Wireless Local area Networks, Wi-Fi, MAC protocols

Résumé

Malgré leur réussite remarquable, les premières versions des normes des réseaux locaux sans fil IEEE 802.11, IEEE 802.11a/b/g WLAN, sont caractérisées par une efficacité spectrale faible qui est devenue insuffisante pour satisfaire la croissance explosive de la demande de capacité et de couverture. Grâce aux progrès considérables dans le domaine des communications sans fil et l'utilisation de la bande de fréquence autour de 5 gigahertz, le standard IEEE 802.11n et plus récemment l'IEEE 802.11ac ont amélioré les débits offerts par la couche physique. Cela a été possible grâce principalement à l'introduction des techniques multi-antennaires (MIMO, pour Multiple-Input Multiple-Output) et des techniques avancées de modulation et de codage. Aujourd'hui, deux décennies après sa première apparition, le Wi-Fi est présenté comme une technologie WLAN permettant des débits supérieurs à 1 gigabit par seconde. Cependant, dans la plupart des scénarios de déploiement du monde réel, il n'est pas possible d'atteindre la pleine capacité offerte par la couche physique. Avec la croissance rapide de la densité des déploiements des WLANs et l'énorme popularité des équipements Wi-Fi, la réutilisation spatiale doit être optimisée. D'autre part, des nouveaux cas d'utilisation sont prévus pour décharger les réseaux cellulaires et pour couvrir des grandes surfaces (stades, gares, etc.). Ces environnements de haute densité représentent un vrai défi pour les générations actuelles de Wi-Fi qui doivent offrir une meilleure qualité à moindre coût.

C'est dans ce contexte que s'inscrit l'objectif de cette thèse qui porte sur l'amélioration de l'efficacité des protocoles de la couche MAC des réseaux WLAN de haute densité. Notamment, un des buts de cette thèse est de contribuer à la préparation de la prochaine génération du standard Wi-Fi : IEEE 802.11ax High Efficiency WLAN (HEW). Plutôt que de continuer à cibler l'augmentation des débits maximums théoriques, nous nous concentrons dans le contexte de HEW sur l'amélioration du débit réel des utilisateurs. Pour cela, on prend en compte tous les autres équipements associés à des WLANs voisins, qui essayent d'accéder au même canal de transmission d'une manière simultanée.

Pour améliorer la performance du Wi-Fi dans ces environnements denses, nous proposons une adaptation dynamique du mécanisme de détection de signal. Comparé au contrôle de la puissance de transmission, le mécanisme proposé est plus incitatif parce que l'utilisateur concerné bénéficie directement de son application. Les résultats de nos simulations

montrent des gains importants en termes de débit atteint dans les scénarios de haute densité. Ensuite, nous étudions l'impact de la nouvelle adaptation sur les mécanismes de sélection de débit actuellement utilisés. D'après les résultats obtenus, l'adaptation proposée peut être appliquée sans avoir besoin de modifications substantielles des algorithmes de sélection de débit.
Pour améliorer l'équité entre les différents utilisateurs, nous élaborons une nouvelle approche distribuée pour adapter conjointement le mécanisme de détection de signal et le contrôle de la puissance de transmission. Cette approche est évaluée ensuite dans différents scénarios de simulation de haute densité où elle prouve sa capacité à résoudre les problèmes d'équité en particulier en présence de nœuds d'anciennes générations dans le réseau, cela tout en améliorant le débit moyen d'un facteur 4 par rapport à la performance conventionnelle du standard.
Enfin, nous concevons et mettons en œuvre une solution centralisée basée sur l'apprentissage à base de réseaux de neurones. Cette approche repose sur l'adaptation conjointe de puissance de transmission et du mécanisme de détection du signal. Cette nouvelle solution bénéficie de la capacité des réseaux de neurones artificiels à modéliser les fonctions non-linéaires complexes pour optimiser la réutilisation spatiale dans les environnements WLAN denses tout en préservant l'équité entre les nœuds en compétition.
Les différentes contributions de ces travaux ont permis d'apporter des solutions novatrices pour les futures générations de la technologie Wi-Fi. Ces solutions que nous avons présentées au sein du groupe de standardisation IEEE 802.11ax sont aujourd'hui identifiées comme très pertinentes pour le prochain standard.

Mots clefs : High Efficiency Wireless Local area Networks, Wi-Fi, MAC protocols

Résumé étendu en Français

0.1 Introduction

Le Wi-Fi est aujourd'hui la référence des réseaux locaux sans fils ou WLAN pour "Wireless Local Area Network". Cette technologie est basée sur les normes du groupe de l'Institut des ingénieurs électriciens et électroniciens (IEEE, pour "Institute of Electrical and Electronics Engineers") 802.11. Depuis les premières spécifications en 1997 jusqu'à la norme la plus récente IEEE 802.11ac [13], une augmentation en débit conséquente a été obtenue avec l'introduction de chaque nouvelle génération. Les attentes, en termes de débit, de portée, de fiabilité et de consommation énergétique, pour les futures générations sont de plus en plus importantes. Il y a donc un réel défi technologique à relever. Une approche permettant d'optimiser les protocoles de la couche d'accès au canal (MAC, pour Medium Access Control) pour augmenter la réutilisation spatiale dans les déploiements de haute densité pourrait offrir des pistes d'amélioration intéressantes pour bénéficier pleinement des capacités offertes de la couche physique ou PHY. C'est le thème que l'on propose d'aborder dans cette thèse.

Dans les vingt dernières années, l'industrie du Wi-Fi a connu une croissance colossale avec la prolifération des appareils équipés des interfaces de communication IEEE 802.11. Cette croissance est impulsée par la nécessité de disposer d'un accès à internet en permanence n'importe quand et n'importe où. Ce besoin a longtemps été accompagné par une augmentation considérable de la taille des données communiquées. Avec l'enrichissement des services offerts dans le domaine de la vidéo en haute définition en "streaming", les jeux vidéo en ligne, la réalité augmentée, etc., il y a un besoin croissant pour des débits plus élevés et une plus grande capacité des réseaux sans fil. Selon un récent rapport de Strategy Analytics [2], 65 % des ménages à travers le monde qui ont accès à internet à haut débit utilisent la technologie Wi-Fi. Cela représente 25 % des ménages dans le monde, ce qui constitue environ 451 millions de ménages. En outre, ABI Research, qui a suivi la livraison des équipements Wi-Fi depuis la première apparition de cette technologie, indique qu'à la fin de 2014, 9,98 milliards d'appareils Wi-Fi ont été vendus dans le monde et qu'environ 4,5 milliards de ces appareils sont en usage quotidien aujourd'hui [3] [4].

Cependant, la combinaison d'une couverture omniprésente et d'une haute capacité est un

défi pour tous les systèmes de communication sans fil. Cette combinaison est encore plus difficile à atteindre pour le Wi-Fi car cette technologie n'a pas été conçue pour fonctionner dans de tels cas d'utilisations extrêmes. Depuis son introduction, cette norme n'a pas cessé d'évoluer. En conséquence, une longue liste d'amendements ont été adoptés et plusieurs générations se sont succédées. La dernière version de la norme IEEE 802.11 [5] qui intègre tous les amendements précédents remonte à 2012. Dans toute son histoire d'évolution, la réussite de la technologie Wi-Fi est due à son prix modeste et son opération simple. Aujourd'hui, les réseaux locaux sans fil (i.e., WLAN ou Wi-Fi) basés sur la norme IEEE 802.11 sont à nouveau contraints d'évoluer afin de garder le même rythme imposé par les nouveaux besoins. Bien que le défi est grand, la technologie Wi-Fi doit garder sa simplicité opérationnelle, la clé de son succès, tout en façonnant sa nouvelle génération.

0.2 Panorama de la norme IEEE 802.11

L'élément de base dans un réseau local sans fil IEEE 802.11 est nommé le BSS (pour "Basic Service Set") et formé d'un point d'accès (AP, pour "Access Point") et des stations (STA, pour "Station") associées à l'AP. L'AP est une STA normale à laquelle on ajoute des fonctionnalités permettant la gestion du BSS (contrôle et synchronisation de toutes les transmissions). Généralement, chaque AP est lié à un système de distribution (DS pour "Distribution System") comme montré par la Figure 1. Le DS assure la liaison de l'AP avec le monde extérieur, typiquement l'internet et dans des autres cas des réseaux locaux étendus ou ESS (pour "Extended Service Set").

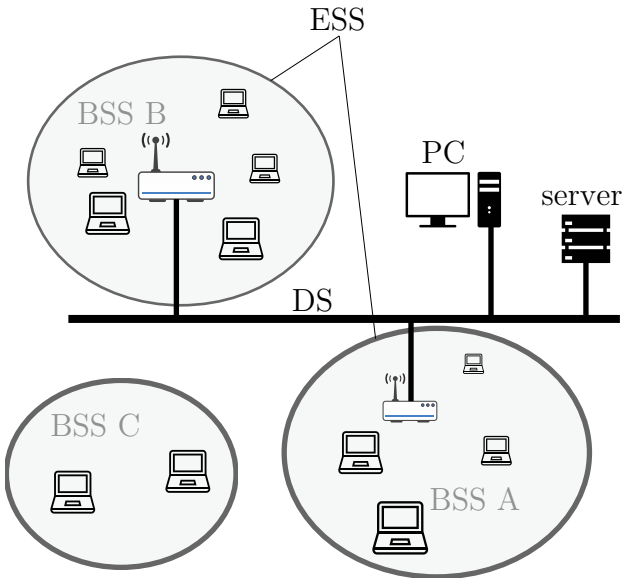

Figure 1 – L'arichecture générale d'un réseau du 802.11

0.2.1 Les protocoles de la couche Media Access Control Layer (MAC)

Les mécanismes de la couche MAC permettent, entre autres, le partage du canal sans fil entre plusieurs utilisateurs. Ainsi, ils doivent tenir compte des spécificités du canal et des éléments physiques atténuateurs. De plus, le signal transmis étant diffusé, les stations qui fonctionnent sur le même canal peuvent "s'entendre", peu importe le réseau (BSS) auquel elles appartiennent, à condition qu'elles soient à portée les unes des autres. Puisqu'en Wi-Fi, toutes les STAs du même BSS utilisent la même fréquence, le canal de communication est dit semi-duplex. Plusieurs mécanismes élémentaires sont alors mis en place pour assurer le partage équitable de ce canal.

Premièrement, toute transmission est précédée d'une période de contention d'accès au canal au cours de laquelle le canal est "écouté" afin d'éviter les collisions. Cette dernière technique est nommée généralement le LBT (pour "Listen Before talk"). Dans le Wi-Fi, le LBT est assuré par deux mécanismes différents. Le premier se situe au niveau de la couche PHY et s'appelle le PCS (pour "Physical Carrier Sensing") qui est connu comme étant le mécanisme de CCA (pour "Clear Channel Assessment"). Deux modes de CCA sont définis par la norme: le ED (pour "Energy Detect") qui quantifie toute sorte d'énergie dans le canal et le CS (pour "Carrier Sensing") qui détecte et décode les signaux 802.11. Le canal est considéré occupé si au moins l'un des deux modes le déclare.

Dans le but d'éviter les collisions de trames causées par des transmissions synchrones, après avoir constaté que le canal est libre et avant de transmettre chaque station doit attendre un temps aléatoire (le mécanisme du "backoff" exponentiel). Ce mécanisme est aussi utilisé suite à une collision afin de la résoudre et éviter sa reproduction.

Deuxièmement, les trames reçues doivent être acquittées par le destinataire (dont l'adresse MAC est informée dans la trame). Si aucun acquittement n'est reçu avant l'expiration d'un "timeout" prédéfini, les trames devront être retransmises.

Troisièmement, le temps d'occupation du canal restant est indiqué dans la trame envoyée afin de protéger l'échange des trames à suivre, qui y sont directement associées (par exemple les trames d'acquittement). Le VCS (pour "Virtual Carrier Sensing") implémente ce dernier mécanisme en utilisant des tableaux d'allocation du canal (NAV, pour "Network Allocation vector") qui sont mis à jour localement par chaque station après la réception d'une trame.

D'ailleurs, puisque les conditions du canal sans fil évoluent au cours du temps, le débit de transmission peut être adapté de manière dynamique grâce aux algorithmes de sélection de débit de la couche PHY. Plus la modulation et le codage utilisés sont robustes et plus le débit transmis est faible.

Pour améliorer l'efficacité de la couche MAC, des mécanismes avancés sont aussi définis. La qualité de service est introduite par la norme 802.11e en définissant les catégories d'accès. A chaque catégorie est attribuée une priorité différente dans le processus d'accès au canal. Certaines catégories sont autorisées à occuper le canal pour plus d'une transmission à la

fois, à condition de ne pas dépasser un temps total prédéfini à chaque accès (TXOP, pour "Transmit Opportunity"). Suite à cela, l'acquittement par bloc de trames a été introduit pour gagner en efficacité temporellement. L'évolution la plus importante des mécanismes de la couche MAC est sans doute l'agrégation des paquets introduite par la norme 802.11n. Cette agrégation consiste à mutualiser les phases de contention et les entêtes de mise en trame pour une meilleure efficacité. Le premier mode d'agrégation se situe au-dessus de la couche MAC et consiste à agréger plusieurs trames MSDU (pour "MAC Service Data Unit") en un A-MSDU. Ainsi, juste au-dessous de la couche MAC, les paquets MPDU (pour "MAC Protocol Data Unit") sont agrégés en un A-MPDU avant d'arriver à la couche PHY.

0.2.2 L'évolution du standard et les nouveaux défis

Les évolutions récentes des normes IEEE 802.11 ont porté principalement sur l'augmentation du débit maximal théoriquement possible par la couche PHY. Le dernier amendement, IEEE 802.11ac, pourrait théoriquement fournir un lien d'un débit maximal de 7 $Gbps$ [1].

Un aperçu des caractéristiques les plus importantes ajoutées à la couche PHY et la couche MAC par les amendements 802.11n et 802.11ac est illustré par la figure 2. Comme on l'explique dans le Chapitre 1 de ce mémoire, le débit de données théorique maximal est à peu près un produit de trois facteurs : la largeur du canal, la densité de la constellation de modulation, et le nombre de flux spatiaux. Par rapport aux spécifications de la couche PHY de la norme 802.11n, la norme 802.11ac a poussé plus fort sur les limites de chacun de ces facteurs.

Étant donné la puissance des mécanismes d'agrégation introduits par la norme 802.11n, la norme 802.11ac en réalité n'a pas beaucoup modifié les caractéristiques de la couche MAC. En effet, l'extension des mécanismes de protection (i.e., RTS/CTS, pour "Request To Send/Clear To Send") a été nécessaire pour l'opération sur des canaux beaucoup plus larges. En outre, la norme 802.11ac a étendu le mécanisme d'accès au canal 802.11n : les mécanismes de VCS et du backoff sont appliqués seulement sur un seul canal de 20 MHz (le canal primaire) et ensuite le mécanisme CCA est utilisé immédiatement avant de transmettre sur chacun des autres canaux secondaires de 20 MHz.

Néanmoins, les débits théoriques maximaux offerts par les derniers avancements techniques de la couche PHY ne peuvent être jamais atteints dans des conditions réelles en raison de nombreuses limitations liées à l'implémentation matérielle (e.g., encombrement des antennes, etc.), aux couches supérieures et leur coûts généraux et de nombreuses autres contraintes imposées par la nature de l'accès partagé au canal sans fil.

De plus, la densité de déploiement des réseaux locaux sans fil (WLAN) est renforcée pour répondre aux besoins de capacité élevée et de couverture omniprésente. Comme on l'explique dans cette thèse, la génération actuelle de la technologie Wi-Fi ne correspond pas aux nouveaux besoins du marché pour les déploiements extérieurs et/ou en haute

[1] Pour 8 flux spatiaux, une bande passante de 160 MHz et en utilisant un intervalle de garde court

	802.11n	802.11ac
MAC	Frame aggregation A-MSDU: 7935 Bytes max. A-MPDU: 65535 Bytes max.	Frame aggregation A-MSDU: 11434 Bytes max. A-MPDU: 1048575 Bytes max.
	Enhanced Block ACK	Always Block ACK
	Protection mechanisms for backward compatibility	Protection and coexistence updated for wider bands
PHY	2.4 and 5 GHz bands	5 GHz band only
	20, 40 MHz channels	20, 40, 80, 160 MHz channels
	1 to 4 spatial streams	1 to 8 spatial streams
	SU MIMO	SU and Downlink MU-MIMO
	16, 64 QAM	16, 64, 256 QAM

Figure 2 – Résumé des importants amélioration apportées par le 802.11n et 802.11ac aux niveaux de la couche physique (PHY) et la couche MAC

densité.

Dans ce contexte, le groupe d'étude (SG, pour "Study Group") IEEE 802.11 HEW (pour "High Efficiency WLAN") [6] a été formé en Mars 2013. Ce SG a étudié les exigences fonctionnelles nécessaires pour répondre aux problèmes identifiés dans les réseaux WLAN actuels. En conséquence, un nouveau "Task Group" (TG) a été lancé en Mars 2014 pour développer les solutions techniques pour la prochaine génération du Wi-Fi. Ce TG est nommé IEEE 802.11ax [7] et travaille à définir les modifications des normes 802.11 des deux couches, la PHY et la MAC. Ces modifications vont permettre l'amélioration du débit moyen par utilisateur d'un facteur de quatre dans un scénario de déploiement dense, tout en maintenant ou en améliorant l'efficacité énergétique par station. Les solutions définies doivent permettre la compatibilité ascendante et la coexistence avec les anciennes générations des équipements IEEE 802.11.

Dans le présent manuscrit, après avoir identifié les principaux défis et enjeux de la technologie Wi-Fi, nous contribuons au développement de la nouvelle norme en abordant la question de la réutilisation spatiale dans les environnements de haute densité de dé-

ploiement. La densité croissante des réseaux Wi-Fi en termes du nombre des APs déployés et le nombre des STAs associées à ces APs pose de nouveaux problèmes de performances. En raison de la nature de l'accès multiple concurrent défini par la norme IEEE 802.11, les utilisateurs Wi-Fi fonctionnant sur la même fréquence partagent le temps d'accès au canal. Dans la même zone géographique, le débit moyen de chaque utilisateur Wi-Fi diminue proportionnellement avec l'augmentation du nombre total des utilisateurs co-canaux. Comme nous le montrons à travers cette thèse, le comportement sur-protecteur des protocoles de la couche MAC aggrave la situation. Bien qu'il y ait un besoin d'atténuer les problèmes de sur-protection, l'équité entre les utilisateurs en contention doit être préservée.

0.3 L'adaptation du Physical Carrier Sensing (PCS) dans les environnements denses

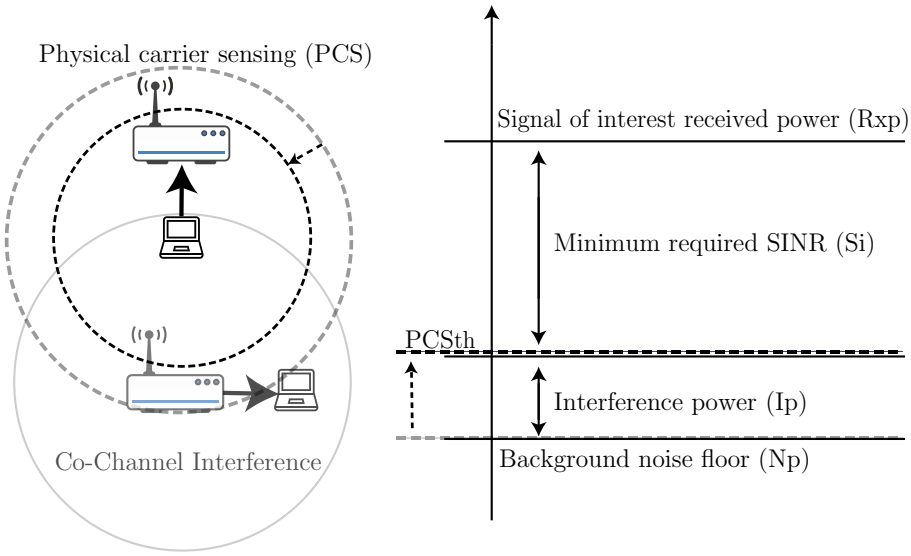

Figure 3 – Physical Carrier Sensing (PCS)

L'adaptation du mécanisme de PCS est proposée comme une solution alternative pour augmenter la réutilisation spatiale sans nuire aux autres utilisateurs. L'augmentation du seuil de PCS, illustrée par la Figure 3, montre un important potentiel afin d'exploiter la capacité offerte par les déploiements denses des réseaux locaux sans fil. Contrairement au contrôle de la puissance de transmission (TPC, pour "Transmit Power Control"), cette solution est plus incitative parce que l'utilisateur concerné bénéficie directement de son application. Pour un scénario de déploiement cellulaire de haute densité, nos résultats de simulation montrent un gain global de 190 % en débit total par rapport à la limite actuelle assumée par la norme 802.11. Cependant, un seuil statique n'est pas la solution la plus appropriée compte tenu du fait que le mécanisme d'accès au canal et la quantité

d'interférences subies dépendent de la position de l'utilisateur dans le BSS et de la topologie du réseau et sa densité. Par conséquent, une approche dynamique, nommé le PCSA (pour, "PCS Adaptation"), est proposée comme un moyen efficace pour adapter dynamiquement le mécanisme de PCS d'une manière locale, sans aucune coordination entre les utilisateurs. Cette approche distribuée est nécessaire en raison du fait que la majorité des déploiements WLAN aujourd'hui ne sont pas coordonnés, n'ayant pas une architecture centralisée et ne sont pas planifiés. Le mécanisme proposé est évalué dans plusieurs scénarios de haute densité et a démontré sa capacité à améliorer la réutilisation spatiale même en présence des anciens utilisateurs (i.e., "legacies") où le TPC échoue. En outre, on a comparé la performance du PCSA avec un mécanisme centralisé d'adaptation du CCA proposé dans [63] et nommé ORCCA (pour "Optimal-rate Clear Channel Assessment Adaptation"). Nos résultats montrent que le PCSA surpasse le ORCCA.

0.4 Améliorer la réutilisation spatiale en préservant l'équité entre les utilisateurs, le Balanced TPC and PCS Adaptation (BTPA)

Pour améliorer l'équité entre les différents utilisateurs, nous élaborons une nouvelle approche distribuée pour adapter conjointement le mécanisme de détection de signal (PCS) et le contrôle de la puissance de transmission (TPC). Nous appelons cette méthode le BTPA (pour "Balanced TPC and PCS Adaptation"). Cette approche est évaluée ensuite dans différents scénarios de simulation de haute densité où il prouve sa capacité à améliorer les niveaux d'équité en particulier en présence des utilisateurs d'anciennes générations dans le réseau, cela tout en améliorant le débit moyen d'un facteur 4 par rapport à la performance conventionnelle du standard.

La méthode proposée consiste à calculer un écart Δ_X tel que

$$\Delta_X[dB] = Rx_p[dBm] - M[dB] - PCS_{default}[dBm] \tag{1}$$

où Rx_p est la puissance reçue en dBm, M est la valeur de marge déjà définie pour le mécanisme de PCSA afin d'éviter les nœuds cachés au sein du même BSS et $PCS_{default}$ est le seuil de PCS par défaut comme défini dans le standard. Cet écart est utilisé ensuite par chaque nœud pour calculer les deux valeurs Δ_{TPC} et Δ_{PCS} qui seront respectivement utilisées pour l'adaptation de la puissance de transmission et le seuil de PCS. Ce calcul se base sur les expressions qui suivent :

$$\Delta_X[dB] = \Delta_{PCS}[dB] + \Delta_{TPC}[dB] \tag{2}$$

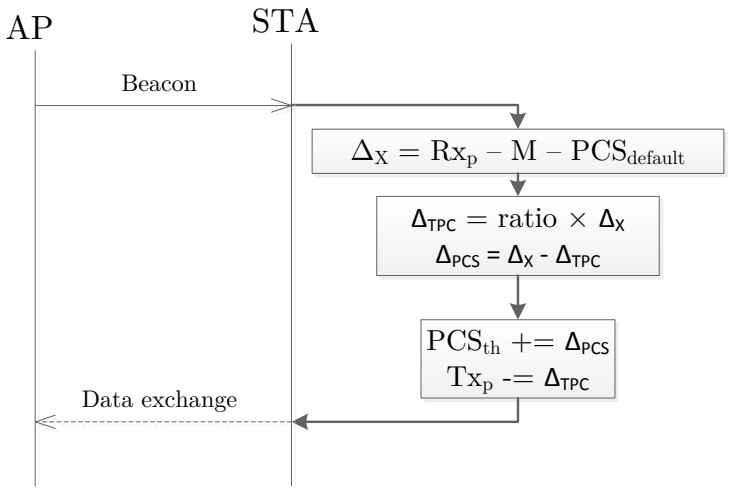

Figure 4 – Un cas de figure d'utilisation du BTPA

$$\Delta_{TPC}[dB] = ratio \times \Delta_X[dB] \tag{3}$$

Pour un simple cas de figure, l'application du BTPA est illustrée par la Figure 4. Dans cet exemple, une nouvelle STA s'associe à un BSS et commence une nouvelle communication avec son AP. A la réception d'une trame de beacon (ou balise) de l'AP, la STA calcule la valeur de Δ_X. Dans une implémentation pratique, il est facile de diffuser la valeur $ratio$ par l'AP dans la trame de beacon. Connaissant le $ratio$, la STA déduit les valeurs de Δ_{PCS} et Δ_{TPC}. La dernière étape consiste à calculer le nouveau seuil de PCS (PCS_{th}) et la puissance de transmission (Tx_p) et à les appliquer avant de procéder à l'échange de données prévu.
Dans un scénario cellulaire de haute densité, on compare la performance des différentes approches en terme de débit moyen atteint par chaque utilisateur. Nous montrons respectivement dans les Figures 5 et 6 les fonctions de répartitions (CDF, pour "Cumulative Distribution Function") de ces débits pour deux cas: (a) sans STAs legacy; (b) en présence des STAs legacy. La pente de la courbe de CDF donne une idée claire sur l'équité entre les différents utilisateurs. On peut remarquer clairement d'après ces courbes que les meilleurs résultats sont obtenus avec le BTPA dans les deux cas. Cette solution améliore le débit moyen ainsi que le niveau de l'équité. On distingue surtout dans le cas (b) (Figure 6) l'inefficacité du TPC en présence des STAs legacy et la capacité du BTPA à maintenir les meilleurs débits moyens avec une pente élevée indiquant une meilleur équité entre les différents utilisateurs.

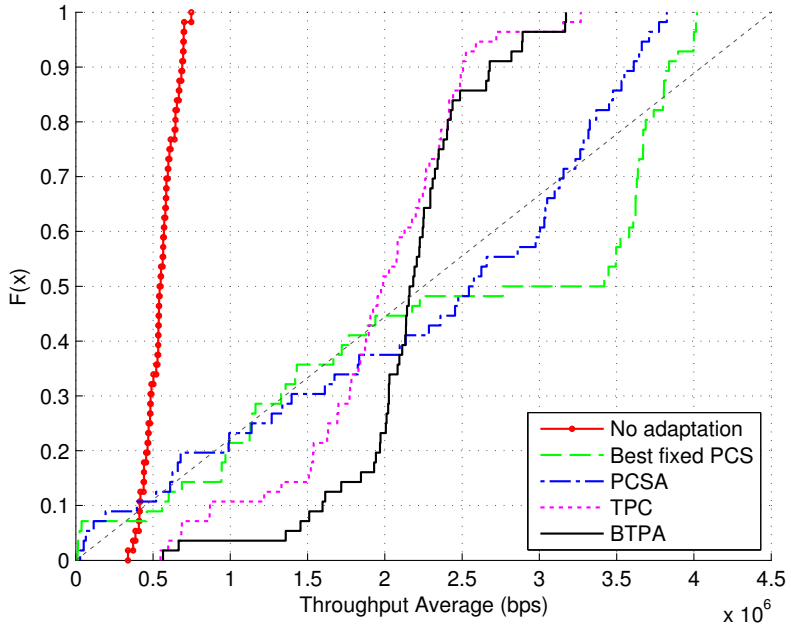

Figure 5 – Comparaison du débit moyen: Transmit Power Control (TPC), Physical Carrier Sensing Adaptation (PCSA), Balanced TPC and PCS Adaptation (BTPA), meilleur PCS fixe, sans aucune adaptaion – Cas (a): sans STAs legacy

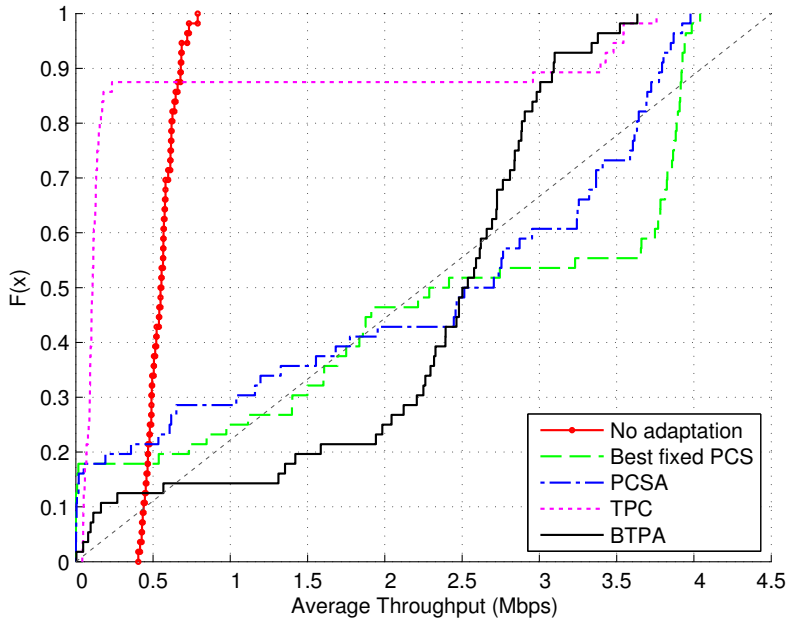

Figure 6 – Comparaison du débit moyen: Transmit Power Control (TPC), Physical Carrier Sensing Adaptation (PCSA), Balanced TPC and PCS Adaptation (BTPA), meilleur PCS fixe, sans aucune adaptaion – Cas (b): en présence des STAs legacy (12.5 % de la totalité des STAs)

0.4.1 La valeur du ratio du mécanisme Balanced TPC and PCS Adaptation (BTPA)

Dans cette partie, on cherche à déterminer la valeur optimale du paramètre $ratio$ dans deux différents scénarios de haute densité. Le premier est le scénario cellulaire et le deuxième est un scénario résidentiel constitué d'un bâtiment de 5 étages de 20 pièces chacune. Pour cette étude, on définit trois configurations en terme de proportion des STAs legacy. Dans la première configuration, 25 % de la totalité des STAs dans chaque scénario sont des STAs legacy (opération conventionnelle sans l'application du BTPA). La deuxième et la troisième configurations contiennent respectivement 50 % et 75 % de STAs legacy. Dans la suite, les STAs non legacy (appliquant le BTPA) sont nommées des STAs "802.11ax". La Figure 7 montre le débit moyen par utilisateur dans le scénario cellulaire pour les trois configurations des STAs legacy par rapport à la valeur du $ratio$. Les même résultats obtenus dans le scénario résidentiel sont montrés par la Figure 8. Dans les deux figures, on sépare les débits des STAs legacy des autres STAs 802.11ax. Cela permet de mettre en évidence l'impact du $ratio$ sur chaque type de STA afin d'étudier la performance en terme d'équité.

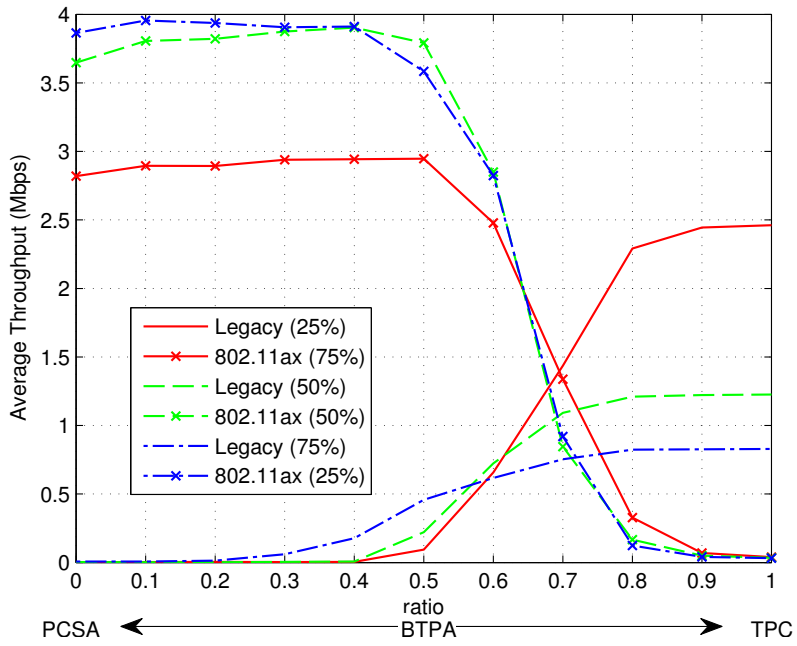

Figure 7 – Débit moyen par utilisateur en fonction de la valeur du paramètre $ratio$ du BTPA en présence des legacy STAs dans le scénario cellulaire

Encore une fois, la valeur optimale du paramètre $ratio$ de BTPA est un compromis entre la valeur utilisée pour atteindre la meilleure performance en débit agrégé (total) ainsi qu'un meilleur niveau de l'équité entre les utilisateurs. Pour les deux scénarios, une valeur du $ratio$ d'environ 0.65 donne des débits équitables entre les STAs legacy et les STAs 802.11ax. En pratique, un $ratio$ de cette valeur atteint le compromis souhaité dans le scénario

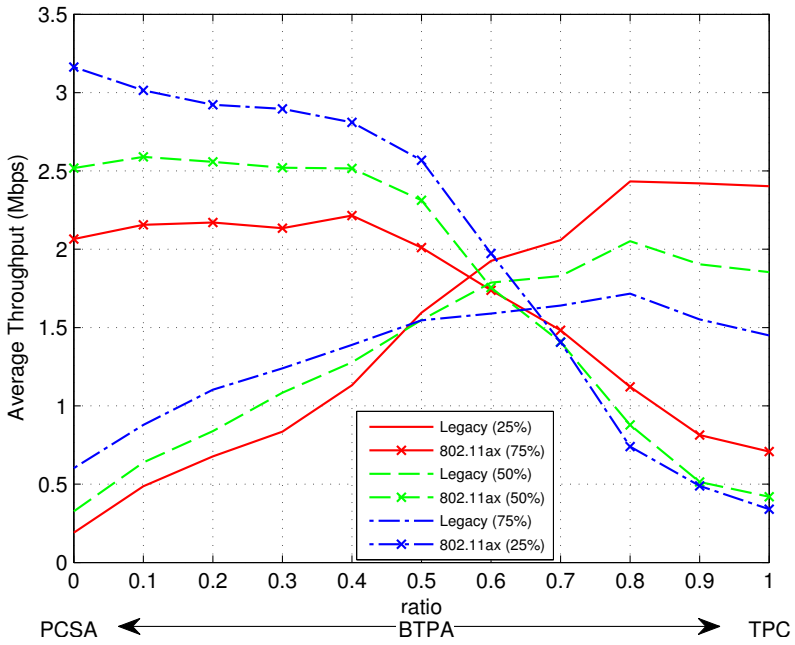

Figure 8 – Débit moyen par utilisateur en fonction de la valeur du paramètre $ratio$ du BTPA en présence des legacy STAs dans le scénario résidentiel

cellulaire ainsi que le scénario résidentiel pour toutes les proportions des utilisateurs legacy. Dans le scénario résidentiel, Pour cette valeur du $ratio$, en présence des STAs legacy, le BTPA améliore le débit total d'environ une fois et demi. Le débit passe de 278.6 $Mbps$ sans l'utilisation du BTPA jusqu'au 392 $Mbps$ quand 25 % des STAs sont 802.11ax (appliquant le BTPA). En termes d'équité, le débit moyen atteint par une STA legacy et une 802.11ax STA dans ce cas est respectivement 1.61 $Mbps$ et 1.68 $Mbps$ au lieu de 1.16 $Mbps$ lorsque il n'y a pas d'adaptation.

0.5 Optimisation basée sur l'apprentissage

Enfin, nous concevons et mettons en œuvre une solution centralisée basée sur les techniques d'apprentissage utilisant les réseaux de neurones. Cette approche repose sur l'adaptation conjointe de puissance de transmission et du mécanisme de détection du signal. Cette nouvelle solution bénéficie de la capacité des réseaux de neurones artificiels à modéliser les fonctions non-linéaires complexes pour optimiser la réutilisation spatiale dans les environnements WLAN denses tout en préservant l'équité entre les nœuds en compétition.

La Figure 9 illustre la procédure générale sur laquelle est fondée notre solution. Après une phase d'enregistrement des nœuds auprès du contrôleur, on passe à une phase de collecte de la base de données qui sera utilisée plus tard pour l'apprentissage et le test. Après que le réseaux de neurones soit suffisamment entrainé sur plusieurs échantillons d'entrés sorties, on teste le niveau d'apprentissage en utilisant d'autres échantillons. Après le succès du

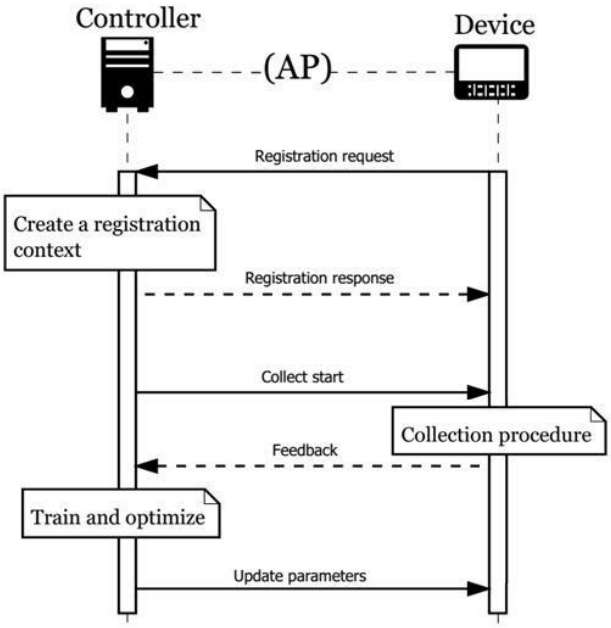

Figure 9 – Procédure générale

test, on passe à la phase d'optimisation des paramètres d'accès au canal.
A travers des nombreux simulations, nous montrons que la technique proposée permet de traiter les cas des nœuds exposés et des nœuds cachés et globalement permet d'améliorer l'équité entre les nœuds dans les environnement denses. Dans la Figure 10, les résultats de simulation en considérant le scénario cellulaire à forte densité sont montrés en fonction de deux valeurs de η (le taux d'optimisation). L'algorithme converge rapidement vers un point stable avec un index d'équité de Jain égal à 0.7 et un débit moyen de 1.5 $Mbps$.

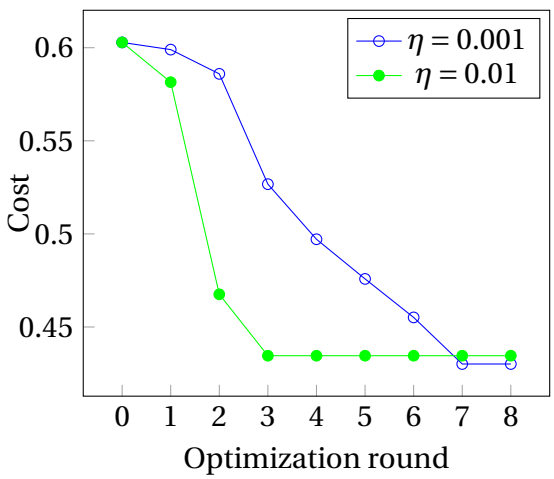

(a) La fonction de cout en fonction du nombre d'itération

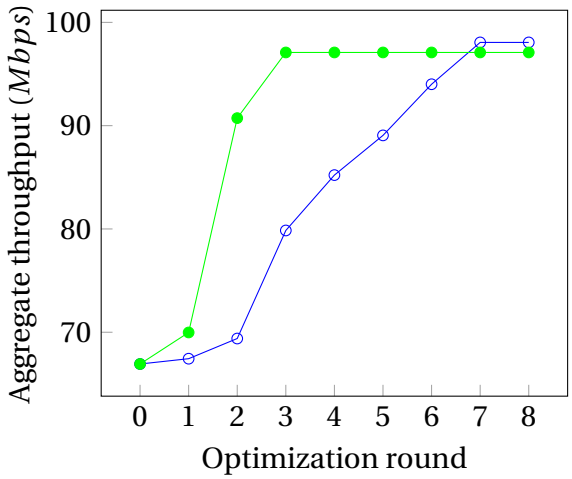

(b) Le débit agrégé en fonction du nombre d'itération

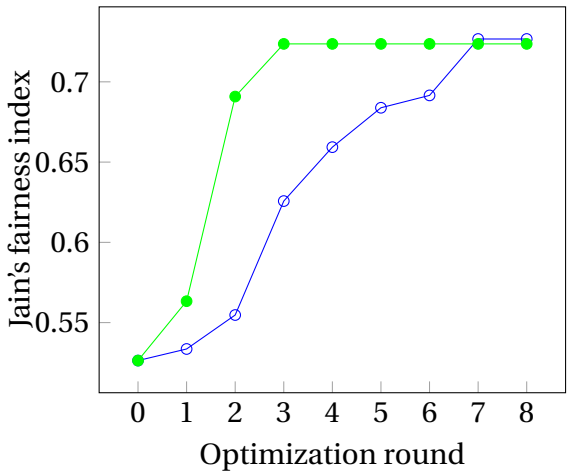

(c) L'index d'équité de Jain (ou "Jain's fairness index")

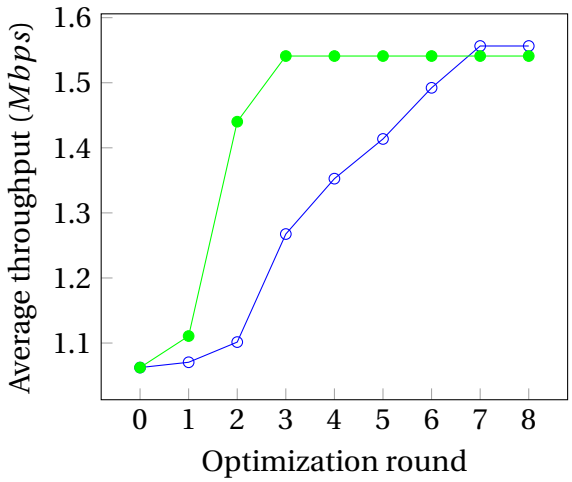

(d) Le débit moyen en fonction du nombre d'itération en fonction du nombre d'itération

Figure 10 – La performance de la solution centralisée dans le scénario cellulaire de haute densité

0.6 Conclusion

Les différentes contributions de ces travaux ont permis d'apporter des solutions novatrices pour les futures générations de la technologie Wi-Fi. Ces solutions que nous avons présentées au sein du groupe de standardisation IEEE 802.11ax sont aujourd'hui identifiées comme très pertinentes pour le prochain standard.

Des nombreuses perspectives de recherche son envisagées comme l'extension des solutions proposées surtout dans le contexte des systèmes LTE-U (pour "LTE on Unlicensed band") et les cas d'utilisation des transmission MIMO Multi-Utilisateurs. Ainsi, les travaux menés dans cette thèse peuvent être étudiés sur le plan de la minimisation de la consommation énergétique dans les réseaux WLANs.

Contents

List of Figures

List of Tables

Glossary

List of Acronyms

3GPP	3rd Generation Partnership Project
A-MPDU	Aggregated MPDU
A-MSDU	Aggregated MSDU
AARF	Adaptive Automatic Rate Fall-back
AC	Access Category
ACK	Acknowledgment
AIFS	Arbitration Inter-Frame Space
ANN	Artificial Neural Network
AP	Access Point
ARF	Automatic Rate Fall-back
BA	Block Acknowledgment
BAR	Block Acknowledgment Request
BER	Bit Error Rate
BPSK	Binary Phase Shift Keying
BSS	Basic Service Set
BTPA	Balanced TPC and PCS Adaptation
CCA	Clear Channel Assessment
CCI	Co-Channel Interference
CCK	Complimentary Code Keying
CDF	Cumulative Distribution Function
CDMA	Code Division Multiple Access
CS	Carrier Sense
CSI	Channel State Information
CSMA/CA	Carrier Sense Multiple Access with Collision Avoidance
CSMA/CD	Carrier Sense Multiple Access with Collision Detection
CSMA	Carrier Sense Multiple Access

CTS Clear To Send
CW Contention Window
DCF Distributed Coordination Function
DIFS DCF Inter-Frame Space
DLL Data Link Layer
DS Distribution System
DSSS Direct Sequence Spread Spectrum
ED Energy Detect
EDCA Enhanced Distributed Channel Access
ESS Extended Service Set
FAST Full Duplex Attachment System
FCC Federal Communications Commission
FDMA Frequency Division Multiple Access
FER Frame Error Rate
FFT Fast Fourier Fransform
FHSS Frequency Hopping Spread Spectrum
FSM Finite State Machine
GI Guard Interval
GO Group Owner
HEW High Efficiency WLAN
HT High Throughput
IBSS Independent BSS
IEEE Institute of Electrical and Electronics Engineers
IFFT Inverse Fast Fourier Transform
IFS Inter-Frame Space
IoE Internet of Everything
ISI Inter-Symbol Interference
ISM Industrial, Scientific and Medical
ITU International Telecommunication Union
LAA Licensed-Assisted Access
LAN Local Area Network
LBT Listen Before Talk
LLC Logical Link Control
LTE Long-Term Evolution
LTE-U LTE in Unlicensed spectrum
MAC Media Access Control Layer
MAN Metropolitan Area Network
MCM Multi-Carrier Modulation
MCS Modulation and Coding Scheme
MIMO Multiple-Input Multiple-Output

MPDU MAC Protocol Data Unit
MSDU MAC Service Data Unit
MSE Mean Squares Error
MU-MIMO Multi-User MIMO
MLP MultiLayer Perception
NAV Network Allocation Vector
OBSS Overlapping BSS
OFDM Orthogonal Frequency Division Multiplexing
OFDMA Orthogonal Frequency Division Multiple Access
ORCCA Optimal-rate Clear Channel Assessment Adaptation
OSI Open Systems Interconnection
P2P Peer-to-Peer
PCF Point Coordination Function
PCS Physical Carrier Sensing
PCSA Physical Carrier Sensing Adaptation
PDU Protocol Data Unit
PER Packet Error Rate
PHY Physical Layer
PLCP Physical Layer Convergence Protocol
PPDU Physical Protocol Data Unit
PSDU Physical Service Data Unit
QAM Quadrature Amplitude Modulation
QoE Quality of Experience
QoS Quality of Service
QPSK Quadrature Phase Shift Keying
RAN Radio Access Network
RIFS Reduced Inter-Frame Space
RTS Request To Send
SA Standard Association
SCM Single Carrier Modulation
SDMA Spatial Division Multiple Access
SDU Service Data Unit
SG Study Group
SIFS Short Inter-Frame Space
SINR Signal to Interference and Noise Ratio
SNR Signal to Noise Ratio
SR Spatial Reuse
SSID Service Set Identifier
STA Station
TBTT Target Beacon Transmission Time

TC Traffic Category
TDMA Time Division Multiple Access
TG Task Group
TPC Transmit Power Control
TXOP Transmit Opportunity
UDP User Datagram Protocol
VCS Virtual Carrier Sensing
VHT Very High Throughput
VoIP Voice over IP
WFA Wi-Fi Alliance
WG Working Group
WLAN Wireless Local Area Network
WSN Wireless Sensor Network
WCDMA Wideband Code Division Multiple Access

List of Symbols

Rx_p reception power level
R code rate
N_{BPSCS} number of coded bits per single carrier for each spatial stream
N_{CBPS} number of coded bits per Orthogonal Frequency Division Multiplexing (OFDM) symbol
N_{DBPS} number of data bits per OFDM symbol
N_{STA} number of non access point stations
N_{AP} number of access points
S_i minimum required SINR for MCS_i
N_P background noise power level
I_P interference power level
$PCS_{default}$ default PCS according to the standard
PCS_{th} physical carrier sensing threshold
Rx_{th} reception sensitivity threshold
PCS_R physical carrier sensing range
M PCSA margin parameter value expressed in dB
Tx_p transmission power level

Introduction

Context and motivations

Today, the most used access technology for communications is wireless. Among the other systems, Wireless Local Area Network (WLAN) gained an outstanding reputation and a wide proliferation. The beginning of the wireless era was announced in 1888 by the Hertz's proof of the existence of electromagnetic waves. Later, Marconi's experiments in 1894 proved the ability to transmit and receive the radio waves over long distances. Afterwards, the radio communication system and radar were designed initially for military use. Accordingly, the development of the spread spectrum modulation was necessary to increase the resistance to noise and establish more secure communications. In 1971, ALOHANET [1], the first wireless packet data communication system was designed at the University of Hawaii. This system defined a random access technique called ALOHA that inspired later a lot of wired and wireless communication technologies.

One of the landmarks for commercial WLAN was allowing the use of the Industrial, Scientific and Medical (ISM) radio bands for the commercial applications of the spread spectrum technology by the United States Federal Communications Commission (FCC) in 1985. Consequently, many proprietary WLAN systems were designed to use the ISM bands such as WaveLan by Bell labs. However, these systems were expensive to deploy and maintain, what prevented the expansion in their use.

In 1990, the Institute of Electrical and Electronics Engineers (IEEE) 802.11 Working Group (WG) started the development of a standard for WLAN. It took seven years to ratify the first IEEE 802.11 standard in 1997. Originally, the goal was to replace Ethernet cables in home and office offering users a higher degree of mobility especially with the increased popularity of laptop computers back then. With the tremendous evolution in the semiconductors industry, IEEE 802.11 WLAN provided a cheap and easy way to make connected computer mobility a reality for everyone and everywhere. To deal with the interoperability of devices

from different vendors, the Wi-Fi Alliance (WFA) was formed in 1999 to certify all IEEE 802.11 devices.

In the last twenty years, the Wi-Fi industry has experienced a colossal growth with the huge spread of IEEE 802.11 equipped devices. This growth is driven by the always-connected trend; the need to have an Internet access all the time, from everywhere is essential today. This need has long been accompanied by a substantial increase in the size of the communicated data traffic. With the enrichment of the offered services for high definition video streaming, video games, augmented reality, etc., there has been an increasing need for higher data rates and larger capacity. According to a recent report from Strategy Analytics [2], 65% of worldwide households that have broadband Internet access are using Wi-Fi connectivity. This represents 25% of the global households, which is approximately 451 million households. Furthermore, ABI Research, which has tracked Wi-Fi shipments since the industry's inception, indicates that at the end of 2014, 9.98 billion Wi-Fi devices have been sold worldwide and that about 4.5 billion Wi-Fi products are in use today [3] [4].

However, the combination of ubiquitous coverage and high capacity requirements is challenging for any wireless communication system. This combination is even more challenging for Wi-Fi because this technology was not designed to operate in such extreme use cases. Since its introduction, this standard has not stopped evolving. Accordingly, a long list of amendments were adopted and different generations succeeded. The last version of the IEEE 802.11 standard [5] that incorporates all the previous amendments dates back to 2012. In all its evolution history, the success of Wi-Fi was due to its low price and its simple operation. As always, the IEEE 802.11 WLAN is again compelled to evolve in order to keep the pace with the new challenges. Although the challenge is big, Wi-Fi has to keep its relative simplicity, the key of its success, while shaping its new generation.

The recent evolutions of IEEE 802.11 mainly focused on increasing peak Physical Layer (PHY) throughputs. The last amendment, IEEE 802.11ac, could theoretically reach 7 $Gbps$ [2]. Nevertheless, such throughputs cannot be reached in real conditions due to many limitations related to practical hardware implementations, higher layers overhead, and many other constraints imposed by the shared access to the wireless medium. Furthermore, the density of deployed WLANs is being stepped up to address the needs for more capacity and coverage. As will be discussed later in this thesis, the present Wi-Fi technology does not match the new needs of the market for outdoor or/and high density deployments use cases.

In this context the IEEE 802.11 High Efficiency WLAN (HEW) Study Group (SG) [6] was formed in March 2013. The IEEE 802.11 HEW studied the functional requirements needed to meet the identified issues of the current Wi-Fi networks. As a result, a new Task Group

[2] For 8 spatial streams and 160 MHz band using a short Guard Interval (GI)

(TG) was launched in March 2014 to develop the technical solutions for the next Wi-Fi generation. This TG is named IEEE 802.11ax [7] and is working to define standardized modifications to both the IEEE 802.11 PHY and the IEEE 802.11 Media Access Control Layer (MAC) that enable four times improvement in the average throughput per device in a dense deployment scenario, while maintaining or improving the power efficiency per station. The defined solutions shall enable backward compatibility and coexistence with legacy IEEE 802.11 devices operating in the same frequency band.

In this work, after identifying the main challenges and issues in current WLAN technology, we contribute to the development of the new Wi-Fi standard by tackling the spatial reuse issue in dense deployments. The increasing density of Wi-Fi networks in terms of deployed Access Point (AP)s and associated Station (STA)s per AP is raising new performance issues. Because of the nature of the multiple access scheme defined by the IEEE 802.11 standard, neighboring Wi-Fi devices operating on the same frequency band share the communication airtime. In the same geographical zone, the average throughput of every Wi-Fi device decreases proportionally with the increase of the number of co-channel operating devices. A conservative configuration of the MAC layer protocols aggravates the situation. Although there is a need to alleviate the overprotection issues, the fairness between the contending devices must be preserved.

We propose in this thesis a new adaptation scheme of the physical carrier sensing used by Wi-Fi transmitters to access the medium. Subsequently, we compare it to the transmission power control approach in terms of enhancing the spatial reuse in dense environments. Then, we study the impact of the proposed technique on the link layer adaptation and how to use it to enhance the currently adopted rate control algorithms. Furthermore, we study the fairness issues incurred by the different approaches and we propose a joint solution that preserves fairness while enhancing the spatial reuse in dense scenarios. Finally, we propose a novel centralized solution based on neural networks to optimize the spatial reuse and resolve fairness issues in fully managed WLANs.

Outline of the thesis

In Chapter 1, we detail the fundamental background of WLANs. The main MAC and PHY layers functionalities of the IEEE 802.11 standard are presented. Subsequently, the major improvements adopted by the most important amendments are discussed. Then, the most relevant use cases for Wi-Fi are identified and the related challenges and issues are described.

In Chapter 2, we depict the solutions proposed in the literature to resolve the previously described problems. Consequently, we list the possible areas to improve the current state

of the art performance and we draw the link with the currently ongoing standardization efforts in the IEEE 802.11 WG.

In Chapter 3, we show the deployment scenarios that are used along this thesis. The simulation tools are presented with their related modifications that were required to fit the needs of our validation process. As a reference performance, the results of some basic tests are shown and discussed at the end of this chapter.

In Chapter 4, we consider two approaches to enhance the spatial reuse of Wi-Fi networks in dense environments. The first is the control of the transmission power that is widely cited in the literature and traditionally used in cellular networks. The second approach is specific to the technologies using a contention-based access scheme like Wi-Fi and consists in an adaptation of the physical carrier sensing protocol. After discussing the advantages of the latter approach in terms of total gain in aggregate throughput, we propose a novel dynamic adaptation of the physical carrier sensing mechanism and compare its performance to other techniques in the state of the art. Through extensive simulations, we show that our proposal outperforms these existing solutions.

In Chapter 5, the impact of the proposed adaptation of the physical carrier sensing is studied in accordance with the link layer adaptation. An improvement to the currently adopted rate control algorithms is proposed and the performance results are shown. This study shows that improving the currently used link adaptation algorithms is essential when dealing the increasing density of Wi-Fi deployments. However, we prove that the solution that we present in Chapter 4 is able to improve the spatial reuse without substantial modifications of the present link layer adaptation mechanisms.

In Chapter 6, to preserve better fairness performance while enhancing spatial reuse, we propose a new distributed adaptation technique that jointly uses the control of the transmission power and the physical carrier sensing. The performance of this proposal is compared to other approaches in two different deployment scenarios and shows the best performance in terms of total gain in throughput and fairness level.

In Chapter 7, we exploit a novel optimization proposal to enhance the spatial reuse in a centralized scheme using artificial neural networks. Since the relation between the access protocol mechanisms and the achieved throughput is very complex, we show that neural networks could be trained to learn this relation and use the modeled function to optimize the MAC mechanisms and parameters.

Finally, we conclude this thesis in the last chapter and provide some potential perspectives for future research activities.

List of the contributions

All the following publications are co-authored with Laurent Cariou, and Jean-François Hélard.

In progress — *"Novel Learning-based spatial reuse optimization in dense WLAN deployments"*, Journal submitted to **EURASIP Journal on Wireless Communications and Networking**

June 2015 — *"Preserving Fairness in Future Super Dense WLANs"*, In the proceedings of the IEEE International Conference on Communications, **ICC '15**, London, UK. pp. 2276-2281.
doi: 10.1109/ICCW.2015.7247520

March 2015 — *"Efficient MAC Protocols Optimization for Future High Density WLANS"*. In the proceeding of the IEEE Wireless Communications and Networking Conference, **WCNC '15**, New Orleans, USA. pp. 1054-1059.
doi: 10.1109/WCNC.2015.7127615

December 2014 — *"Carrier Sensing-aware Rate Control Mechanism For Future Efficient WLANs"*. In the proceedings of the International Conference On Network of the Future, **NoF '14**, Paris, France. pp. 1-6.
doi: 10.1109/NOF.2014.7119777

April 2014 — *"Improving the Capacity of Future IEEE 802.11 High Efficiency WLANs"*. In proceedings of The International Conference on Telecommunications, **ICT '14**, Lisbon, Portugal. pp. 303-307.
doi: 10.1109/ICT.2014.6845128

The below patent is co-authored with Laurent Cariou.

September 2014 — *"Procédé de détermination de seuils de signaux WiFi et station WiFi associée"*, **Patent** deposit, (Déclaration d'invention, France 1458554)

The following presentations are co-authored with Laurent Cariou and presented to the standardization committee at the **IEEE 802.11ax** TG.

April 2014 — *"MAC simulation results for Dynamic sensitivity control (DSC - CCA adaptation) and transmit power control (TPC)"*, IEEE 802.11-14/523r0

September 2014 — *"OBSS reuse mechanism which preserves fairness"*, IEEE 802.11-14/1207r1

1 Wi-Fi after two decades of evolution

1.1 Introduction

Wi-Fi, which started in 1997 as a wireless local area network connectivity technology to replace cables in office and home, has become a leading wireless technology invading all electronic devices. Today, more than 4 billion Wi-Fi chipsets are operating around the world [4]. Going back 25 years, after the decision of the Federal Communications Commission (FCC) to open Industrial, Scientific and Medical (ISM) bands allowing their use without the need of a wireless license, many vendors of wireless equipment developed their proprietary solutions for wireless devices operating in these unlicensed bands. As a consequence, equipments from one vendor could not communicate with the equipments from another.

Inspired by the success of the Ethernet, the wireline networking technology based on the Institute of Electrical and Electronics Engineers (IEEE) 802.3 standard, quickly several vendors realized that a common wireless standard would make sense too. Consequently, a new standardization committee called 802.11 Working Group (WG) was set up within the IEEE. It took around seven years to ratify the first 802.11 standard that allowed a data rate of 2 $Mbps$. Later, the newly standardized technology needed a consumer friendly name. Many suggested names were given, such as *FlankSpeed* of *DragonFly*, but the winner was *Wi-Fi* for *Wireless-Fidelity*. Since then, the evolution of the Wi-Fi technology has never ceased driven by its increasing proliferation.

Today, Wi-Fi equipped devices are present everywhere around us. This technology is the easiest way to enable several devices in home, office, coffee shops, venues, etc., to share a broadband Internet connection. The latest Wi-Fi devices are able to communicate with data rates approaching 1 $Gbps$. In this chapter, we describe the technical fundamentals behind Wi-Fi. Then, we depict the main amendments that contributed to the tremendous evolution of this technology.

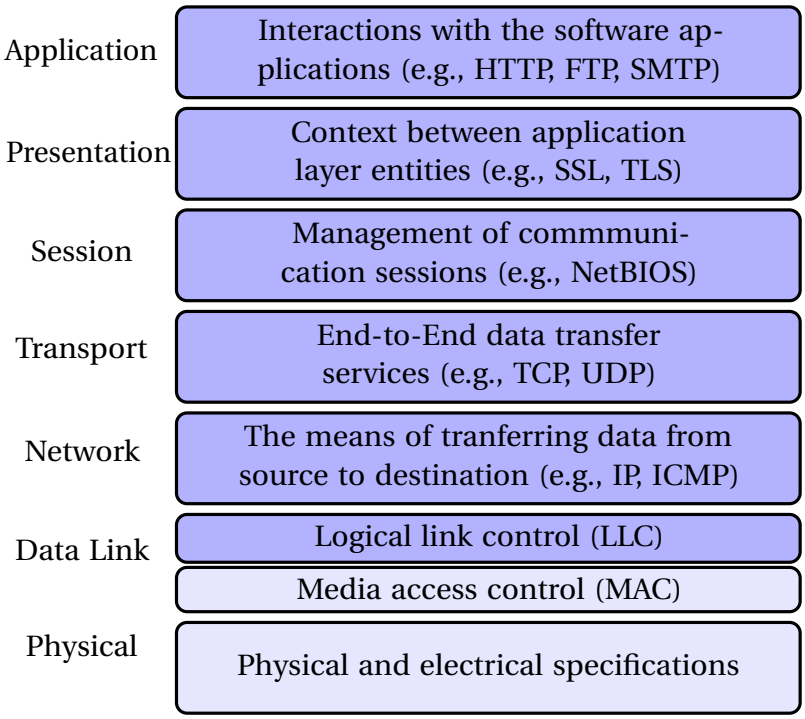

Figure 1.1 – OSI reference model (ISO/IEC 7498-1, 1994)

1.2 IEEE 802.11 protocol and network architecture

The IEEE 802.11 standard [5] is member of the IEEE 802 family that deals with Local Area Network (LAN) and Metropolitan Area Network (MAN) standardization. The 802 standards reference model is based on the Open Systems Interconnection (OSI) networking reference model shown in Figure 1.1. More precisely, the services and protocols specified in 802 map to the lower two layers (Data Link and Physical) of the seven-layers OSI reference model. The 802.11 standard defines multiple Physical Layer (PHY) layers and a common Media Access Control Layer (MAC) layer for wireless local area networking [5]. As the most of the 802 family's members, the 802.11 inherits the 802 reference model and the 48-bit universal addressing scheme. The 802.11 MAC and 802.2 Logical Link Control (LLC) sublayers together form the Data Link Layer (DLL) layer of the OSI model and the 802.11 PHY represents the physical layer.

The basic protocol architecture of the 802.11 standard is illustrated in Figure 1.2. In this layered architecture, each layer, PHY and MAC, offers services to the layer directly above it. The user data is transferred between these layers in the form of Service Data Unit (SDU). The data unit received by the MAC from the LLC and delivered by the MAC to the LLC is called MAC Service Data Unit (MSDU). The PHY receives data from the MAC and send data to the MAC through the Physical Service Data Unit (PSDU). Between two different nodes, the exchanged data takes place in the form of a Protocol Data Unit (PDU). The MAC layers of two peer nodes exchange data using a MAC Protocol Data Unit (MPDU). The PHY

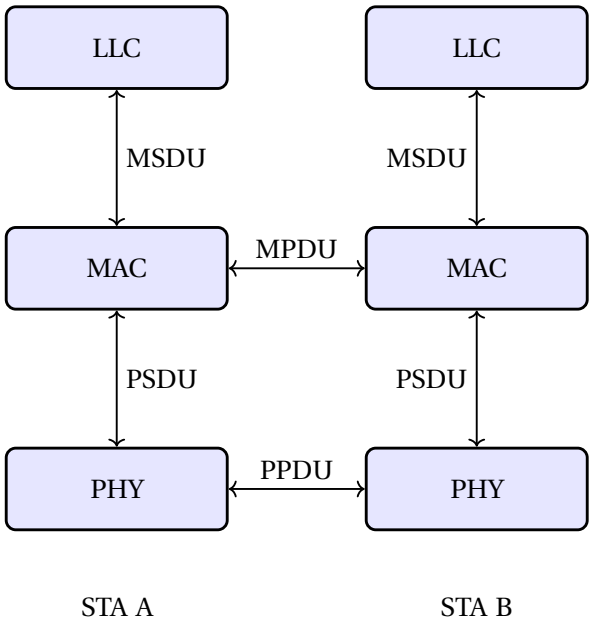

Figure 1.2 – Protocol architecture and messaging

layers of two peer nodes exchange data through a Physical Protocol Data Unit (PPDU).

In 802.11 standard, the term Station (STA) is used to refer to the device that incorporates the MAC and PHY entities. In real world, this device is the network interface card in a computing equipment. On the other hand, the Access Point (AP) is a special type of STA having additional features and functions essentially to manage the communications within a basic 802.11 network. The basic building block of an 802.11 Wireless Local Area Network (WLAN) is termed as Basic Service Set (BSS). Typically, multiple STAs within the same geographic area, in order to communicate with each other or with a distant entity, associate to a central device which is the AP. This type of 802.11 WLAN is called an infrastructure BSS and is represented by the BSSs A and B in Figure 1.3. All the communications within an infrastructure BSS pass through the AP. Normally, there is no direct communication between associated STAs. An Extended Service Set (ESS) is formed when multiple BSSs are interconnected by a Distribution System (DS). Within an ESS, the devices (STAs and APs) are able to communicate directly at the MAC layer. In practice, the DS is usually an Ethernet LAN where the APs play the role of Ethernet bridges. Consequently, the 802.11 devices are also able to address LAN devices (connected to the DS) at the MAC layer. It is worth mentioning that in typical production deployments the different BSSs does not coordinate their operation.

Another mode of operation of a BSS is formed in an ad-hoc fashion where the STAs communicate directly with each other. This operation mode is called Independent BSS (IBSS). The BSS C in Figure 1.3 illustrates an example of an IBSS. Furthermore, to improve the Peer-to-Peer (P2P) operation, the Wi-Fi Alliance (WFA) developed a specification for direct

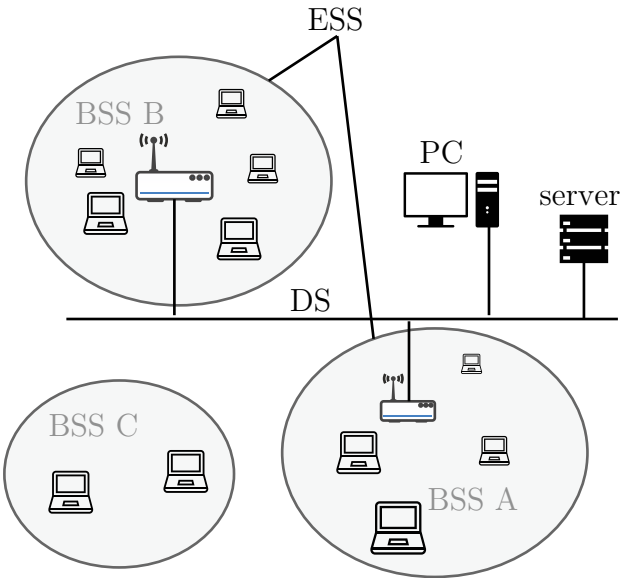

Figure 1.3 – The 802.11 network architecture

communication between Wi-Fi devices without being associated to an AP. This specification is called Wi-Fi Direct and can be seen as a variation of the IBSS. However, Wi-Fi Direct differs from the IBSS in the sense that one of the peers assumes a role similar to that of an AP in an infrastructure BSS. The device assuming this role is called the Group Owner (GO). The other peer devices associate with the GO. However, what differs a Wi-Fi Direct network from an infrastructure BSS is that the GO does not provide the access to a distribution system and it could be a mobile battery powered device.

1.3 Media Access Control Layer (MAC) basics

Among other functionalities, the MAC layer coordinates the access to the shared medium allowing the communication of multiple devices over a common wireless channel. In addition, the MAC layer provides the addressing scheme that permits the identification of these different devices. Mainly, this layer is responsible for resolving the contention between the communicating devices so that the limited radio resources are shared efficiently and fairly. The first version of the 802.11 standard was influenced by the success of the Ethernet which was standardized as 802.3. In fact, in terms of channel access and addressing, 802.11 is similar to Ethernet. For that reason, the 802.11 is often referred to as wireless Ethernet. The 802.3 or Ethernet would not exist without that simple distributed access protocol that is called the Carrier Sense Multiple Access (CSMA). Similarly, the 802.11 MAC adopted the same simple yet efficient contention-based distributed access scheme. Another common aspect between Ethernet and 802.11 is the use of the same 48-bit addressing space. This made these two technologies compatible at the DLL layer.

With CSMA, if a node wants to transmit, it has to listen to the communication medium for a predefined period. If the channel is sensed to be *idle* or free, meaning that there is no other transmissions occurring in the sensed channel, the node is permitted to transmit. In contrast, if the channel is sensed to be *busy*, the node assumes that another node in the network is transmitting and defers its transmission. This is generally known as the Listen Before Talk (LBT) mechanism. The original Ethernet, assuming a shared medium, used a variation called Carrier Sense Multiple Access with Collision Detection (CSMA/CD). After sensing the status of the channel and determining that the medium is *idle*, the nodes transmits and continue to listen to the medium. This is possible, since the Ethernet communication medium (cable) is bidirectional, thus the node is able to transmit and receive simultaneously. Consequently, while transmitting in an Ethernet medium, the node is able to receive its own transmission and hence any other initiated transmission resulting in a collision is detected by the transmitting nodes. When a collision is detected, the two colliding nodes countdown a random backoff period before trying to transmit again.

However, in a wireless communication medium it is not possible to detect a collision directly in the same way as in Ethernet. As a general rule, wireless devices operate in a half-duplex mode due to the fact that when a device's transmitter is transmitting, a part of the signal's energy leaks into the receiving path preventing the device from a simultaneous reception of another signal. Thus, the 802.11 defines another access scheme variation called Carrier Sense Multiple Access with Collision Avoidance (CSMA/CA). As its name says, the transmitter using CSMA/CA attempts to avoid the collision because detecting it is not feasible. Once the medium is sensed to be *idle*, the node waits another period chosen randomly during which it continues to sense the medium. At the end of this period, if the medium is still *idle*, the node begins its transmission. The aim of this random period is to reduce the probability of a collision to occur because another node potentially waiting to transmit would likely choose a different random period.

Furthermore, since the wireless medium is very different from the wired medium, other features are needed to assure successful communications using this simple contention-based access protocol. Firstly, the wireless medium is error prone and have a low latency. Hence, a data link level error correction and recovery mechanism is needed. Secondly, in a wireless context, the maximum range of a transmitted signal is determined by the ability of the receiver to decode the attenuated signal. Consequently, not all devices are able to hear the transmission of all other devices. MAC protocols need to take into account this fact to maintain a good performance. Thirdly, the distance between the transmitter and the receiver affects greatly the signal and determines the supported data rates. Additionally, the conditions of the wireless channel are variable in time due to environment changes or the mobility of the communicating nodes. Therefore, devices need a mechanism to adapt

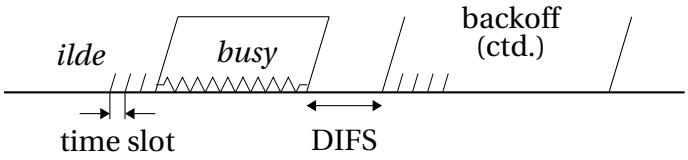

Figure 1.4 – Illustration of the distributed coordination function

their transmission data rate to optimize their achieved throughput.

1.3.1 Scanning and joining a BSS

The AP in an infrastructure BSS and the GO in a P2P network periodically broadcast beacon frames. The time interval between two beacon transmissions is predefined as the Target Beacon Transmission Time (TBTT). However, the medium may be sensed as busy at the exact time scheduled using the TBTT. For that reason, the beacons are transmitted as close as possible to the TBTT schedule. The beacon frame contains regulatory information such as the country code, the maximum allowable transmission power and the available channels. Additionally, a beacon carries information to manage the BSS and a list of its capabilities.

To become aware of the existence of an operating BSS, a STA scans the medium. The 802.11 standard defines two types of scanning, passive and active. The passive scanning is generally the most used type and consists in listening to the communication channel seeking for beacon transmissions. The STA may switch to other channels during passive scanning to look for these transmissions. Since it is just a receive only operation, the passive scanning is allowed in all regulatory domains. When the STA discovers the AP, it may ask for further information about the BSS using a probe request frame. The concerned AP responds with a probe response containing the information that was not present in the beacon frame. On the other hand, the active scanning is used when the regulatory domain allows its use and it consists on broadcasting a probe request on a specific channel to discover all the APs that are operating on that channel. A STA can switch to other channels and send probe requests to scan these channels for operating APs. Each AP that receives the probe request responds with a prob response that the capabilities of the BSS.

1.3.2 Channel access

The IEEE 802.11 standard defines a mandatory Distributed Coordination Function (DCF) and an optional Point Coordination Function (PCF). The DCF is based on the CSMA/CA mechanism. Every device willing to transmit chooses from a predefined Contention Window (CW) interval a random backoff timer. Before transmitting, the device senses the

energy in the wireless channel for a fixed duration, the DCF Inter-Frame Space (DIFS). After that, the device begins to countdown the backoff timer after every *idle* time slot. When the backoff timer reaches zero, the device starts its transmission. As shown in Figure 1.4, during the countdown, if the channel becomes *busy* the device freezes the timer, waits for the channel to return again *idle* for a DIFS before continuing the countdown.

1.3.2.1 Carrier sensing

To determine the state of the medium, DCF defines two distinct types of carrier sensing functions. The first function is the Physical Carrier Sensing (PCS) that is called the Clear Channel Assessment (CCA) procedure. Logically residing in the PHY, the PCS is composed of two related functions, the Energy Detect (ED) and the Carrier Sense (CS). According to the standard, the CCA reports a *busy* medium if at least one of these two functions detects the medium as *busy*.

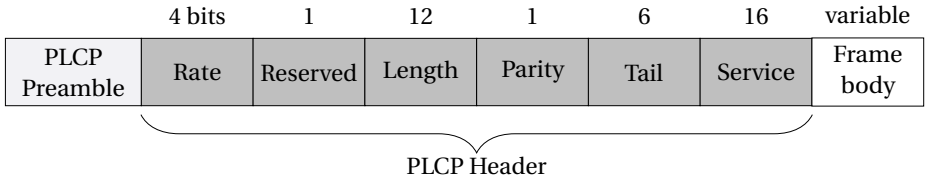

Figure 1.5 – PLCP frame format (IEEE Std 802.11-2012)

Using ED the device samples the energy in the medium and compares it to a predefined threshold. The ED threshold is often referred to as the PCS threshold or CCA sensitivity and is defined in the standard as the minimum modulation and coding rate sensitivity of $-82\ dBm$ for a 802.11 signal (see Section 20.3.21.5.2 is [5]). However, for a non-802.11 signal, the receiver reports the medium as busy if the sensed energy exceeds $-62\ dBm$ (20 dBm above the minimum modulation and coding rate sensitivity). The other function composing the CCA is the CS that consists in decoding the 802.11 Physical Layer Convergence Protocol (PLCP) header to determine for how long the medium remains *busy*. This technique is called preamble detect with frame length deferral. The PLCP header shown in Figure 1.5 contains among other fields the Length and Rate of the MPDU that are used by the CS mechanism to predict the duration of the frame.

On the other side, the Virtual Carrier Sensing (VCS) resides in the MAC and hence uses the Duration field of the MAC header shown in Figure 1.6 to determine how long the medium will stay *busy*. The operation of the VCS is based on the Network Allocation Vector (NAV) that is updated using the information extracted from the Duration field. The reference of the Duration field is the end of the last symbol of the related PPDU and it indicates the duration for which the transmitting device expects the medium to be busy. It is worth mentioning that the neighboring devices need to successfully decode the corresponding

frame to be able to update their NAVs. This function is meant to augment the PCS. A device assumes the medium as *idle* only when both PCS and VCS indicate an *idle* state.

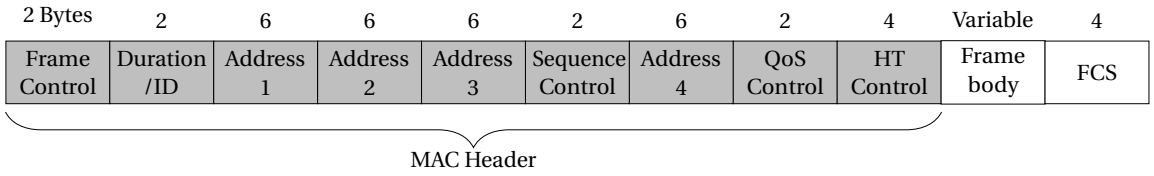

Figure 1.6 – MAC frame format (IEEE Std 802.11-2012)

1.3.2.2 Basic frame exchange

Once a device has gained access to the medium, it interleaves the transmitted frames with a Short Inter-Frame Space (SIFS). This is a minimum gap to keep between frames in a sequence so that another device will not gain access to the medium during that frame sequence. In practice any other device will sense the medium as *busy*, thus it defers for a DIFS which is longer than SIFS. To prevent the monopolization of the medium, some rules are defined to limit the duration of these sequences and the types of the exchanged frames.

Upon a successful reception of a data frame, the receiving device replies with a positive Acknowledgment (ACK) frame. Consequently, if the sender device does not receive the ACK frame, it assumes that the corresponding data frame was not received and tries to retransmit it. Obviously, broadcast and multicast data frames are not acknowledged this way. In an 802.11 network, only unicast frames benefit from the reliability provided by the ACK mechanism.

A basic frame exchange is depicted in Figure 1.7. In the illustrated example, STA_A is transmitting data to STA_B. After a contention period (i.e., a DIFS followed by a random backoff period during which the medium remains *idle*), STA_A gains access to the medium and transmits its first frame addressed to STA_B. The latter succeeds to correctly decode the frame and hence responds with an ACK. Upon the reception of the ACK frame, STA_A starts a new channel access attempt in order to send the next frame. As with the second frame

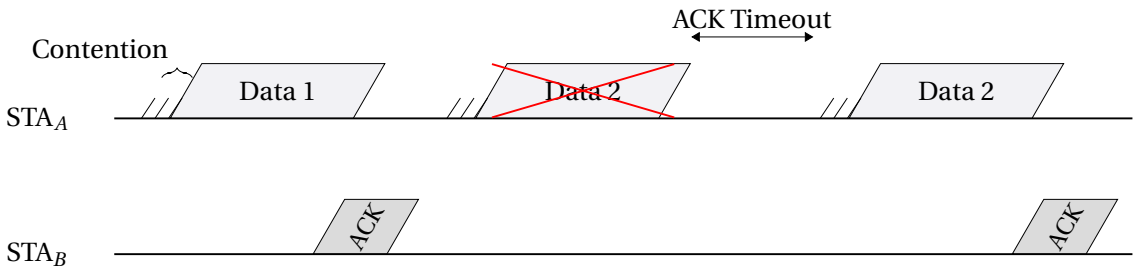

Figure 1.7 – Basic sequence of Data/ACK exchange

in Figure 1.7, STA_B fails to correctly decode the frame. As a result, STA_A will not receive an ACK and on that account it will start a new channel access to retransmit the same data frame.

Initially, the CW is set to its minimum value CW_{min}. In case of a retransmission, the CW is doubled until the CW_{max} is reached. After a successful MPDU transmission (i.e., the reception of an ACK), the CW is set again to its initial value CW_{min}. Actually, the device choses randomly a backoff in the range of [0,CW]. The number of retransmission of an MSDU is indeed limited. When the counter of retransmission of a particular MSDU exceeds a configured retry limit, the MSDU is discarded.

1.3.2.3 Request To Send (RTS)/Clear To Send (CTS) handshake

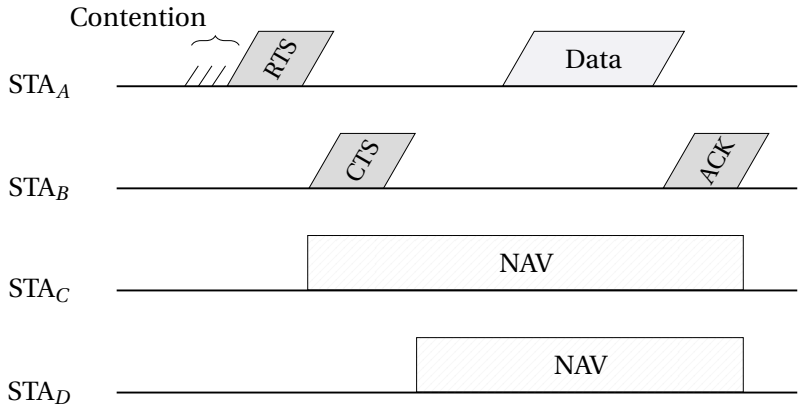

Figure 1.8 – Request To Send (RTS)/Request To Send (RTS) handshaking and Virtual Carrier Sensing (VCS)

Additionally to the previously described basic access method, the 802.11 standard defines an optional four-way handshake. This access method is called Request To Send (RTS)/Clear To Send (CTS) and consists of exchanging two control frames prior to any data frame exchange. After the contention period, the device that gains the access to the medium sends an RTS. After decoding correctly this frame, the destination device waits for SIFS and responds with a CTS. Finally, the transmitter device begins data transmission after a SIFS starting from the reception of the CTS. These control frames include the duration of the data exchange and hence all the devices that are able to successfully decode them update their NAV accordingly. The described access mechanism is illustrated in Figure 1.8 where four STAs are depicted as follows. STA_B and STA_C are in the range of STA_A. STA_D is out of the range of STA_A but in the range of STA_B. A STA is in the range of another STA when they hear the transmissions of each other and defer their own transmissions accordingly. It is worth mentioning that even if the CCA senses the channel as *idle*, the device can't transmit during the time period indexed by the NAV (i.e., the VCS mechanism). The aim of the optional RTS/CTS handshaking is to cope with the hidden node problem where an

interfering co-channel transmitter prevents another communication from being successful received. RTS/CTS protects this communication by extending the region protected by VCS to the receiver's surroundings. This problem and the limitation of RTS/CTS are discussed later in this chapter.

1.4 Physical Layer (PHY) basics and its evolution

1.4.1 Traditional 802.11 frequency bands

The original IEEE 802.11 standard [8] defined three different PHYs. An infrared-based PHY, a 2.4 GHz Frequency Hopping Spread Spectrum (FHSS), and a 2.4 GHz Direct Sequence Spread Spectrum (DSSS). Later in 1999, two new amendments to the original standard defined an enhanced data rate PHY based on the DSSS in the 2.4 GHz band using a Complimentary Code Keying (CCK) (i.e., the 802.11b [9]) and another new PHY operating in the 5 GHz band (i.e., the 802.11a [10]). The former amendment was able of increasing the communication data rate to 11 $Mbps$. Consequently, the IEEE 802.11b-compliant devices achieved important market success thanks to the attractive data rates that they offered. Actually, the markets for infrared and FHSS-based 802.11 PHY have failed to materialize.

The 802.11a amendment introduced the Orthogonal Frequency Division Multiplexing (OFDM) to the 802.11 standard. Operating at the 5 GHz band, this OFDM-based PHY offered data rates of up to 54 $Mbps$. However, the adoption of this new PHY in new products has been very slow. An important aspect that slowed the adoption of 802.11a is the backward compatibility constraint. To benefit from the high data rates offered by the 802.11a and retain at the same time the compatibility with the huge number of 802.11b devices already operating at the 2.4 GHz band, the manufacturers needed to implement two radios on the same device. Besides that, especially in the United States, the non-military operation in the 5 GHz band was possible only on some selected channels.

After modifying the rules governing the 2.4 GHz band to permit the use of OFDM, the FCC opened the door to the development of an 802.11 OFDM-based PHY operating at 2.4 GHz. Consequently, the 802.11g amendment [11], ratified in 2003, extended possible data rates to up to 54 $Mbps$. The new specification knew a huge market and has been quickly adopted all over the world. Obviously, the new 802.11g devices are backward compatible with the 802.11b devices what boosted their expansion.

In Table 1.1, the main features of each of six different PHYs for 802.11 are listed. The depicted data rates are the maximum theoretical PHY data rates using a single spatial stream. The evolution of the 802.11 standard continued with the 802.11n [12] that in-

Table 1.1 – The different 802.11 PHYs in a glance (2.4 and 5 GHz bands)

Aspect \ PHY	802.11	802.11a	802.11b	802.11g	802.11n (HT)	802.11ac (VHT)
Year	1997	1999	1999	2003	2009	2013
Modulation	DSSS	OFDM	DSSS/CCK	OFDM	OFDM	OFDM
Frequency (GHz)	2.4	5	2.4	2.4	2.4, 5	5
Bandwidth (MHz)	25	20	25	25	20, 40	20, 40, 80, 160
Max PHY data rate ($Mbps$)	2	54	11	54	150	866.7

creased substantially the PHY data rates using Multiple-Input Multiple-Output (MIMO) techniques and 40 MHz channels bandwidth. Afterwards, 802.11ac [13] improved the enhancements introduced by 802.11n by providing the operation over wider bandwidth channels (80 and 160 MHz), new 256 Quadrature Amplitude Modulation (QAM)-based Modulation and Coding Scheme (MCS)s, and Multi-User MIMO (MU-MIMO). While the 802.11n amendment is referred to as High Throughput (HT), its successor, the 802.11ac, is referred to as Very High Throughput (VHT).

1.4.2 WLAN operation in unconventional frequency bands

Since its first appearance, the operation of 802.11 WLANs was limited to the 2.4 and 5 GHz frequency bands. However, due to its success, many other applications are envisioned for this technology. To address these needs, the 802.11 WG has launched multiple Task Group (TG)s to extend the operation over the unlicensed 60 GHz band (i.e., the millimeter-wave or "mmWave") on one hand and over the frequency bands below 1 GHz on another hand. The 802.11ad amendment [14] defines the "mmWave" operation of WLAN that is known as "WiGig" and targets short range high data rates communications. For sub 1 GHz operation, 802.11af [15] specifies the opportunistic WLANs operation over TV white space (e.g., 470-790 MHz in Europe) for while 802.11ah [16] defines the operation at unlicensed bands below 1 GHz (e.g., 863-868 MHz in Europe). The PHY layers of 802.11ad and 802.11ah is designed based on that of 802.11ac (i.e., the 802.11ah PHY is a 10 times down-clocked version of the 802.11ac PHY). The purpose behind these two amendments is to extend the communication range to address the increase needs for long-range, large-scale, low-rate and low-power sensor networks for various applications in the context of Internet of Everything (IoE) (i.e., smart metering, smart grid, etc.). In this thesis, we study the 802.11 operating in traditional 2.4 and 5 GHz frequency bands. However, since CSMA/CA is also a part of the amendments operating at sub 1 GHz and 60 GHz bands,

our proposed solutions could be applied where there is a need for high spatial reuse and dense deployments.

1.4.3 Orthogonal Frequency Division Multiplexing (OFDM)

In high data rate communication systems like WLAN, using wide bandwidth is indispensable. For a wideband communication channel, when the bandwidth of the transmitted signal exceeds the value for which the channel is still considered flat (i.e., coherence bandwidth), the channel is termed as frequency-selective [17]. In multipath propagation environments, the delay spread of the received signal is high and hence the channel is indeed frequency-selective. In a frequency selective-channel, the Single Carrier Modulation (SCM) systems are vulnerable to Inter-Symbol Interference (ISI) caused by multipath propagation and narrow-band co-channel interference. The compensation of the linear distortion caused by the frequency selectivity is done by equalization. The complexity of the equalization procedure implementation increases importantly with the number of data symbol intervals.

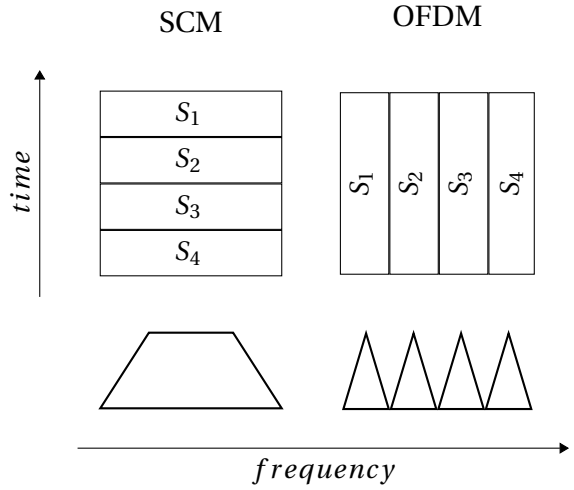

Figure 1.9 – Comparison between Single Carrier Modulation (SCM) and Orthogonal Frequency Division Multiplexing (OFDM)

An alternative to the SCM is the Multi-Carrier Modulation (MCM), where the data stream is divided into multiple bit streams, each of which having lower bit rate than the original stream. The resulting substreams are used to modulate several frequency subcarriers. Accordingly, the substreams are transmitted in parallel and each subcarrier is separately equalized by a simple gain and phase factor. The OFDM is a special form of MCM that was patented in 1970 in the United States. In OFDM the separation between the subcarriers (Δf) is chosen to be equal to the inverse to the symbol period (T). In that way, the subcarriers are orthogonal since the main lobe of a subcarrier coincide with the nulls of the adjacent subcarriers. Figure 1.9 illustrates a simple comparison between SCM and OFDM.

Furthermore, a Guard Interval (GI) is added to cope with the performance impairments caused by the ISI between adjacent OFDM symbols. For instance, an 802.11a OFDM symbol having a total time of 4 μs disposes of 0.8 μs for the GI. This GI is in the most of OFDM systems a copy of the last part of the OFDM symbol. The generation of the multiple subcarriers is done simply by performing an Inverse Fast Fourier Transform (IFFT) processing at the transmitter on blocks of M data symbols. Accordingly, an OFDM baseband waveform can be expressed as follows:

$$s(t) = \frac{1}{N}\sum_{k} X_k exp(j2\pi k\Delta f t) \qquad 0 \leq t < T \tag{1.1}$$

Where N is the number of IFFT samples, Δf is frequency spacing, T is IFFT symbol period with $\Delta f = \frac{1}{T}$, and X_k is the set of $IFFT$ coefficients.

At the receiver, the extraction of the subcarriers is done by performing the Fast Fourier Fransform (FFT) operation on blocks of M received samples as shown in Equation (1.2). $s(n)$ is the received waveform signal after being sampled.

$$X_k = \sum_{n} s(n) exp(-j2\pi k\frac{n}{N}) \tag{1.2}$$

The reader is invited to refer to [18] and [19] for further detailed information about OFDM and its implementation in wireless networks.

1.4.4 Multiple-Input Multiple-Output (MIMO)

To improve the performance of the PHY layer, 802.11n introduced MIMO systems. In MIMO multiple antennas are used both at the transmitter and the receiver. In such a way, the receiver can benefit from spatial diversity, and the transmitter can spatially multiplex different streams of data. With spatial diversity, the receiver has two different copies of the same signal coming from different paths. Hence, the decoding can largely benefit from this diversity. With spatial division multiplexing, the data rate is multiplied by the number of spatial streams since everyone corresponds to an independent data stream [20]. 802.11ac expands on MIMO defined in 802.11n to enable MU-MIMO. This technique allows a simultaneous transmission to multiple devices using different spatial streams and hence improves the network capacity.

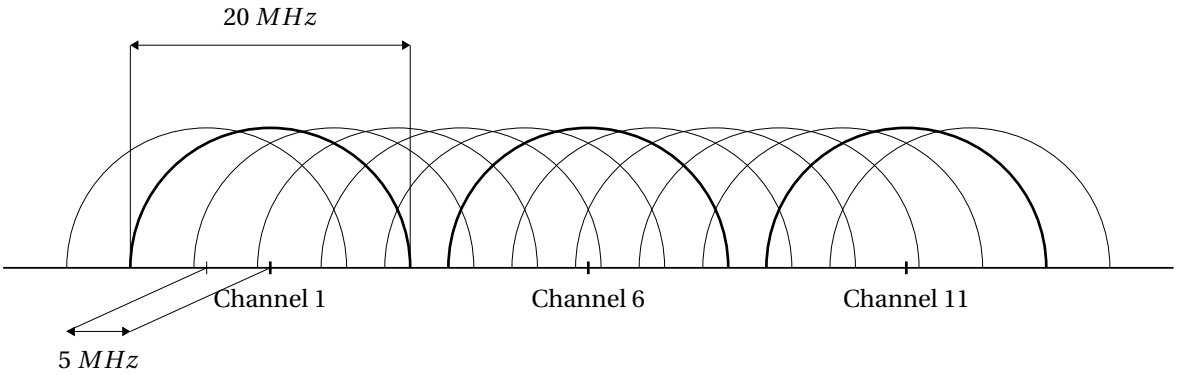

Figure 1.10 – Frequency channel allocation in the 2.4 GHz spectrum

1.4.5 Frequency channels

The available ISM spectrum is divided into operating channels of 20 MHz width. The separation between the center frequencies of two adjacent channels is 5 MHz. As shown in Figure 1.10, only three 20 MHz channels are orthogonal in the 2.4 GHz band. Starting from the first frequency of the specific band (f_{start}), the center frequencies of the operating channels are given as follows.

$$f_c(MHz) = f_{start}(MHz) + 5 \times ch_n \tag{1.3}$$

Where ch_n is the channel number ranging from 0 to 200 for the 5 GHz band and from 1 to 13 for the 2.4 GHz band. The 20 MHz channel allocation in Europe is given in Table 1.2. The operating class is an index into a set of predefined values for radio operation in a regulatory domain.

Table 1.2 – The 20 MHz channel allocation in Europe

Band (GHz)	Operating class	ch_n	f_c (MHz)	Tx power limit (mW)
2.4-2.483	4	$1,2,...,13$	$2412,2417,...,2472$	100
5.15-5.25	1	$36,40,44,48$	$5180,5200,5220,5240$	200
5.25-5.35	2	$52,56,60,64$	$5260,5280,5300,5320$	200
5.47-5.725	3	$100,104,...,140$	$5500,5520,...,5700$	1000

An important feature introduced by 802.11n is the support of channel bonding with an optional 40 MHz operation. This is done by using two adjacent 20 MHz channels and allows direct doubling of the PHY data rate achieved by a single 20 MHz channel. With this channel bandwidth expansion, 802.11n makes use of the spaces reserved between non-overlapping channels to achieve increased spectral efficiency in the used bandwidth. Later, 802.11ac defined the operation of wider channels. By bonding two 40 MHz channels, the operation over an 80 MHz channel is possible. Again two 80 MHz channels are used

to form a 160 MHz channel width. A new feature in 802.11ac is the possibility of using non-contiguous channels to form wider channels. Consequently the 160 MHz channel is termed as 80+80 MHz.

According to the 5 GHz band channel allocation in Europe shown in Table 1.2, 19 non-overlapping 20 MHz channels are available which is pretty enough for high density environments. However, because of the increasing demand for higher data rates, wider channels are needed. In Europe, only four 80 MHz bonded channels are possible or just two 160 MHz channels width. Having said that, we notice that the number of non-overlapping channels stays always a limiting factor in future dense deployments.

1.4.6 Modulation and Coding Scheme (MCS)

For the 802.11n HT PHY, a list of the 20 MHz MCS parameters and data rates using a single spatial stream is shown in Table 1.3. These values are obtained for a guard interval of 800 ns. Since OFDM is based on the orthogonality of the different subcarriers, it is sensitive to frequency shifts (i.e., leading to ISI) caused by user mobility and multipath channels, etc. For that reason, not all the available subcarriers are populated with data. Pilot subcarriers are needed to maintain the orthogonality through phase tracking [19].

Table 1.3 – The different MCS parameters for a 20 MHz channel with a single spatial stream (IEEE std 802.11-2012)

MCS index	Modulation	R	N_{BPSCS}	N_{CBPS}	N_{DBPS}	Data rate ($Mbps$)
0	BPSK	1/2	1	52	26	6.5
1	QPSK	1/2	2	104	52	13.0
2	QPSK	3/4	2	104	78	19.5
3	16-QAM	1/2	4	208	104	26.0
4	16-QAM	3/4	4	208	156	39.0
5	64-QAM	2/3	6	312	208	52.0
6	64-QAM	3/4	6	312	234	58.5
7	64-QAM	5/6	6	312	260	65

Each 20 MHz channel, whether it's 802.11a/g/n/ac, is composed of 64 subcarriers spaced by $\Delta f = 312.5\ KHz$ apart (64-point FFT sampling). 802.11a/g use 48 subcarriers for data, 4 for pilot, and 12 as null subcarriers. 802.11n/ac use 52 subcarriers for data, 4 for pilot, and 8 as null.

The data rate is the result of dividing N_{DBPS} (i.e., the number of data bits per OFDM symbol) by the total symbol duration (i.e., 4 μs). R is code rate, N_{BPSCS} is the number of coded bits per single carrier for each spatial stream, and N_{CBPS} is the number of coded bits per OFDM symbol. Later, the 802.11ac amendment increased the modulation size to

256-QAM and thus the two lines of Table 1.4 could be added to Table 1.3 to form the MCSs supported by 802.11ac using a single spatial stream.

Table 1.4 – The MCS parameters introduced by the IEEE std 802.11ac-2013 for a 20 MHz channel with a single spatial stream

MCS index	Modulation	R	N_{BPSCS}	N_{CBPS}	N_{DBPS}	Data rate ($Mbps$)
8	256-QAM	3/4	8	416	312	78
9	256-QAM	5/6	8	416	n/a	n/a

1.5 MAC performance enhancements

As described earlier in this chapter and shown in Table 1.1, each new 802.11 PHY offered around five-fold data rate increase compared to the previous one. Even with the higher data rates offered by the enhanced PHYs, the real world throughput performance cannot be improved without enhancing the MAC layer protocols. In fact, without enhancing these protocols, the fixed overhead in the MAC prevents the upper layers from experiencing the gain in throughput supported by the PHY. It was clear in the standardization process that MAC had to be enhanced to enable the 802.11 end user to benefit from the improved PHY. The key MAC throughput enhancements were introduced by 802.11n. The most important among them are the frame aggregation and the enhanced block acknowledgment.

However, the enhancements developed by 802.11n are based on prior features introduced by 802.11e amendment [21]. The main contribution of the 802.11e is the extension of DCF that permitted 802.11 to support the Quality of Service (QoS). Additionally, 802.11e defined important features like transmit opportunity and block acknowledgment that permitted higher resource utilization efficiency using data bursting.

1.5.1 Enhanced Distributed Channel Access (EDCA)

In 2005, the 802.11e amendment extended the basic contention-based access scheme (i.e., DCF) to implement different transmission priorities in order to support QoS. The newly introduced mechanism, i.e., the Enhanced Distributed Channel Access (EDCA), defines four Access Category (AC)s. Each one of the ACs is characterized by a set of access parameters values. These values are defined to prioritize the channel access for one AC over another. When an MSDU is tagged with one of the user priorities defined by the MAC bridging protocol (802.1D), then this MSDU belongs to the Traffic Category (TC) with that user priority. Table 1.5 shows the different ACs and their mapping with the 802.1D user priorities.

Accordingly, the traffic load is sorted into four queues. Each queue represents one of the

Table 1.5 – The different Access Categories (AC) of EDCA and their mapping to the 802.1D user priorities

Priority	AC	Description	802.1D user priority
Lowest	AC_BK	Background	1
	AC_BE	Best effort	0
	AC_VI	Video	4
Highest	AC_VO	Audio	6

ACs as shown in Figure 1.11. To access the medium, an EDCA access function instance operates independently on each queue. The EDCA access function is similar to the previously described DCF, however the contending device deffer for an Arbitration Inter-Frame Space (AIFS) instead of DIFS. In fact, each AC has its own AIFS value referenced as AIFS[AC] and the CW of an AC is referenced as CW[AC]. In case of an internal collision between two or more EDCA instances, the highest priority AC gains the access and the others behave as an external collision occurred (i.e., doubling the CW[AC] and reattempting the access).

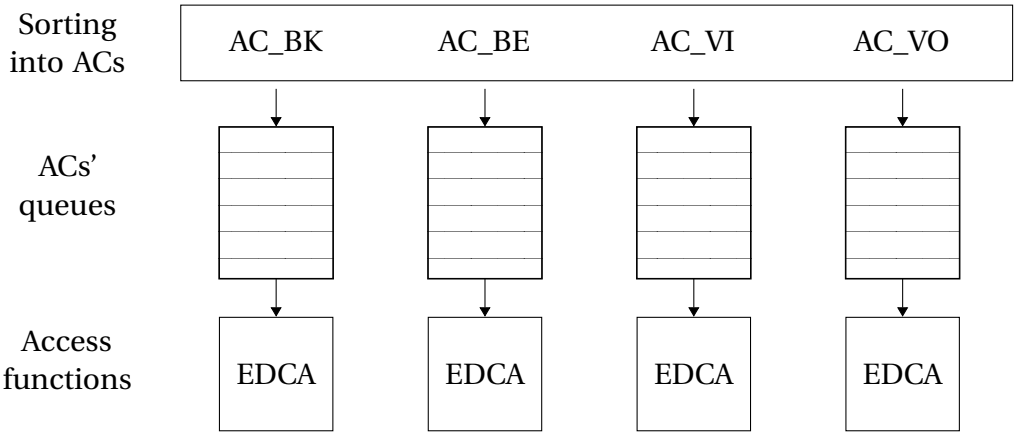

Figure 1.11 – A reference implementation of the EDCA (IEEE Std 802.11-2012)

1.5.1.1 Transmit Opportunity

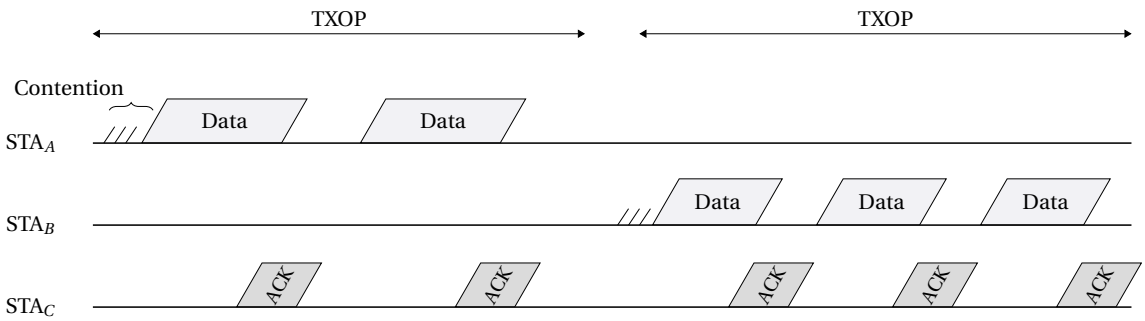

Figure 1.12 – TXOP sequences with two different PHYs

Another important feature introduced by the 802.11e is the Transmit Opportunity (TXOP) than defines an interval of time during which a device transmits data belonging to the same TC. Through the channel access procedure, a device obtains the TXOP for a particular TC and hence transmits data, control, and management frames and receives responses as long as the frame sequence duration does not exceed the TXOP limit for the related TC. The aim of the TXOP is to share the resources fairly between different contending devices. As shown in Figure 1.12, using TXOP does not mean that two different devices (with different PHY data rates) will achieve the same throughput. However, these devices will be using an equal amount of airtime.

1.5.1.2 Block Acknowledgment

The QoS Data frame is introduced by 802.11e and includes a QoS Control Field that carries necessary information to manage QoS. Subsequently, the ACK policy subfield determines how the frame is acknowledged by the receiver by carrying one of the following values: Normal ACK, No ACK, No Explicit ACK, or Block ACK. Under Block ACK policy, upon receiving correctly a QoS Data frame, the device has to just record its reception. Instead of responding with an ACK individually for every received frame, with Block ACK, a sequence of frames are acknowledged using a single Block Acknowledgment (BA) frame. In contrast with the Normal ACK policy, the Block ACK is session oriented. A device must establish a Block ACK session with its peer for each TC.

1.5.2 Aggregation

Due to the fixed overhead in the preamble and Inter-Frame Space (IFS), when the physical data rate increases, the MAC efficiency drops quickly. Since the preamble is always transmitted at lower rate, the airtime percentage occupied by the preamble increases as the duration of data payload gets shorter due to higher data rate. Moreover, to support multiple spatial streams, preambles need to be longer introducing additional fixed overhead. For a set of data rates, the relative overhead caused by the preamble is shown in Figure 1.13. These values are calculated for a typical data frame of 1500 $Bytes$.

Basing on the Block ACK introduced by the 802.11e, 802.11n defined a burst data mode where data frames are sent back-to-back separated by a Reduced Inter-Frame Space (RIFS) instead of SIFS that was needed to switch from reception to transmission. Taking things further, the IFS could be totally eliminated altogether with the preambles of the burst frames. Accordingly, all these data frames are concatenated in a single data transmission in the form of an aggregated frame. This is the key performance enhancement of the 802.11n MAC layer.

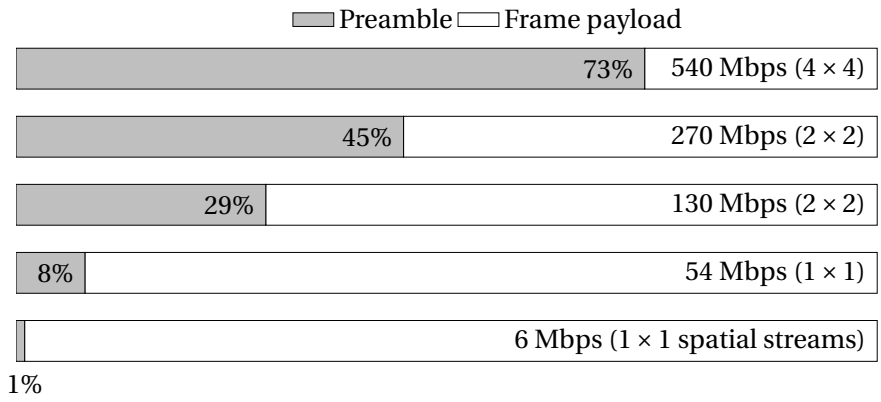

Figure 1.13 – Preamble overhead at different PHY data rates (fixed frame size)

As shown in Figure 1.14, the frame aggregation as defined by 802.11n can be applied before the MAC protocol layer or/and after this layer. Referencing to Figure 1.2, at the top of the MAC resides the MSDU aggregation (A-MSDU) and at the bottom resides the MPDU aggregation (A-MPDU). On account of implementation considerations, the maximum A-MSDU size is defined as 7935 Bytes for HT and 11454 Bytes for VHT.

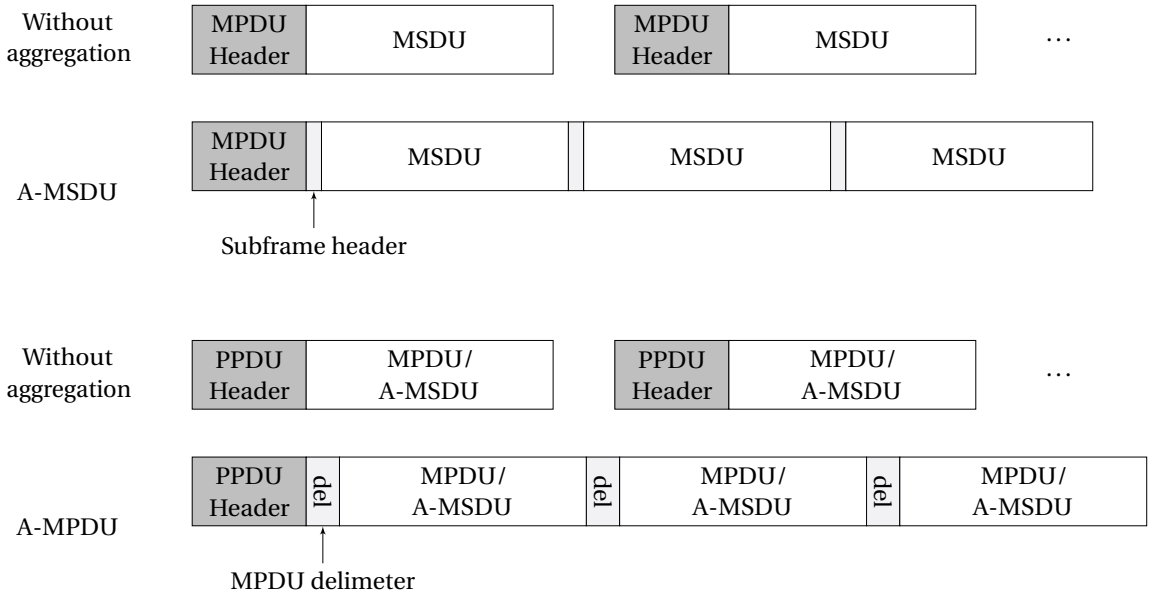

Figure 1.14 – The different types of frame aggregation

1.5.3 Enhanced Block Acknowledgment

Since the Block ACK was defined by the 802.11e before the introduction of frame aggregation, this mechanism has to evolve to support operation with the new aggregation features. However, since the aggregated frame is seen as a single PHY transmission, it is obvious that an ACK policy similar to the original Normal ACK is suitable for this situation. For that reason, when the aggregated QoS data frames are received with an ACK policy set to Normal

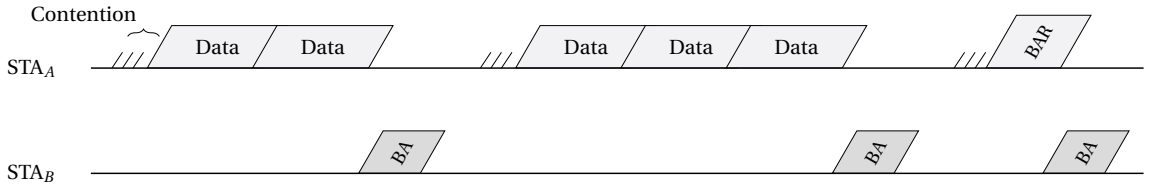

Figure 1.15 – TXOP sequences with frame aggregation and block acknowledgment (Normal ACK policy)

ACK, the receiver responds with a BA. Moreover, the 802.11n introduced compressed BA with an 8 Bytes bitmap (the original BA has 128 Bytes bitmap) what reduced the memory and processing resources at the receiver and the airtime overhead.

With the introduction of frame aggregation and enhancing the Block ACK mechanism, a typical data exchange is shown in Figure 1.15. The final Block Acknowledgment Request (BAR) and BA response exchange is performed when a lot of frame errors cause the discard of an MPDU after exceeding the retransmission limit. In practice, a BAR is needed to flush the reorder buffer at the receiver.

1.5.4 Summary of the major 802.11 enhanced features

An overview of the most important features added to the PHY and MAC layers in 802.11n and 802.11ac is illustrated in Figure 1.16. As detailed earlier in this Chapter, the maximum theoretical data rate is roughly a product of three factors: the channel bandwidth, the constellation density, and the number of spatial streams. Compared to the PHY specifications of 802.11n, 802.11ac has pushed harder on the boundaries on each of these factors. Given the power of the aggregation mechanisms introduced by 802.11n, 802.11ac actually did not add much to the MAC features. Indeed, extending the protection mechanisms (i.e., RTS/CTS) was needed to accommodate the wider channels. Furthermore, 802.11ac has extended the 802.11n channel access mechanism: virtual carrier sense and backoff occur on a single 20 MHz primary channel and CCA is then used for the remaining 20 MHz sub-channels immediately before transmitting on them.

	802.11n	802.11ac
MAC	Frame aggregation A-MSDU: 7935 Bytes max. A-MPDU: 65535 Bytes max.	Frame aggregation A-MSDU: 11434 Bytes max. A-MPDU: 1048575 Bytes max.
	Enhanced Block ACK	Always Block ACK
	Protection mechanisms for backward compatibility	Protection and coexistence updated for wider bands
PHY	2.4 and 5 GHz bands	5 GHz band only
	20, 40 MHz channels	20, 40, 80, 160 MHz channels
	1 to 4 spatial streams	1 to 8 spatial streams
	SU MIMO	SU and Downlink MU-MIMO
	16, 64 QAM	16, 64, 256 QAM

Figure 1.16 – Summary of the most important 802.11n and 802.11ac PHY and MAC enhancements

1.6 Challenges of the current standard

After almost two decades of evolution, the 802.11 standard is enough mature to assure trustworthy wireless broadband connectivity. Low cost, operation on unlicensed spectrum, ease of deployment and maintenance, and legacy interoperability have made Wi-Fi one of the greatest success stories of communication technologies in the last century. Due to this success, a tremendous number of electric devices are equipped today with at least one Wi-Fi interface. These devices vary from the traditional laptops, tablets, and smartphones to more unconventional Wi-Fi enabled devices like refrigerators, coffee machines and others.

The importance of Wi-Fi is increasing as a Radio Access Network (RAN) technology promising seamless wireless access with high data rates. Wi-Fi is seen today as the best suitable technology for offloading overloaded cellular networks. In order to respond to the increasing demand in coverage and capacity, more Wi-Fi APs are deployed to serve a growing number of STAs. This trend that is likely to continue is leading to high density deployment environments where satisfying capacity and coverage requirements at the same time is challenging. These dense Wi-Fi deployment scenarios include: dense apartment buildings, stadiums, dense city squares and streets, large venues and exhibition halls, shopping malls, airports and train stations, etc.

For mobile operators, Wi-Fi, as it is today, is likely unable to provide a high Quality of Experience (QoE) predictable in all the previous deployment scenarios. Several issues in the PHY and MAC layers are to be addressed before considering Wi-Fi as a serious carrier-grade RAN technology for these challenging deployments. In the following, we describe the identified problems before giving the general improvement directions. For reasons of clarity, these problems are divided into two categories. The first deals with issues related to a high density of STAs within a single BSS. The second includes the issues linked to a high density of BSSs and associated STAs.

1.6.1 High density of STAs per BSS

1.6.1.1 Frame collisions

In dense STAs scenarios, when the network is heavily loaded, a large number of devices may be waiting for the medium to go *idle* having accumulated packets to send in their queues while the medium was *busy*. Since the number of backoff intervals is limited, two or more devices may chose accidentally the same backoff interval. This results in a synchronous interference of the simultaneous transmissions inside the BSS. The probability for such collisions to occur increases with the number of contending STAs. In practice, the collision

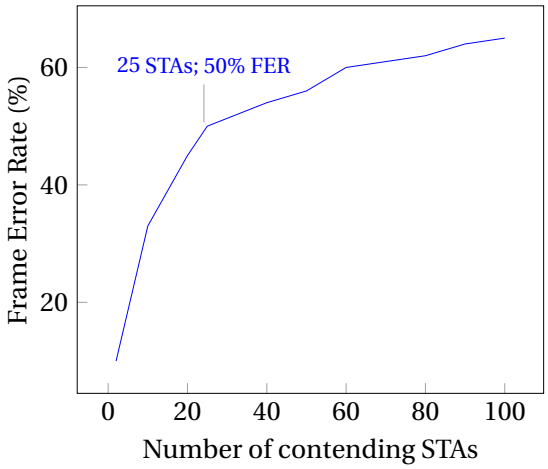

Figure 1.17 – Average STA frame error rate due to collisions in terms of STAs number within a single BSS

avoidance mechanism of the CSMA/CA arrives to its limits when the number of STAs exceeds a certain limit. Figure 1.17 emphasizes this fact by showing the Frame Error Rate (FER) percentage due only to collisions within a single BSS with a growing number of contending STAs.

1.6.1.2 Rate control mechanisms and collisions

The problem of synchronous interference is aggravated using of imperfect rate control mechanisms. The purpose of rate control is to use more robust MCS when the channel conditions become bad (i.e., insufficient Signal to Interference and Noise Ratio (SINR)) and rasing the MCS again for higher data rates when the channel conditions are better. As will be discussed in details later in Chapter 5, the currently adopted rate control mechanisms are far from being perfect especially when the number of contending STAs increases. These mechanism are designed to lower the used MCS when the FER increases and vice versa. However, most of the implemented algorithms does not raise back the MCS as quick as lowering it. Once the MCS is lowered, it is difficult to raise it back in a short term.

Since the detection of a collision is not possible as previously explained, every collision will trigger the rate control algorithm that will decrease the rate even if the channels conditions are not bad. In other words, most of the rate control mechanisms are not able to differentiate between collisions and bit errors caused by low SINR values. Obviously, using lower MCS to face collisions won't help. In contrast, using lower MCSs for future transmissions will increase the transmission duration and hence the probability to have other collisions.

1.6.1.3 Airtime unfairness between STAs

The DCF is conceived to ensure fair channel resources sharing among multiple STAs within the same contention domain (typically the BSS). Ultimately, DCF guarantees equal long term throughput for every STA. However, due to many factors, this fairness is threatened and unfairness situations are likely to happen. The most important factors affecting the channel airtime fairness are:

- **Different PHYs:** the new IEEE 802.11 generations of the standard are always designed to be backward compatible with older generations. This interoperability prevents the devices implementing the latest generation from benefiting fully from their new features. In a BSS where all the devices including the AP are 802.11n capable, a single 802.11b device joining the network is enough to disrupt the performance of the entire BSS. Since the 802.11b device can't use HT data rates, it occupies most of the airtime preventing other 802.11n capable devices from accessing the channel. As a result, the throughput of the entire network goes down to the maximum throughput provided by the slowest device's PHY.
- **Different channel conditions in a large BSS:** any other cause leading to different MCSs (i.e., data rates) used by the devices of the same BSS leads to the same consequences of unfairness. It is common in WLAN that an associated device experiences a bad radio link to the AP because of the far distance separating them or due to an obstacle. To overcome the situation, the device uses lower MCS that tolerates the bad channel conditions. The lower data rate means longer transmission duration and hence less airtime for other devices. Authors in [22] reveal this issue and state that the CSMA/CA technique is naturally causing this problem since it guarantees an equal channel access probability to all hosts.
- **Uplink versus downlink:** another issue regarding the airtime unfairness is related to the direction of the transmission. As a general rule, the 802.11 DCF does not guarantee fairness between uplink and downlink transmission flows occurring in the same BSS. In a BSS having N_{STA} associated STAs, the channel access probability of the AP is similar to that of a non-AP STA equal to $\frac{1}{1+N_{STA}}$. Consequently, when all the devices have data to send, uplink flows have more chances than downlink flows.

1.6.1.4 Hidden node problem

The hidden node problem is a well-known issue related to CSMA/CA. This access scheme relies mainly on the capability of a transmitter to sense the potential transmissions of all the neighboring devices. However, in many situations a device will not be able to sense other devices and/or vice versa. A typical case-scenario is when two STAs are separated

with an opaque wall as shown in Figure 1.18. Although STA_A and STA_B are reaching their AP without any problem (i.e., no frame losses due to channel errors), they are not able to sense each other because of the signal attenuation due to the wall penetration loss. In another case-scenario, the STAs are far away from each other located at the apposite sides of the AP and separated by several walls. This is the case in a residence having one AP.

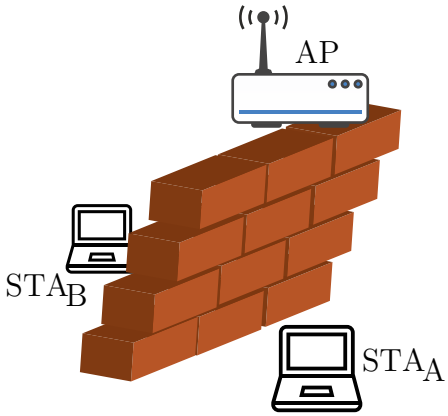

Figure 1.18 – Hidden node problem typical case-scenario

When a device is not sensed by others, its transmissions are simply ignored. In other words, CCA on other devices records the medium as *idle* despite the transmissions of the hidden node. So far the synchronous backoff countdown is the only cause of collisions. Nevertheless, on account of the hidden node case-scenarios, the collision may occur asynchronously for a different reason. In Figure 1.18, while STA_A is transmitting, STA_B finishes its backoff countdown and starts its own transmission that distorts that of STA_B. In a situation where all the STAs are hidden from each other, the performance of CSMA/CA is identical to ALOHA [1].

1.6.1.5 The limitations of the Request To Send (RTS)/Clear To Send (CTS)

As stated earlier in this chapter, the RTS/CTS handshake was introduced to solve the hidden node problem. Actually, this handshaking accentuates the VCS mechanism where a device sets its NAV using the duration field of decoded data frames that are destined to another device. Generally, data frames are sent using high MCSs that tolerate less the noise and interference. Using more robust frames would increase the chances of successfully setting the NAV of all the neighboring devices and hence preventing any potential hidden node. Since the RTS is sent by the initiator and the CTS by the destination device, all the devices around the initiator and around the destination set their NAV according to the upcoming transmission duration. Under the hypothesis of perfect channel conditions, only RTS frames are possibly subject to synchronous collisions. In that sense, RTS/CTS protects the data frame exchange that follows it.

In order to be decoded by all the devices in the BSS including any potential legacy device

(i.e., 802.11b), the RTS and CTS frames are sent with a very low data rate (typically 1 $Mbps$). Indeed, the use of RTS/CTS consumes airtime and introduces more overhead to the network. Authors in [23] state that in some cases RTS/CTS performs worse than the basic access scheme of the CSMA/CA. Moreover, it is proven in [24] that RTS/CTS is not able to solve all interference problems. Furthermore, sent at lower MCS, the RTS and CTS frames covers more devices in the neighborhood resulting in the creation of the exposed node that is discussed in details in the next paragraph. On that account, vendors and network administrators are very careful about using RTS/CTS in their networks and many chose to turn it off [25]. However, when legacy devices are present in the network (e.g., 802.11g STA in an 802.11n BSS), RTS/CTS cannot be avoided as a protection mechanism for backward compatibility.

1.6.2 High density of BSSs

The other dimension of high density WLAN environment issues is the high density of deployed APs. This can be coupled with high density of associated STAs (e.g., stadium, large venue, airport, etc.) or a moderate density of STAs (e.g., residential building, street, etc.). In both cases, the high density case-scenarios are classified into two groups depending on the deployment manner. In the first group comes the majority of WLAN deployments that are dominating since the introduction of Wi-Fi. In these deployments, the APs are installed individually without any planning (home networks). These APs are commonly managed by different entities and obviously does not coordinate their operations. As a result the WLAN environment belonging to the first group is chaotic and can't rely on any explicit coordination between the different BSSs. In contrast, a deployment belonging to the second group is administrated by a single entity (i.e., service provider or operator). Normally, the deployed APs here are managed in a centralized way by a controller device. As a general rule, the networks of the second group are carefully planned, cleverly deployed, and continually maintained and monitored. However, many real-world scenarios are combinations of these two groups where, for instance, multiple standalone self-managed BSSs (installed in home, shops, etc.) overlap with controlled networks managed by a common service provider.

1.6.2.1 Overlapping BSS (OBSS)

As a whole, the principal limiting factor for increasing the density of deployed APs is interference. When the distance between neighboring co-channel BSSs fall behind a minimum value, these BSSs overlap (transmissions occurring in one BSS are sensed in the neighboring overlapping BSSs). As a consequence, the transmissions of some STAs in one BSS affect some STAs in another BSS. This is commonly referred to as the Overlapping

BSS (OBSS) problem. As explained earlier in this chapter, the number of available frequency channels is limited and the fact that the access to these channels is not licensed attracted many other technologies that are sharing today the spectrum with WLANs. Since the demand on capacity is escalating continuously, deploying more APs is necessary since the capacity of one AP is limited as shown previously. In these circumstances, the OBSS problem is likely to be more produced.

All the issues described in a single BSS with high density of STAs can be extended to cover STAs belonging to different OBSSs. For instance, a legacy STA belonging to an OBSS affects the airtime fairness in the neighboring OBSS. Furthermore, when talking about OBSS problems, a STA in one BSS may be hidden to the STAs belonging of an overlapping BSS. Obviously, the reason is that two or more OBSSs share the same channel and hence their devices contend to gain access as if they are belonging to a single BSS.

1.6.2.2 Capture effect

An important phenomenon that we have to take into account when considering concurrent co-channel transmissions among different BSSs is the capture effect. In practice, radio receivers are able to demodulate a signal from one transmitter even if another simultaneous signal is being transmitted over the same channel [26] [27]. The capture properties particularities depend on the implementation of the radio receiver. Some receivers are able to differentiate between two signals having almost the same strength [28]. However, depending on the time when the interfering signal arrives to the receiver, there are two possible cases when talking about capture effect. The first case is called the strongest-first where the signal of interest is received at a higher power and arrives first to the receiver. After the synchronization with the strongest signal, a weaker interfering signal can't prevent the reception of the strongest one. The second case is when the interfering signal arrives prior to the signal of interest. While the radio receiver has been synchronized with the interfering signal (i.e., in an infrastructure-based WLAN, it would be a co-channel transmission from a neighboring OBSS), the arrival of the signal of interest (the strongest) disrupts the reception of the first signal and results in the loss of the two packets. The second case is called strongest-last capture effect.

1.6.2.3 Exposed node problem

In high density deployments, the channel access airtime is shared among overlapping OBSSs. That means that the channel may be sensed *busy* because a STA in a neighboring BSS is transmitting. In that way the carrier sensing part of the CSMA/CA fulfills its role by preventing the initiation of another transmission that disrupts the reception of the transmission occurring in the neighboring BSS. However, there are cases where two

simultaneous transmissions over the same channel are possible. In these cases, due to multiple reasons, the SINR experienced at the devices simultaneously receiving from their respective peer devices is satisfactory. When a possible successful transmission of a device is wrongly forbidden by the carrier sensing procedure, that device is called an exposed node. The presence of exposed node problem degrades the performance of the whole system. Logically, this problem is more prevalent in dense environments where it may prevent the densification from attaining its objective of increased capacity. As we will see later in details, the overprotecting behavior of CSMA/CA is limiting the performance of 802.11 networks in dense deployments. To meet the increasing demands for WLAN capacity, more spatial reuse is needed along with network densification in order to prevent exposed node scenarios.

1.7 Summary

In this chapter the technical background of WLAN is presented. The evolution of the IEEE 802.11 standard is discussed in the light of the needs that motivated the different amendments. The MAC layer improvements have been shown to be crucial after presenting the main PHY layer enhancements. It is clear that the ultimate performance of WLAN system is always limited by the MAC layer performance. This is due mainly to the nature of the contention-based multiple access scheme, as detailed earlier in this chapter. Although many important improvements were introduced with the different amendments, the IEEE 802.11 WLAN efficiency is still questionable especially when the density of deployed APs increases. Along with the increasing demand on capacity, many challenging case-scenarios are identified. The issues that the upcoming generation of the standard has to cope with are discussed in this first chapter. In the second chapter we see how research and standardization societies have been dealing with these issues. The main areas and directions of improvements are presented and deeply discussed.

2 Towards super dense Wi-Fi – state of the art

2.1 Introduction

After depicting the fundamental background related to IEEE 802.11 Wireless Local Area Network (WLAN)s in the first chapter, we describe how the performance of these networks is analyzed in the literature. When proposing new features to enhance the standard, the performance of the new version of the protocols must be tested to validate it and predict its possible drawbacks and limits. In Section 2.2, the different approaches used to analyze the 802.11 WLANs are presented. Subsequently, the limitations of these approaches are described. Following the identification of the main problems and challenges facing WLANs in Chapter 1, we show in Section 2.4 the main directions of improvements of the 802.11 technology. A list of potential candidate solutions is presented and discussed in Sections (2.5) and (2.6). Although many improvement techniques are possible, the combination of two or more of those techniques are proposed to boost the gain in performance. Throughout these sections, the state of the art concerning the different presented directions and approaches is reviewed with a special focus on the scope of spatial reuse in dense environments. In Section 2.3, some important alternatives of the Carrier Sense Multiple Access with Collision Avoidance (CSMA/CA) scheme are presented. It is commonly argued that future WLAN solutions must be built on top of the CSMA/CA without replacing it. In the same section the trade-off between centralized and distributed approaches is considered. Next, in Section 2.9, we explain how we are entering the era of super dense Wi-Fi before introducing the standardization group that is preparing for the next generation of this technology. In the last Section we summarize all the discussed topics of this chapter.

2.2 IEEE 802.11 WLAN performance analysis

Evaluating the performance of the random access based Media Access Control Layer (MAC) protocols is one of the most critical parts when studying the performance of 802.11

networks. This evaluation is carried out using different approaches. In the literature, in order to evaluate their performance, the MAC protocols are modeled via simulation tools, testbeds or theoretical models. While the analytical approach tries to model the different protocols through mathematical equations, testbeds reproduce a real network on a small scale using adapted hardware devices or prototypes. On another hand, simulation literally mimic the real protocol behavior using software programs. This allows more flexible models than those implemented in testbeds thanks to the software flexibility. At the same time, simulations enable addressing particular case-scenarios under specific conditions while analytical modeling gives general insights related to the characteristics of the modeled protocol.

2.2.1 DCF analytical performance modeling

Traditionally, analytical models of the distributed MAC protocols are designed based on stochastic processes with various approximations and assumptions. These models are conceived to provide an approximation of the network performance in generic scenarios.

2.2.1.1 Maximum theoretical throughput of a single link

The different parameters specified by the IEEE 802.11 standard are used to calculate the maximum throughput that can be achieved by an 802.11 transmitter. These parameters include the length of the various headers of the different sublayers (see Figure 1.2), the different Inter-Frame Space (IFS) used during the contention period and the random backoff time ($T_{backoff}$). For instance, without accounting for channel errors and management frames (e.g., beacons, probes, etc.), the maximum theoretical throughput ($Throughput_{max}$) achieved using the basic channel access scheme (described in Section 1.3) is calculated as follows.

$$Throughput_{max} = \frac{Size\ of\ an\ \text{MSDU}}{T_{\text{DIFS}} + T_{backoff} + T_{frame} + T_{\text{SIFS}} + T_{\text{ACK}}} \tag{2.1}$$

Where T_{DIFS} and T_{SIFS} are respectively the DCF Inter-Frame Space (DIFS) and Short Inter-Frame Space (SIFS) durations, T_{ACK} and T_{frame} are respectively the time durations needed to transmit the Acknowledgment (ACK) and the data frames including the preamble and the headers. Note that T_{frame} depends on the Modulation and Coding Scheme (MCS) selected for the ongoing data transmission and the size of the transmitted data.

This calculation can be extended to take into account the eventual packet loss due to bit errors. Knowing the Bit Error Rate (BER) for the MCS in use, the Frame Error Rate (FER) is calculated for an MAC Service Data Unit (MSDU) of a fixed size. Consequently, the

probability of a transmission to succeed after i retransmissions is given by:

$$Pr_{success}^{(i)} = (1 - Pr_{success})^{(i-1)} Pr_{success} \tag{2.2}$$

Where $Pr_{success} = 1 - \text{FER}$. As previously described, Contention Window (CW) is doubled after each retransmission. Hence an average $T_{backoff}^{(i)}$ is calculated to take into account the total backoff time after i retransmissions [29]. Finally, $Throughput_{max}$ becomes:

$$Throughput_{max} = \frac{Size\ of\ an\ \text{MSDU}}{Pr_{success}^{(j)} \sum_{i=1}^{j-1} \left(T_{frame}^{(i)} \right) + T_{frame}^{(0)}} \tag{2.3}$$

For the basic access scheme, $T_{frame}^{(i)} = T_{\text{DIFS}} + T_{backoff}^{(i)} + T_{frame} + T_{\text{SIFS}} + T_{\text{ACK}}$. Many extensions to these calculations are easily performed in order to account for more advanced features of the different 802.11 amendments (e.g., Request To Send (RTS)/Clear To Send (CTS) handshaking, frame aggregation, block acknowledgment, Quality of Service (QoS) support, etc.). Moreover, other contributions propose conducting offline measurements on real devices to build a mapping table between the Signal to Noise Ratio (SNR) and the corresponding throughput [30] [31]. Such methods are used to provide a per link capacity estimations. However, they are valid only for a single transmitter-receiver link where the transmitter is not competing with other potential devices in order to access to the communication channel. In a Basic Service Set (BSS), multiple devices contend for gaining access what raises the possibility of having frame collisions (1.6.1). The previous approaches are not capable of capturing the backoff mechanism in presence of multiple contending devices.

2.2.1.2 Offered and carried load analysis

To estimate the capacity of a WLAN, multiple models are proposed in the literature. One of the earliest models is based on the analysis of the carried and the offered load. For the offered load, this approach assumes an infinite number of devices generating traffic following a Poisson process with a given aggregate packet generation rate. On the other hand, packet transmission and retransmission is modeled by another Poisson process with a defined packet rate. This technique was widely used to analyze the performance in terms of delay for slotted and non-slotted ALOHA and Carrier Sense Multiple Access (CSMA) [32] [33] [34]. The analysis offered by this approach, in contrast to practical systems, assumes an infinite devices number and an homogeneous network.

2.2.1.3 Markov chain model

The most widely used technique in MAC protocols performance modeling is the Markov chain. Basically, Markov analysis is used to model the different states of a whole communication system [35]. Earlier works considers a simple MAC in a homogeneous system where a device have only two states. In the first state, frames are waiting in the buffer. The second states represent an empty buffer with a probability of generating a new frame following Bernoulli law. The number of states in these models equals the number of devices. To model more advanced MAC protocols, multi-dimensional Markov chains are used. Due to the increasing complexity of these models, they are limited to homogeneous networks with a small number of devices having small buffers [34].

A different approach of the Markov analysis models the state of an individual device instead of modeling the whole system composed of multiple devices. Accordingly, the backoff procedure of an individual device in a WLAN is modeled via a two-dimensional Markov chain. Originally, this model is used to study the saturation throughput of the 802.11 Distributed Coordination Function (DCF) [36] [37]. Then it was extended to model the Enhanced Distributed Channel Access (EDCA) introduced by the IEEE 802.11e [21] [38] [39].

In order to solve the model, the state transition probabilities of the Markov chain must be found. Normally, the traffic is assumed to be Bernoulli or Poisson to maintain the Markov chain memoryless. In other cases, the traffic is assumed saturated so that a device has always at least a buffered frame for transmission. These assumptions are introduced to simplify the resolution of the model. However, deciding the transition probability matrix of the Markov chain remains complex especially when the number of states increases. This number increases with the number of devices and the complexity of the modeled protocol.

2.2.1.4 Renewal process

Another approach to model the backoff and the channel access behavior of a device using CSMA/CA is based on renewal processes theory [40]. According to their proposal, authors in [41] consider a three-level renewal process that models the renewal cycle of a device using CSMA/CA. The renewal cycle is defined as the period between two consecutive successful frame transmissions from the same device. This definition permits a direct relation to the MAC throughput and average time of a frame. It has been argued that the complexity of the performance analysis using the previous framework does not scale up with the complexity of the MAC protocols (e.g., backoff channel access policies) as in Markov chain based models. Moreover, using the same approach, a performance modeling for unsaturated traffic operation is proposed.

2.2.2 Limitations of the analytical models

In the literature, the majority of the models designed to analyze the performance of the 802.11 DCF are based on the Markov chain model [37]. While these models are useful to understand the theoretical limits of a 802.11 network, they are not accurate when there is a high degradation and unfairness issues in the modeled network. In these models the interference is ideally modeled and as a result, the throughputs achieved by the modeled CSMA/CA protocols are biased. The most important limitation related to our work is that these models do not consider the Physical Carrier Sensing (PCS) mechanism neither the capture effect. Moreover, the previously described models are not capable of modeling a multiple BSSs network. Authors in [42] proposed a method to estimate the capacity of multi-BSS WLAN (i.e., Extended Service Set (ESS)). However, in their model, each BSS is treated alone ignoring the evident inter-BSS interactions.

In practice, many considerations make modeling multiple BSS performance analytically complex. Firstly, taking into account the eventual interferences between different BSSs is not trivial. These interferences may result from using overlapping channels in neighboring BSSs (adjacent channel interferences) or from the presence of Overlapping BSS (OBSS)s (co-channel interferences). Secondly, the hidden node problem is complicated to model especially if the hidden node is in an OBSS. Thirdly, modeling the rate control mechanisms is a real challenge mainly because the majority of these mechanisms are proprietary solutions. Authors in [43] proposed a capacity model for 802.11 multiple BSS networks. However, in their work, they recognize the complexity of modeling practical rate control and link adaptation mechanisms. Furthermore, their model does not take into account the exposed node problem.

2.2.3 Performance analysis in standardization process

In standardization, performance evaluation and analysis are mostly based on simulations. System level simulations allow a fast performance assessment of new protocols under various case-scenarios. These simulations are widely employed and recognized as effective tools to study new technical solutions. As we will see in details in Chapter 3, a system simulator makes an abstraction of the physical layer and hence permits packet-level simulations. In practice, the validation of new protocols via simulation tools is of paramount importance, since it allows to substitute the experimental analysis with simulation one. This is typically less expensive and easier to setup. Moreover, a simulation approach allows to perform analyses that respond to the “What-if ...?” questions without the need of effectively implementing the new functionalities in real devices.

An 802.11 simulation model implements the functionalities defined by the standard and

permits their modification and the implementation of new functionalities. Thanks to an event-driven approach, modeling the interaction between different entities is easily implementable. Accordingly, the randomness of the MAC protocols is naturally modeled as it happens in real world networks. Hence the interference caused by one BSS on another is inherently taken into account.

In order to obtain comparable results, the different simulation tools configurations are specified in the standardization process. Multiple scenarios are defined to perform the calibration between the different simulators. In Chapter 3, the scenarios considered for the evaluation purpose in this thesis are described and linked to the scenarios proposed by the current 802.11 Task Group (TG). Moreover, the different evaluation metrics are defined to generate coherent interpretation of the results.

2.3 CSMA/CA, alternatives or improvements

By surveying the literature, we identify many proposals for alternative mechanisms to replace the CSMA/CA protocol. In [44], the authors argue that the approach adopted by the CSMA/CA protocol is not sufficient to simultaneously resolve all the problems previously discussed in Chapter 1. Accordingly, the authors propose an alternative cross layer protocol called Full Duplex Attachment System (FAST). The proposal defines two parts. The first part is the Physical Layer (PHY) layer attachment coding to transmit control information over the wireless medium without impacting on the throughput of the data traffic. This is possible by modulating the information into interference-like signals and attaching them to the signal of interest. This scheme is inspired from interference cancellation methods based on the work conducted in [45] and [46]. The second part is the MAC layer attachment sense that is responsible of identifying hidden and exposed nodes by exploiting the control information sent using the first part. The results show that FAST achieves a gain of 180 % in user throughput over CSMA/CA. However, this work is considered immature mainly because the compatibility of full duplex attachment coding is not deeply investigated.

An alternative technique to CSMA/CA is presented in [47] to exploit the advantages of directional communications in 802.11 ad hoc WLANs. Globally, the omnidirectional antennas are inefficient in terms of spatial reuse especially in contention based access networks. To cope with this inefficiency, directional antennas are proposed in the literature [48] [49]. However, relying on the 802.11 conventional CSMA/CA is a limiting factor. The authors in [50] show that deafness problem is caused when using directional antennas with on top of CSMA/CA. Deafness happens when a receiver that is beamformed to a given direction becomes unreachable by a corresponding transmitter. For that reason, authors in [47] propose a mechanism called EDirection where the MAC layer instructs the PHY layer to

listen to unblocked sectors only instead of continuously carrier sensing towards unavailable sectors. The authors show an important performance improvement when comparing EDirection to the omni-directional and the conventional directional antennas.

Another proposed solution to cope with the inefficiency issues of the CSMA/CA mechnism is presented in [51]. The solution consists in a hybrid MAC protocol that switches between conventional CSMA/CA and a Time Division Multiple Access (TDMA) scheme depending on the interference conditions. Authors propose an interference estimation scheme based on measurements reported periodically by all the Station (STA)s to their corresponding Access Point (AP)s. The proposed schemes needs a coordination protocol between all the APs of the ESS. Additionally, all the coordinated APs must be synchronized to avoid slot overlap due to timing inaccuracies. Consequently, these APs negotiate about switching from CSMA/CA to the TDMA scheme (or vice-versa) after exchanging all the necessary information related to interference. Based on the conducted simulations, the authors show a good potential of the proposed framework in terms of aggregate throughput and fairness among the different BSSs. However, this work does not discuss the coordination protocol that is needed to implement the proposal. Furthermore, the impact of the signaling overhead introduced by the information exchange and the time slotted scheme is not taken into account by the authors.

In practice, the Point Coordination Function (PCF) that is standardized since the earlier versions of the 802.11 standard has never found its way into the production stage. This fact gives an important indication about the nature of the access schemes in the next Wi-Fi generation. Anyhow, for the next generation of the IEEE 802.11 standard, there is no intention to replace the CSMA/CA protocol. The main reason behind that is the interoperability with the previous generations of devices (i.e., legacy devices) that are widely operating today (i.e., 802.11b/g/n/ac). Another reason is the coexistence with other networks that are sharing the spectrum. These networks include neighboring WLANs and other technologies like Wireless Sensor Network (WSN)s (e.g., IEEE 802.15.4 [52]), and Bluetooth (i.e., IEEE 802.15.1 [53]). In this context, CSMA/CA offers a simple but effective multiple access scheme to share the unlicensed frequency bands among these contending networks. Any other scheme to manage the multiple access to the shared medium (e.g., TDMA, Frequency Division Multiple Access (FDMA), or Code Division Multiple Access (CDMA)) will introduce a higher degree of complexity in implementation and operation than that of the CSMA/CA. This complexity will deprive Wi-Fi technology from its distinctive character among other wireless technologies. As discussed in Chapter 1, a key factor of the success of Wi-Fi is its affordable price and the simplicity of its design. Accordingly, the scope of any technical amendment to the future standard must consider the CSMA/CA protocol as the backbone of the 802.11 MAC.

2.4 Enhancing the performance of the future Wi-Fi networks

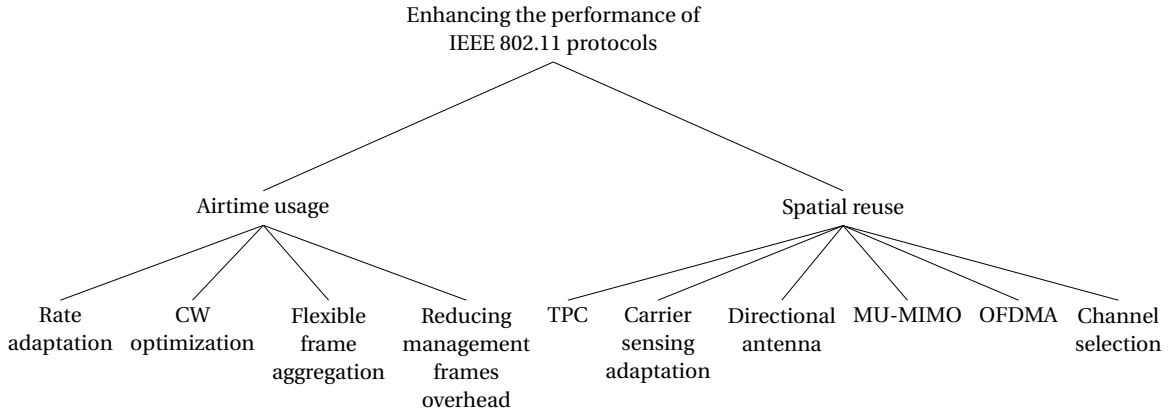

Figure 2.1 – Different approaches to enhance the performance of IEEE 802.11 protocols

Mainly because of their historical success, future generation of 802.11 WLANs face three important challenges. Obviously, the number of connected devices will continue to grow especially with the beginning of the Internet of Everything (IoE) era. To serve these devices, APs are continuously deployed covering more and more new areas. As a result, the first major challenge facing future WLANs is the high density of the operating environments. The second challenge is driven by the nature of the modern usage of the Internet where the dominating contents are high definition real time audio and video. These applications are significantly increasing the demand on higher end users throughputs. Thirdly, 802.11 WLANs are real candidates to offload data from saturated cellular networks. This new use case represents a main challenge for the next generation of the 802.11 standard, since operators need efficient WLANs to maintain high Quality of Experience (QoE) for their end users.

Evolving and optimizing the protocols defined by the MAC and PHY layers is necessary to keep pace with the increasingly imposing challenges. In Figure 2.1, we list the different enhancement fields and possible features. For clarity, we have grouped the envisioned solutions into two categories: access time optimization which includes solutions in the temporal domain and spatial reuse category that combine the solutions in the space and frequency domains.

2.5 Access time optimization

As we already saw in Section 1.6, the main efficiency issues in modern WLAN systems are due to the basic intrinsic parts of DCF employed by the 802.11 devices to access the channel. The backoff procedure, the inter-frame spacing, the frame headers, the management overhead, the synchronous collisions and retransmissions decreases the time that a device spend transmitting useful data when it succeeds to gain access to the

channel. In this section we describe the main improvement areas related to the access time optimization.

2.5.1 Contention parameters optimization

Better utilization of the channel is possible in time domain through the optimization of the backoff algorithm used by the CSMA/CA as a collision avoidance mechanism. An important approach studied in [54] is optimizing the value of CW. The authors have shown that exponential backoff may lead to short term unfairness issues. Moreover, setting the CW appropriately is sufficient for a stable throughput when the number of users actively contending is known and the time wasted on collisions is estimable. In these circumstances, the authors suggest to completely disable the exponential backoff. The authors show in [55] that such a technique is effective in reducing the penalty due to selfish adaptation of the communication link and rate control. Furthermore, authors in [56] argue that the backoff mechanism introduces delay degradation in a saturated network. Accordingly, different backoff schemes are studied and a polynomial backoff procedure is proposed and shown to have the same performance as the exponential backoff but without delay degradation. In the context of dense deployments, as shown in [57], linear backoff is more efficient than reseting the CW to CW_{min} after a successful transmission.

2.5.2 Rate control

The rate control mechanism is an effective way to improve the overall system performance in IEEE 802.11 multirate networks. It consists in assessing the conditions of the communication channel in the aim of choosing the best data rate according to the current state of the channel. This adaptation is challenging due to the fluctuating wireless channel conditions. A detailed survey about the different rate adaptation schemes designed for IEEE 802.11 WLANs is presented in [58]. After comparing the performance of these multiple rate adaptation techniques, the authors conclude that raise many open issues. They highlight that an effective rate adaptation algorithm must be able to differentiate between a bit error and a frame collisions, which is not the case of the most representative schemes of these algorithms. Furthermore, in dense environments, due to the large number of contending nodes, the packet collisions trigger unfairly the rate control mechanism to decrease the transmission data rate. As we will see in Chapter 5, this behavior has a detrimental effect on the performance of 802.11 WLANs.

2.5.3 Flexible frame aggregation

Frame aggregation is clearly the most important enhancement related to airtime efficiency that was introduced in 2009 by the IEEE 802.11n amendment. As explained in Section 1.5.2, frame headers and inter-frame spacing overhead are reduced by aggregating short frames into a longer frame. Enabling more flexible aggregation schemes is mandatory to cope with the real world traffic where the size of frames varies widely. When the channel is saturated, aggregating frames is of utmost importance because it reduces the airtime and hence permits an efficient use of the channel. However, if the channel is not saturated, the applications may be satisfied without even aggregating the frames at the MAC layer. Moreover, if the channel experiences bad conditions and hence the BER is relatively high, limiting the size of a retransmitted frame increases the efficiency. For instance, if an MSDU within an Aggregated MSDU (A-MSDU) is not correctly decoded, all the A-MSDU is to be retransmitted by the sender. Additionally, for audio or video real time applications (e.g., Voice over IP (VoIP)), despite enhanced throughput, jitter increases with aggregation as shown in [59]. Flexible frame aggregation schemes must decide whether to activate the aggregation or not and whether to use A-MSDU, Aggregated MPDU (A-MPDU), or both.

2.5.4 Reducing management frames overhead

Exchanging control and management frames consumes a large amount of the airtime. The overhead introduced by these exchanges is important for two reasons. Firstly, in order to tolerate bad channel conditions, they are transmitted at lower bit rates. Secondly, some of these frames are sent periodically (e.g., beacons every Target Beacon Transmission Time (TBTT), ACK frame after every successful reception, etc.). In addition, advanced PHY technical features enabling multi-user transmissions introduces more frequent control frames exchange for synchronization purposes.

Reducing the overhead caused by the management and control frames is an important way to increase the efficiency of the airtime used to transfer the application's layer data. For instance, if a beacon of 373 $Bytes$ is transmitted every 102.4 ms at 1 $Mbps$ then it the transmission time is 3.226 ms. The resulting beacons airtime utilization per Service Set Identifier (SSID) is3.15 %. With 7 SSIDs that would be 22.05 %, and with 15 SSIDs that would be 47.26 %. For those reasons, many network administrators configure their APs with higher TBTT values to reduce beacon frames overhead especially when their network broadcasts a large number of SSIDs.

2.6 Spatial reuse

Basically, increasing the density of WLAN deployment is possible by shrinking the BSS size (i.e., the zone where STAs are associated to a given AP). This size is markedly lower than the actual maximum coverage area of the AP (i.e., where the transmitted signal propagates). For that reason, even when applying frequency reuse patterns, some co-channel BSSs overlap and hence the CSMA/CA domain becomes larger and the communication resources are shared among more and more devices. This is known as the OBSS problem as discussed in Section 1.6.2. In this section we identify the directions where improvements are possible in the aim of enhancing the spatial reuse in dense environments.

2.6.1 Channel selection

In the context of infrastructure based IEEE 802.11 WLANs, a channel selection mechanism is needed in order to mitigate the interference caused by the neighboring overlapping BSSs. In practice, as discussed in Section 1.6.2, there are two groups of WLAN deployments: centrally managed and uncoordinated. In the first category where a controller manages all the APs belonging to it, the channel selection is decided by the controller. The strategy adopted by the majority of the deployed channel assignment techniques is to assign the available channels to different APs in such a way to minimize the generated interference among the controlled BSSs. The mission of a channel assignment mechanism is more critical in uncoordinated deployments because of the absence of the common management of the different APs. Moreover, in this case the placement of the APs is neither planned nor controllable. APs are placed in a particular geographical location, usually fixed, that we cannot optimize prior to the channel assignment. Controlling APs placement is only possible in the centrally managed category of WLAN deployments. However, in reality, managed and unmanaged WLANs coexist in the same geographical area and may overlap. Authors in [60] provide a survey of the different schemes of channel assignment and a qualitative comparison between them.

2.6.2 The control of the transmission power

In wireless networks, the control of the transmission power is an efficient way to manage interferences, save energy and enhance the connectivity. In this thesis, we use Transmit Power Control (TPC) to refer in a general way to the mechanisms consisting on controlling the power used for transmissions. Power control in mobile cellular networks has been widely studied and extensively developed in both directions of the communication, uplink (i.e., from the user equipment to the base station) and downlink (i.e., from the base station to the user equipment). In modern cellular networks, TPC plays an essential role especially

with the increasing density of deployments, the increasing demand on capacity, and the increasing number of energy constrained mobile user equipments (i.e., smartphones, tablets, and other connected objects ...). The basic idea of TPC is to reduce the transmission power to a minimum value while meeting the required Signal to Interference and Noise Ratio (SINR) needed to successfully decode the signal of interest by the receiver. An extensive discussion of the techniques, models, and methodologies of TPC in cellular networks is provided in [61].

Although, the idea of TPC is simple, applying it to the 802.11 WLAN based system is very challenging as argued in [62]. When reducing the transmission power, there is more chance to create hidden node issues. In infrastructure based WLAN, the AP must be very careful when applying TPC because the associated STAs located at the edge of the BSS will experience lower SNR and may loose their connectivity. From the STAs point of view, reducing the transmission power erroneously may create hidden nodes inside the BSS. Moreover, as consequence of using lower power, the experienced SINR at the receivers decreases what forces the transmitter to use lower MCSs (having more robust modulation and coding). Consequently, since transmission data rates become lower, they take more airtime and hence the probability of synchronous collision increases. Furthermore, it is true that lower transmission power means lower energy consumption when transmitting a frame. However, due to the previously described drawbacks, retransmissions are more likely to happen and hence in longterm, the power consumption may be higher. A detailed study in this thesis shows why TPC is hardly finding its way to the production stage in WLAN industry.

2.6.3 Enhancing the Clear Channel Assessment (CCA) mechanism

Solutions and techniques adopted in cellular networks have always been exploited to increase the spatial reuse in high density WLANs. However, the difference in the access schemes between the cellular and the WLAN technologies does not allow exploiting these solutions with the same relevance in both technologies. Practically, the specificity of DCF demands different approaches than those adopted in cellular world where the access is scheduled and the communications are fully coordinated. One of the mechanisms that is specific to the 802.11 world and does not exist in the cellular networks technologies is the Clear Channel Assessment (CCA) (see Section 1.3.2). This mechanism plays a fundamental role in determining the size of the contention domain (i.e., the protection region around the device that is currently transmitting where other co-channel transmissions can't be initiated simultaneously). In dense infrastructure-based WLAN topologies, this protection range impacts directly the amount of spatial reuse between OBSSs. Basically, there are two opposite approaches regarding the optimization of the CCA mechanism. While the first approach aims at increasing the protection range around the transmitter, the second aims

at decreasing this range for more aggressive access to the shared medium.

Following the first approach, the optimization of high density network design is considered in [63]. To tolerate co-channel interference, the authors propose tuning the parameters of the MAC layer, particularly the CCA threshold. More specifically, the proposal is a centralized solution based on periodic measurements provided by all the devices of the network and processed by a central controller. After an exhaustive search in all possible values, the controller deduces an optimal network wide CCA and MCS values that maximize the aggregate network throughput. After arguing that the 802.11a environment is noise-limited and the 802.11b is interference-limited, the CCA tuning is observed to be useless in the 802.11a environments. As will be shown later in this Chapter 3, the magnitude of the density considered by the work in [63] is way lower than the envisioned network densities for future WLANs that we are targeting in our work (i.e., envisioned scenarios are about 20 times more dense than that of [63]). This fact deeply affects the findings, the analysis and obviously the results of the mentioned work. Additionally, in their simulation scenario, the authors have not considered uplink traffic which does not reflect the real world traffic trends today.

Another work in [64] considers the second approach to increase the spatial reuse between concurrent transmitters in a large ad hoc network. In conventional multi-hop ad hoc networks, the carrier sensing is configured to be sensitive in order to defer neighboring interferers during local transmissions. Although the high sensitivity level results in a high probability for a transmission to be successful, it reduces the spatial reuse of the entire ad hoc network. To increase the performance of multi-hop ad hoc networks, the authors proposes a carrier sensing adaptation scheme. The solution is based on the exchange of local measurements and channel conditions estimations between neighboring nodes. Therefore, an additional overhead is added to the system because the measured informations need to be periodically flooded over the network.

2.6.4 Multi-user transmission protocols

Conventionally, in 802.11 WLAN systems, only one device can transmit at a time over the same channel. Within a BSS, only one communication between the AP and a STA is supported. Letting multiple devices transmit simultaneously in same BSS increases the capacity of that BSS. Basically, Multi-User MIMO (MU-MIMO) and Orthogonal Frequency Division Multiple Access (OFDMA) are the potential technologies to make that happen.

MU-MIMO is a technique to enable different devices to transmit simultaneously on the same frequency channel by spatially multiplexing multiple data streams belonging to different users using multiple antennas. In this sense, the MU-MIMO is a form of Spatial Division Multiple Access (SDMA). The challenges of designing MU-MIMO MAC protocols

are presented in [65]. The MU-MIMO feature was introduced by the 802.11ac amendment [13] only in the downlink communication path. OFDMA, the multi-user version of Orthogonal Frequency Division Multiplexing (OFDM) (Section 1.4.3), was the other option proposed during the standardization process. The multi-user access in OFDMA is achieved by assigning subsets of subcarriers to individual users. In 802.11ac, SDMA was preferred over OFDMA for downlink because it showed higher theoretical throughputs when APs have more antennas than STAs. However, the overhead engendered by the MU-MIMO protocol limits its usage only to demanding applications. It is believed that OFDMA is able to aggregate less demanding users applications with lower overhead. This would be very efficient in real world high density scenarios.

For now, multi-user transmissions in the uplink communication path are not supported. However, generally speaking, the uplink traffic is strongly growing mainly because of the cloud storage trends. In dense environments, this uplink traffic becomes quite important (e.g., uploading multimedia content to social networks, new live streaming applications, etc.). Uplink multi-user transmission is an interesting solution to increase the spectral efficiency of WLAN systems. In 802.11ac uplink, MU-MIMO was left aside mainly because of the complexity of achieving synchronization between different STAs. In order to bring uplink multi-user transmissions to 802.11 WLANs, efforts are needed to avoid strong frequency offset between users, power difference between received signals and unsynchronized packet arrivals at the AP. This cannot be done without enabling a sort of scheduling on top of CSMA/CA. However, any envisioned mechanism will have a MAC overhead that needs to stay low in order to preserve the efficiency of the multi-user transmission scheme.

2.6.5 Massive MIMO and network MIMO

Long term solutions that are envisioned for future WLANs include using a large number of antennas to serve a large number of users or to null the interferences caused to other users within a cooperating network. In a massive Multiple-Input Multiple-Output (MIMO) context, the AP has an antenna array of multiple tens of antennas and uses them to serve nearly every STA by a different point-to-point spatial stream [66]. Indeed, the cost of such an AP is high. Additionally, there are many issues regarding the needed Channel State Information (CSI) information, the extra processing complexity, and the higher energy consumption due to the number of antennas.

In a MIMO network system, each AP is equipped with multiple antennas and thanks to the coordination between the different BSSs, interference cancellation is realized by data and CSI exchange. In such a system, joint downlink transmission from different APs is possible using beamforming techniques. Basically, multiple coordinating APs are able to operate as if they were a large array of antennas. This results in a reduction in the co-channel

transmissions interference and increases the spatial reuse of the system [67]. However, many challenging issues are yet to be solved including the constrained synchronization requirements among the APs.

2.7 Combining different approaches

We have presented in Section 2.4 the main areas where enhancements to the current standard are possible. Obviously, a candidate solution may consist in combining two or more of the previously described approaches. For instance, managing the interferences in chaotic WLAN deployments is addressed in [68] by a joint adaptation of the transmission power and the data rate. Starting from a large WiFi mapping database (i.e., street-level maps of WiFi APs from *WifiMaps.com* and Intel Place Lab in [69] [70]), the authors study the effect of interference in unplanned and unmanaged WLAN systems. Using trace-driven simulations, authors show that power control and channel selection may ameliorate the user throughput and the fairness. Accordingly, a distributed power control based data rate adaptation algorithm is proposed and evaluated. Another joint adaptation is considered in [63] where authors propose a combination of rate control and CCA adaptation following a centralized scheme in order to minimize interferences caused by hidden nodes. In [71], authors propose a centralized solution to manage enterprise WLANs. Using active probing interference measurement, a joint optimization of channel selection and power control is designed.

2.8 Centralized or distributed strategy ?

One of the perpetual basic questions for any solution for enhancing WLAN performance is whether a centralized or distributed architecture is preferable. While the majority of the conventional WLANs are completely unmanaged (e.g., home), enterprise grade WLANs are deployed following a centralized approach (e.g., office). In centralized WLANs, functionalities such as security, device management and control, load and association balancing, and transmission power are controlled by central device called the controller. Each AP in the controlled system communicates with the controller to manage these functions. In distributed WLANs, the functionalities for each AP resides within that AP. Some WLAN providers implement a highly distributed design to deploy enterprise WLANs without the use of any centralized controller [72]. Some of these implementations propose a cooperative control between the different APs belonging to the same domain. However, the amount of overhead introduced by the coordination frames exchanged periodically in such a network is always questionable. Regardless of the exact application of the network, the main advantage for distributed architectures is the survivability in the event of the loss of the controller. On the other hand, centralized architectures have the advantage of

offering less expensive APs (i.e., thin APs) because they do not require high resources for complex processing.

We believe that an efficient solution has to cope with the diversity of the real world scenarios. However, the more the solution is distributed the more it goes with the spirit of the 802.11 WLAN. Keeping this technology as simple as possible was and will stay the key of its success. Additionally, even if we consider deployment scenarios where managing and controlling all the APs by a common entity is possible, the presence of other single BSSs in proximity of the controlled deployment is largely expected. In such scenarios the system must be designed to take into account the presence of these possible interferers. Moreover, if the controller fails, the APs have to figure out how to operate individually to prevent a single point of failure problem. For these reasons our contributions throughout this thesis are able to address these scenarios in centralized and distributed manner.

2.9 Next Wi-Fi generation for high density and high efficiency performance

2.9.1 Towards high density WLAN

Nowadays Wi-Fi networks are deployed in diverse environments characterized by a high density of APs and STAs in geographically limited area. This is driven by the need for ubiquitous coverage to be always connected to the world wide web. The fast evolving technology has boosted the expansion of WLAN ready devices and pushed the prices of hardware equipment down. For instance, a normal Wi-Fi network interface card is so cheap that it is embedded into almost all types of computing and communication devices such as smart phones, notebooks and tablets. With millions of hot-spots deployed around the world, Wi-Fi is rapidly becoming ubiquitous. Nowadays, urban environments are showing a huge number of deployed APs and connected STAs [73].

Besides the need for ubiquity, nowadays applications are indeed more aggressive in terms of network resources. Gaming, high definition video, augmented reality and others are examples of daily used applications categories. To respond to these demands, the IEEE 802.11 working group [74] had always an interest in increasing the peak bit-rate. While in IEEE 802.11n [12] it reached 150 $Mbps$ per spatial stream, the new IEEE 802.11ac amendment [13] is announcing almost 1 $Gbps$ per stream. It is important to mention here that these bit-rates are theoretical; real networks never attain these upper bounds. That is due to the contention nature of the MAC layer mechanisms of the IEEE 802.11 standard along with the interference problem discussed earlier in Chapter 1.

In these dense environments, performance degradation is caused by co-channel inter-

ferences and higher number of contending devices resulting in exposed nodes and sever collisions (see Section 1.6 for details). As already identified by the research community, the exponentially growing wireless traffic demand can only be addressed and satisfied by increasing the number of access points and combining different wireless access technologies [75]. Authors in [76] conclude that Wi-Fi is the best indoor wireless solution to offload mobile data traffic from cellular networks. Following this trend, operators and service providers started to deploy denser Wi-Fi networks by building femto-cells and installing more Wi-Fi hotspots in public areas for mobile data offloading. Consequently, more mobile data traffic is predicted to be injected in Wi-Fi networks to relieve the overloaded mobile cellular networks [77]. As a result, the share of offloaded mobile data traffic is expected to increase from 33 % in 2012 to 47 % in 2017 (see [78]).

All the aforementioned facts mean that we are entering the era of super dense Wi-Fi environments. To handle the boom in the demand for wireless communications, densifying is the most sustainable solution as it enhances the spectral efficiency. The sad part is that the original form of Wi-Fi is not made for such a high density deployment. As we discussed in Section 1.6, the default contention-based multiple access protocol defined in the IEEE 802.11 standard [5] suffers from serious performance degradation in dense environments. Future Wi-Fi devices generation have to be conceived in the light of the aforementioned challenges by improving the efficiency of their PHY and MAC protocols.

2.9.2 IEEE 802.11ax: the future Wi-Fi standard

Over the past decade, substantial enhancements have been introduced by the successive amendments of the IEEE 802.11 (see Section 1.4 and Section 1.5). However, in all the past generations of the standard (e.g., 802.11n/ac), the efforts of the standardization have been mainly focused on increasing the theoretical peak throughput for a transmitter-receiver link. In other words, the focus was mainly on the performance of a single BSS regardless of the inter-BSS impacts.

The IEEE 802.11 High Efficiency WLAN (HEW) Study Group (SG) was created in March 2013 to define the scope of the next main amendment to the standard. Following the identification of the main issues and challenges that would need to be solved, the SG decided to take an other approach, different from that of its predecessors, by focusing on improving the real world performance and the end user QoE. The track took by the IEEE 802.11 HEW initiative targets enhancing the efficiency and performance of WLANs in a dense multi-BSSs use cases. This would make them even better complements to cellular mobile networks.

Orange was a key driver behind the creation of the HEW SG, pushing the standardization community to change the objective that drove the past standard amendments [79]. Later

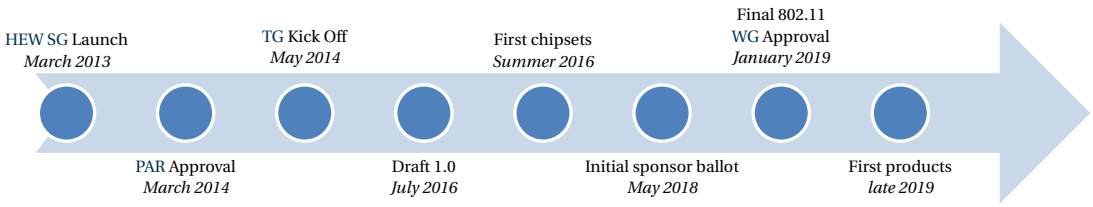

Figure 2.2 – IEEE 802.11ax project predicted timeline

on, HEW SG voted in January 2014 to approve the documents defining the scope and objectives of the next Wi-Fi generation. Therefore, a TG was created in May 2014 to actually define the new specification document. Following the nomenclature of previous well-known Wi-Fi standards (e.g., 802.11a/b/g/n/ac), the new amendment is called 802.11ax [7].

Figure 2.2 depicts the envisioned timeline of the 802.11ax. The first draft of the specification document is expected in July 2016. Later on, in May 2018, the draft is expected to be submitted to the IEEE Standard Association (SA) for initial sponsor ballot. The final 802.11 Working Group (WG) approval awaited for January 2019. Accordingly, it was anticipated that first products implementing the new standard would start to appear in late 2019. However, earlier 802.11ax chipsets are expected in summer 2016 right after the publication of the Draft 1.0.

2.9.3 Spatial reuse ad hoc group

In its November 2014 meeting, the 802.11ax TG approved the creation of four ad hoc groups. Each one of these groups treats separately one of the following aspects: MAC, PHY, Multiuser, and Spatial reuse. The 802.11ax Spatial Reuse (SR) ad hoc group discusses matter that improves spatial frequency reuse and other mechanisms that enhance the concurrent use of the wireless medium by multiple devices. The features discussed in the SR ad hoc group aim at improving OBSS operation in dense WLAN environments.

2.10 Summary

We discussed in this chapter the different methodologies used to evaluate the performance of 802.11 WLANs. Choosing the best methodology depends on the real needs behind its deployment. For instance, for general perspectives studies, mathematical models are capable of evaluating the performance of WLAN protocols in general situations. However, in order to test new functionalities in scenarios more close to real world, simulation is preferred. Simulators allow mimicking the details of a protocol and assessing its performance in very specific scenarios. This is very advantageous when designing a new solution as a candidate

for a future standard. Later on, we structured the solutions envisioned for the next 802.11 WLAN generation around two main axis: access time optimization and spatial reuse. Globally, the investigated solution directions are chosen in the light of the challenges facing the future WLANs previously discussed in Chapter 1. The increasing density of the WLAN environments is the main limiting factor for a carrier grade WLAN experience. Higher QoE is needed to permit the 802.11 technology to realize its promise in integrating operator's networks for traffic offloading. Denser deployments are needed to address the explosion of demand for wireless network capacity. In this context, the 802.11 WG created the HEW SG that resulted in the establishment of a new TG called IEEE 802.11ax. This TG is responsible of preparing the new specification for the next generation of Wi-Fi technology. The subject addressed by this thesis is firmly aligned with these ongoing preparations for the next Wi-Fi generation. In Chapter 3, the different scenarios considered in this work are explained and the simulation models are described in details.

3 Scenarios and Simulation tools

3.1 Introduction

As discussed in Chapter 2, evaluating the performance of a WLAN system is a critical task. Choosing the best fitted evaluation methodology and tools is not straightforward process. That is mainly due to the large number of tools available and the diversity of the approaches and methodologies adopted by these tools. On another hand, defining the scenarios and the use cases the most representative of the today's and tomorrow's WLAN environments is crucial. In this chapter, we start to define in Section 3.2 the different simulation scenarios considered for performance evaluation in this thesis. Moreover, in Section 3.3, we describe the simulation platform used throughout this thesis. In order to simulate the performance of WLANs in high density environments, we have improved the default WLAN simulation model provided by OPNET Modeler. The main improvements and modifications to the standard simulation model are described in Section 3.4. Finally, in order to draw a clear baseline reference for the performance of the simulation model, we conduct some basic simulations and show the results in Section 3.5.

3.2 Simulation scenarios

The work on the definition of the scenarios used in this thesis started earlier than the formation of the HEW SG creation. However, based on the identification of the challenges that the future WLANs have to cope with, we had a clear understanding of the scope of the most important scenarios. A key aspect to capture is the high density deployments and their impact on the performance of a WLAN system. Later on, after the formation of the SG, a document describing the evaluation methodology started to take shape. Today, the document in [80] defines all the simulation scenarios to be used for the performance evaluation of new features proposed in the TGax [1]. The different contributions on sce-

[1] TGax is used in the rest of this thesis to refer to the IEEE 802.11ax Task Group (TG)

narios details from various companies are consolidated in this document and continually revised and updated. Four main scenarios are described, including: (1) residential scenario, (2) enterprise scenario, (3) indoor small BSSs scenario, and (4) outdoor large BSSs scenario. Below, we describe the scenarios considered in this thesis, we highlight their main characteristics and discuss the metrics used for evaluation.

3.2.1 Cellular scenario

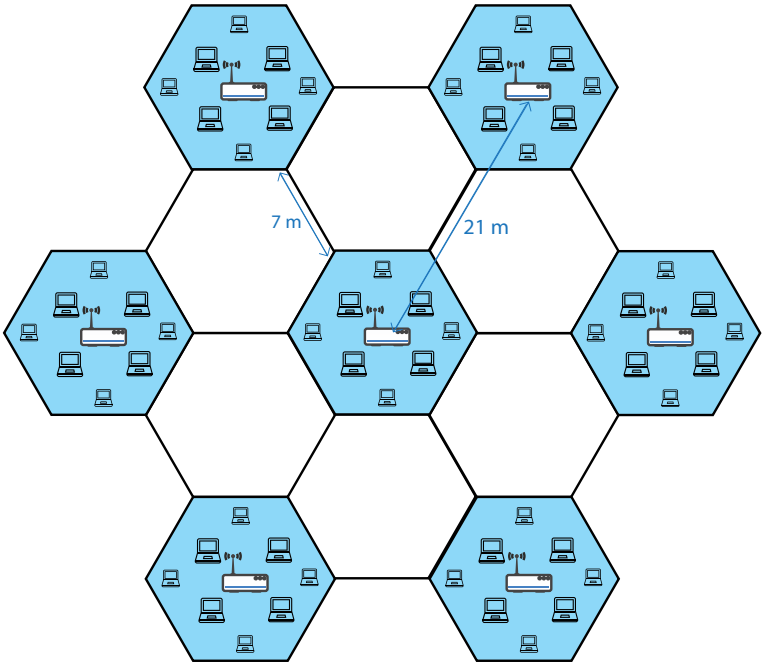

Figure 3.1 – Cellular scenario network topology

The cellular scenario is designed to model real world deployments with high density of APs and STAs that are initially highlighted in [81]. These deployments are considered by the Wi-Fi Alliance (WFA) as prioritized usage models for future WLANs. This scenario simulates a crowded place like a stadium or a train station. In such environments, the deployment of the infrastructure network is usually planned. To simplify the simulation complexity and the interpretations of the results, an hexagonal BSS layout is considered with frequency reuse pattern. In fact, the presented cellular scenario is aligned with the scenario number (3) of the TGax simulation scenarios document [80].

Figure 3.1 shows the cellular network topology of this scenario. It consists of 8 BSSs, in each of which an AP is placed in the center of an hexagon of radius of 7 m representing a cell. In each BSS, 8 STAs are randomly placed at a distance of 2 to 5 meters from their AP. The cellular deployment is based on a cluster of three frequency channels (frequency reuse 3). We suppose an ideal channel selection, in the sense that the network is ideally preplanned in terms of frequency resources. This results in 21 m of distance separation between two

neighboring co-channel APs. Frequency reuse 3 is the most realistic configuration in high density APs scenarios and it represents the majority of the planned deployments today. As discussed in Section 1.4.5, only 3 non-overlapping channels are available in the 2.4 GHz frequency band. Moreover, using 80 MHz channel width for higher data rates leads to only 4 non-overlapping channels in the 5 GHz band. For the sake of clarity and reducing the simulation time, we chose to simulate the operation over one of the three channels. For that reason, Figure 3.1 depicts a set of co-channel BSSs only. Since we are only considering co-channel interference, this does not limit the generality of our simulations. All the important parameters describing the cellular scenario are listed in Table 3.1. Most of these parameters are set in accordance with HEW simulation scenarios as defined in [81]? and [80]?.

Table 3.1 – Cellular scenario parameters

Parameter	Value
General parameters	
Network topology layout	Regular symmetric hexagonal grid (hexagon radius: 7 m)
APs location	At the center of the hexagon
STAs location	Randomly distributed in the hexagon (2 to 5 meters from the AP)
Number of STAs per BSS	8
Frequency reuse	3
Standard version	802.11n
Simulation run duration	3 min
PHY Layer parameters	
Radio band	5 GHz
Bandwidth	20 MHz
Path loss	Path loss model in Equation (3.2)
Number of antennas for each device	1
OFDM Guard Interval (GI)	Long (800 ns)
MAC Layer parameters	
Maximum number of retransmissions	7
Default RTS/CTS setting	Disabled
Default rate control setting	Enabled
Traffic Access Category (AC)	AC_BE (best effort with default Enhanced Distributed Channel Access (EDCA) parameters)
Max size of Aggregated MSDU (A-MSDU)	3839 $Bytes$
Max size of Aggregated MPDU (A-MPDU)	8191 $Bytes$
Default transmission power - APs	15 dBm
Default transmission power - STAs	15 dBm
Default physical carrier sensing threshold - APs	-82 dBm
Default physical carrier sensing threshold - STAs	-82 dBm
Application traffic parameters	
Transport protocol	User Datagram protocol (UDP)
Uplink traffic	Full buffer
Downlink traffic	Full buffer

3.2.2 Residential scenario

This scenario represents a dense apartment building that was initially proposed in HEW SG by [82]. Indeed, this represents a real world situation that is common in urban areas and crowded cities. The main purpose of such practical scenario is involving interference between APs placed in the different apartment units. As a general rule, residential APs are installed arbitrary without any planning. This leads in chaotic WLAN environments where many BSSs operating on the same channel overlaps creating the OBSS problem (Section 1.6.2). The network topology of the residential scenario is depicted in Figure 3.2.

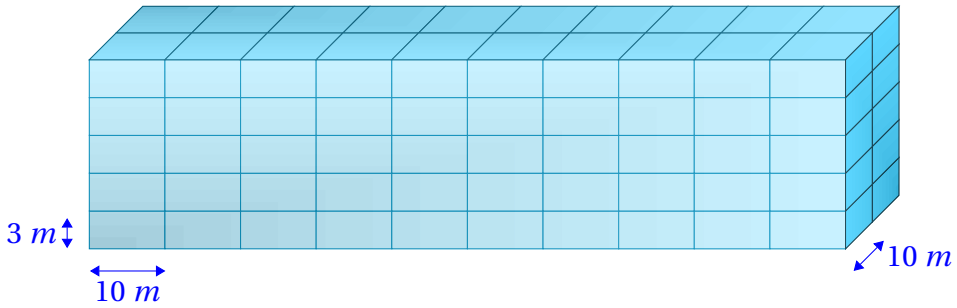

Figure 3.2 – Residential scenario building layout

It consists of a multistory building with story height of 3 m. Each floor is composed of 20 apartment units of 10 m × 10 m. The number of APs in the whole building is N_{AP}. These APs are randomly distributed over the totality of the units following a uniform distribution. By default, an AP is randomly located within its unit. However, there is an option to fix the location of all the APs in the center of their units. Each apartment unit that includes an AP has N_{STA} STAs randomly located (uniform distribution) inside it. By default, all the STAs of the unit X are associated with AP of unit X. The simulation parameters are set conformity with those chosen in the TGax simulation document [80]. The most important of these parameters are listed in Table 3.2 with their default value. Obviously, the main difference when comparing to the cellular scenario is the propagation path loss model. The same traffic parameters are used in both scenarios for the sake of throughput performance comparison.

Table 3.2 – Residential scenario parameters

Parameter	Value
General parameters	
Network topology layout	Regular multistory building composed of 5 floors. Each floor has 3 m height and contains 20 “10 m × 10 m" apartments
Default APs location	Randomly located inside the apartment
STAs location	Randomly located inside the apartment
Nodes elevation	1.5 m above the apartment’s floor level
Total number of APs	N_{AP} randomly distributed on the apartments
Number of STAs per apartment	N_{STA}
Frequency reuse	3
Standard version	802.11n
Simulation run duration	3 min
PHY Layer parameters	
Radio band	5 GHz
Bandwidth	20 MHz
Path loss	Path loss model in Equation (3.3)
Number of antennas for each device	1
OFDM Guard Interval (GI)	Long (800 ns)
MAC Layer parameters	
Maximum number of retransmissions	7
Default RTS/CTS setting	Disabled
Default rate control setting	Enabled
Traffic Access Category (AC)	AC_BE (best effort with default EDCA parameters)
Max size of Aggregated MSDU (A-MSDU)	3839 $Bytes$
Max size of Aggregated MPDU (A-MPDU)	8191 $Bytes$
Default transmission power - APs	21 dBm
Default transmission power - STAs	21 dBm
Default physical carrier sensing threshold - APs	-82 dBm
Default physical carrier sensing threshold - STAs	-82 dBm
Application traffic parameters	
Transport protocol	User Datagram protocol (UDP)
Uplink traffic	Full buffer
Downlink traffic	Full buffer

3.2.3 Evaluation metrics

Since the new standardization efforts are aiming at enhancing the real world performance of Wi-Fi networks, the metrics used to evaluate the simulated network performance must reflect real world QoE. TGax evaluation methodology document [83] defines the evaluation of spectrum efficiency improvement in both link level and system level simulations. For our system level simulations we use the following metrics to evaluate the system performance.

- Individual throughput (per-device) that is measured at the MAC level by the number of bits of MAC payload successfully received over the measurement period and forwarded to the higher layer. This metric is used to measure the user experience in the area covered by one or multiple BSSs in different simulation scenarios.
- Global throughout (or aggregate throughput) is the aggregation of all the per-device throughputs over the simulated network. This metric gives an overall idea about the capacity gain achieved by a proposed solution.
- Average throughput is obtained by averaging all the per-device throughputs over the measurement period. This metric provides a clear indication about the throughput gain experienced by a device in the simulated scenario.
- Cumulative Distribution Function (CDF) curves of the per-device throughputs that defines the percentage of devices having an individual throughput less than or equal certain throughput value. This metric is of paramount importance to study the fairness issues and the enhancements offered by the proposed solutions. Additionally, we have three different types of the CDF curves.
  - 5 percentiles: measures the minimum throughput of devices in all the BSSs of the simulated network.
  - 50 percentiles: provides a clearer indication about the average throughput of all the devices belonging to the different BSSs with a stress on the potential fairness issues between these devices.
  - 95 percentiles: measures the performance of the majority of the devices giving.

3.3 Simulation tools

Simulators are substantially important for the R&D community to evaluate new enhancements to standard-based protocols. Such importance is more pronounced when these enhancements are contributions to new standards. Calibrated simulators allow to compare different approaches and proposals in the same scenario or the same solution in different use cases. Network simulators for WLAN are either system level or link level depending on

the implementation of the MAC and PHY layers. Link level simulators are PHY layer centric that include very fine-grained wireless channel propagation models and bit level processing. Such simulations aim at studying the BER performance in terms of SNR values. By implementing the full transmission-reception chains, the focus is put on the performance of a single communication link between a transmitter and its receiver by evaluating its PHY capacity. On the other hand, system level simulators focus on the higher layers. For WLAN, the MAC layer protocols are finely implemented and simulated. In order to achieve higher scalability and lower simulation time on large scenarios, the PHY layer is simplified. The abstraction of the PHY is possible using BER to SNR lookup tables, analytical models, or other techniques. Despite the fact that the PHY layer is abstracted, system level simulators enable the evaluation of WLAN performance in real world scenarios by simulating the modeled system over time. A well established PHY model minimizes the impact of this abstraction on the system performance. NS-3 and OPNET are two recognized system level network simulators that are briefly presented in the rest of this section.

NS-3 [84], is the third generation of the popular communication network system simulator NS [2]. NS is an event-driven simulator written in C and C++ that is primarily used in research and academia. This simulator is an open source software publicly available under the GNU GPLv2 license [85] for research, development, and use. At the beginning of the project of this thesis, the latest release of NS-3 was the 3.16 that includes plenty of wireless modules such as LTE, WiMax and Wi-Fi. However, the Wi-Fi module was limited to the following functionalities:

- Basic 802.11 DCF with infrastructure and ad hoc modes,
- 802.11a, b, and g PHY layers,
- The EDCA and queueing extensions of 802.11e.

Neither High Throughput (HT) nor Very High Throughput (VHT) operation was provided by the standard Wi-Fi module of NS-3. An internal project within Orange Labs was launched to implement new features including:

- 802.11n and ac PHY layers (preambles and data rates),
- Channel bonding (operation on 40/80/160 MHz channels),
- MAC functionalities like frame aggregation (A-MSDU and A-MPDU),
- MU-MIMO.

[2] Stands for Network Simulator

At that time, the project was far from being completed and many features were partially implemented. For that reason, we choose to use OPNET instead for the continuation of the studies.

OPNET Modeler [3] [86] is a well known commercial product used by industrial engineers and academic researchers to model and simulate almost all communication technologies. It is widely used to test and demonstrate technology designs and proprietary wireless protocols. The simulations in OPNET are based on a discrete event-driven engine and a user interface to analyze and design communication networks. Standard OPNET models are written in C and structured using a Finite State Machine (FSM) that represents the different processing states of a modeled entity.

3.3.1 Overview of the WLAN node model in OPNET

In this section, we describe briefly the simulation model of a WLAN node in OPNET. As shown in Figure 3.3, the modeling of the PHY and MAC layers of a WLAN node is compromised of the "wlan_port_tx" (radio transmitter), the "wlan_port_rx" (radio receiver), and the "wireless_lan_mac". The higher layers of the Open Systems Interconnection (OSI) model (see Figure 1.1) are modeled by the rest of the processes as illustrated in Figure 3.3. The PHY layer functionalities are modeled through multiple pipeline stages. The radio transceiver pipeline consists of fourteen stages, most of which are implemented at the radio receiver side. The radio pipeline models the wireless channel by implementing the propagation and the error models. All the MAC layer protocols are modeled by the "wireless_lan_mac" process model.

The WLAN node model included in the OPNET Modeler 17.5 (the latest available version at the time) implements the following features:

- Basic 802.11 DCF and PCF with infrastructure and ad hoc modes,
- 802.11e EDCA full functionalities,
- Block ACK mechanisms,
- Frame aggregation (A-MSDU and A-MPDU),
- 802.11n PHY,
- 40 MHz HT operation.

[3] Renamed to Riverbed Modeler after the acquisition of OPNET technologies by Riverbed

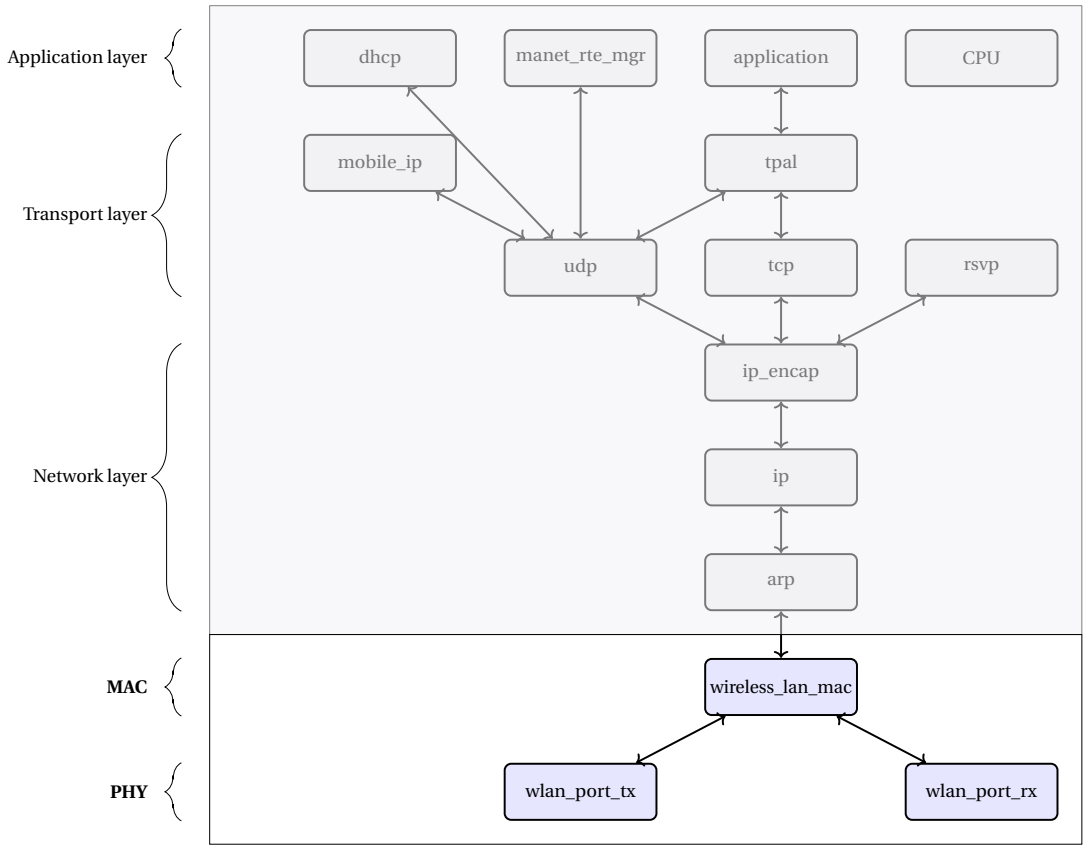

Figure 3.3 – OPNET simulation node model of a WLAN workstation

3.4 Improvements and modifications of the simulation model

Throughout the different phases of the thesis project, many modifications to the standard OPNET model have been made to enhance the simulation model or to add a new functionality.

3.4.1 Propagation channel model

The path loss model is implemented in the "wlan_power" pipeline stage at the radio receiver. The default OPNET 17.5 model implements the standard Friis path loss for wireless propagation with a path loss exponent equal to two. Which is a free space path loss model that in not appropriate for the scenarios described above. Accordingly, we added new models for path loss to the default simulation model. Typically, the International Telecommunication Union (ITU) Urban Micro (UMi) model defined by the ITU-R SG [87] for hexagonal cell layout as follows:

$$PL(d_{TR}) = 22.7 + 36.7\log(d_{TR}) + 26\log(f_c) \tag{3.1}$$

where d_{TR} is the distance separating the transmitter and its receiver expressed in meters, and f_c is the central frequency of the transmitted signal given in GHz. A modified version of this model is used within the cellular simulation scenario that is previously described in this chapter. This model is defined in [81] as follows.

$$PL(d_{TR}) = 23.3 + 36.7\log(d_{TR}) + 21\log(\frac{f_c}{0.9}) \tag{3.2}$$

Another implemented path loss model is that of the residential scenario. In this case, we take into account the penetration losses due to the walls of the different apartments. The resulting expression is as follows:

$$PL(d_{TR}) = 40.05 + 20\log(\frac{f_c}{2.4}) + 20\log(min(d_{TR},5)) + (d_{TR} > 5)35\log(\frac{d_{TR}}{5}) + 18.3F^{((F+2)/(F+1)-0.46)} + 5W \tag{3.3}$$

where F is the number of floors traversed by the signal before arriving to the corresponding receiver, and W is the number of walls traversed in both direction of the horizontal plan.

3.4.2 Error rate model

Before introducing the modifications made to the default, it is necessary to summarize briefly how error events are generated in OPNET. Recalling that the PHY layer is modeled through the radio pipeline stages. Whenever a transmission occurs throughout the simulated network, almost all the pipeline stages are executed at each receiver. The reception power of a packet is calculated at the receiver power radio pipeline stage ("wlan_power") basing on many factors such as the transmission power, the distance separating the transmitter from the receiver, the frequency, the antenna gains at the transmission and reception.

While receiving a packet, all the interfering signals arriving to the same radio receiver are accumulated by the interference noise stage ("wlan_inoise"). Accordingly, the SINR value is calculated at the ("wlan_snr") stage using the values already calculated in the previous stages of the pipeline (e.g., received power, interference, and background noise). In practice, the SINR is updated upon the arrival of any interfering signal and remains constant until the next interfering signal. Next, in the bit error rate model ("wlan_ber"), the probability of bit error (i.e., BER) is calculated during each constant SINR interval (packet segment). In the default OPNET implementation, the BER is obtained using the SINR value from a lookup table that corresponds to the given uncoded modulation scheme. The error allocation pipeline stage ("wlan_error") is responsible of estimating the number of bit errors in packet segment having a constant BER over the segment and the length of

the affected segment. The process continues over all the potential segments during the reception of the packet to find the cumulative number of bit errors in the entire packet. Basing on this final value, the error correction pipeline stage ("wlan_ecc") decides if the packet is successfully received or not using a preselected error correction threshold.

3.4.2.1 The problem of the default error model

The problem resides in the BER calculation. In fact, the predefined SINR to BER mapping are available per modulation type and required SINR per bit (i.e., $\frac{E_b}{N_0}$). However, the standard model in OPNET applies instead the SINR per modulated symbol (i.e., $\frac{E_s}{N_0}$). This erroneous calculation of the BER leads to a significant deviation from the correct values especially when the used modulation is higher. The impact of this error is shown in Figure 3.5 where the performance of the default OPNET error model is depicted. As a result, the minimum SINR values for: MCS_0,MCS_1, and MCS_2; MCS_3, and MCS_4; MCS_5, MCS_6, and MCS_7 are erroneously identical.

Furthermore, accepting or rejecting a received packet in the default OPNET model relies on the error correction threshold selected at the receiver. Practically, this threshold defines the maximum number of bit errors in a packet that can be corrected by some coding scheme. Accordingly, the error correction threshold can be set differently for different error correction code types. While this is an essential setting in modeling the coding scheme, there is no standard or documented way to set it. This aspect remains unclear in the standard error model of OPNET.

3.4.2.2 The new implementation of the error model

In a contribution to the public contributed models of OPNET Modeler [88], authors have reported the same problem in the default error model and propose to solve it by providing new modulation curves taking into account the different modulation and coding schemes. To calculate the $\frac{E_b}{N_0}$, the authors suggest to add a processing gain to the effective SINR calculated by the default model. Even if this improves the default model, but it is not the most comprehensive approach as authors themselves note. In fact, with the proposed solution, the issues related to the error correction code usage is always present. Determining the error correction threshold value that yields to a target Packet Error Rate (PER) value for a given SINR using a known MCS is not a straightforward process.

In our model, we implement a new error model that solves completely the shortcoming of the standard OPNET model. For the OFDM modulation, the implemented model description and its validation can be found in [89]. After calculating the uncoded BER using the SINR value (i.e., $\frac{E_s}{N_0}$ calculated in the "wlan_snr" pipeline stage) over each segment

of the packet using the analytical model described in [89] and [90], a binary convolution coded transmission with hard-decision viterbi decoding scheme is used to determine the PER. Practically, the coded BER is calculated using the following expression.

$$BER_{coded} = \frac{1}{2b} \sum_{d=d_{min}}^{\infty} \beta_d D^d \tag{3.4}$$

Where D is the probability that an incorrect decoding path of distance d is chosen and is given by $D = \sqrt{4p(1-p)}$, p is the uncoded BER shown in Table 3.3 where $Q(x) = \frac{1}{2} erfc(\frac{x}{\sqrt{2}})$ [4], d_{min} is the free distance of the convolutional code, b is given in Table 3.3, and β is the number of bits in error in each case that depends on the modulation and coding scheme and is given by Table 3.1.1 and Table 3.1.2 of the document [89]. Finally, the packet error probability is given in terms of the packet size in bits n_{bits} as follows.

$$PER = 1 - (1 - BER_{coded})^{n_{bits}} \tag{3.5}$$

Table 3.3 – Summary of the different bit error rate model parameters

MCS index	Modulation	R	Data rate ($Mbps$)	p	b
0	BPSK	1/2	6.5	$Q(\sqrt{2SINR})$	1
1	QPSK	1/2	13.0	$Q(\sqrt{SINR})$	1
2	QPSK	3/4	19.5	$Q(\sqrt{SINR})$	3
3	16-QAM	1/2	26.0	$\frac{3}{4}Q(\frac{\sqrt{SINR}}{5})$	1
4	16-QAM	3/4	39.0	$\frac{3}{4}Q(\frac{\sqrt{SINR}}{5})$	3
5	64-QAM	2/3	52.0	$\frac{7}{12}Q(\frac{\sqrt{SINR}}{21})$	2
6	64-QAM	3/4	58.5	$\frac{7}{12}Q(\frac{\sqrt{SINR}}{21})$	3
7	64-QAM	5/6	65	$\frac{7}{12}Q(\frac{\sqrt{SINR}}{21})$	5

In order to decide if a packet is successfully received and decoded by the radio receiver, a random packet error probability value is drawn from a uniform distribution. If the PER calculated by Equation (3.5) is lower than the random value, the packet is accepted and forwarded to the higher layer.

3.4.3 Rate control

One of the basic limitations of the standard WLAN model under OPNET is the absence of any link adaptation for variable transmission rate operation. The MCS used for data

[4] $erfc(x) = \frac{2}{\pi} \int_{t=x}^{\infty} e^{-t^2} dt$ is the complementary error function

transmission by a WLAN device is static throughout the simulation. However, a part of this thesis studies the implication of the rate control mechanisms on the performance. Accordingly, as we will discuss in details in Chapter 5, the rate control mechanism proposed by [91] has been implemented by modifying the "wireless_lan_mac" process model. By employing only local information, the transmitter determines the quality of the radio link and decides to switch accordingly to higher or lower data rate (i.e., MCS). The advantage such a mechanism is that it does not require any changes to the standard 802.11. Moreover since the radio link quality is determined basing on local information, no overheard is added to the system and the operation is fully distributed. The basic performance of this link adaptation mechanism is discussed in Section 3.5.

3.5 Baseline performance

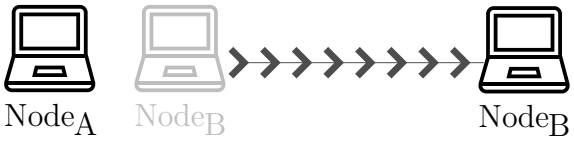

Figure 3.4 – Baseline performance simulation scenario

In this section we study the baseline performance of the modified simulation model. This serves as a point of reference for all the simulations conducted in the rest of this thesis. For the sake of this analysis, we consider a simple network scenario consisting of a single link that is illustrated in Figure 3.4.

Table 3.4 – Baseline performance scenario parameters

Parameter	**Value**
Standard version	802.11n
Radio band	5 GHz
Bandwidth	20 MHz
Path loss	Path loss model in Equation (3.2)
Background noise	-130 dBm
Number of antennas for each device	1
Maximum number of retransmissions	7
Transmission power	15 dBm
Physical carrier sensing threshold	-82 dBm
Traffic	Full buffer
Simulation run duration	5 min

This scenario consists of two WLAN devices (two OPNET WLAN node models), $Node_A$ that represents the transmitter node and $Node_B$ representing the receiver node. The default

simulation parameters are listed in Table 3.4. During the simulation run, the receiver node ($Node_B$) moves away from the transmitter.

3.5.1 Fixed Modulation and Coding Scheme (MCS)

Here we discuss the baseline performance using fixed transmission data rate (fixed MCS) throughout the simulation duration. The same simulation run is repeated for each one of the 8 MCSs listed in Table 3.3. The throughput received at $Node_B$ is continuously measured while this node moves away from $Node_A$ (the transmitter). At the same time, the corresponding SINR values of the successfully received packets are obtained and averaged over the measurement period. The same measurement period is used to calculate the throughput. Consequently we derive the throughput performance in terms of achieved SINR at $Node_B$. It is worth mentioning here that because of the absence of any source of interference, the SINR can be obtained through simple calculation using the reception power at $Node_B$ and the background noise shown in the table of parameters.

3.5.1.1 Default error rate model performance

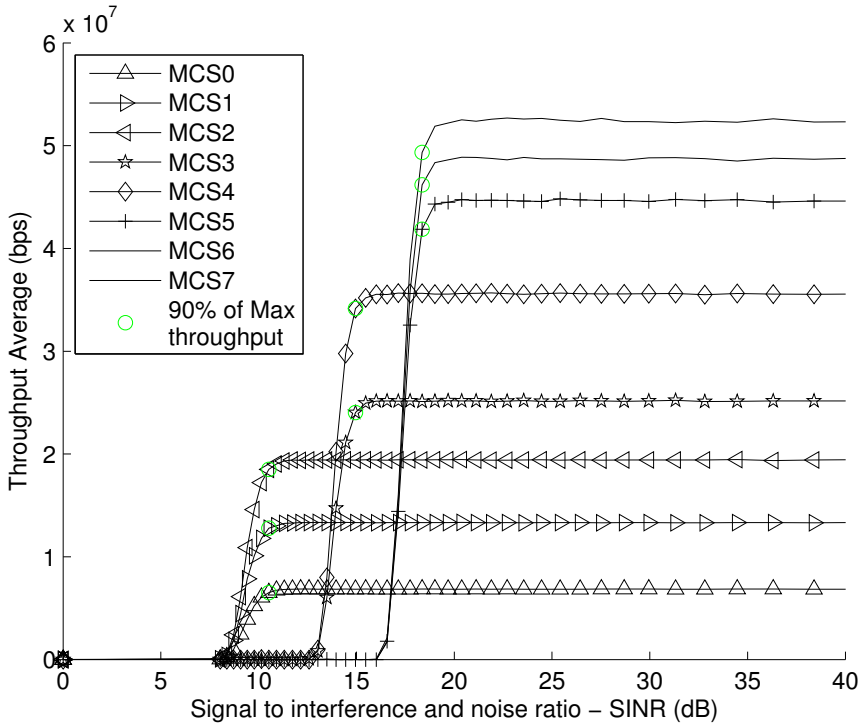

Figure 3.5 – Fixed MCS baseline performance using the default error rate model. Throughput measured at $Node_B$ in terms of SINR

.

First, we show the performance of the default implementation of the error rate model in OPNET 17.5 that is already discussed in Section 3.4.2. The throughput obtained by the

different MCSs is plotted in terms of the achieved SINR of the packets received by $Node_B$. As previously stated, the default error model does not consider the effect of the different coding schemes. The impact of this erroneous implementation is clearly visible in Figure 3.5.

The minimum SINR values needed for different MCSs using the same modulation scheme but not the same channel coding rate are identical. To highlight this fact, we plot, for each MCS curve, the point where the throughput attains 90 % of its maximum value. Indeed, this implies that the transmission ranges using these MCSs (having the same minimum SINR) are also identical. Obviously, this behavior is invalid and needs to be corrected for credible simulations for multi data rate operation.

3.5.1.2 Performance overview with the new error rate model

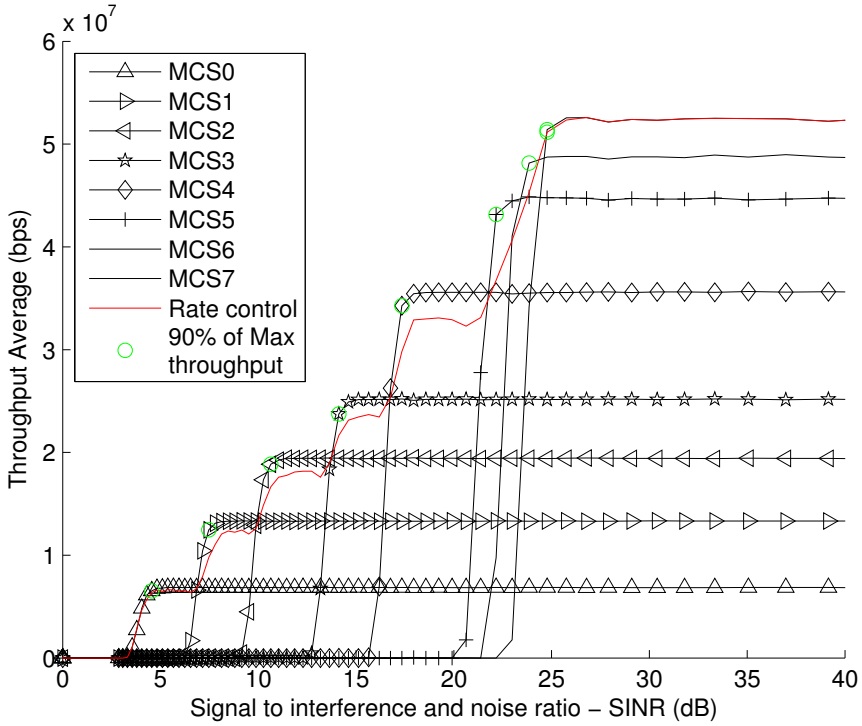

Figure 3.6 – Fixed MCS baseline performance using the modified error rate model. Throughput measured at $Node_B$ in terms of SINR.

To correct the flawed error rate model, we implement an entirely new error model as described in Section 3.4.2. In this Section we study the baseline performance of the simulation model using the new error rate implementation. In the beginning, using the same previous approach, Figure 3.6 illustrates the throughput achieved using the different MCSs in terms of SINR. Comparing to the default model performance in Figure 3.5, it is clear that the new error rate model is taking into account the coding scheme and is achieving realistic throughput performance.

It is interesting here to give an idea about the propagation distances accomplished by the different MCS configurations. The throughput achieved using each MCS is plotted in Figure 3.7 in terms of the distance traveled by the signal before reaching the receiver.

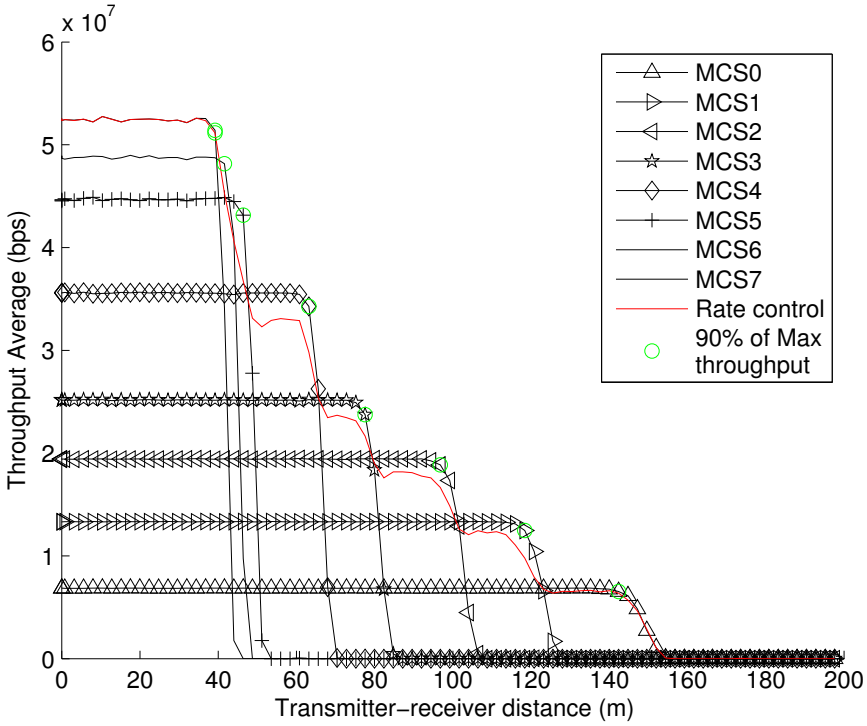

Figure 3.7 – Fixed MCS baseline performance using the modified error rate model. Throughput measured at $Node_B$ in terms of the distance separating $Node_B$ from $Node_A$.

3.5.2 Adaptive Modulation and Coding Scheme (MCS)

In order to evaluate the basic performance of the adaptive MCS scheme, we activate the rate control algorithm described in Section 3.4.3. The modified error rate model is used for this evaluation and for the rest of the thesis. The aim of this section is to validate that the implemented rate control mechanism is operating correctly. A more advanced study that analyses the different rate control approaches and their deficiencies is conducted later in Chapter 5.

The throughput achieved using the rate control mechanism is shown in Figure 3.6 in terms of SINR and in Figure 3.7 in terms of the transmitter-receiver distance. While $Node_B$ moves away from $Node_A$ the reception power of $Node_A$'s transmissions decreases. Hence, the SINR calculated at $Node_B$ decreases to the extent that a high MCS cannot be correctly decoded. Consequently, some frames are lost and retransmitted. At this point, the role of the rate control mechanism is to adapt the MCS in use to the situation. Accordingly, in this case (when transmitter-receiver distance increases), the rate control mechanism

uses lower MCS that are able to propagate further. What we have described is the expected correct behavior of the rate control implementation that is validated through the achieved throughput in Figures (3.6) and (3.7). As shown in these figures, the throughput curve of the rate control case is the envelope of all the fixed MCS curves.

3.6 Summary

The main objective of this chapter is to present the performance evaluation tools and the different scenarios that are used in this thesis to evaluate and analyze the performance of the multiple proposed solutions. The chapter starts by describing the simulation scenarios, their characteristics, and what are the perspectives of their design (what aspects of the future WLAN networks they are supposed to capture). Then, a brief discussion about the metrics used for the performance analysis is presented, their definition, and what they practically measure. Defining these scenarios is an important step that allows to investigate the strong and weak points of each enhancement in the light of representative real world circumstances.

Another important subject covered by this chapter is the simulation platform. A description of the most recognized network simulation approaches is provided. Then, two system level simulators, namely NS-3 and OPNET are highlighted before describing in details the WLAN simulation model provided by OPNET. After identifying some flawed aspects of the default WLAN model in OPNET, we provide a description of the modifications that we made to correct them. Finally, we carry out an analysis of the baseline performance of the simulation model that is needed as a reference point for the advanced simulation throughout the following chapters.

4 Enhancing spatial reuse in dense Wi-Fi environments

4.1 Introduction

In future's high density Wireless Local Area Network (WLAN)s, to improve the overall capacity of the network, optimizing the Media Access Control Layer (MAC) layer protocols and mechanisms is more than necessary. Traditionally, it's clear in the literature that Transmit Power Control (TPC) is identified as one of the most powerful tools for optimizing wireless networks performance and efficiency by managing interferences. However, TPC is not always possible to implement due to hardware and licensing limitations on one hand, and on the other, its unbalanced use results in starvation situations where some nodes can't achieve successful transmissions.

In the context of IEEE 802.11 WLANs, the Clear Channel Assessment (CCA) is an essential mechanism to assess the shared wireless medium for other currently occurring communications before initiating any transmission. Although the variety of WLAN environments and the specificity of each type of deployment, the standardized CCA mechanism has remained the same without modifications. As we show in this chapter, the adaptation of this mechanism is proving its effectiveness in enhancing the capacity of a high density system. This adaptation is preferable to TPC that behaves aggressively towards transmitters having lower transmit power as we discuss later.

4.2 Context and motivations

The increasing density in deploying WLANs is due to an exponential need for omnipresent coverage. Additionally, WLAN devices are supporting a wide variety of demanding applications and services such as voice, video, cloud access (for remote storage and computing) and hence capacity demand are aggressively increasing. While the massive deployment is necessary to meet these needs in coverage and capacity on an evolving basis, it raises the amount of interference between different Wi-Fi networks. This interference results in

sub-optimal user throughput due to contention [68], and therefore attenuates the global network performance. The neighboring Access Point (AP)s that operate on the same channel suffer from Co-Channel Interference (CCI) that may degrade severely the wireless communication quality. Since Wi-Fi operates on Industrial, Scientific and Medical (ISM) 2.4 and 5.8 GHz unlicensed radio bands, it is limited to a few number of orthogonal channels. Given the intent for omnipresent Wi-Fi, this lack of orthogonal channels quantity has made Overlapping BSS (OBSS) problem inevitable (see Section 1.6.2).

After two decades of targeting higher peak theoretical throughputs in a single link, standardization aims are changing. Today, the intention is to improve the efficiency of the current IEEE 802.11 WLAN on the way to support this drastic increasing need for capacity, omnipresence, and higher performance. It's clear that the MAC layer protocols of the IEEE 802.11 need many optimization efforts to enhance the WLAN performance in today's dense deployments. In this context, the IEEE announced the creation of a new IEEE 802.11 Study Group (SG) to define the scope of a future IEEE 802.11 amendment with the aim of enhancing the efficiency and the performance of WLAN challenging deployments. The 802.11 High Efficiency WLAN (HEW) SG [6] has led to the creation of a new Task Group (TG) within the 802.11 Working Group (WG): the 802.11ax. At the time of writing this thesis, the TGax is preparing the new 802.11 MAC and Physical Layer (PHY) specifications considering use cases including dense network environments with large numbers of access points and stations. The reader is referred to Section 2.9 for more details concerning the predicted timeline of the standardization process.

One of the most promising solutions, that is discussed since the earliest meetings of the HEW SG, lies on increasing spatial reuse between neighboring networks as discussed earlier in this thesis in Section 2.6. The power level used for transmission dictates the interference projected on neighboring communication links. Therefore, controlling the transmission power (TPC) is suggested in the literature [92] to reduce the CCI damage and increase the amount of spatial reuse. In fact, this solution was brought from the power control adopted in cellular networks. As we will see later in this chapter, due to the difference between the channel access scheme adopted in WLAN and the cellular networks, TPC is not the best technique to enhance spatial reuse in 802.11 WLANs because it alters the symmetry of the communications.

Yet, another technique, that is specific to WLAN's contention-based access, has proved its efficiency in managing interferences and spatial reuse. This technique consists on optimizing and adapting the CCA mechanism. More precisely, the standard physical carrier sensing part of this mechanism (see Section 1.3.2 for details) is identified as overprotective in dense deployments [93]. Compared to TPC, CCA adaptation can bring the same results but without harming severely the symmetry of the communications. Another advantage is that a node benefits from applying CCA threshold adaptation without relying on all the

neighboring nodes to do so. While TPC fails if not all the adjacent WLANs apply it, CCA adaptation doesn't need their compliance.

4.3 Hidden and exposed node regions

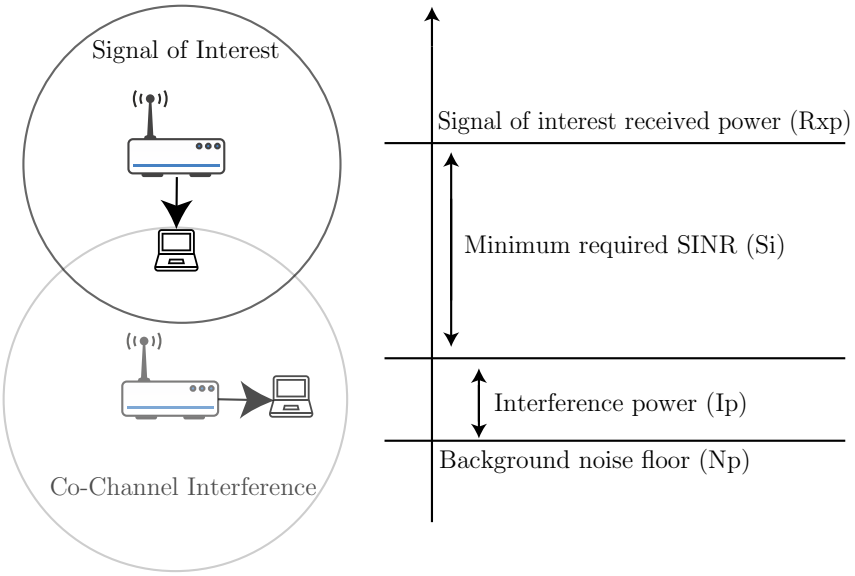

Figure 4.1 – Signal to Interference and Noise Ratio (SINR)

Depending on the data rate used to transmit, a communication is sustained only if the corresponding Signal to Interference and Noise Ratio (SINR) at the receiver exceeds certain mandatory minimum value. As represented in Figure 4.1, S_i is the minimum required SINR for a Modulation and Coding Scheme (MCS) of index i, namely MCS_i. This is translated by the following expression.

$$SINR \geq S_i \tag{4.1}$$

Where the SINR is defined by

$$SINR = \frac{Rx_p}{N_P + I_P} \tag{4.2}$$

where Rx_p is the power of the signal of interest at the receiver, N_P is the background noise level and I_P is the interference power at the receiver's close vicinity. Notably, CCI is one of the greatest challenges threatening wireless communications. This challenge is more pronounced in dense WLAN environments since co-channel Basic Service Set (BSS)s are deployed closer to each other. Basing on the illustration of Figure 4.1, the interference region is defined as the region around the receiver where any co-channel transmission (considered as CCI) can decrease the SINR of the signal of interest below the acceptable threshold S_i. The region around a node in which any occurring transmission is detected,

thanks to the carrier sensing mechanism, is termed the detection region of that node.

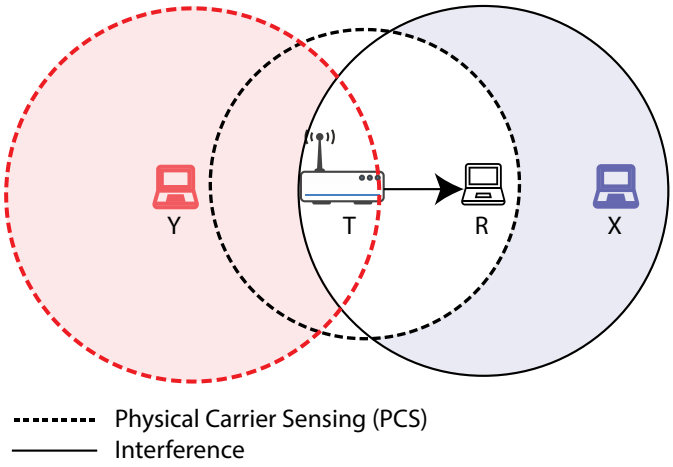

Figure 4.2 – Hidden and exposed node regions

In the literature, two main problems are identified to be detrimental to WLAN performance. Namely, the hidden and exposed node problems caused by the distributed nature of the channel access in IEEE 802.11 WLANs [94] [95]. To explain these problems, we consider the scenario shown in Figure 4.2. When a potential interferer X is outside the detection range of a transmitter T, X is defined as a hidden node with respect to T. Note that, in order to threaten the transmission of T, X must be in the interference region of R, the intended receiver of X. In this case, it is impossible to achieve successful transmissions by X and T simultaneously because X transmissions will corrupt the reception at R. Otherwise, if X is outside the interference region of R, it can transmit at the same time as T without any problem.

In another situation, T may be in the detection region of node Y. Thus any transmission initiated by T will be detected by Y and, as a consequence, the medium is inferred to be busy. Although, as shown in Figure 4.2, Y is outside the interference region of the intended receiver of T (i.e., R) and therefore its transmission will not interfere with the ongoing transmission of T. In that way, Y is banned unfairly from transmitting and is termed an exposed node. This loss of possible transmission opportunities decreases the overall performance of the network. This decrease is more significant when the deployments become more and more dense.

To cope with the hidden and exposed node problems, one can think about identifying all the possibly hidden and/or exposed nodes and trying to avoid them in a per-communication basis. However, any similar approach is highly cost-ineffective in terms of complexity and overhead. In practice, a node may be considered as 'hidden' with respect to a specific transmitter-receiver communicating pair but not with respect to another pair. Additionally, a reception may be corrupted due to the superposition of two or more signals

transmitted simultaneously by two or more devices that are not considered as hidden nodes if they are transmitting individually. Moreover, any mechanism aiming at identifying hidden and/or exposed nodes cannot be designed without adding more overhead burden to the network (e.g., exchanging statistics and new management frames, etc.).

4.4 Transmit Power Control (TPC)

As mentioned before, TPC is the traditional intuitive way to manage interferences and increase the spatial reuse in wireless networks. As shown in Figure 4.3, decreasing the transmission power of the possible interferers helps to fulfill the required SINR (S_i) at the neighboring receivers. In that way, the transmission ranges in the neighboring networks are shrunk and hence more reuse is permitted.

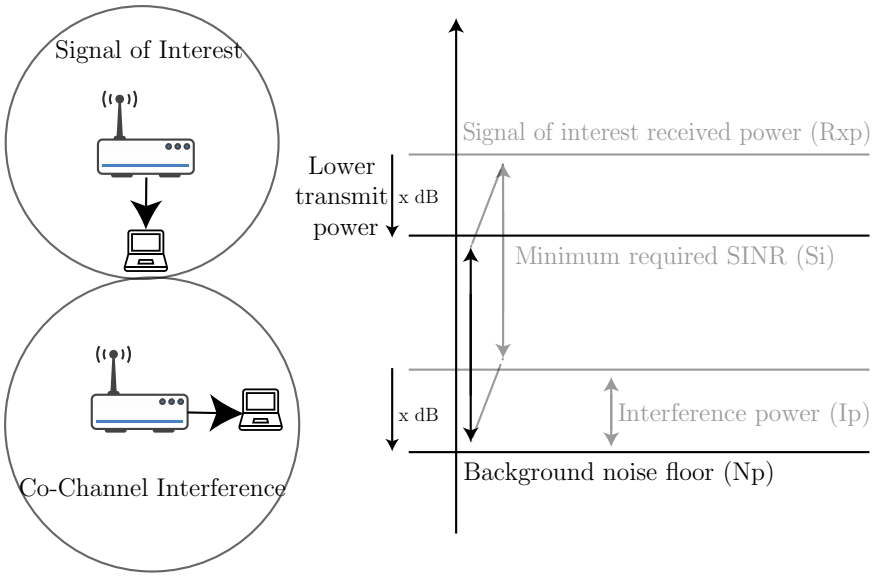

Figure 4.3 – Transmit Power Control (TPC)

4.4.1 Transmit Power Control (TPC) in cellular networks

In cellular networks, a frequency division multiplex is possible inside the same cell. Thus, the transmission power is controlled by the base station individually for each user apart from others. This kind of power control is used in almost all the mobile communication technology (e.g;, Code Division Multiple Access (CDMA), Wideband Code Division Multiple Access (WCDMA), Long-Term Evolution (LTE), etc.). Such closed loop scheme is possible thanks to the centralized hierarchy present in cellular networks and the adopted Frequency Division Multiple Access (FDMA) scheme. Unfortunately, in WLANs, all the nodes of the same BSS share the same frequency and we can't always assume a centralized deployment.

Despite this, TPC stays important due to two reasons:

- Mobile nodes are energy limited devices and they have to use efficiently their power resources. TPC is a key solution to decrease the power consumption.

- The transmission power dictates the interference power perceived at neighboring nodes.

Mainly for these reasons, researchers tried to find solutions to adapt TPC to WLANs.

4.4.2 Challenges of Transmit Power Control (TPC) in WLAN systems

It is interesting to note that TPC is standardized since 2003 by the IEEE 802.11h amendment [96] but it has hardly found its way to the production stage. Although, for networks with centralized controllers, TPC is relatively simple to implement, it was only applied on APs but never on Station (STA)s. In such situations, the APs that are connected to a common controller apply TPC to reduce their transmit power, however the STAs associated to these APs still transmit with their full power. The main reason behind this is related to the nature of TPC which is selfless. If a node reduces its transmission power by applying the TPC, that will promote the neighboring transmissions because they are no more bothered by the transmissions of that node. Consequently, the other nodes will benefit directly and not the node that applied the TPC. Another industrial constraint when envisioning TPC for WLAN devices is the cost of its implementation. As we earlier discussed in Chapter 1, Wi-Fi chips for end user devices are designed to be cheap. The presence of high performance amplifiers increases the cost of a Wi-Fi chip. Even in the recent discussions of the different TGax, it's clear that there are no incitations to apply TPC in STAs.

Moreover, in networks which lack a central regulator, power control proves to be much more difficult to implement and apply. Since centralized coordination between nodes is very difficult, it is necessary for each node to regulate its own transmission power autonomously. This behavior creates an asymmetric application of TPC and hence different transmission powers for different nodes. Again, the selfless feature of TPC will prevent real networks from taking this approach. The detrimental effect of this asymmetry is argued by many researchers [97] [98] [99]. It has been proven that in such situation, TPC leads to the starvation of the unprivileged nodes [100], [62]. Actually, TPC is more problematic to achieve in a distributed manner because it will foster higher power transmitters, that are not applying power control, at the expense of lower power transmitters that are applying it.

4.5 Physical Carrier Sensing (PCS)

Recalling that the Distributed Coordination Function (DCF) function described by the IEEE 802.11 standard [5] is based on a well known medium access scheme, the Carrier Sense Multiple Access with Collision Avoidance (CSMA/CA). The multiple access to the communication medium is defined by CSMA/CA to be contention-based. In that way, all the nodes in the same physical area compete to transmit on the half-duplex medium of a single frequency. This physical area is termed "contention domain". While one node is transmitting, all other nodes of the same contention domain must wait until it finishes. The decision whether a node is in the same contention domain of a transmitter is based on the value of the Physical Carrier Sensing (PCS) threshold that is part of the CCA mechanism (see Section 1.3.2 for more details about CCA). Briefly, if the in-band signal energy crosses this threshold, CCA is held busy until the medium energy is below the threshold again.

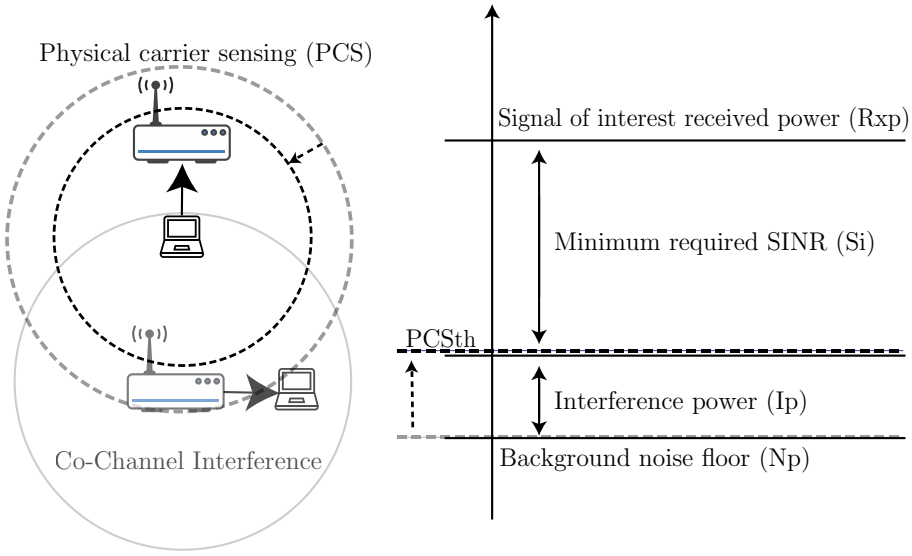

Figure 4.4 – Physical Carrier Sensing (PCS)

Due to the direct role of the carrier sensing mechanism in accessing the shared medium, specifically the PCS, its adaptation is indeed effective in managing interferences and leveraging the spatial reuse in WLANs. Interestingly enough, the adaptation of the PCS is one of the solutions currently discussed in the newly created IEEE 802.11ax TG. As will be shown in the sequel, this promising solution is highly efficient in dense environments. The most important feature of this approach is that there is an incentive to adopt it in production. Contrary to TPC, the node applying PCS adaptation will benefit directly from its application.

The current carrier sensing mechanism is over conservative in today's dense environments. An important number of nodes in these dense networks are exposed to the transmissions

of the neighboring co-channel networks. Thus, the available spectrum is not efficiently exploited and the system is loosing a great amount of possible spatial reuse. In carrier sensing adaptation, instead of decreasing its transmission power, a node will decrease its sensitivity in detecting signals in its environment. In Figure 4.4, the PCS threshold is increased so that tolerable interferences are prohibited from triggering busy channel assessments. Consequently, in situations where the signal of interest is received with a power sufficiently higher than the interference power, the reuse between neighboring networks will be possible.

Let us take a simple example from real world deployment scenarios to explain the effect of modifying the PCS threshold. This example includes two neighboring BSSs depicted in Figure 4.5. For a PCS threshold equal to T_{1a}, the PCS range of AP_1 (equal to R_{1a}) covers the STA_{2x} that's associated to AP_2 of the neighboring WLAN. The previous statement means that AP_1 is not able to transmit at the same time as STA_{2x}. This fact is very harmful for the BSS_1, since AP_1 is obliged to stay silent when STA_{2x} is transmitting. Add to this the fact that, in almost all WLANs, the most important amount of data is directed from the AP towards its STAs. Clearly, the PCS range R_{1a} is reducing the aggregated capacity of this network by restricting possible concurrent transmissions. Now let's consider T_{1b} (given $T_{1b} > T_{1a}$) as the PCS threshold of AP_1. Here, in contrast to the previous case, the PCS range has been shrunk sufficiently (R_{1b}) to let simultaneous transmission for both AP_1 and STA_{2x} and thus increasing the spatial reuse.

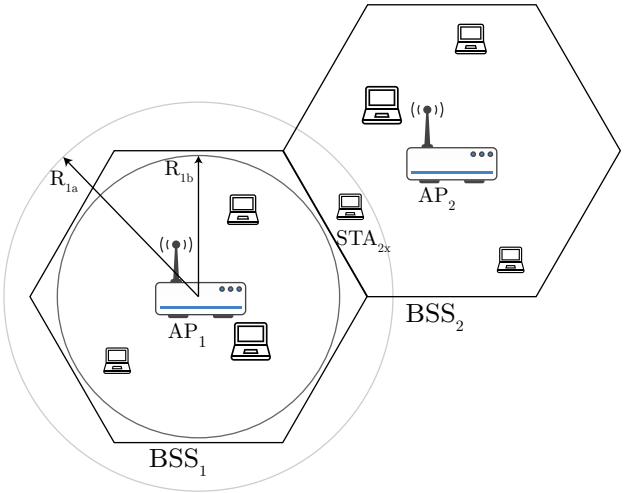

Figure 4.5 – Increasing spatial reuse with Physical Carrier Sensing (PCS) – an example

It's worth pointing out that simultaneous transmissions of STA_{2x} are still received by AP_1, but the latter ignores them because their received power is below the new PCS threshold T_{1b}. However, these transmissions are treated by AP_1 as interferences. So, if STA_{2x} is highly loaded and there are other devices belonging to neighboring BSSs and having the same effect on AP_1, one can imagine a drop in the achieved SINR at AP_1. This fact brings

to light the necessity of establishing a trade-off between spatial reuse and interference level. Furthermore, the results' analysis reveals that in dense environments, thanks to short distances, the SINR values stay high enough assuring successful transmissions.

As shown in the previous example, if the carrier sensing threshold is increased, more concurrent transmissions are permitted. Additionally, by decreasing the carrier sensing (protection) region, the number of contending devices decreases and hence the probability of synchronous collisions is reduced. However, generally speaking, this behavior may involve more interference because the communication range of the node will decrease and it becomes less aware of other concurrent transmissions. Interestingly enough, the simulations prove that in dense environments this behavior is of minor importance due to short distances between transmitter-receiver nodes in dense environments and the capture effect discussed in Section 1.6.2.2.

4.5.1 Increasing the PCS threshold in high density deployment scenario

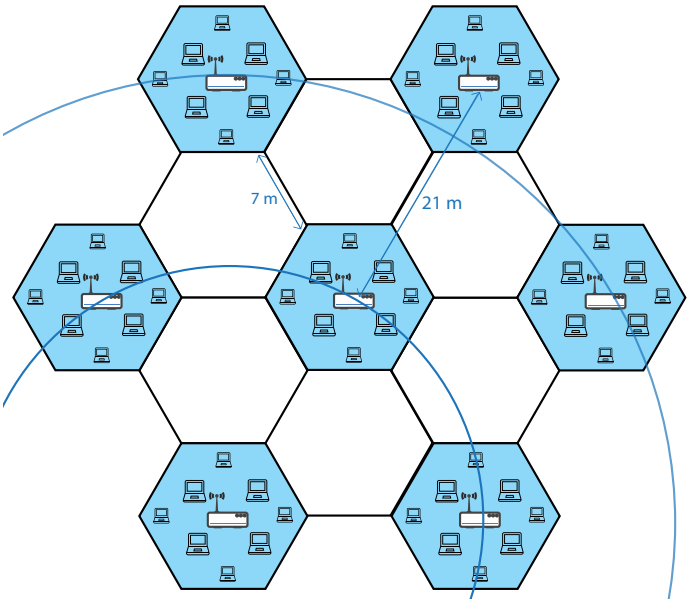

Figure 4.6 – Cellular scenario network topology

In this section, we consider the cellular scenario previously described in Section 3.2.1. The cellular topology illustrated in Figure 4.6 consists of 6 BSSs forming the first tier around a central BSS. If we consider the south east corner BSS, then the central BSS is in the first tier and the BSS of the north west corner of the topology belongs to the second tier. The default settings depicted in Table 3.1 are used for the simulation setup. However, for these simulations, to be as close as possible to a current real world deployed network, the TPC is only applied on the AP. For that purpose, the APs are transmitting at 6 dBm and the STAs at 15 dBm. Additionally, all the traffic is generated by the APs towards their STAs (i.e., only downlink). Since all the traffic is in downlink, the transmission power configuration will

not affect severely the symmetry of the communications.

First, we discuss the results obtained when varying the PCS threshold between −82 and −65 dBm on all the devices of the considered scenario. The global (or aggregate) throughput is plotted in terms of PCS threshold variation. In Figure 4.7, one can distinguish three important parts: −82 dBm, from −81 to −75 dBm, and from −74 to −65 dBm. As considered in the IEEE 802.11 standard's CCA requirements [5] (Section 20.3.21.5.2) and as widely used in todays WLANs, −82 dBm is the default PCS threshold value, and thus it is used as a reference to compute the gain percentage when using other threshold values. In the present document, we refer to this value as $PCS_{default}$. When PCS threshold is less or equal to −82 dBm, any considered AP affects the transmissions of the STAs belonging to the second tier of the cellular topology. In other words, all the devices of the first tier and some STAs belonging to the second tier are exposed to the transmissions of the considered AP. Starting from −81 dBm, all the devices of the second tier can transmit simultaneously with the considered AP, therefore the global throughput of the network increases (to 100 %).

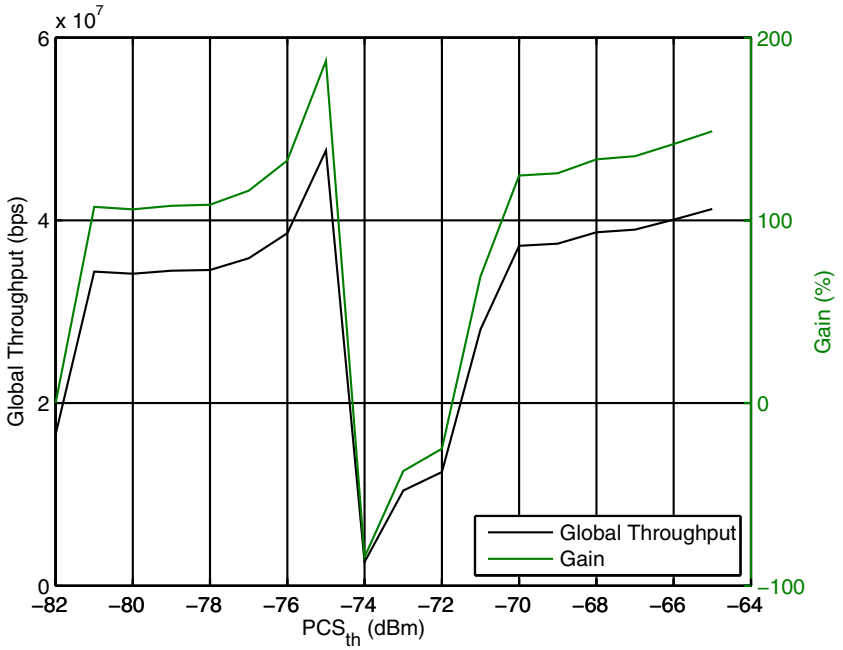

Figure 4.7 – Achieved global (aggregate) throughput gain in terms of PCS threshold

Considering any AP in the cellular scenario (Figure 3.1), let it be AP_x, the received power of its transmissions at one of the closest APs (belonging to the first tier around AP_x) is −75 dBm. The maximum global throughput gain is obtained when the PCS threshold is set to −75 dBm (190 %). For this value, the PCS range covers the APs of the first tier, meaning that the considered AP_x can't transmit simultaneously with these APs. When these concurrent transmissions are permitted (PCS threshold equal to −74 dBm), the gain becomes negative. Note that at this point the majority of the STAs belonging to neighboring

BSSs are prohibited from responding to their APs, thus a mass of retry attempts and unsuccessful transmissions lead to this critical decrease. The gain returns to a positive value when the PCS threshold exceeds $-71\ dBm$. Recalling that the closest STA belonging to a BSS of the first tier receives AP_x's signal at $-71\ dBm$. Since the traffic is downlink, the STAs only communicate management frames with their corresponding APs, mainly Acknowledgment (ACK) frames. Since all the STAs belonging to the BSSs of the first tier can transmit concurrently with AP_x only when their PCS threshold is greater than $-71\ dBm$, the throughput gain becomes positive beyond this value. After that, the gain continue it's recover because the BSSs are more and more isolated in terms of PCS range. This isolation is translated into a higher amount of concurrent transmissions.

At this stage, it is clear that the PCS threshold as defined in the standard is over conservative. As illustrated in Figure 4.7, increasing the value of this threshold in densely deployed WLANs allows higher global throughputs. The gain in aggregate throughput attains 190 %: a two folds increase compared to the conventional performance. However, choosing the appropriate value of PCS threshold is an essential process to obtain the maximum gain. A direct conclusion of these first observations is that the network topology must be considered in this process. The best PCS range depends on the distance separating a device from the other co-channel devices belonging to neighboring BSSs. In this experiment, we considered the same PCS for all the devices of the topology (i.e., a network wide PCS). However, it is interesting to study a per node dynamic PCS adaptation. This is the subject of the following sections of this chapter.

4.5.1.1 In presence of legacy devices

As previously discussed in Chapter 1, a primary consideration in the IEEE 802.11 WG standardization process is ensuring backward compatibility with older standards. Future devices implementing the new specifications must interoperate with legacy devices when their are present in the same BSS. To investigate the effect of the presence of these legacy devices, a test of the previous section is conducted here without increasing the PCS_{th} on N STAs (i.e., N legacy STAs). These N STAs are selected randomly from the different BSSs. Two simulation sets are carried out for $N = 8$ (14 % of STAs) and $N = 16$ (28 % of STAs). The key question is: how much aggregate throughput will be affected by the presence of these legacy STAs?

Figure 4.8 illustrates the global (aggregate) throughput achieved in each situation. One can clearly observe the effect of the presence of the STAs that are not modifying their threshold (i.e., the decrease in the aggregate throughput). However, this effect is more severe when the PCS_{th} of the non-legacy devices exceeds $-74\ dBm$. Above this value, the PCS of each node does not cover other nodes belonging to other BSSs. In such a situation, the presence

of STAs behaving differently will be more noticeable. The legacy STAs, having their PCS_{th} fixed to $-82\ dBm$, are prohibited from gaining access to the channel by the transmissions of the neighboring APs. Thus, they will not be able to acknowledge their APs. Therefore, their destined traffic will experience higher losses, which results in the decrease of the throughput. As depicted in Figure 4.8, the legacy devices representing 14 % and 28 % of the total number of STAs result in throughput losses up to 37 % and 68 % respectively (for PCS_{th} greater than $-70\ dBm$). Both previous cases still have important gains in global throughput when the PCS_{th} is optimally adapted.

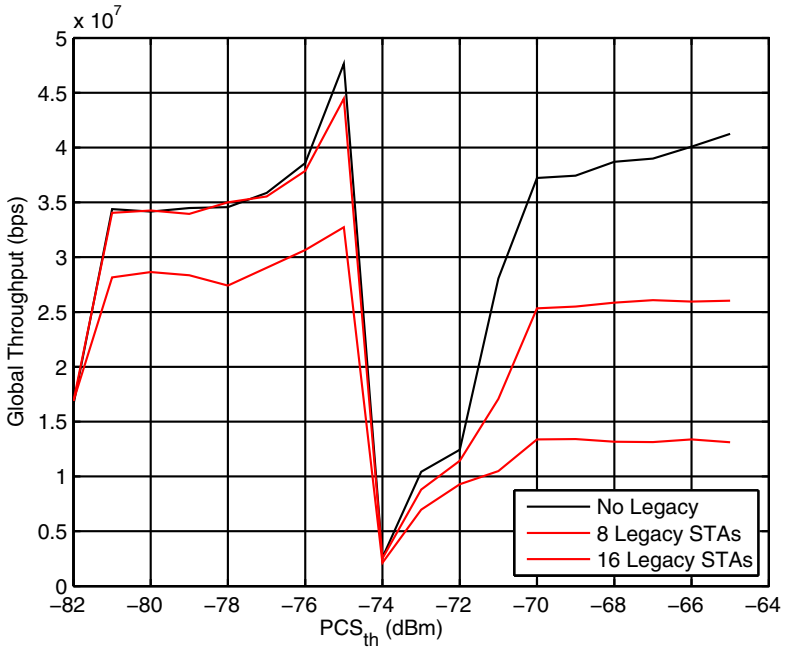

Figure 4.8 – Achieved global (aggregate) throughput in terms of PCS threshold - The effect of legacy devices

From the above, it's clear that the growing heterogeneity of the present WLANs in terms of standard versions can't be ignored. This diversity challenge and the obligation of being backward compatible with older devices (legacies) necessitate flexible, autonomous, and dynamic solutions. While centralized schemes can be envisioned in specific cases where a single authority is responsible of all the co-located WLANs, distributed schemes are preferred for the majority of WLAN deployments. In the following sections, we propose a dynamic distributed adaptation of the PCS mechanism and we evaluate its performance in real world scenarios.

4.6 Communication model

Before coping with any data link layer adaptation, we define a convenient propagation model for wireless communication to understand the radio channel characteristics. The

received power at the intended receiver is expressed in its linear form as follows:

$$Rx_p(d) = Rx_p(d_0)\left(\frac{d_0}{d}\right)^{\gamma} \tag{4.3}$$

where d is the distance between the transmitter and the receiver and d_0 is a reference distance close to the transmitter (e.g., $d_0 = 1m$).

4.6.1 Transmission range

The maximum distance that a signal can travel before being successfully received by its destination is the transmission range. The latter distance is calculated in the absence of any interference, and is given by

$$Rx_R = d_0\left(\frac{Rx_p(d_0)}{max(N_P S_i, Rx_{th})}\right)^{\frac{1}{\gamma}} \tag{4.4}$$

where S_i is the minimum required SINR, Rx_{th} is the reception threshold that denotes the minimum power level of a received signal, and N_P is the noise power. Actually, the receiver can decode a received packet with high probability of success if and only if the received power exceeds Rx_{th} and the corresponding SINR is greater than S_i. It's worth to mention that both, S_i and Rx_{th}, depend on the used coding and modulation schemes.

In dense WLAN with high spatial reuse, the transmission ranges are quite small and the Rx_{th} is greater than $N_P S_i$. Consequently, the transmission range becomes

$$Rx_R = d_0\left(\frac{Rx_p(d_0)}{Rx_{th}}\right)^{\frac{1}{\gamma}} \tag{4.5}$$

4.6.2 Physical Carrier Sensing range

The distance from a transmitter within which any detected communication causes the deferral of the pending transmission is defined to be the Physical Carrier Sensing range (PCS_R). This range is given by

$$PCS_R = d_0\left(\frac{Rx_p(d_0)}{PCS_{th}}\right)^{\frac{1}{\gamma}} \tag{4.6}$$

where PCS_{th} is the Physical Carrier Sensing threshold expressed here in Watts, which is defined as the minimum power level sensed by the transmitter to infer that the medium is busy. If the sum of signals power sensed in the medium is less than PCS_{th}, then the transmitter reports the medium as *idle* and initiates its pending transmission.

4.6.3 Interference range

As defined earlier in Section 4.3, the interference range can be expressed as follows.

$$I_R = d \left(\frac{1}{\frac{1}{S_i} - \left(\frac{d}{d_0}\right)^{\gamma} \frac{N_P}{P_r(d_0)}} \right)^{\frac{1}{\gamma}} \tag{4.7}$$

If we consider an interference limited environment where noise power is negligible (i.e., $N_P \approx 0$), the interference range becomes

$$I_R = S_i^{\frac{1}{\gamma}} d \tag{4.8}$$

4.7 New margin-based Physical Carrier Sensing (PCS) adaptation

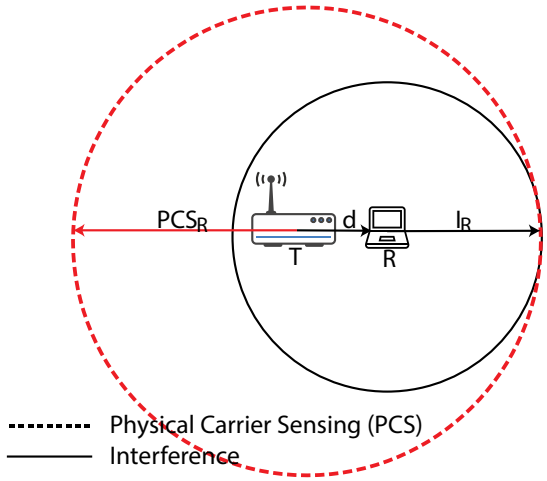

Figure 4.9 – Hidden node problem mitigation

The aforementioned definition of the hidden node problem leaves no doubt about the fundamental role played by the PCS in mitigating it. Simply, the interferer located outside the carrier sensing region of a given transmitter is considered as a hidden node for that transmitter. So, if all nodes located in the interference region are covered by the PCS, the hidden node problem will be resolved. The previous statement is illustrated in Figure 4.9 and translated by the following expression:

$$PCS_R \geq d + I_R \tag{4.9}$$

Using Equation (4.3), (4.6), (4.8), and (4.9) we obtain

$$PCS_{th} \leq Rx_p(d) \frac{1}{\left(1 + S_i^{\frac{1}{\gamma}}\right)^{\gamma}} \tag{4.10}$$

Supposing that the powers in the linear form are expressed in milliwatts, in logarithmic form, the previous equation is expressed as follows

$$PCS_{th}[dBm] \leq Rx_p(d)[dBm] - \gamma 10 \log\left(1 + S_i^{\frac{1}{\gamma}}\right) \tag{4.11}$$

Let M be the value needed to cover the hidden node region. The minimum value of this margin M is given by

$$M[dB] \geq \gamma 10 \log\left(1 + S_i^{\frac{1}{\gamma}}\right) \tag{4.12}$$

Increasing M more than the needed value to cover the hidden region will create the previously described exposed node region. As explained before, the presence of exposed nodes in the network decreases the system's spatial reuse because possible concurrent transmissions are prohibited by the conservative PCS. For that reason, the margin M must be set to the minimum value allowed by Equation (4.12) in order to prevent exposed situations.

4.7.1 Dynamic physical carrier sensing adaptation

In order to confirm the efficiency of PCS in enhancing spatial reuse in dense deployments and hence increasing the aggregate throughput of the network, a dynamic adaptation algorithm is proposed here and evaluated in the following section. The incentive behind this dynamic scheme is to cope with variability of the wireless channel and the randomness of the interference levels in space and time. In the proposed scheme, each device adapts its PCS threshold in terms of the power received from its communication peer. For instance, in an infrastructure BSS, all the communications are held between an AP and a STA. In such a case, the STA adapts its PCS threshold according to the power level received from its AP and vice-versa. This adaptation consists in adding an appropriate margin value to the received power to prevent hidden regions. Therefore the PCS threshold of each device is obtained as follows

$$PCS_{th}[dBm] = Rx_p[dBm] - M[dB] \tag{4.13}$$

where PCS_{th} and Rx_p are expressed in dBm, and M is the margin value in dB. We call this margin-based PCS adaptation scheme Physical Carrier Sensing Adaptation (PCSA).

A STA uses the algorithm depicted in Figure 4.10 to calculate the reception power level Rx_p used in Equation (4.13). Since an AP transmits periodically beacon frames that are robustly modulated, we chose to use the reception power of beacons in when the PCSA is applied at the STA. Moreover, the STA calculates a moving average of the beacon frames received power (Avg_{Rxp} expressed in its linear form) to ensure smooth adaptation of the PCS particularly when the wireless channel quality is severely fluctuating.

Input : Beacon forwarded to the MAC layer
Output : Received power average value (Avg_{Rx_p})

Rx_p: received power
Avg_{Rx_p}: moving average of Rx_p

```
while True do
    if beacon received from AP then
        get Rx_p of the received beacon
        if First beacon after update then
            Avg_Rxp = Rx_p
        else
            Avg_Rxp = 1/2 (Avg_Rxp + Rx_p)
        end
    end
end
```

Figure 4.10 – Algorithm used by the Station (STA) to calculate the received power (Rx_p) that is used for the margin-based dynamic Physical Carrier Sensing Adaptation (PCSA)

An AP applies the same expression (Equation (4.13)) to adapt its PCS, however, the calculation of the Rx_p differs of that of a STA. As described in the algorithm shown in Figure 4.11, the AP uses the minimum reception power from its associated STAs (Min_{Rx_p}). This prevents the creation of hidden STAs inside the same BSS. Accordingly, the AP records the reception power of all the associated STAs before running the PCSA. The $Min_{Rx_p}Ready$ is set to *True* by the algorithm in Figure 4.11 when the Min_{Rx_p} value is ready to be used by the PCSA. After receiving packets from all the associated STAs ($H = A$), if the AP receives a packet from an already associated STA, the new Min_{Rx_p} is calculated as the average of its old value with the new minimum reception power. This is meant to tolerate the fluctuations of the communication channel.

Following the PCSA, the PCS threshold of a STA is adapted depending on the position of that STA, the distance separating it from its AP, and the wireless channel quality. In that sense this scheme takes into account the topology of the WLAN system. Firstly, the PCSA runs at the AP, then at the STAs. The PCSA is conceived to be run periodically during the operation of the network. However, it is highly important to trigger PCSA when a new STA

attaches to the network.

Input : Packet forwarded to the MAC layer
List of associated STAs
Output : Minimum received power value (Min_{Rx_p})
Minimum received power ready ($Min_{Rx_p}Ready$)

Rx_p: received power
Min_{Rx_p}: the minimum received power
$Min_{Rx_p}Ready$: set to True when the Min_{Rx_p} is ready
STA_{addr}: the MAC address of an associated STA
A: set of associated STAs' addresses
H: set of heard STAs' addresses

```
while True do
    if packet received from a STA then
        get STA_addr
        get Rx_p of the received packet
        if First packet after update then
            H = ∅
            Min_Rx_p = Rx_p
        else
            if Rx_p < Min_Rx_p then
                if H = A then
                    Min_Rx_p = 1/2 (Min_Rx_p + Rx_p)
                else
                    Min_Rx_p = Rx_p
                end
            end
        end
        if STA_addr ∉ H then
            update H
        end
        if H = A then
            Min_Rx_p Ready = True
        else
            Min_Rx_p Ready = False
        end
    end
end
```

Figure 4.11 – Algorithm used by the Access Point (AP) to calculate the received power (Rx_p) that is used for the margin-based dynamic Physical Carrier Sensing Adaptation (PCSA)

4.8 Evaluation and discussion

To evaluate the performance of PCSA, we consider the cellular scenario described in Chapter 3 Section 3.2.1. The network topology defining this scenario is illustrated in Figure 3.1. Table 3.1 lists the simulation system parameters related.

4.8.1 Physical Carrier Sensing Adaptation (PCSA) performance

Initially, it is interesting to show the effect of the adaptation on the aggregate throughput in these dense network scenarios. In this chapter, we are not studying the implications of the rate control mechanism that will be the subject of Chapter 5. Accordingly, to isolate the effect of rate control on the performance of PCSA and TPC, we chose in this part not to use any rate control, hence we fix the transmission data rate. Specifically, all the transmitters are configured to transmit using the MCS_7 (64-QAM modulation scheme and 5/6 coding rate).

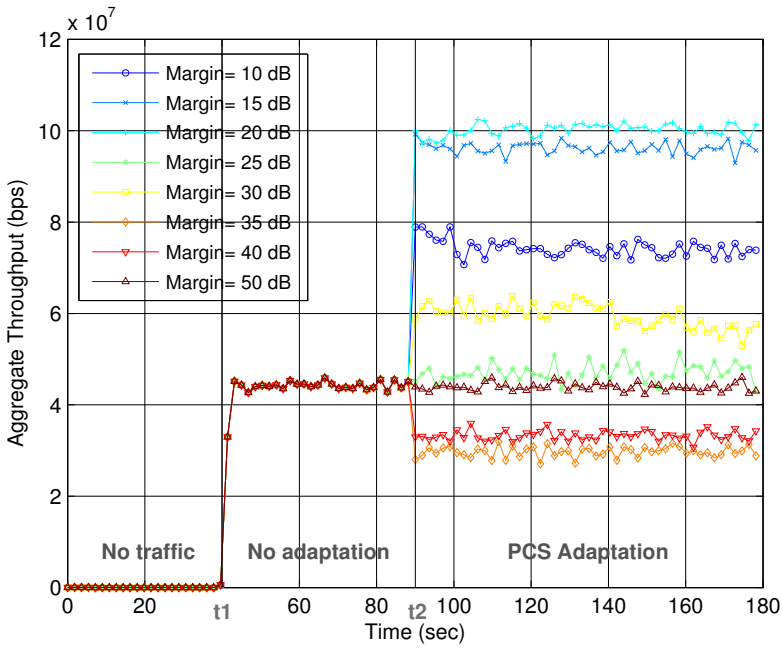

Figure 4.12 – Aggregate throughput performance of the margin-based Physical Carrier Sensing Adaptation (PCSA)

For different margin values, Figure 4.12 depicts the aggregate throughput with respect to the simulation time. This throughput includes all traffic successfully received by the MAC layer of all nodes. All the nodes start their transmissions at $t1 = 40s$ but they don't apply the PCSA until $t2 = 90s$. In the interval between $t1$ and $t2$, the PCS_{th} is set to the standard value of $-82\ dBm$. This interval simulates the conventional operation of currently deployed WLANs described previously as over-conservative because of the large carrier

sensing range.

After adapting the PCS_{th} using Equation (4.13), the carrier sensing range is contracted. Thus, more concurrent transmissions are permitted, and as a consequence, as shown in Figure 4.12, the aggregate throughput is largely increased for some margin values. It is interesting to note here that the aggregate throughput is not increased for all the values of M. The performance of each value is related to the number of co-channel nodes covered by the protection region. For instance, large margin values lead to carrier sensing ranges smaller than the minimum PCS_R and thus create detrimental hidden node problems. For that reason, in the results shown in Figure 4.12, the margins greater than 40 dB lead to lower aggregate throughput. The best aggregate throughput is achieved with a margin M equal to 20 dB. For this margin value, the application of PCSA leads to a gain of 126 % in aggregate throughput (from 45 $Mbps$ to 102 $Mbps$).

4.8.2 Comparable Transmit Power Control scheme

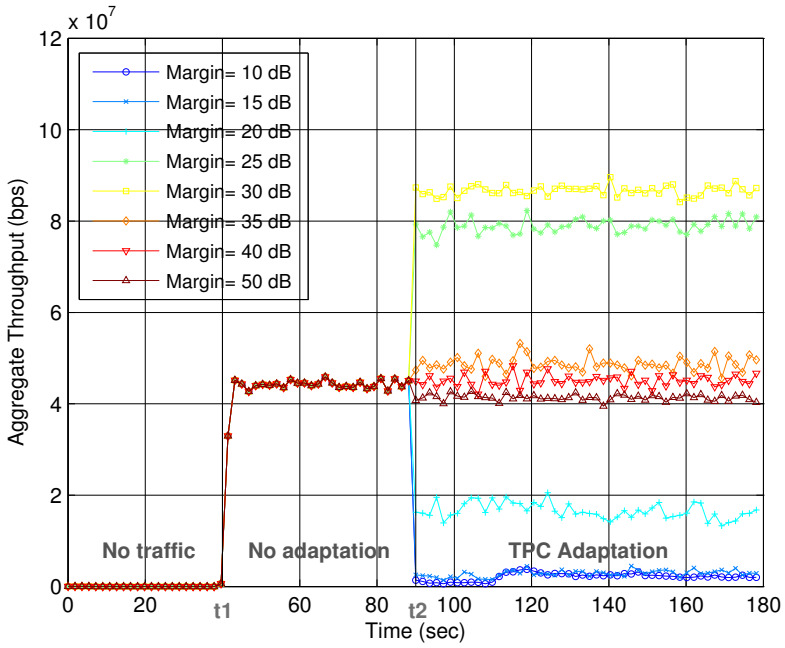

Figure 4.13 – Aggregate throughput performance of the margin-based Transmit Power Control (TPC)

This section introduces a new TPC algorithm that is fairly comparable to the PCSA described above. Each node adapts its transmit power so that its transmission is received at a margin above the traditional PCS_{th} (-82 dBm) by the intended receiver. In that way, the shrinking ratio of the sensitivity range is maintained the same as the PCSA case. This adaptation algorithm is used to compare the performance of TPC versus PCSA.

Figure 4.13 shows the aggregate throughput obtained before applying TPC ($t1 < t < t2$)

and after its application ($t > t2$) for different margin values. For the cellular scenario, the highest aggregate throughput is obtained with a margin equal to 30 dB. Furthermore, when using lower margin values, the TPC adaptation leads to inconsiderable aggregate throughputs. This is due to the very low transmit power that does not succeed in satisfying the required SINR (S_i). Interestingly enough, PCSA outperforms TPC which achieves around 93 % of maximum gain in aggregate throughput (from 45 $Mbps$ to 87 $Mbps$).

Another potential inconvenient for the TPC is related to the transceiver hardware aspect. Actually, with lower margins, the resulting transmit powers are extremely low. Unfortunately, for hardware limitations, it is difficult to transmit or receive using these insignificant power values. The applicability of TPC on the existing 802.11 network interface cards is questionable as shown in the work carried out in [101]. Inevitably, this problem must be considered when comparing TPC to other approaches like PCSA. In the future, the evolving technology may be able to cope with this limitation.

4.8.3 PCSA performance in presence of peer-to-peer communications

In this section we study the impact of the presence of Peer-to-Peer (P2P) pairs on the performance of PCSA in dense WLAN deployments. For this study, we consider the cellular scenario with two different cases basing on the location of the P2P pairs in the cellular topology with regards to the infrastructure BSSs. In the first case, as depicted in Figure 4.14, we place a P2P pair inside each cell containing an infrastructure BSS. In the second case, we move each pair to the neighboring empty cell as shown in Figure 4.15 (all the pairs are moved the same distance in the same direction). All the devices of the simulated network, including the P2P devices, are applying PCSA at the adaptation stage (starting at $t2$). Recalling that each cell that is shown empty in the cellular scenario contains in practice an infrastructure BSS operating on an orthogonal channel to that of the BSSs figuring in the topology. Consequently, we study here also whether it is more beneficial for the whole system performance to configure the P2P pairs located inside a cell with the same channel of that cell or another orthogonal channel. For these simulations, the same setup used in the previous section applies here with a margin $M = 20\ dB$. Each P2P pair is configured with a full buffer User Datagram Protocol (UDP) flow in one direction. The distance separating the two devices belonging to the same pair is only 1 m.

The results in terms of aggregate throughput of both cases are plotted in Figure 4.16. The 'P2P inside' curve represents the throughput achieved by the first case (Figure 4.14). In both cases, PCSA succeeded to enhance the performance, however, in the second case (i.e. 'P2P outside'), the enhancement is very slight. In practice, at the adaptation interval, the P2P are able to transmit simultaneously with the neighboring BSSs when they are placed outside their cells (second case). In the first case, even after the adaptation, the P2P

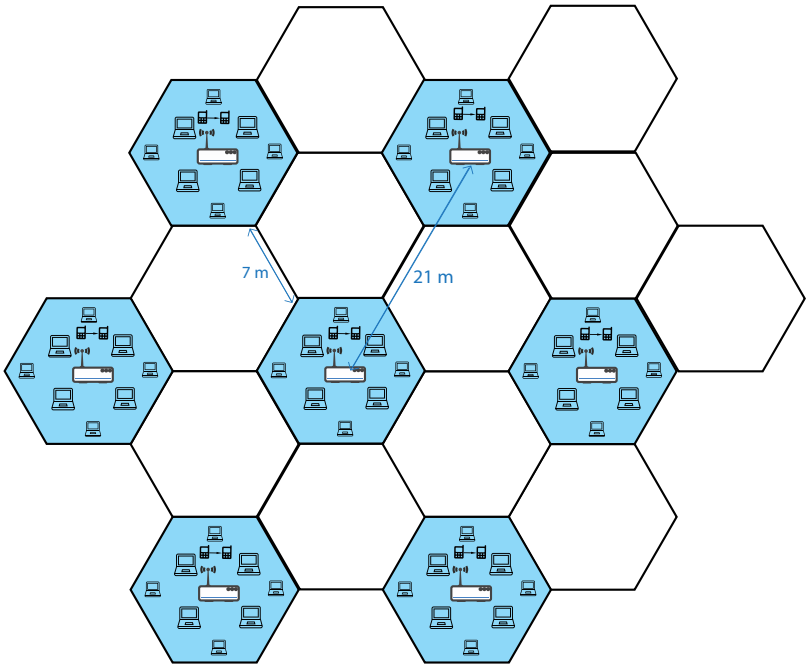

Figure 4.14 – Cellular scenario network topology in presence of Peer-to-Peer (P2P) pairs – case 1: inside

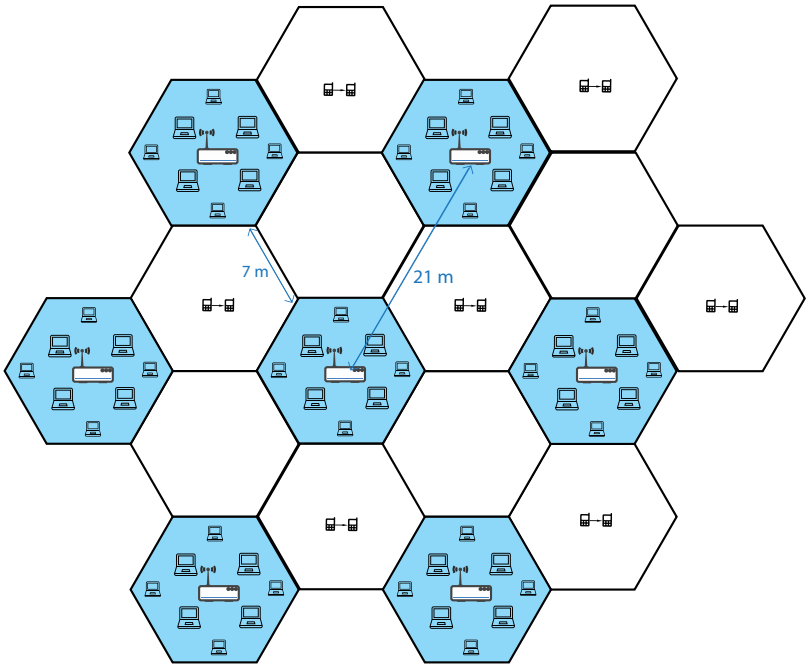

Figure 4.15 – Cellular scenario network topology in presence of Peer-to-Peer (P2P) pairs – case 2: outside

pairs and the infrastructure BSS remain in the same contention domain and hence defer for the transmissions of each other. According to our results, in high density scenarios with frequency reuse patterns, a better throughput performance is guaranteed with PCSA when the P2P pairs operate on the same frequency channel of the BSS with which they are overlapping.

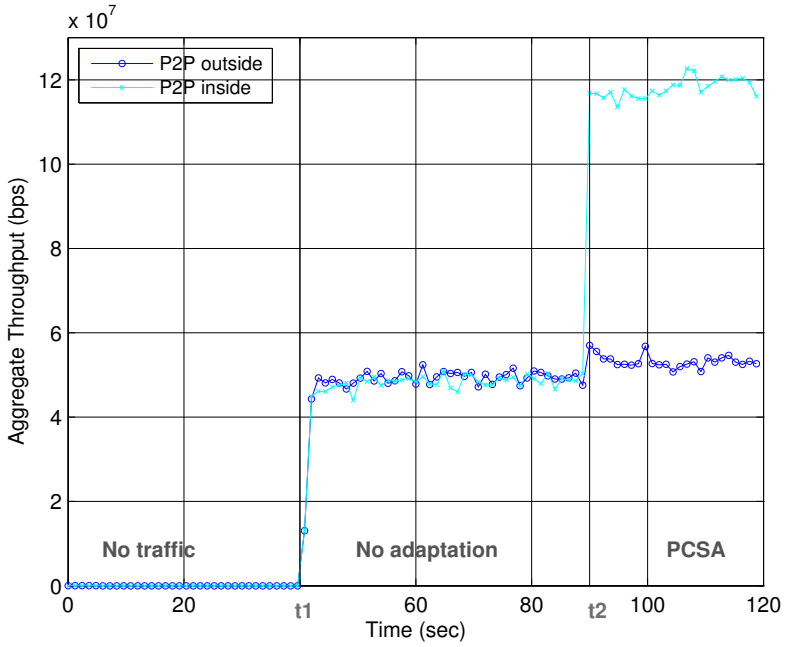

Figure 4.16 – Aggregate throughput performance of Physical Carrier Sensing Adaptation (PCSA) in presence of Peer-to-Peer (P2P) pairs

4.8.4 PCSA versus TPC in presence of legacy devices

Wi-Fi deployment is somehow chaotic [68] in terms of diversity in managing authorities and lack of planning [102]. Therefore, any proposed enhancement must take into account the possibility of coexistence between different versions of devices that are not adopting the same solutions (i.e., legacy devices). In this scene, it is necessary to study the impact of legacy devices on the performance of a system applying new solutions.

In this section, the performance of the two approaches, PCSA and the TPC, is studied in the presence of legacy devices that do not implement either the PCSA or the TPC algorithms. The simulation conducted in this study considers the cellular scenario with 7 legacy STAs (12.5 % of the total number of STAs). These legacy STAs are selected randomly, one from each BSS. In the sequel, we investigate the impact of the presence of these STAs on the aggregate throughput of the system for both adaptation approaches: the PCSA and TPC.

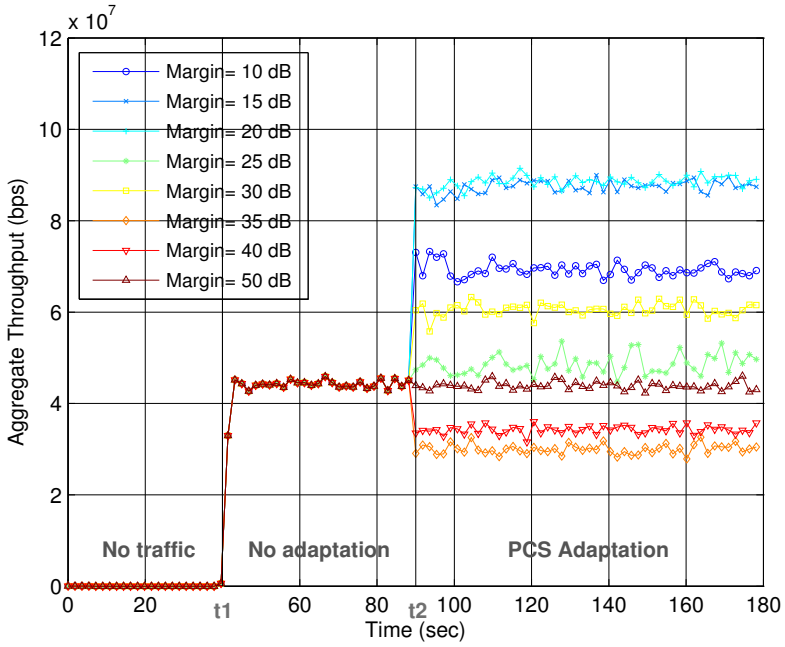

Figure 4.17 – PCSA performance in terms of aggregate throughput in presence of legacy devices

Figure 4.17 and Figure 4.18 show the resulting aggregate throughput when applying the PCSA and the TPC schemes, respectively. It is clear that PCSA shows greater ability to tolerate the presence of legacy devices than TPC. For the PCSA approach, the maximum aggregate throughput is decreased by 10 % compared to the case where there are no legacy device (Section 4.8.1 Figure 4.12). On the other hand, in the case of TPC, comparing the results of Figure 4.13 and 4.18, we can see that the presence of 7 legacy STAs causes more than 35 % of aggregate throughput decrease. While all other STAs are decreasing their transmit power according to the previously described algorithm, these 7 STAs continue

transmitting using their highest power. Therefore, as described earlier in this chapter, the STAs transmitting with higher power dominate the channel access. The other STAs that apply the TPC remain exposed to the ongoing dominating transmissions.

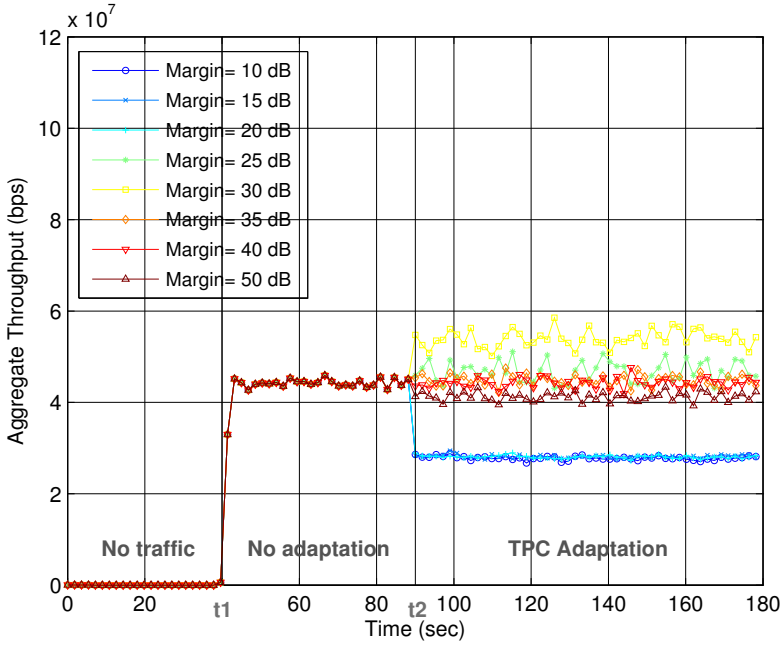

Figure 4.18 – Margin-based TPC performance in terms of aggregate throughput in presence of legacy devices

As a conclusion of this section, results show that in the case of TPC, the devices that don't apply TPC will have more chance to transmit. However, in the PCSA case, the advantage is for the devices that apply the adaptation because they are able to transmit simultaneously with others since they are no more exposed. To cope with the increasing density of WLANs, the medium access mechanisms that are based on contention must be somehow aggressive. Thanks to the short distances between the transmitters and their receivers, the SINR condition (Equation (4.1)) is satisfied even with the presence of co-channel simultaneous communications. This is due mainly to the capture effect described in Section 1.6.2. The aim of PCSA is to adapt the PCS mechanism properly to the density of the environment in a way to increase the spatial reuse.

4.8.5 Physical Carrier Sensing Adaptation (PCSA) versus Optimal-rate Clear Channel Assessment Adaptation (ORCCA)

In [63], authors perform an analytical study of the CCA implications in environments where co-channel APs are deployed in a regular lattice. CCA threshold is the term used by the authors to refer to the PCS threshold. They conclude after this analysis that using optimum CCA threshold in high density networks is substantially important for better

throughput performance. However, the authors argue that the optimization problem that they formulated in their analytical study cannot be analytically generalized and solved for other random topologies. For that reason, authors propose a heuristic algorithm, named Optimal-rate Clear Channel Assessment Adaptation (ORCCA) that sets a network wide CCA threshold (i.e., the same value for all the devices) of a given managed network purely based on channel measurements. Following this algorithm, each AP keeps track of the signal strengths (I_P) of all the neighboring co-channel APs. Authors assume that the interference level at a STA is equal to the interference level at the serving AP which is a restrictive assumption. ORCCA assumes that all the APs of the network are managed by a central controller and that they send measurement reports periodically to that controller. Accordingly, ORCCA is a centralized scheme that can't be applied to unmanaged WLAN deployments.

Following ORCCA, each AP calculates the maximum allowable interference level while supporting data rate i to communicate with the associated STA having the weakest received signal strength. This is calculated as follows:

$$I_i = \left(\frac{Min_{Rx_p}}{S_i}\right) - N_P \tag{4.14}$$

where Min_{Rx_p} is the weakest Rx_p from the associated STAs, S_i is the minimum SINR required for data rate i, and N_P is the background noise level. If $I_i > 0$, then the CCA threshold value of the concerned AP to support data rate i is equal to I_i. Otherwise, data rate i cannot be supported in the BSS. Accordingly, all the APs of the managed network report to the controller their calculated CCA thresholds for the different modulation and coding schemes. Additionally, after sorting the different reception power levels of its neighboring APs transmissions in ascending order (i.e., $I_{P_1} < I_{P_2} < ... < I_{P_M}$), each AP finds the smallest index m such that

$$\sum_{l=1}^{M} I_{P_l} = \sum_{l=1}^{m} I_{P_l} + \sum_{l=m+1}^{M} I_{P_l} \tag{4.15}$$

and

$$\sum_{l=m+1}^{M} I_{P_l} < I_i \tag{4.16}$$

Basing on the index m, each AP calculates γ_i, which is the achievable throughput when $(m+1)$ APs share the channel capacity using the modulation and coding scheme i. The capacity is simply considered as the data rate offered by the scheme i. However, in practice, as explained earlier in Chapter 1, due to the MAC overhead, especially the time spent by the

transmitter while contending to gain access according to DCF, the achieved throughput cannot reach the offered PHY data rate. This is another restrictive assumption of ORCCA.

Having all the CCA_i and γ_i values from all the APs, the controller performs an exhaustive search to determine the CCA threshold value ($\geq CCA_i$) that maximizes the network throughput. This throughput is equal to the aggregation of all the γ_i values.

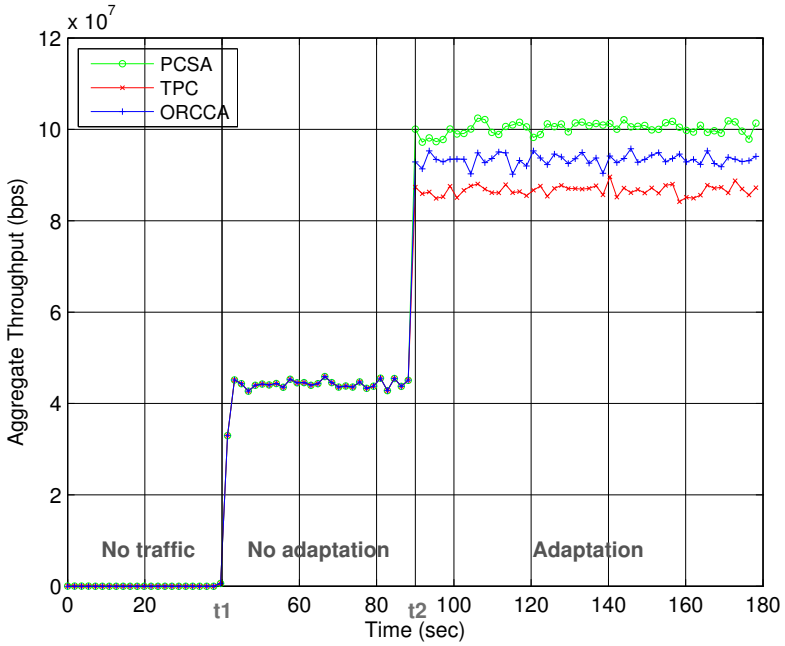

Figure 4.19 – Aggregate throughput performance: Physical Carrier Sensing Adaptation (PCSA) versus Optimal-rate Clear Channel Assessment Adaptation (ORCCA)

For comparison purposes, we implement ORCCA in our simulation model and we analyze its performance having the same conditions and configurations as in Section 4.8.1. In Figure 4.19, we show the aggregate throughput achieved with three different schemes: ORCCA, PCSA, and TPC. In their evaluation, authors of [63] show that their proposed mechanism improves the aggregate throughput by about 260 % in a regular lattice topology with saturated downlink only traffic. In our scenario, because of the higher deployment density and the bidirectional traffic, ORCCA results in around 100 % improvement in the aggregate throughput. However, as shown in Figure 4.19 and discussed in Section 4.8.1, PCSA outperforms ORCCA and TPC by achieving about 120 % of gain in global throughput. This has many explanations, firstly, the authors assume a symmetric communication channel in the sense that the interference level at the AP is considered to be equal to that at the STA and vice-versa. Secondly, ORCCA uses a network wide value for PCS which limits the adaptability of the mechanism. Additionally, in terms of complexity, PCSA is much simpler than ORCCA to be implemented in real networks. On one hand, it does not need periodic channel measurements, on the other hand there is no need for any supplementary overhead to process and exchange the collected measurements. Moreover, determining

the optimum CCA threshold in ORCCA lies on an exhaustive search over i (MCS index) and l (AP index). This raise a question about the complexity and the scalability of ORCCA. For instance, 802.11ac supports up to 80 different MCSs for a single spatial stream systems and up to 640 MCSs for 8 spatial streams. Multiplying the number of supported MCSs by the number of APs results in an important number of combinations. To conclude, as we have shown and discussed, PCSA is more efficient in terms of throughput performance, complexity, and overhead.

4.9 Summary

In this chapter, we highlighted the importance of increasing the spatial reuse in dense networks. When co-channel APs are deployed closer to each other, the default CSMA/CA mechanism behaves over-conservatively. This behavior prevents the network densification from attaining its goal which is increasing the capacity of the WLAN system. Instead, due to the OBSS problem, the neighboring co-channel WLANs share the transmission airtime and hence the capacity of the channel.

To cope with this over-protection problem, two mechanisms are presented: the control of the transmission power (TPC) and the adaptation of the physical carrier sensing (PCSA). While TPC is widely used in cellular wireless networks technologies, we show that its use in WLANs is critical and needs the compliance of all the neighboring BSSs which is not feasible for the majority of WLAN deployments. These deployments are highly independent and does not belong to the same management entity. The presence of legacy devices makes things even worst when dealing with TPC, because these devices cause the starvation of the TPC compliant devices.

The adaptation of the PCS mechanism is proposed as an alternative solution to increase the spatial reuse without harming the legacy devices. Increasing the PCS threshold show an important potential in leveraging the capacity of densely deployed WLANs. For a dense IEEE 802.11n network topology, our simulations show a global gain of 190 % in aggregate throughput compared to the current bound assumed by the standard MAC layer protocols. However, a static threshold is not the most adequate solution given the fact that the access mechanism and the amount of endured interferences depend on the location of the device and the topology of the network. Consequently, a dynamic adaptation (i.e., PCSA) is introduced in this chapter permitting an effective way to adapt the PCS mechanism locally without any coordination between devices. This distributed approach is needed due to the fact that the majority of WLAN deployments are not centrally coordinated, unmanaged, and unplanned. The proposed mechanism is evaluated in relevant high density WLAN deployments and has shown its ability to enhance spatial reuse even in presence of legacy devices where TPC fails. Furthermore, we showed that PCSA outperforms ORCCA, a

centralized CCA adaptation mechanism proposed in [63]. In the next chapter, we study the performance of PCSA in presence of conventional rate control mechanisms. Moreover, a detailed study concerning the fairness of PCSA is conducted in Chapter 6 and a new solution is proposed.

5 Improved rate control mechanisms

5.1 Introduction

In the previous chapter, we proposed the Physical Carrier Sensing Adaptation (PCSA) mechanism to increase the spatial reuse in a dense Wireless Local Area Network (WLAN) scenario. In the evaluation of PCSA, a fixed data rate was assumed. However in WLANs, the data rate control is an important mechanism that needs to be adapted for better performance. The interest of the present chapter is to investigate the performance of PCSA in presence of rate control.

As detailed in Chapter 1, the IEEE 802.11 standard [5] supports a wide variety of transmission rates. By employing different combinations of signal Modulation and Coding Scheme (MCS), a large number of bit rates is possible. For example, an IEEE 802.11n [12] device is able to transmit over eight different data rates using only one single spatial stream (see Section 1.4.6). With Multiple-Input Multiple-Output (MIMO) systems, the number of possible data rates may reach 24. This multiple rate capability offers a wide range of supported transmission modes and hence the ability to adapt the used mode to the network environment. In other words, the transmitter is able to select the most suitable MCS based on the status of the communication channel. While low MCSs can tolerate higher amount of interferences, higher MCSs can offer higher data rates.

While the standard [5] lists the MCSs supported by each Physical Layer (PHY) specification with their associated data rates (see Table 1.3 and 1.4), it does not describe which MCS to be used and in which circumstances. In practice, like other aspects that does not alter the interoperability between different WLAN products, the standard leaves the question of MCS selection to the manufacturers. In the literature, many efforts were made to design efficient rate adaptation algorithms. The current products in the market are implementing different proprietary solutions to cope with this issue. The majority of these solutions are based on the well-known Automatic Rate Fall-back (ARF) algorithm that was implemented

initially by Lucent in its WaveLan-II product [103]. However, this algorithm tends often to use lower MCSs. While this may help to tolerate channel errors, using lower MCSs wont help when collisions are the major cause of packet loss (especially in dense WLAN deployments). This problem is discussed in this chapter and an enhancement to the current rate control mechanisms based on PCSA is proposed to cope with these unnecessary MCS decrements.

5.2 Context and motivations

5.2.1 Rate control

The main idea behind rate control is to fortify the communication in case of bad wireless channel conditions. This is done by decreasing the transmission bit rate and using more robust MCS. On the other hand, an efficient rate control mechanism should benefit from the good channel state to increase the transmission rate opportunistically to improve the system throughput.

As already mentioned in the introduction, rate control algorithms are implementation specific. However, generally, they are based on measurements and estimations of the Packet Error Rate (PER). These algorithms track the PER variation to infer the status of the channel and hence adapt the transmission MCS correspondingly. Although the efficiency of a MCS at a given moment depends on the receiver's channel state at that moment, almost all the rate control algorithms are sender-based. This means that the sender estimates the channel state and decides which MCS to use, not the receiver. This decision is based on the information tracked locally by the transmitter. Particularly, the Acknowledgment (ACK) history is used to deduce the current PER.

The multi-rate capabilities of the IEEE 802.11 WLAN PHY and the need for high performance under varying conditions necessitate a dynamic adaptation of the transmission during runtime. Due to the critical role of the rate adaptation mechanism, the performance of any Media Access Control Layer (MAC) enhancement needs to be studied and analyzed in the light of practical rate adaptation algorithms. Before going into this study, it is important to see how different MCS configurations impact the performance when the spatial reuse is enhanced in dense WLAN deployments throw higher Physical Carrier Sensing (PCS) threshold (PCS_{th}).

5.2.2 Modulation and Coding Scheme (MCS) impact on less protective Physical Carrier Sensing (PCS)

For a better understanding of the implications of rate control, it is worth recalling the main causes of packet loss in WLANs. Packet loss happens for two different reasons: synchronous interferences (collisions) and asynchronous interferences. As argued in [104], [105] and others, the majority of rate control schemes are not able to differentiate the nature of the interference which is the cause of their inefficiency in collision dominated environments as will be shown in the sequel.

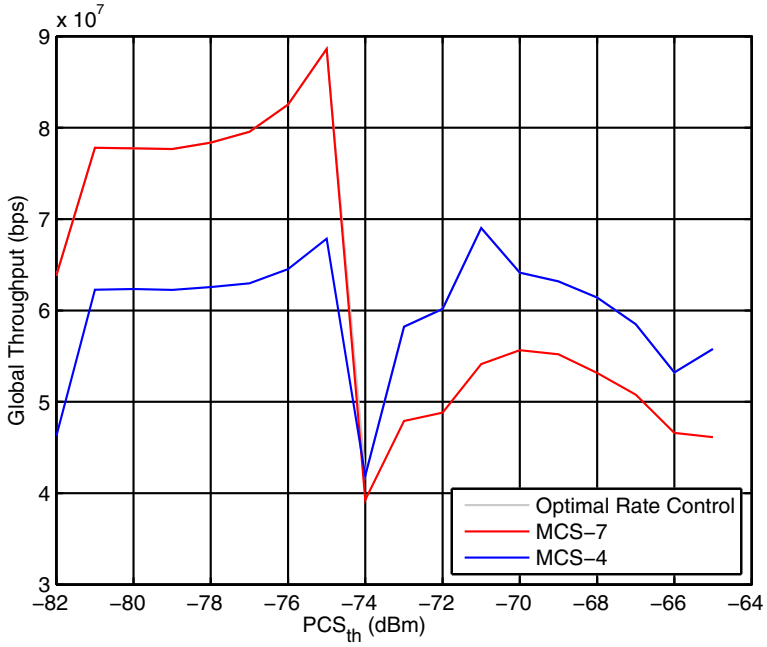

Figure 5.1 – Achieved global (aggregate) throughput in terms of PCS threshold - Modulation and Coding Scheme (MCS) impact

In this scenario, we look at the cellular simulation scenario (described in Section 3.2.1) with the same configurations used in Section 4.5.1. However the rate control algorithm is disabled here and two sets of simulations are performed, in each one a different MCS is chosen. The global (aggregate) throughput of the network is collected and represented in Figure 5.1. The first observation when comparing these results to those obtained with enabled rate control algorithm (Figure 4.7) is that this algorithm is not performing optimally. It is not able to adapt the transmission MCS to the changing PCS_{th}. Another observation is that the distance between two neighboring co-channel Access Point (AP)s plays a fundamental role in the effectiveness of the used MCS. In the cellular simulation scenario, this distance is equal to 21 meters. The received signal power at this distance is $-75\ dBm$. As shown in Fig 5.1, the maximum throughput is observed when using the higher MCS (MCS_7) at a PCS threshold that covers these neighboring APs ($-75\ dBm$). For the lower MCS case, the maximum throughput is achieved for a PCS_{th} equal to $-71\ dBm$.

In the simulation, this belongs to the case where the PCS range of each AP does not include any node from other Basic Service Set (BSS)s. Next, the above observations are analyzed in details and the appropriate resulting conclusions are highlighted.

If one wants to use high data rates, the first tier of neighboring co-channel APs must be covered by the PCS. The transmissions of the closest co-channel APs are very detrimental for the central AP and thus they must be covered. Actually, these transmissions are treated as interference signals at the central AP and thus the Signal to Interference and Noise Ratio (SINR) of the signal of interest inside the central BSS is lowered. Not covering these surrounding APs increases the amount of interferences significantly and expanding the carrier sensing range further than needed may raise the probability of collisions. That's because more nodes are included in the same contention domain. In this case, the packet loss is due to synchronous back-off time where the channel status may be sufficiently fine for successful transmissions. As shown in Figure 5.1, lower data rate does not perform better in this case because the SINR values at the receivers are high enough. In contrast, shrinking WLANs by contracting the physical carrier sensing range must be accompanied with lower transmission rates to tolerate the increasing amount of interferences caused by concurrent transmissions. Here a robust MCS can tolerate lower SINR and thus can ameliorate the achieved aggregate throughput (Figure 5.1).

To conclude this section, an efficient rate control algorithm must operate jointly with the PCS threshold adaptation algorithm. When the latter threshold is increased (the PCS range is contracted), the used data rate must be decreased to tolerate lower SINR values. However, very low MCSs, caused by unnecessary rate control triggered decrements, must be prevented when possible to maintain high throughputs. In practice, thanks to the short transmitter-receiver distances in dense environments, very low MCSs are rarely needed.

5.2.3 Automatic Rate Fall-back (ARF) link adaptation family

ARF [103] is one of the most popular rate control algorithms implemented in today's WLAN products. Figure 5.2 illustrates how ARF operates. In its implementation, ARF defines two counters: one to count the number of successfully transmitted packets ("succeededPackets"), and another that counts the number of failed packets ("failedPackets"). The success counter is incremented for every packet acknowledged by the receiver. If the ACK response is not received by the transmitter before the related timeout for any reason, the failure counter is incremented by *one* and the success counter is reset to *zero*. However, if the ACK response is received before the expiration of the timeout, the success counter is incremented and the failure counter is reset to *zero*.

In the original ARF algorithm, *two* consecutive failures reported by the failure counter (i.e., "decreaseThreshold"= 2) result in an MCS downshift (−−MCS). However, the sender cannot upshift the MCS (++MCS) before counting *ten* consecutive succeeded packets (i.e., "increaseThreshold"= 10). Yet, if the next packet (i.e., the eleventh one which is termed as probe packet) is failed, ARF automatically falls back to the previous MCS without waiting for another consecutive failure. Normally, ARF, like other conventional rate control algorithms, operates using all the MCSs supported by the transmitter. Thus, "MCSmin" is the most robust available MCS and the "MCSmax" is least robust supported MCS having the highest data rate.

The majority of the practical rate control algorithms [91], [106], [104], [107] and [108] are based on the same principle as ARF. All these rate adaptation schemes implement the previously described upshift/downshift counters or use statistics of packet delivery based on the ACK feedback.

In [106], the Adaptive Automatic Rate Fall-back (AARF) is proposed as an enhancement of ARF. Authors of [106] argue that the best data rate to choose to optimize the achieved throughput is the highest data rate whose PER produces a low number of retransmissions. Obviously, higher rates can achieve higher throughput but their higher PERs generate more retransmissions, which then decreases the application level (i.e., useful) throughput. The authors explain that ARF can recognize this best rate and use it extensively but it also tries constantly (every 10 successfully transmitted consecutive packets) to use a higher rate to be able to react to channel condition changes. According to the authors, this process can be costly since the regular transmission failures generated by ARF decrease the application throughput. For the authors of [106], ARF is unable to stabilize the performance for long periods because it handles long-term variations of the wireless medium by the same mechanism used to handle the short-term variation which is not efficient. For that reason, AARF is proposed to avoid the described issue by changing the "increaseThreshold" at runtime to better reflect the channel conditions changes. Accordingly, the "increaseThreshold" starts by a value of 10 but it is doubled (up to 50) when a probe packet fails. The "increaseThreshold" is reset to its initial value (10) after two consecutive failed transmissions. On the other hand, the failure threshold in AARF is left the same as that used in ARF (i.e., "decreaseThreshold"= 2).

Authors in [91] consider another more advanced variation of the ARF algorithm where the success threshold (i.e., "increaseThreshold") is dynamically adapted during runtime according to the speed at which the link quality is changing. The authors argue that fast changing channel quality requires a small success threshold value so that the used data rate can keep up with the channel variations. Accordingly in their proposal, they define two different success threshold configurations, slow and fast, such that in the slow configuration the "increaseThreshold" is set higher than that in the fast configuration.

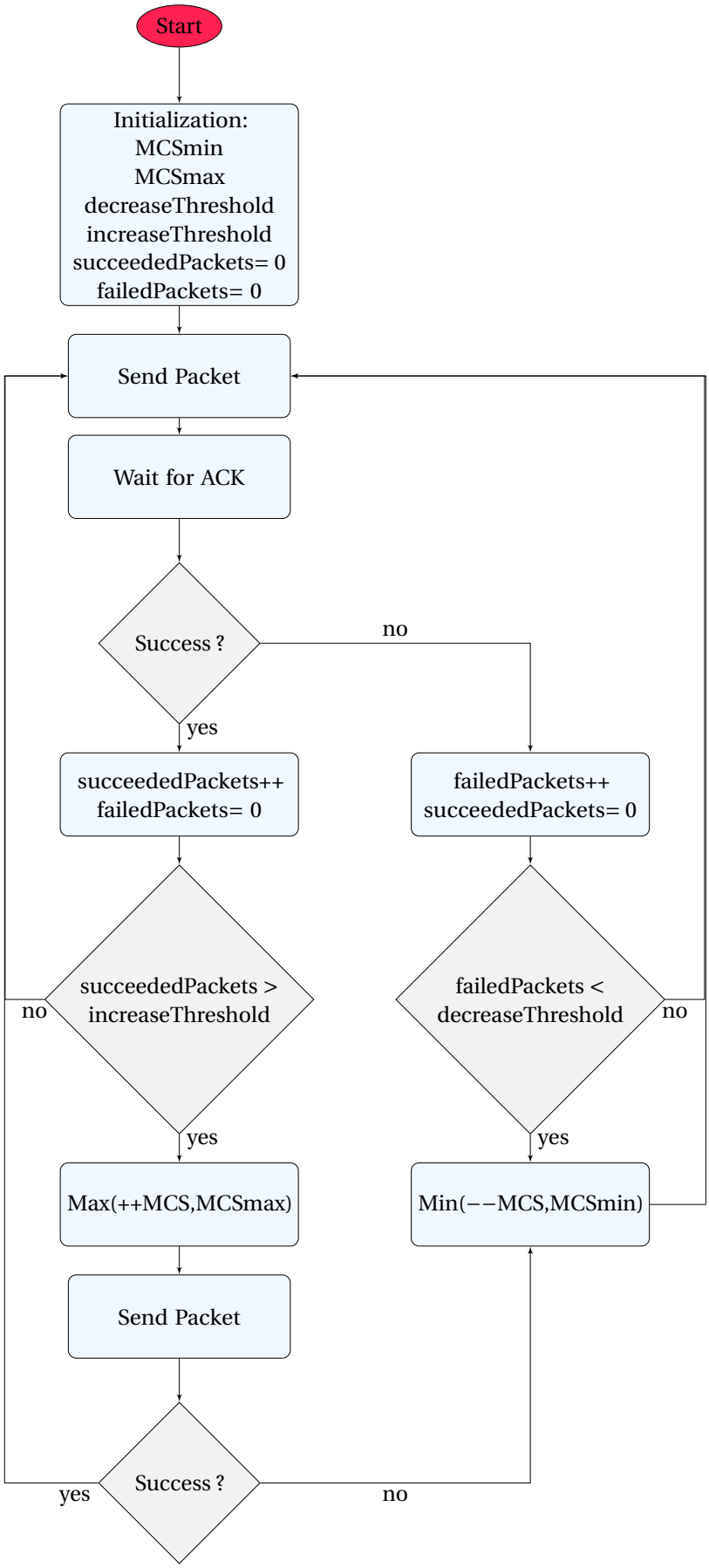

Figure 5.2 – Automatic Rate Fall-back (ARF) rate control – functional overview

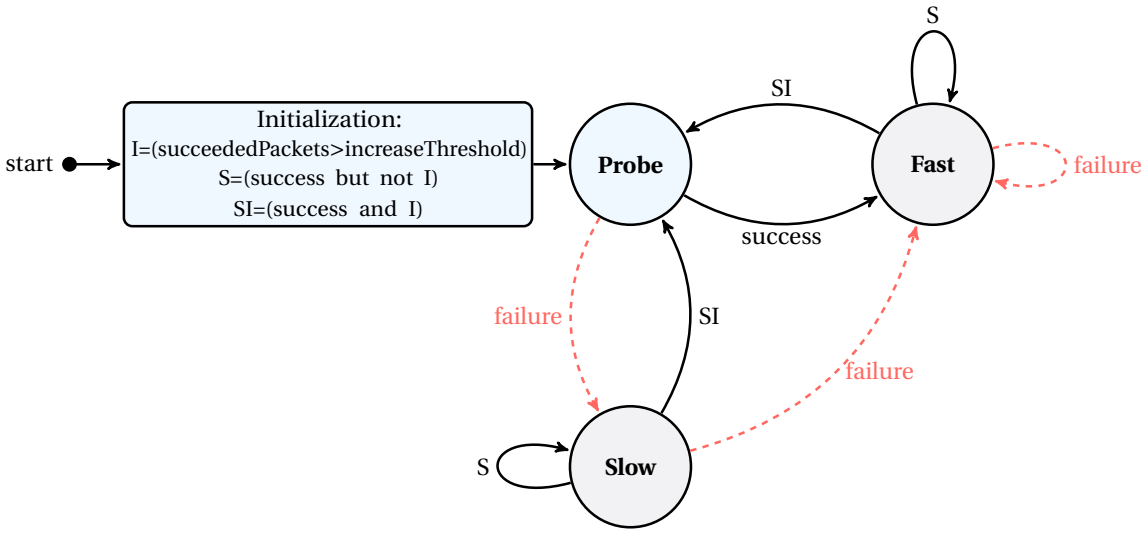

Figure 5.3 – Adapting the success threshold according to Chevillat et al.

The transition diagram in Figure 5.3 illustrates how the success threshold is adapted. If the probe packet succeeds (ACK received by the transmitter), the fast configuration is applied (lower "increaseThreshold"). The process returns to the probe state only when the "succeededPackets" counter exceeds the "increaseThreshold". However, if the probe packet fails, the slow configuration is applied (higher "increaseThreshold"). Now, if the next transmission fails, the process returns directly to the fast configuration because the channel quality is quickly changing and hence lower "increaseThreshold" is required. Concerning the failure threshold (i.e., "decreaseThreshold"), it is always set to 1.

5.2.4 Conservative behavior detriments in dense environments

It is clear that the operation of ARF-like rate control algorithms tends always to decrease the used MCS (the "decreaseThreshold" is always much lower than the "increaseThreshold"). The reason behind is to protect the communication from any degradation in the channel state. However, since the packet loss is not always due to bad channel conditions, the MCS (data rate) decrement is not always helpful. In some situations where collisions are more likely to happen, using lower MCSs degrades the performance of the network. In dense environments, the SINR values are more probably satisfied thanks to the close distance between the transmitter and the receiver. Nevertheless, because of the high number of contending nodes, collisions may happen frequently producing packet loss. These collisions are due to synchronous transmissions due to backoff countdown overlap or hidden node problems. In this case, reducing the MCS will increase the probability of collisions since the transmissions are occupying more airtime over the communication channel. Hence, instead of improving the PER, these conservative rate control algorithms

will end up using the lowest MCS decreasing with that the aggregate throughput of the network.

In this context, this work proposes a new way to cope with the problem of conventional rate control caused by unnecessary rate decrements. In a dense WLAN environment, using the PCSA described in Chapter 4, the achieved SINR values are bounded with certain minimum [109]. Consequently, the rate control algorithm is prevented from using low MCSs that are more robust than needed.

5.3 Carrier Sensing-aware Rate Control

In this section, the rate control mechanism is enhanced by preventing the use of lower MCSs in situations where the channel state tolerates higher MCSs. Basing on the adaptation of the PCS that we have discussed in Chapter 4, it is possible to define a lower bound for S_i. Using Equation (4.11), we get the following:

$$S_i \geq \left(10^{\left(\frac{Rxp(d)-PCS_{th}}{10^{\gamma}}\right)} - 1\right)^{\gamma} \tag{5.1}$$

Consequently, the minimum SINR achieved by any transmission is defined by Equation (5.1). Having that in mind, the usage of the MCSs needed for the SINR values lower than this minimum can be prevented. In practice, the rate control algorithm will not be allowed to use all the MCS list supported by the PHY. This list is updated so that only the reasonable MCSs that fit the situation are used. By this way, the aggregate throughput is enhanced because the rate control is deriving the maximum benefit from the supported MCSs.

As explained earlier in this chapter, the currently used rate control schemes are not able to identify the cause of the packet loss. Such loss may be caused by bad channel conditions or by a synchronous collision due to simultaneous packet transmissions. While decreasing the MCS helps to overcome channel errors, this will never help in case of collisions. Furthermore, lower MCSs may produce more collisions because packets using these MCSs are transmitted slower than other packets using higher MCSs. For sure, low MCSs consume more channel airtime and hence reduce the communication system efficiency.

The goal of our proposal is to prevent the use of low MCSs where the major cause of packet loss is collision and not bad channel state. Today, the density of WLANs is dramatically increasing. The APs are deployed closely to each other to serve the increasing number of WLAN users. These high density environments suffer from a high collision probability because of the large number of contending transmitters. Since the distance between the Station (STA)s and their APs is short, the achieved SINR is normally advantageous. In these situations, the spatial reuse is efficiently enhanced by adapting the medium access

mechanism as shown in [93] and [110]. However, because of the high probability of collisions between the contending transmitters, the implemented rate control algorithms will decrease their MCSs depriving the network from the possible performance improvement targeted by this adaptation.

To cope with that situation, PCSA is followed by an update of the MCS list used by the rate control algorithm to prevent it from using unwanted MCSs. Once an MCS is banned, it will not be considered again until another PCSA allows it. This approach proves its efficiency in improving the performance of the network as will be shown in the evaluation section.

5.4 Evaluation and discussion

For this evaluation we consider the cellular scenario (see Section 3.2.1) with the same configurations used in Section 4.8.1. Recalling that the rate control algorithm [91] described earlier in Section 5.2.3 is implemented and used for the rest of the evaluations of this work. Many simulation runs are conducted. In each of which the MCS list used by the rate control algorithm is modified on all the devices. The first run "*MCS All*" represents the normal operation of the rate control scheme, where all the supported MCSs are allowed. This run will serve as a reference to deduce the gain when applying the proposed approach.

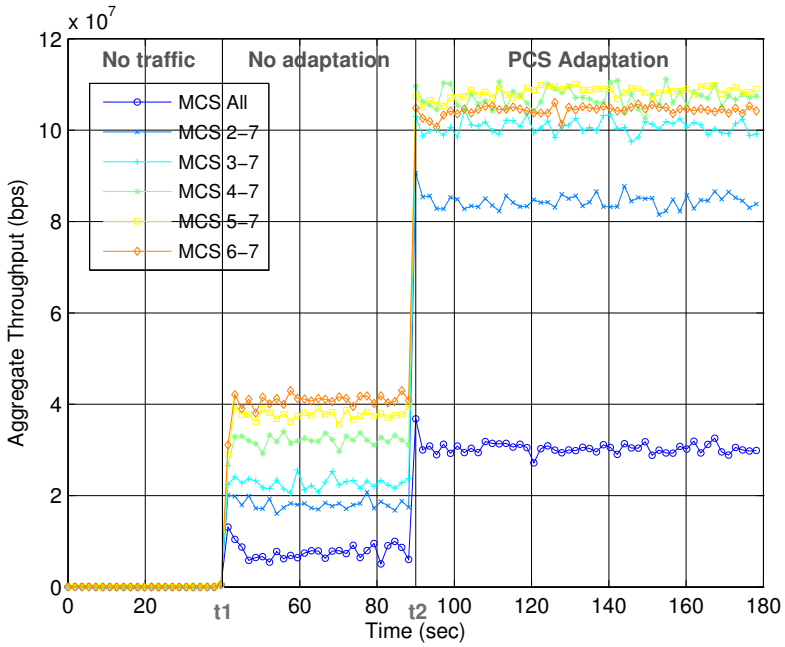

Figure 5.4 – Aggregate throughput performance

The throughput received by each node is collected and the aggregated value is plotted with respect to time in Figure 5.4. As shown in this figure, each simulation run is divided into 3 stages. In the first stage ($Time < t1$) there is no traffic generated by the flows, this

stage is meant to be the initialization stage. The traffic is initiated at $t1$ but PCSA is not applied until $t2$. We show the aggregate throughput before the adaptation ($t1 \leq Time < t2$) for different MCS list configurations to highlight the effect of PCSA on the rate control. This brings to light the gain produced by the carrier sensing-aware rate control approach proposed here.

The aggregate throughput is increased up to 260 % with the proposed adaptation scheme. It is worth noticing that the worst case is when all the supported MCSs are allowed (i.e. "*MCS All*"). The scenario "*MCS 5-7*" where only the MCSs of index 5, 6 and 7 are used is the best performing scenario in terms of aggregate throughput. Certainly, the set of MCS performing the best depends on many criteria, one of them is topology. Accordingly, for other topologies we may have a different MCS set that brings the maximum aggregate throughput. An important thing to notice in Figure 5.4 is the difference in maximum aggregate throughput achieved in the situation where PCSA is not applied ($t1 \leq Time < t2$) and the other one where it is applied ($Time > t2$). When applying PCSA with conventional rate control algorithms, the provided spatial reuse is downgraded by the unnecessary MCS downshifts performed by these algorithms. By limiting the used MCS set, as previously described, knowing that after applying PCSA a certain minimum SINR is always achieved, the network will highly benefit from the additional spatial reuse.

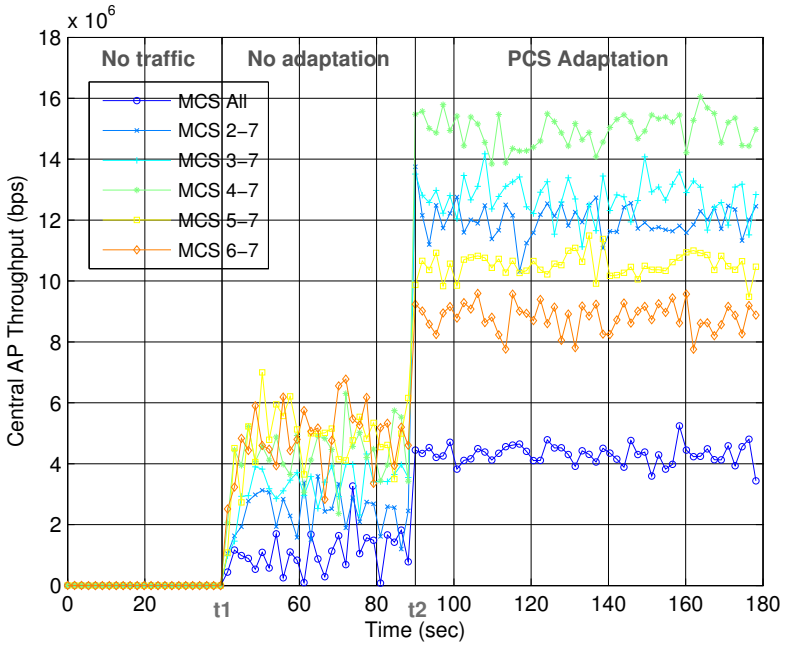

Figure 5.5 – Central AP achieved throughput

The aggregate throughput only tells half the story. It is interesting to look at the worst case throughput performance represented by the central AP in the simulated topology (see Figure 3.1). This AP, belonging to the central BSS, experiences the greater amount of interference from the surrounding BSSs. Figure 5.5 shows the average throughput

received by this AP in terms of simulation time. The same previously described logic of the three simulation stages is valid here also. In spite of the bad situation of this AP, the achieved gain in the adaptation stage ($Time > t2$) is relatively the same gain brought to the aggregate throughput. While the highest aggregate throughput is achieved with the MCS configuration *"MCS 5-7"*, for the central AP the best MCS configuration is the *"MCS 4-7"*. This is due to the fact that this AP is the receiver the most exposed to the interference and hence a more robust MCS (i.e. MCS_4) enhances the achieved throughput.

5.5 Summary

In this chapter we showed that achieving more spatial reuse in high density WLANs is more efficient with an adapted rate control algorithm. The latter is able to benefit from the variety of the modulation and coding schemes defined in the standard. However, in dense environments, due to unnecessary decrements in the transmission bit rate, the currently adopted rate control schemes do not achieve the best performance. To cope with this problem, we proposed in this chapter a carrier sensing-aware rate control approach that sets the minimum used bit rate following a physical carrier sensing adaptation. Simulation results show that the proposed approach is able to achieve a gain of 260 % in the network throughput. This simple, yet effective adaptation proved that PCSA is able to operate jointly with conventional rate control mechanisms without the necessity of substantial modifications.

In the next chapter, we analyze the performance of PCSA and Transmit Power Control (TPC) in terms of throughput fairness among nodes. Consequently, to enhance this performance, we propose a new solution that preserves high fairness levels while leveraging the spatial reuse in dense WLAN deployments.

6 Balanced Transmit power control and Physical carrier sensing Adaptation (BTPA)

6.1 Introduction

In this chapter, to cope with the challenges raised by the increasing density of IEEE 802.11 Wireless Local Area Network (WLAN)s that we already discussed in Chapter 1, we investigate a new combination of transmit power control and physical carrier sensing adaptation to leverage the spatial reuse in high density deployments. While each of these techniques when applied separately is efficient in enhancing the performance of such dense scenarios, they suffer from serious fairness issues. After highlighting these issues in a dense simulation scenario, a new joint solution is proposed to elevate the unfairness problem especially in the presence of legacy nodes in the network. Extensive simulations show that the proposed technique is able to ameliorate the fairness in different situations, while improving the average throughput by 4 times compared to the standard performance. Our results prove that the balanced adaptation of the transmission power control and the physical carrier sensing achieves the desired trade-off between the enhanced spatial reuse and the fairness level among different contending devices. This is proven in two different deployment scenarios: the cellular and the residential scenarios described in Chapter 3.

6.2 Context and motivation

A detailed study evaluating separately the Transmit Power Control (TPC) and the Physical Carrier Sensing Adaptation (PCSA) is conducted in [110] and discussed in Chapter 4. In particularly, we have shown that in the presence of a given number of legacy devices, the aggregate throughput decreases by 10 % when applying PCSA while it decreases by 35 % when applying TPC (see Section 4.8.4 for details). It is true that in the presence of

legacy devices, the PCSA overall performance does not suffer from serious degradation as that of TPC. However, the fairness between the contending nodes is altered. Since the coexistence of the future Wi-Fi generation with legacy devices should not be compromised, it is important to give a particular attention to the fairness aspect issues while enhancing the performance in dense deployments.

On the other hand, 3rd Generation Partnership Project (3GPP) is currently specifying Long-Term Evolution (LTE) operation in the unlicensed band, under the name of Licensed-Assisted Access (LAA). Future LAA devices will operate on the same bands as the IEEE 802.11. The fair co-existence of LAA and Wi-Fi in unlicensed spectrum is an important research topic and industrial concern today. The work presented in this chapter is also fully relevant for the design of LAA channel access mechanism, in order to ensure a fair coexistence between the different technologies operating on the unlicensed spectrum and an efficient operation in dense environments.

To extend the previous study that we conducted in Chapter 4, we intend in the present chapter to improve the situation by preserving higher degree of fairness especially in presence of legacy devices in future super dense environments. In the rest of this chapter, a new approach that combines the PCSA and the TPC is proposed and shows its effectiveness in different scenarios.

6.3 Related SINR Expression

Depending on the transmission data rate, a communication is sustained only if the corresponding Signal to Interference and Noise Ratio (SINR) at the receiver exceeds certain mandatory value. Let S_i be the minimum required SINR for a Modulation and Coding Scheme (MCS) of index i, namely MCS_i. The achieved SINR is expressed by

$$SINR = \frac{Rx_p}{N_P + I_P} \tag{6.1}$$

where Rx_p is the received power, N_P is the background noise and I_P is the interference power at the receiver. All the previous power levels are expressed in watt (W) here. The received power is a function of the transmission power Tx_p and the propagation distance d as defined in Equation (6.2)

$$Rx_p = Tx_p \times d^{-\gamma} \tag{6.2}$$

where γ is the path loss exponent. For a successful reception, the following equation must be satisfied.

$$SINR \geq S_i \tag{6.3}$$

As shown in [110], the relation between the PCS_{th} and the reception power Rx_{th} is expressed in its linear form as follows.

$$\frac{Rx_p}{PCS_{th}} = \left(1 + S_i^{\frac{1}{\gamma}}\right)^{\gamma} \tag{6.4}$$

Accordingly, the SINR can be expressed by:

$$S_i = \left(\left(\frac{Rx_p}{PCS_{th}}\right)^{\frac{1}{\gamma}} - 1\right)^{\gamma} \tag{6.5}$$

and making use of Equation (6.2) and (6.5), we get the following.

$$S_i = \left(\frac{1}{d}\left(\frac{Tx_p}{PCS_{th}}\right)^{\frac{1}{\gamma}} - 1\right)^{\gamma} \tag{6.6}$$

The above expression shows the reflection of the transmission power and the carrier sensing on the SINR. While transmitting at higher power increases the signal to noise ratio, the same increase can be obtained by decreasing the carrier sensing threshold. This shows that the TPC and the PCSA affect similarly the achieved signal to noise ratio and consequently the resulting throughput. This is verified later in this work by the simulation results.

6.4 Proposed Balanced Transmit Power Control (TPC) and Physical Carrier Sensing (PCS) Adaptation (BTPA)

As explained before, a conventional Wi-Fi Station (STA) transmits with the highest power. Yet, except for a minority of deployment scenarios, reduced transmission powers are

sufficient to achieve an SINR satisfying Equation (6.3). Especially for short and medium transmitter-receiver distance where the S_i of the highest available MCS can be achieved with transmission powers much lower than the maximum power. Actually, when using the highest MCS, increasing the SINR more than the appropriate S_i will not bring important throughput gain. In high dense Wi-Fi environments, using lower transmission powers by applying TPC schemes is advantageous to shrink the transmission ranges and limit the co-channel interferences. Moreover, using TPC is intuitive to decrease the energy consumption for green communications.

On another hand, when the co-channel Basic Service Set (BSS)s are close to each other, if the Physical Carrier Sensing (PCS) is not adapted, the transmitters will lose the possibility of simultaneous communications because of the overlapped areas where the STAs of one BSS are exposed to the communications occurring in a neighboring co-channel OBSS. Again, since the distance between the communicating nodes is short in dense networks, S_i is eventually satisfied despite the potential interference caused by co-channel simultaneous transmissions. Adapting the PCS is essential to enhance the reuse of the limited Wi-Fi frequency bands when super densifying is imminent.

Having in mind the above considerations, we propose in the sequel the Balanced TPC and PCS Adaptation (BTPA). Proceeding from the margin-based PCSA adaptation that we originally proposed in [110] and already described in Chapter 4, every node calculates its PCS threshold in decibel scale as follows:

$$PCS_{th}[dBm] = Rx_p[dBm] - M[dB] \tag{6.7}$$

where M stands for the $margin$ parameter, a dB value defined for all the nodes of the given scenario and is related to the topology.

On the other side, we proposed in [110] the following TPC scheme. Every node reduces its transmission power so that its signal is received at a $margin$ (M) above the default minimum sensitivity threshold $PCS_{default}$ ($-82\ dBm$ in the case of 20 MHz bandwidth).

Let Δ_X be the difference between the traditional sensitivity $PCS_{default}$ and the adapted PCS_{th} as expressed below:

$$\Delta_X[dB] = Rx_p[dBm] - M[dB] - PCS_{default}[dBm] \tag{6.8}$$

Figure 6.1 – Balanced Transmit power control (TPC) and Physical carrier sensing (PCS) Adaptation (BTPA) – the $ratio$

According to the PCSA, the PCS_{th} is increased by Δ_X to adapt the carrier sensing mechanism. Instead of that, in the BTPA, Δ_X is used to adapt both the carrier sensing and the transmission power. Accordingly, the PCS_{th} will be increased by Δ_{PCS} dB and the transmission power will be decreased by Δ_{TPC} dB. The following equations show how the values of Δ_{PCS} and Δ_{TPC} are calculated using the $ratio$.

$$\Delta_X[dB] = \Delta_{PCS}[dB] + \Delta_{TPC}[dB] \tag{6.9}$$

$$\Delta_{TPC}[dB] = ratio \times \Delta_X[dB] \tag{6.10}$$

As depicted in Figure 6.1, a $ratio$ equal to 0 means no TPC, i.e., the PCS is increased by Δ_X. Increasing the $ratio$ means introducing more and more TPC. If the $ratio$ is set to 1, the Δ_{TPC} value would be equal to Δ_X and the node performs only a TPC without PCSA. This rule is proposed in order that each mechanism (PCSA and TPC) counteracts the unfairness of the other mechanism.

For a simple scenario, the application of BTPA is illustrated in Figure 6.2. In this example, a new STA associates to an existing BSS and starts a new communication with its Access Point (AP). Upon the reception of a beacon frame from the AP, the STA calculates Δ_X value. From an implementation point of view, it is simple to broadcast the $ratio$ value in the beacon frame itself. Knowing the $ratio$, the STA deduces the values of Δ_{PCS} and Δ_{TPC}. The last step is to calculate the new carrier sensing threshold (PCS_{th}) and transmission power (Tx_p) parameters and apply them before proceeding to the intended data exchange.

6.5 Evaluation

To study the fairness problem and evaluate the proposed solution, we consider first the cellular scenario described in Section 3.2.1.

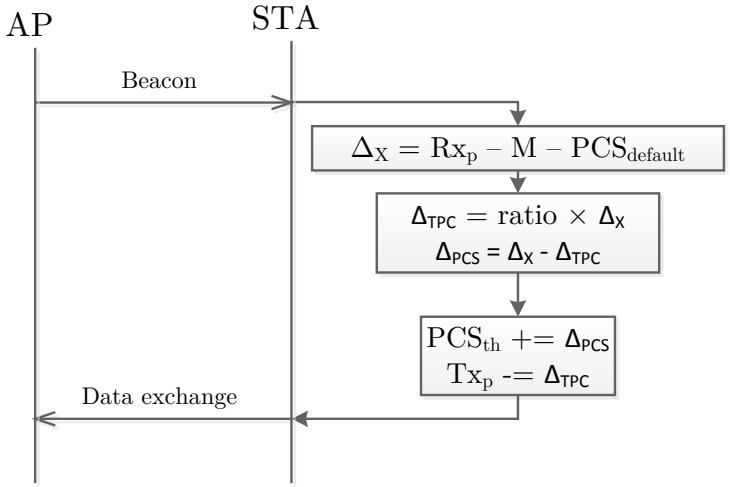

Figure 6.2 – Balanced Transmit power control (TPC) and Physical carrier sensing (PCS) Adaptation (BTPA) – an example

This scenario consists of a high density cellular deployment as depicted in Figure 3.1. Table 3.1 presents a summary of the main simulation system parameters. All the simulated nodes implement the IEEE 802.11n Media Access Control Layer (MAC) and Physical Layer (PHY), operate in 20 MHz band and have only one spatial stream (i.e., one antenna). A User Datagram Protocol (UDP) full buffer traffic generator is configured on all nodes. The default transmission power is 15 dBm and the default PCS threshold is as defined by the standard for 20 MHz bandwidth, -82 dBm. For each of the adaptation mechanisms we chose the $margin$ value achieving the best performance in terms of aggregate throughput. As shown in Chapter 4, for PCSA, M = 20 dB achieves the best performance in terms of aggregate throughput. However, for TPC, the best performance is obtained using M = 30 dB. For BTPA, the best aggregate throughput performance is obtained when M = 20 dB. Furthermore, the rate control algorithm approach described in Chapter 5 is activated with the best MCS configuration (i.e., *"MCS 4-7"*).

6.5.1 Performance comparison

In this section, we compare the performance in terms of throughput fairness of five different modes: no adaptation (applying default settings), the best fixed PCS threshold, PCSA, TPC, and the proposed BTPA. The first mode serves as a reference and reflects the conventional Wi-Fi deployments today. For BTPA, we consider a $ratio$ of 0.5 to carry out this comparison. Later in this chapter, we study the optimal value of the $ratio$ in terms of the number of legacy nodes present in the network. After running the same simulation scenario for the different adaptation mechanisms, the Cumulative Distribution

Function (CDF) of the average individual throughputs achieved by all the STAs is calculated. The slope of the CDF curve is a good indication of fairness. The more the slope is positively steep, the more fairly the throughput is distributed among nodes.

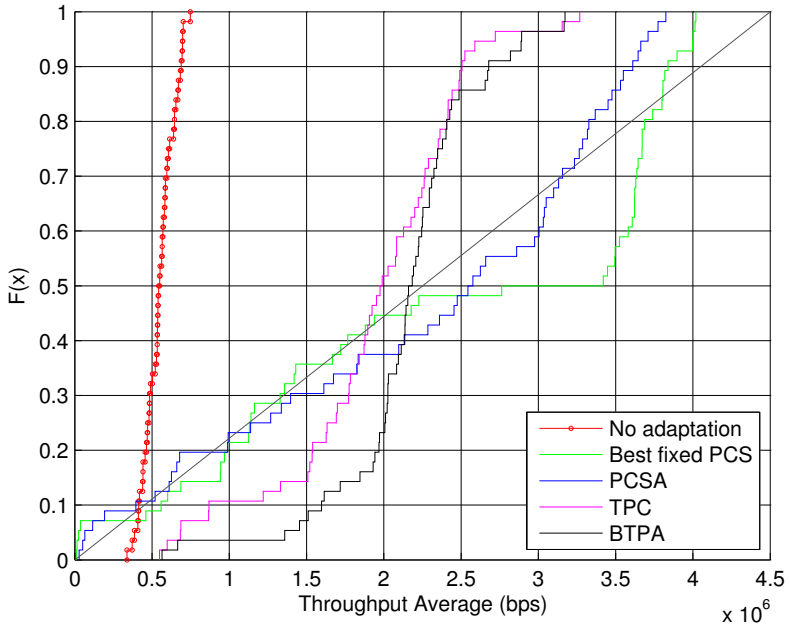

Figure 6.3 – Average throughput performance comparison: Transmit Power Control (TPC), Physical Carrier Sensing Adaptation (PCSA), Balanced TPC and PCS Adaptation (BTPA), Best fixed PCS, and no adaptation – Case (a): without legacy STAs

For all the conducted simulations, we consider two cases: the first (case (a)) does not include any legacy node (all the nodes are able to apply the corresponding adaptation scheme); the second (case (b)) consists of configuring one legacy STA per BSS (this STA applies the default carrier sensing and transmission power parameters). In the latter case, the number of legacy STAs represents 12.5 % of the total number of STAs present in the cellular scenario. The CDFs of the first and the second case are plotted respectively in Figures 6.3 and 6.4 and represented by the function $F(X)$. In the sequel, the non-legacy STAs are called 802.11ax STAs.

6.5.1.1 In the absence of any legacy node

In the absence of legacy nodes, the unfairness is caused by the asymmetry of the communication links. This asymmetry is linked to the fact that different nodes may have different carrier sensing and transmission power parameters. This can be clearly seen in Figure 6.3 when looking to the CDF of the no adaptation mode where the parameters are set to their default values, and hence are the same for all the nodes. It is true that the best fairness (the steepest slope) is achieved by this mode, but the aggregate throughput is the lowest as depicted in Table 6.1 for case (a).

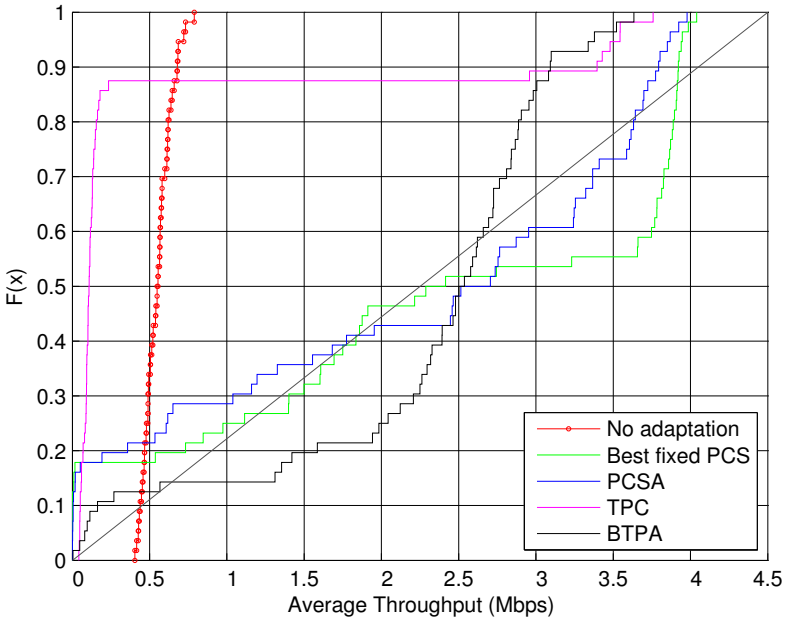

Figure 6.4 – Average throughput performance comparison: Transmit Power Control (TPC), Physical Carrier Sensing Adaptation (PCSA), Balanced TPC and PCS Adaptation (BTPA), Best fixed PCS, and no adaptation – Case (b): with legacy STAs (12.5 % of total STAs)

This is due to the lack of spatial reuse and the related Overlapping BSS (OBSS) problem. As detailed before, the traditional carrier sensing and transmission power parameters are over-conservative and prevent possible concurrent transmissions.

It is worth noting here that the proposed mechanism (i.e., BTPA) achieves the best performance among the other adaptation modes since it is able to preserve the highest degree of fairness all in accomplishing high aggregate throughput. As shown in Table 6.1 for case (a), the highest aggregate throughputs are achieved by the best fixed PCS mode. That is caused by the symmetry ensured by the fixed PCS configuration (all the nodes having the same PCS_{th} and Tx_p), on one hand, and the non optimal BTPA $ratio$ chosen for this part of the simulations (0.5), on the other. However, this highest aggregate throughputs is obtained in detriment of the fairness performance clearly identified when comparing the corresponding curves' slopes with that of BTPA (see Figure 6.3). As previously argued in chapter 4, when there's full compliance, TPC achieves good performance. This is why TPC, in absence of legacy nodes, approaches BTPA in terms of performance as shown in Figure 6.3.

6.5.1.2 In the presence of legacy nodes

When legacy nodes are present in the network, all the adaptation modes are challenged. The worst performance is that of TPC as shown clearly in Figure 6.4 and Table 6.1 for case

(b). As discussed before, the legacy STAs (12.5 % of STAs) using the highest power cause the starvation of the 802.11ax STAs that represent 87.5 % of STAs. All the 802.11ax STAs are impacted since there is one legacy STA in each BSS. As a consequence, the average throughput achieved using TPC is marginal for $F(X) \leq 0.88$ as depicted in Figure 6.4. It is clear now why device manufacturers and network administrators are not considering a widespread TPC application.

To the contrary of TPC that favors legacy nodes, adapting the carrier sensing favors the 802.11ax nodes. Consequently, the performance of the best fixed PCS and the PCSA is slightly harmed as the slopes of their corresponding $F(X)$ curves are less steep in Figure 6.4 and their aggregate throughput is decreased as recorded in Table 6.1 for case (b).

Again, the best performance is achieved by BTPA. In spite of the presence of the legacy devices, our proposal is able to achieve a high aggregate throughput with the best degree of fairness. Oddly, comparing to case (a), the aggregate throughput achieved by BTPA is higher in case (b) where 12.5 % of STAs are legacy. This is due to the non optimal $ratio$ value assumed in this part of the simulations leading to less airtime share for legacy STAs (as shown when $F(X) \leq 0.14$), and hence more throughput achieved by the remaining 87.5 % of STAs (the 802.11ax STAs). This brings to light the importance of an optimal BTPA $ratio$ for higher levels of fairness between different nodes.

Table 6.1 – Aggregate throughput performance in the cellular scenario – Case (a): without legacy STAs; Case (b): with legacy STAs (12.5 % of total STAs)

Mode	No adaptation	Best fixed PCS	PCSA	TPC	BTPA
Aggregate throughput (Mbps)	(a) 30.69 (b) 30.69	(a) 136.3 (b) 132.1	(a) 125.6 (b) 120.8	(a) 108.5 (b) 29.19	(a) 126.8 (b) 128.2

6.6 Ratio value in presence of legacy devices

Choosing the value of the BTPA's $ratio$ may depend on multiple factors. In this section, we examine the effect of the number of legacy nodes present in the network on the optimal value of the $ratio$ parameter. For this purpose, the simulation is run for different $ratio$ values ranging from 0 to 1 as depicted in Figure 6.1. The BTPA is applied as described by equations (6.9) and (6.10).

6.6.1 Cellular scenario

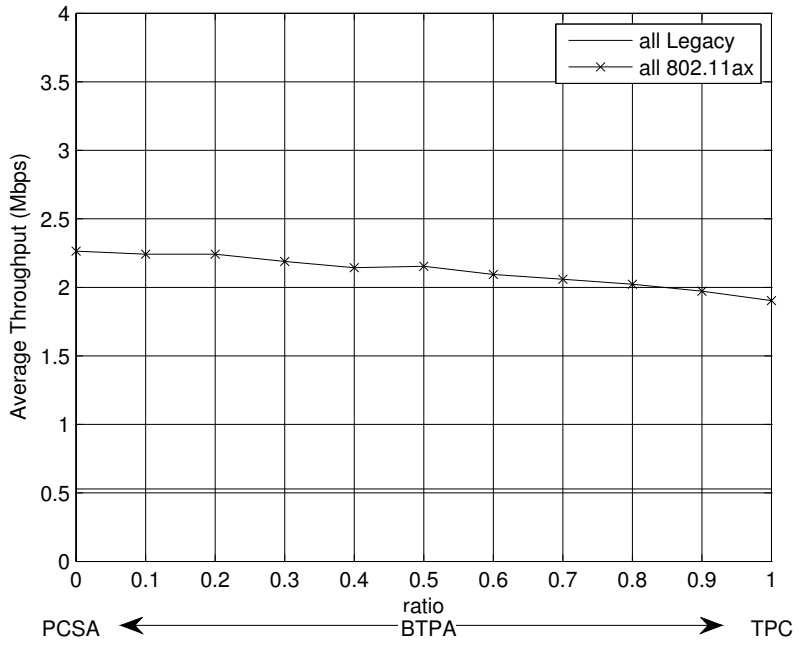

Figure 6.5 – Average throughput performance in terms of the $ratio$ of the BTPA in presence of legacy nodes in the cellular scenario – All legacy versus all 802.11ax

Firstly, we look at the cellular scenario with the same configurations used in Section 6.5. As a reference, Figure 6.5 compares, in terms of average throughput, two independent simulation configurations: the *all legacy* where all the nodes apply the default settings as in conventional networks (i.e., no BTPA); and the *all 802.11ax* where all the nodes apply BTPA. For the latter, the $ratio$ is varied from 0 (PCSA only) to 1 (TPC only). This comparison shows the important gain in average throughput achieved by the proposed solution (BTPA). For instance, the average throughput increases from 0.5 $Mbps$ to 2.15 $Mbps$ for $ratio = 0.5$ (more than four times). The average throughput achieved by applying BTPA on all the nodes (i.e., *all 802.11ax* configuration) is quite stable but slightly better with lower ratio as shown in Figure 6.5.

To bring to light the effect of the presence of legacy STAs in the network on the optimal BTPA $ratio$, we consider three configurations with different proportions of legacy STAs. In the first configuration 25 % of STAs are legacy, in the second 50 % are legacy, and in the third 75 % of STAs are legacy. The corresponding simulation results are presented in Figure 6.6 where the average throughput achieved by the legacy STAs is separated from that achieved by the 802.11ax STAs. Accordingly, for each of the three configurations we have two average throughput curves respectively for the legacy and the 802.11ax STAs.

For all of the three configurations, when the BTPA's $ratio$ is below 0.5 the average throughput achieved by the 802.11ax STAs is quite stable at its maximum attained level.

Yet, the legacy STAs are almost not able to transmit for these values of BTPA's $ratio$. This observation is reasonable recalling the fact that PCSA favors the 802.11ax nodes. Increasing the $ratio$ above 0.5 increases the average throughput achieved by the legacy STAs.

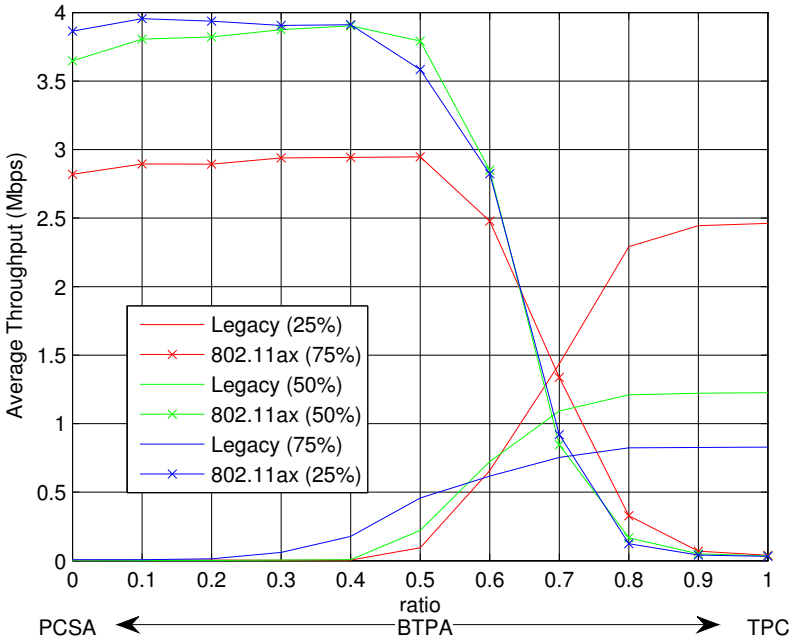

Figure 6.6 – Average throughput performance in terms of the $ratio$ of the BTPA in presence of legacy nodes in the cellular scenario – Legacy and 802.11ax

Normally, in ordinary situations where the coexistence is unavoidable, fairness means aiming at equitable throughput for all nodes whether they are legacy or not. The results in Figure 6.6 show that BTPA is able to achieve this fairness for any proportion of legacy devices. For instance, for the simulated scenario, for a $ratio$ around 0.7, the averaged throughputs achieved by all the nodes are very close. Accordingly, BTPA can be parametrized with a $ratio \approx 0.7$ so that a legacy device achieves the same throughput as an 802.11ax device. This achieved throughput is always higher than that obtained without the use of BTPA despite the number of legacy devices present in the network.

Although the main aim of the proposed BTPA is to enhance the fairness among nodes particularly in presence of legacy STAs, the aggregate throughput must be maintained at high values to fully benefit from the intended gain in spatial reuse. Figure 6.7 shows the aggregate throughput achieved by each of the previous three configurations. The $ratio$ should be chosen so as to maximize the aggregate throughput (i.e., as close as possible to 0.5) while ensuring the best possible fairness level. The latter goal depends on the definition of fairness by the network administration policy. However, as previously discussed, obtaining the same performance for both categories of devices legacies and 802.11ax requires a $ratio$ value close to 0.7. Consequently, for the cellular scenario studied in this section, a $ratio \approx 0.65$ allows a good trade-off to reach the previous objectives.

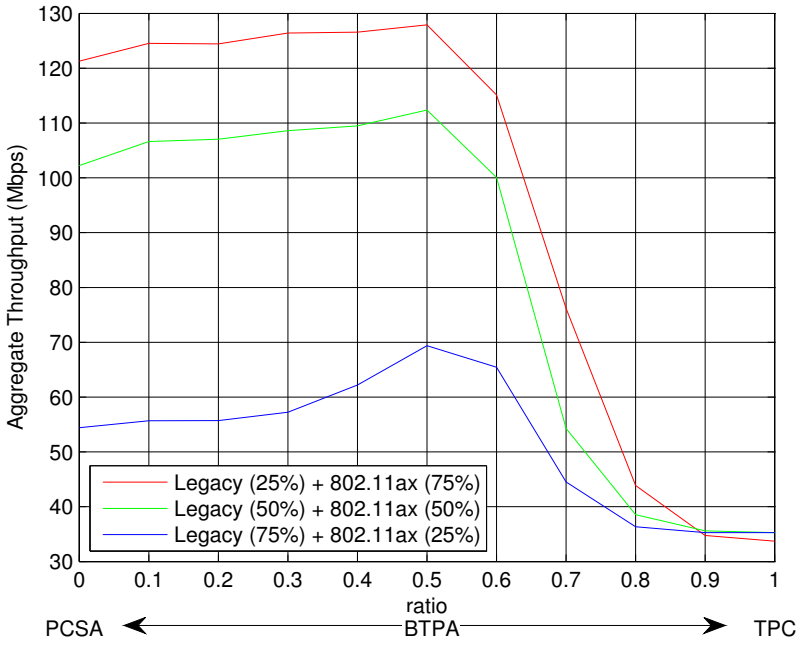

Figure 6.7 – Aggregate throughput performance in terms of the $ratio$ of the BTPA in presence of legacy nodes in the cellular scenario – Legacy and 802.11ax

6.6.2 Residential scenario

In this section we consider the residential scenario that is already introduced in Chapter 3. As described in Section 3.2.2 and illustrated in Figure 3.1, this scenario presents a dense residential building of 5 floors each one consisted of 20 apartments. Each apartment has a $10m \times 10m \times 3m$ size. In our simulations, 30 APs are randomly distributed over the apartments of the building. Each of these AP is placed at the center of an apartment. In each apartment including an AP, 8 STAs are randomly placed within the walls of that apartment and are associated to the AP of the same apartment. Accordingly, for each random drop, an apartment may include one and only one BSS. The full description of PHY and MAC layer parameters used in these simulations is detailed in Table 3.2.

Figure 6.8 shows a $2D$ layout of each floor of the residential scenario for a random drop as previously explained. An AP is illustrated by a star while a STA is illustrated by a circle. All the nodes are located at 1.5 m above the floor level of their corresponding apartment.

To compare the performance of BTPA in this scenario with that in the cellular scenario discussed in Section 6.6.1, we consider a similar representation of the obtained results. Firstly, we show the average throughput performance of two configurations: the *all legacy* and the *all 802.11ax*. We plot these results in Figure 6.9 with respect to the BTPA's $ratio$.

The first observation is that the performance of BTPA when all the nodes are applying it (i.e., *all 802.11ax*) varies according to the value of the $ratio$ parameter. The average throughput

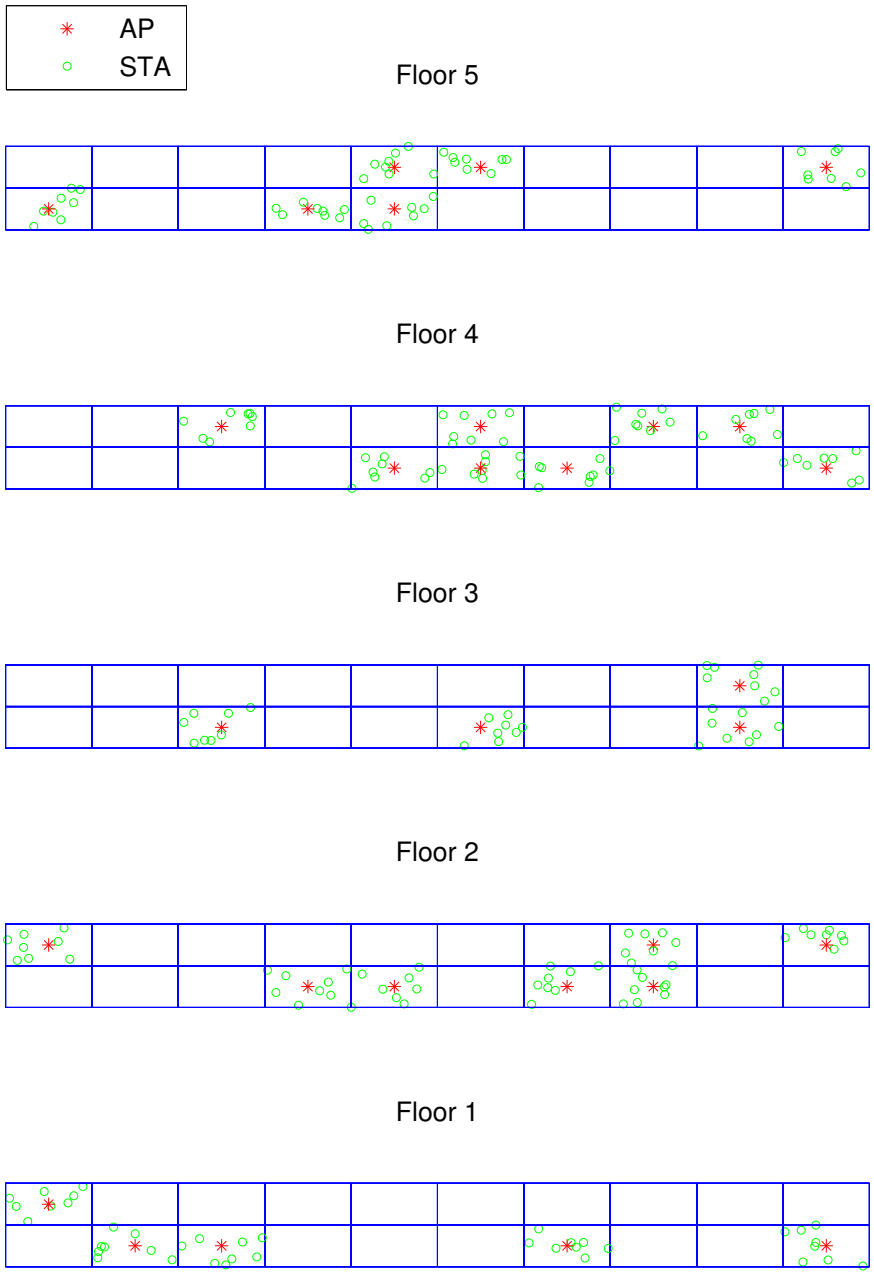

Figure 6.8 – Residential scenario $2D$ layout for the different floors – example of one drop

of an 802.11ax node is always better than that of a legacy node when all the nodes are 802.11ax. However, the gain obtained in this case is higher with a higher BTPA's $ratio$ value. In other words, in the residential scenario, if all the nodes are 802.11ax compliant, applying TPC jointly with PCSA guarantees better enhancement of the spatial reuse.

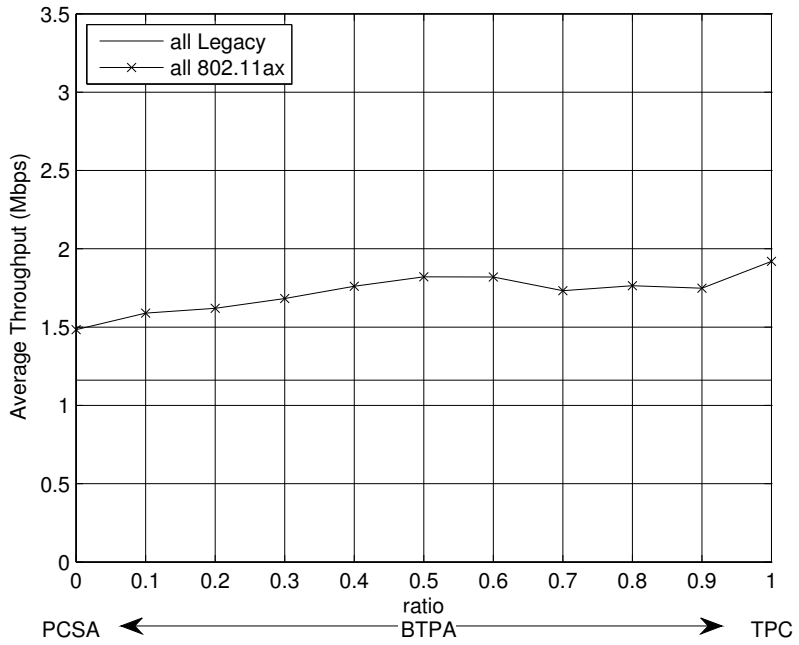

Figure 6.9 – Average throughput performance in terms of the $ratio$ of the BTPA in presence of legacy nodes in the residential scenario – All legacy versus all 802.11ax

In Figure 6.10, we show the average throughput resulting of the three legacy configurations having respectively 25 %, 50 %, and 75 % of the legacy STAs. That is equivalent to 2, 4, and 6 legacy STAs respectively in each apartment including an operating BSS.

As previously discussed in the preceding section for the cellular scenario, Figure 6.10 asserts again that while TPC favors the legacy STAs (curves without a plus marker increase when $ratio$ increases), PCSA favors the 802.11ax STAs (curves with a plus marker increase when $ratio$ decreases). However, in contrast to the cellular scenario results (shown in Figure 6.6), in the residential scenario with 30 randomly located BSSs (each one consisting of an AP and 8 STAs), there is no extreme starvation for any value of the $ratio$ parameter. Regardless the category of the device (802.11ax or legacy) and regardless of the BTPA's $ratio$ value, each device is achieving a none zero throughput as shown in Figure 6.10. This is mainly due to the different node density between the two scenarios and the impact of the path loss model used in the residential scenario.

Depending on the interoperability policy between legacy and 802.11ax devices that may be defined in the standard or configured by a network administrator, the BTPA's $ratio$ is set differently. For instance, if the goal is to have the same performance despite if the device is

802.11ax or not, the optimal $ratio$ is a value between 0.5 and 0.7 as shown in Figure 6.10 with slight difference depending on the proportion of legacy devices in the network.

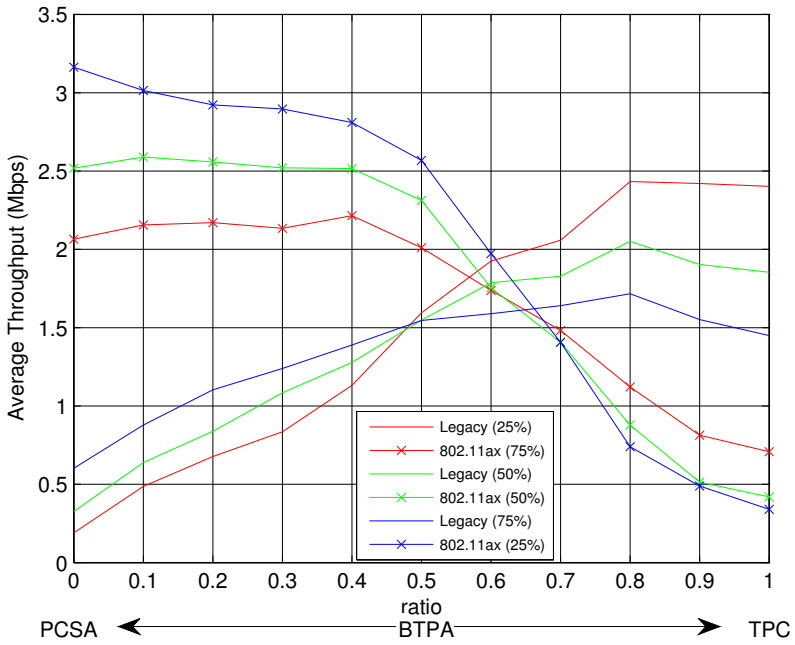

Figure 6.10 – Average throughput performance in terms of the $ratio$ of the BTPA in presence of legacy nodes in the residential scenario – Legacy and 802.11ax

When all the devices are legacies, the aggregate throughput in the cellular scenario (see Table 6.1) is around 30.69 $Mbps$. This is equivalent to an average throughput approximately equal to 4 $Mbps$ per BSS and consequently an average throughput of 0.5 $Mbps$ per device in accordance with the results shown in Figure 6.5 for *all Legacy*. In the residential scenario, as shown in Table 6.2, the legacy performance is much better since we have an aggregate throughput of 280 $Mbps$ which gives an average throughput approximately equal to 9 $Mbps$ per BSS and hence we get an average throughput slightly greater than 1 $Mbps$ as the results shown in Figure 6.9 confirm. The cause behind this performance is the network topology and the propagation channel characteristics. In the cellular scenario there are no obstacles between the co-channel BSSs and hence the interferences are more severe than in the residential scenario. In the latter the separating walls and floors attenuate greatly the signal because of their penetration loss (see Table 3.2).

Table 6.2 – Aggregate throughputs in the residential scenario

Mode	No adaptation	BTPA (*all 802.11ax*)	BTPA (25 % Legacy)	BTPA (50 % Legacy)	BTPA (75 % Legacy)
Max aggregate throughput (Mbps)	278.6	505.2	466.6	463.4	432.4

With the application of BTPA, the maximum aggregate throughput achieved in the cellular scenario with the absence of any legacy device is equal to 126.8 $Mbps$ which is equivalent to approximately 18.1 $Mbps$ per BSS. While in the residential scenario the maximum aggregate throughput reaches 505.2 $Mbps$ (see Table 6.2) which is equivalent in average to 16.84 $Mbps$ per BSS. This shows that BTPA is able to greatly enhance the spatial reuse despite the density, the topology, and the propagation channel characteristics.

With the presence of legacy devices, the maximum aggregate throughput is decreased by 15 % when 75 % of STAs are legacies in the residential scenario as shown in Table 6.2. While in the cellular scenario the same proportion of legacies decreases the aggregate throughput by 45 %. This emphasizes again the difference between the two topologies. However, it should be mentioned here that BTPA is able to largely enhance the throughput performance in both scenarios even in presence of legacy devices.

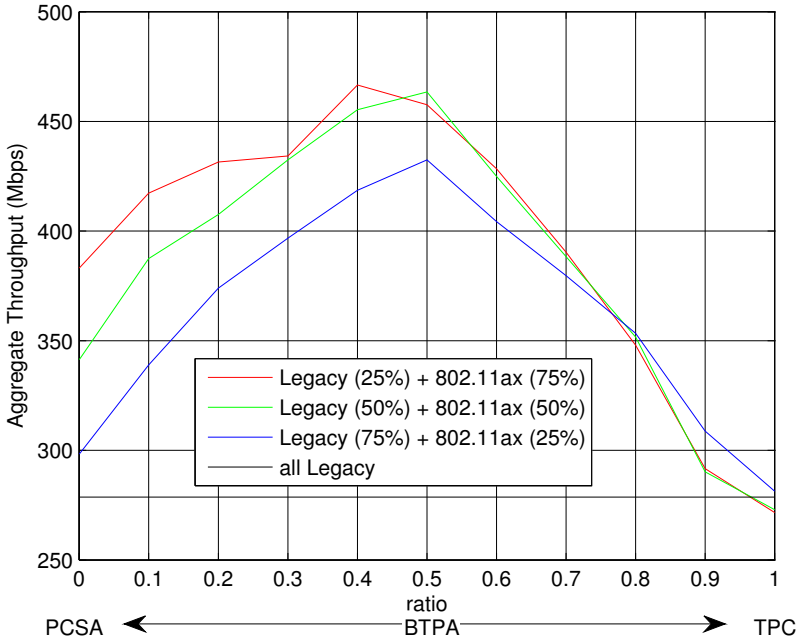

Figure 6.11 – Aggregate throughput performance in terms of the $ratio$ of the BTPA in presence of legacy nodes in the residential scenario – Legacy and 802.11ax

Again, the optimal value of the BTPA's $ratio$ is a trade-off between the value achieving the best aggregate throughput performance and the highest level of fairness among devices. Interestingly enough, the optimal $ratio$ value of 7 that we already concluded for the cellular scenario is close to that we obtain in the residential scenario. In practice, a $ratio \approx 0.65$ achieves the desired trade-off in the residential scenarios for all the proportions of legacy devices. For this value of the $ratio$ in the residential scenario, in presence of legacy STAs, BTPA enhances the aggregate throughput by around one and half fold (e.g., from 278.6 $Mbps$ in *all Legacy* scenario to 392 $Mbps$ when 25 % of STAs are 802.11ax as shown in Figure 6.11). In terms of fairness, the average throughput achieved by a legacy STA and an

802.11ax STA in this case is respectively 1.61 $Mbps$ and 1.68 $Mbps$ instead of 1.16 $Mbps$ when there is no adaptation (i.e., $allLegacy$ scenario).

6.7 Summary

In future super dense Wi-Fi deployments, the contention-based access mechanism defined in the IEEE 802.11 standard by the Distributed Coordination Function (DCF) is challenged. The same challenge will be faced by the expected operation of LTE on the unlicensed bands. To attain the goal of the densification, i.e., increasing the system capacity, the spatial reuse needs to be leveraged. In this chapter, the envisioned carrier sensing and transmission power adaptation that we have already presented in Chapter 4 are questioned and their unfairness issues are highlighted. Consequently, a balanced adaptation combining these two techniques is proposed and shows an outperforming fairness along with four fold increase in average throughput.

Particularly, by choosing optimally the BTPA's $ratio$ parameter, an equal average throughput can be achieved by any STA in the network whether it is a legacy STA or not. Our results show that this can be realized for any number of legacy STAs present in the network. The BTPA approach could also be used for future 3GPP LAA channel access mechanisms to cope with the coexistence of different technologies especially in dense environments.

Originally, BTPA is designed in a distributed manner in the sense that there is no need for coordination between contending devices. As discussed in Chapter 1, such distributed approach is needed for the majority of WLAN deployments that are unplanned and unmanaged. Despite this original design intention, BTPA could be simply adopted in centrally managed network deployments where the common controlling entity defines the optimal $ratio$ value basing on its clear view of the network topology, nodes capabilities and density.

However, for these managed networks, it is certainly more suitable to envision fully centralized solutions. In practice, the controller device offers the capability to collect from the controlled BSSs all the needed information to perform intelligent spatial reuse enhancement. We investigate this approach in the following chapter by exploiting the capability of Artificial Neural Network (ANN)s to optimize the channel access mechanism.

7 Learning-based spatial reuse optimization

7.1 Introduction

In enterprise infrastructure-based Wireless Local Area Network (WLAN) deployments, a centralized management entity controls all the Basic Service Set (BSS)s belonging to the managed Extended Service Set (ESS). To enhance the WLAN performance in these deployments, designing fully centralized solutions benefiting from the presence of the central controller is more efficient than applying other distributed solutions.

In this chapter, we propose a new centralized solution to jointly adapt the transmission power and the physical carrier sensing based on artificial neural networks. The major intent of the proposed solution is to resolve the fairness issues while enhancing the spatial reuse in dense Wi-Fi environments. This work is the first to use artificial neural networks to improve spatial reuse in dense WLAN environments. For the evaluation of our proposal, the new designed algorithm is implemented in OPNET Modeler. Relevant scenarios are simulated to assess the efficiency of the proposal in terms of addressing starvation issues caused by hidden and exposed node problems. The extensive simulations show that our learning-based solution is able to resolve the hidden and exposed node problems and improve the performance of high density Wi-Fi deployments in terms of achieved throughput and fairness among contending nodes.

7.2 Introduction to Artificial Neural Networks

Originally, the design of the Artificial Neural Network (ANN) [111]? was inspired from neurobiology. In practice, ANN derives its computing power through its parallel distributed structure that gives it the ability to learn and therefore to generalize by producing reasonable outputs for new unseen inputs. The properties of ANN can be summarized as the following: input-output mapping capability, adaptivity, nonlinearity, and fault tolerance.

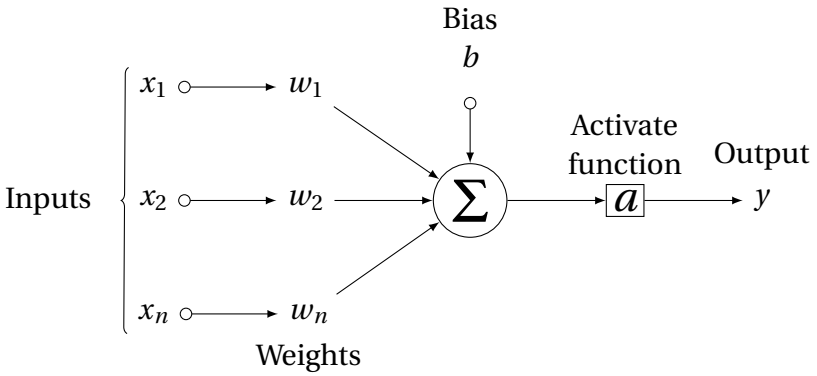

Figure 7.1 – The structure of an artificial neuron

7.2.1 An artificial neuron

The artificial neuron is the basic block of an ANN. The architecture of this fundamental processing unit is shown in Figure 7.1. Accordingly, the transfer function through a single neuron is defined as follows

$$y = a(\sum_{i=1}^{n} w_i x_i + b) \tag{7.1}$$

where y is the output of the neurone, $a(.)$ is the activation function, n is the number of inputs to the neuron, w_i is the weight of input i, x_i is the value of input i, and b is the bias value. Depending on the problem that the ANN needs to solve, the activation function can be a step function, a linear function or a non-linear sigmoid function.

7.2.2 An artificial neural network

Although a single artificial neuron has no usefulness in solving problems, ANNs are capable of solving complex real world problems. An ANN is obtained by combining multiple artificial neurons. These single neurons are distributed over several layers, namely input, hidden and output layers. The number of hidden layers and the interconnections between different neurons can be defined in different ways resulting in different ANN topologies [111].

Building the topology of an ANN is just half of the task before being able to use this ANN to solve the given problem. An ANN needs to learn how to respond to given inputs. The learning (or training) step can be achieved in a supervised, unsupervised, or reinforcement way. The unsupervised approach consists on setting the weights and biases to values that minimize a predefined error function.

7.2.3 The weights update

In the training phase, the training data is fed into inputs, then the output of a neuron is calculated as described in Equation (7.1). This procedure is repeated for all neurons at the input layer, then at the hidden layer(s), and finally at the output layer. Afterwards, the error values are calculated based on the desired output value and the actual output value. This error is used to update the weights of all the connections in the ANN. This update is done by a back propagation of the error value, meaning that the weights connecting the output layer neurons to the last hidden layer neurons are updated in the first place. When all the weights are updated, the ANN is ready for the next epoch of the training phase. The maximum number of epochs is predefined depending on the specific problem and the available dataset. The commonly used error function is the Mean Squares Error (MSE) that is defined by

$$MSE = \frac{1}{2}(\sum_{m=1}^{M}\sum_{i=1}^{K}(desired\_output_i^m - current\_output_i^m)) \tag{7.2}$$

where M is the number of training datasets. When the calculated value of the MSE is less or equal to the predefined desired MSE (MSE_{des}), the training is stopped and the ANN is considered as sufficiently trained. Furthermore, the stop point may be controlled by other customized metrics.

7.2.4 Why Artificial Neural Networks ?

The impact of the Media Access Control Layer (MAC) protocols on the network performance is very complicated to model. Usually, as we discussed in Chapter 2, researchers provide a set of unrealistic assumptions of ideal channel conditions and homogeneous link qualities to simplify their studies. However, these assumptions result in biased results that don't reflect the real life situations. Consequently, optimization efforts basing on these impractical models result in suboptimal solutions.

The relation between the individually achieved throughputs for every node and the MAC parameters used on every node is nonlinear, complex and time variant which is very difficult to predict using an analytical model [112]. This is the motivation behind the use of ANNs to model this highly complicated relation. When the network is sufficiently trained, it will model the aforementioned relation between outputs and inputs. This model can be used to minimize a cost function to determine the best MAC parameters values for each node in order to enhance the performance of the network. For this optimization we have to define a real-time learning and adaptation algorithm.

7.2.5 Related Applications of Artificial Neural Networks in the literature

In the literature, artificial neural networks are employed to model nonlinear relationship between the inputs and the outputs of a given system. The power of neural networks resides in their capability to approximate nonlinear functions. In [113], authors consider a multi-layered feed-forward neural network as a "universal approximator".

Typical problems addressed by neural networks include pattern recognition, clustering, data compression, signal processing, image processing and control problems. In telecommunications, ANNs are implemented for many applications, such as equalizers, adaptive beam-forming, self organizing networks, network design and management, routing protocols, localization, etc. ANNs are also proposed in the literature to enhance the performance of WLANs. In [114], authors propose an adaptation of the transmission data rate based on ANN to improve the aggregate throughput of a WLAN system. Quality of Service (QoS) provisioning is addressed in [115] using fuzzy logic control to enhance the IEEE 802.11e Enhanced Distributed Channel Access (EDCA) function [21]. Other important applications of the ANN theory in WLAN systems include indoor localization [116], channel estimation [117], frame size adaptation [118], and channel allocation [119].

An adaptive algorithm is proposed in [120] to satisfy a predefined user throughput requirement by optimizing some back-off mechanism parameters. Precisely, the minimum Contention Window (CW_{min}) and the Arbitration Inter-Frame Space (AIFS) are chosen as the adaptable parameters. After propagating the current values of these parameters over a multilayer neural network, the corresponding output is compared to the desired throughput to calculate the training error. Once the MSE is satisfied, the trained neural network is used to optimize the input parameters using a back-propagation mechanism. This optimization consists in minimizing the following cost-reward function:

$$Wang\_Cost = \sum_{i=1}^{K} \frac{(T_i - T\_THR_i)^2}{T\_THR_i} \tag{7.3}$$

where, T_i is the result of the forward-propagation over the ANN at the neuron i of the output layer (i.e., the throughput value estimated by the ANN for user i) and T_THR_i is the required user throughput of user i.

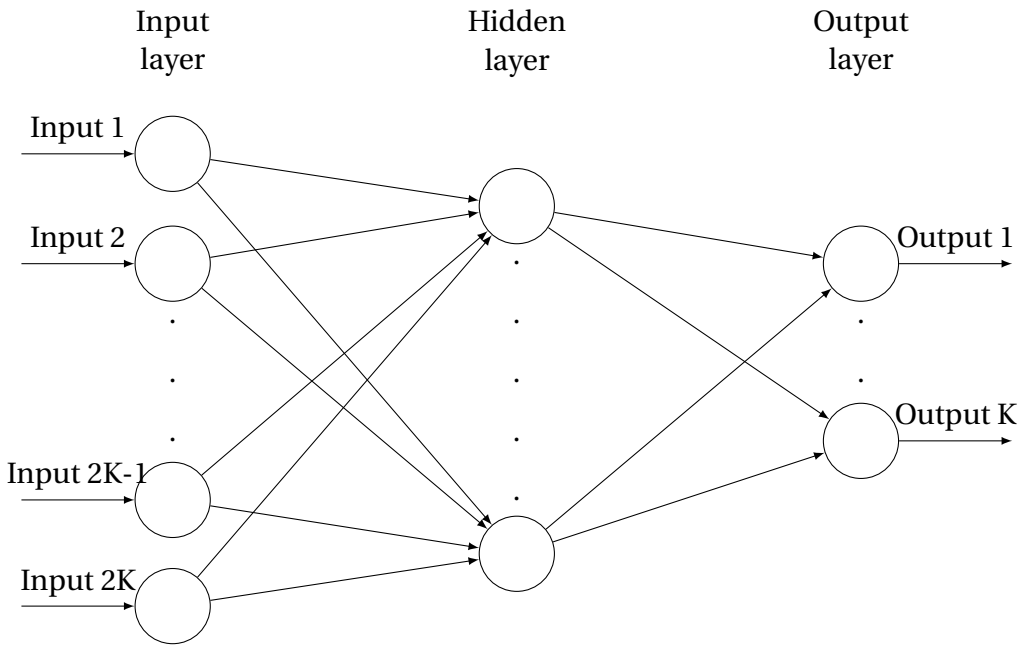

Figure 7.2 – Proposed neural network topology

7.3 The proposed system model

In this work, we chose the MultiLayer Perception (MLP), the most common ANN topology [111]. We consider an ANN topology of three layers: the input layer of index $l = 0$, one hidden layer ($l = 1$) and the output layer ($l = 2$). As shown in Figure 7.2, the input layer contains $2K$ neurons, where K is the number of WLAN nodes in the network. Since we are considering the joint optimization of the Physical Carrier Sensing (PCS) threshold (PCS_{th}) and the transmit power (Tx_p), then we need to adapt $2K$ parameters (two parameters for each WLAN node). The output layer consists of K neurons because we consider the throughput achieved by every node. However, the number of neurons in the hidden layer HN_{nb} is determined according to the complexity of the learning process. The value of HN_{nb} is indicated later in the evaluation part.

By the means of this ANN, we aim to model the correlation function $cf(.)$ between the throughput (Thr) achieved by the different WLAN nodes of the network and their associated MAC parameters.

$$(Thr_1, Thr_2, ..., Thr_K) = cf(PCS_{th_1}, Tx\_p_1, PCS_{th_2}, Tx_{p_2}, ..., PCS_{th_K}, Tx_{p_K}) \quad (7.4)$$

The aim of this study is to enhance the performance of the network in terms of through-

put and preserving fairness between nodes. To chose the new adapted parameters, a minimization of the following cost function is proposed.

$$Cost_{fairness} = 1 - \frac{(\sum_{i=1}^{K} x_i)^2}{K \sum_{i=1}^{K} x_i^2} \tag{7.5}$$

Minimizing this cost is equivalent to the maximization of the Jain's fairness index [121]. This index rates the fairness of a set of throughput values where K is the number of nodes and x_i is the throughput achieved at the i^{th} node. The values generated by the Jain's index have a range between 0 and 1, where a value of 1 means the best fairness. Minimizing the cost function in Equation (7.5) is the same as approaching 1 for the Jain's index.

Although the aim is to preserve fairness in individual achieved throughput, we have to maintain a minimum average throughput per device. Accordingly, X_T is defined as the individual average throughput target. Below X_T, the average throughput achieved by a given device needs to be enhanced. To satisfy this throughput requirement, we need to minimize the expression described in Equation (7.6).

$$Cost_T = \sum_{i=1}^{K} \frac{(X_T - x_i)^2}{X_T} \tag{7.6}$$

For the final cost (Equation 7.7) used by the proposed algorithm, the previously defined costs are summed together. The term multiplied by $Cost_T$ is used to normalize it so that it will produce the same weight in the total cost as $Cost_{fairness}$.

$$Cost_{tot} = \frac{1}{2} Cost_{fairness} + \frac{1}{2 \sum_{i=1}^{K} X_T} Cost_T \tag{7.7}$$

7.4 The new optimization algorithm – Updating the MAC parameters

Let $\psi_i^{(n)}$ the value of the i^{th} MAC parameter of the current adaptation that has an index n. In practice, since the activation function of the input layer is linear, the i^{th} neuron of

the input layer of the ANN has an output equal to $\psi_i^{(n)}$. A summary of the most important symbols used in this section is listed in Table 7.1.

Table 7.1 – Summary of the symbols with their descriptions

Symbol	Description in ANN	Description related to WLAN
l	Layer index ($l = 0, 1, 2$)	See Equation (7.4) and Figure (7.2)
$\psi_i^{(n)}$	The value of the parameter i at the n^{th} adaptation	The current values of PCS threshold PCS_{th} and transmission power Tx_p of a node
$\psi_i^{(n+1)}$	The optimized value of the parameter i	The optimized values of PCS threshold PCS_{th} and transmission power Tx_p of a node
$a_i^{(n)}(l)$	The output value of i^{th} neuron of the l^{th} at the n^{th} adaptation	e.g., $a_i^{(n)}(2)$ is the throughput value of the user i

For the $(n+1)^{th}$ adaptation, the i^{th} MAC parameter is adapted by incrementing or decrementing it by $\Delta\psi_i^{(n)}$.

$$\psi_i^{(n+1)} = \psi_i^{(n)} + \Delta\psi_i^{(n)} \tag{7.8}$$

Where $1 \leq i \leq 2K$ at the layer $l = 0$. To minimize the cost function with respect to $\psi_i^{(n)}$, according to the gradient descent optimization technique, $\Delta\psi_i^{(n)}$ is equal to the negative gradient of the cost function as follows.

$$\Delta\psi_i^{(n)} = -\eta \frac{\delta Cost}{\delta \psi_i^{(n)}} \tag{7.9}$$

where η is the update rate of the optimization process. Introducing the activation function at layer l to Equation (7.9), we obtain

$$\frac{\delta Cost}{\delta \psi_i^{(n)}} = -\frac{\delta Cost}{\delta a_i^{(n)}(l)} \times \frac{\delta a_i^{(n)}(l)}{\delta \psi_i^{(n)}} \tag{7.10}$$

Let's consider

$$\lambda_i^{(n)}(l) = -\frac{\delta Cost}{\delta a_i^{(n)}(l)} \tag{7.11}$$

At the output layer $l = 2$, $\lambda_i^{(n)}(l)$ is given by

$$\lambda_i^{(n)}(2) = -\frac{\delta Cost}{\delta a_i^{(n)}(2)} \tag{7.12}$$

where $1 \leq i \leq K$ at the layer $l = 2$ and $a_i^{(n)}(2)$ is the activation function value calculated at the output layer after the feed forward process previously described. It is worth mentioning here that $a_i^{(n)}(2)$ is the throughput of node $\lambda_i^{(n)}(0)$ are then derived from $\lambda_i^{(n)}(1)$ $(1 \leq i \leq HN_{nb}$ at the hidden layer where $l = 1)$ that are derived from $\lambda_i^{(n)}(2)$, all using the chain-rule manner described by

$$\lambda_i^{(n)}(l) = \sum_{j=1}^{N_{l+1}} \lambda_j^{(n)}(l+1) a'_j(l+1) w_{ij}(l+1) \tag{7.13}$$

however, according to Equation (7.11), we have

$$\lambda_i^{(n)}(0) = -\frac{\delta Cost}{\delta a_i^{(n)}(0)} = -\frac{\delta Cost}{\delta \psi_i^{(n)}} \tag{7.14}$$

since $a_i^{(n)}(0)$ (the i^{th} input of the ANN) is equal to $\psi_i^{(n)}$ (the current value of the i^{th} parameter). Equation (7.8) becomes

$$\psi_i^{(n+1)} = \psi_i^{(n)} + \eta \lambda_i^{(n)}(0) \tag{7.15}$$

Our proposal reposes on the expression of Equation (7.15) to calculate the new adapted parameters during the optimization process.

7.5 Implementation of the proposed solution

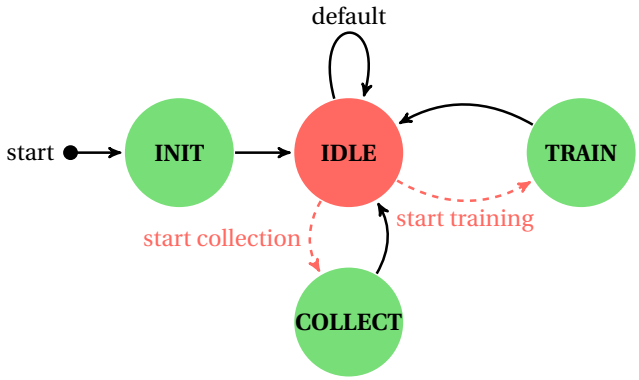

Figure 7.3 – Controller Process Model

We used OPNET modeler 17.5 as the simulation tool. OPNET is a system level simulator that implements the PHY and MAC layers described by the IEEE 802.11n standard. The essential procedures of the proposed solution are described in this section.

A new OPNET node model is created to simulate the controller entity. The process model

is represented by its finite state machine shown in Figure 7.3. The ANN is created in the initialization phase INIT, then the process enters the IDLE state and remains there until the next scheduled collection time. The collection event releases the process that enters the COLLECT state. At the end of the collection procedure, the process returns to the IDLE state and waits for the training event. Once fired, process goes to the TRAIN state, trains the ANN and returns to the IDLE state.

7.5.1 Overview on the proposed solution

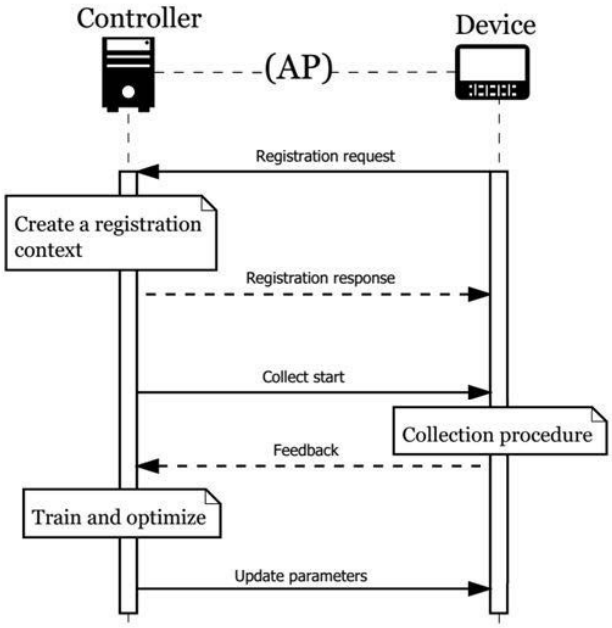

Figure 7.4 – General procedure

As shown in Figure 7.4, each device has to send a registration request to the controller. In practical deployments, an Access Point (AP) is connected directly to the controller. However, all the communications between a Station (STA) and the controller are provided through the AP to which the STA is associated. Upon receipt of the registration request, the controller creates a registration context specific to the requesting device. The controller affirms or denies the registration with an appropriate registration response. A newly associated device can have the latest optimized parameters via this response.

At a predefined moment, the controller sends a collection start command to all the registered devices. The collection procedure is described in details in the next section. After collecting all the datasets, the controller performs an on-line training for the previously created neural network. Then, the trained neural network is used to adapt the parameters of the devices. The optimization procedure is described later in this chapter.

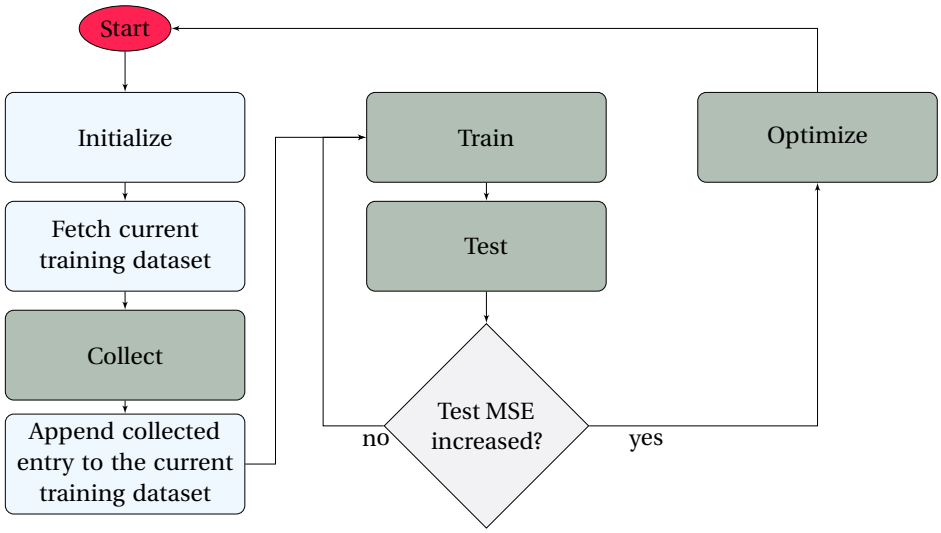

Figure 7.5 – Overall look to the proposed algorithm

Finally, the controller sends the optimized parameters values to the corresponding devices. After receiving the update parameters request, each device applies the new parameters and continues its normal operation. According to the circumstances and the predefined policies, the controller is able to send a new collection command whenever it needs.

7.5.2 The different procedures of the proposed algorithm

After examining every procedure apart from others, the overall algorithm is shown in Figure 7.5. The optimization round consists of returning to the start step after running through the different steps depicted in the flowchart. An optimization round n begins by an initialization phase where the ANN is created and configured. Then, the current version of the training dataset is fetched. As it will be described in details later on, initially the offline dataset is divided randomly into two parts, one is a part of the training dataset and the other constitutes the testing dataset. The fetched dataset is the offline training part appended to the previously collected dataset entries during past optimization rounds ($< n$). Then, a new collection procedure starts and the resulting dataset entry is appended to the fetched training dataset. At this point, we are ready to proceed to the training phase described in Section 7.5.3. After that, the ANN is tested using the testing dataset as outlined in Section 7.5.4. If the resulting testing MSE increases compared to that of the previous optimization round ($n-1$), the process quits the training phase and enters the optimization procedure (see Section 7.5.5). At the end of the optimization procedure, the process returns to the start point and a new optimization round ($n+1$) starts.

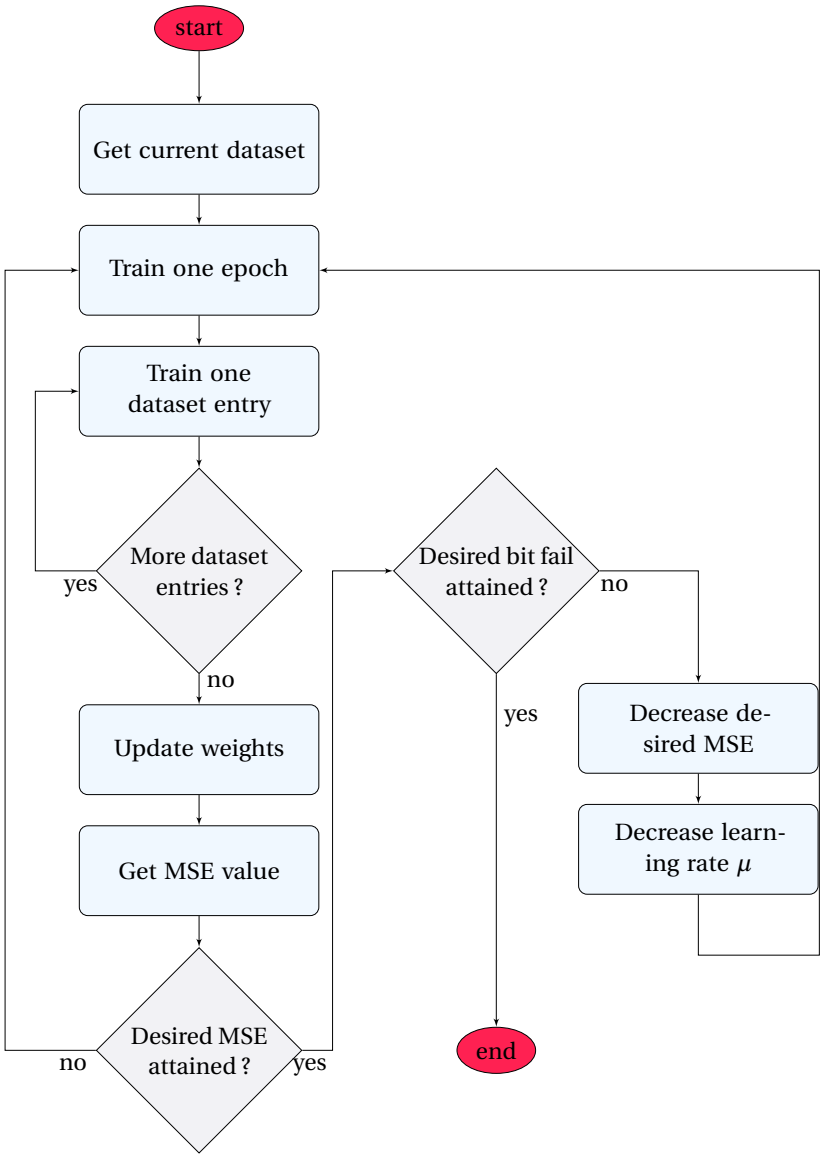

Figure 7.6 – Training procedure details

7.5.3 Training procedure

In this section we describe the training procedure of the ANN. The latter is based on two types of datasets, the first is collected offline (when the real network is not in operational mode) and the second is the result of an online collection (while the normal system operation).

The offline dataset is divided into two separate datasets. The first part is used as the initial part of the training dataset, while the second part is used to test the ANN during the training process. The testing procedure is an important player in determining the end of the training process and the beginning of the optimization process.

The online dataset is the complementary part of the training data set. After every optimization round, the collected dataset entry is appended to the latest training dataset. Accordingly, the ANN is trained with an incremental training dataset, increasing in size after each optimization round. This assures an adaptive behavior of the proposed solution.

The detailed training procedure is depicted in Figure 7.6. To increase the robustness of the training phase, we integrate two test levels to verify if the network is successfully trained or not. To implement our approach, we consider two different criteria. One of them is the well known desired Mean Square Error (MSE_{des}). The other criteria is the number of output errors exceeding certain absolute value (the desired fail limit FL_{des}) that's equivalent to the difference between the output neuron value and the related value in the dataset. We define the desired fail number ratio FNr_{des} as the ratio of output errors exceeding FL_{des} to the total number of output values in the training dataset (number of ANN's outputs K times the number of dataset entries DSe_{nb}). Accordingly, the first test level consists of a verification whether the current MSE value is less than MSE_{des} value. Once the desired MSE is satisfied, we move to the second test level by testing the number of fails. If the latter does not satisfy the predefined FN_{des} value, the MSE_{des} and the learning rate μ are decreased.

7.5.4 Testing procedure

The testing procedure consists of fetching the offline testing dataset entries and running the ANN for one epoch. Obviously, this run will not affect the trained ANN, meaning that the weights are not updated. Consequently, the testing MSE value is calculated to be used later to conclude if the ANN is enough trained or not. Figure 7.7 depicts the described procedure.

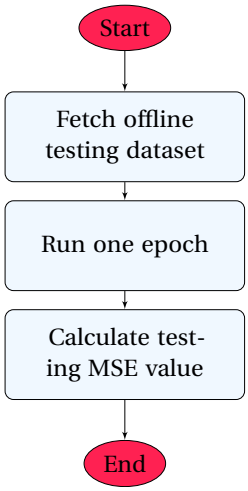

Figure 7.7 – Testing procedure details

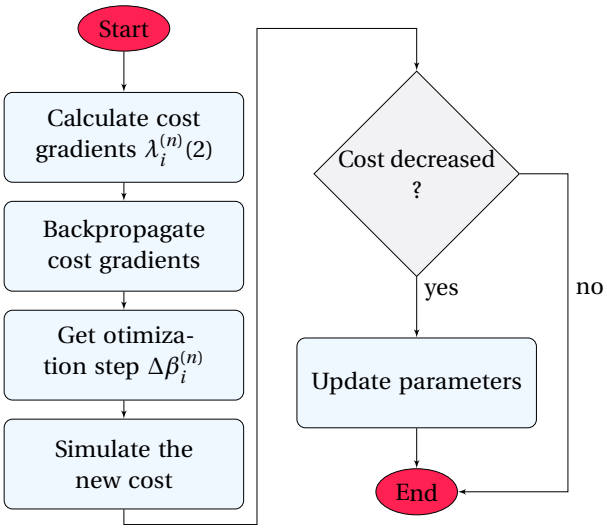

Figure 7.8 – Optimization procedure details

7.5.5 The optimization procedure

The optimization procedure described in this section integrates the analytical algorithm early detailed in Section 7.4. The working flow of the implemented optimization procedure is shown in Figure 7.8. Firstly, the gradients of the cost function are calculated at the last layer of the ANN as described in Equation (7.12). Then, these values are backpropagated through the ANN as described by Equation (7.13). Consequently, the $\Delta\psi$ values that will be used to adapt the MAC parameters are obtained as described by Equation (7.14). In order to get the new optimized MAC parameters, each $\Delta\psi$ value is added to its related old MAC parameter value as shown by Equation (7.8). The update rate η determines how much the optimization process is aggressive in updating MAC parameters. Unless otherwise stated, the update rate η is set to its default value indicated in Table (7.2).

Before sending the newly updated parameters $\psi_i^{(n+1)}$ to their corresponding nodes, their performance is verified by simulating the resulting cost using the trained ANN. This step will prevent an unnecessary parameters update that may alter the current performance of the operational network. If the simulated cost is better than the current cost (cost decreases), an update message is sent back to every registered node asking them to configure their transmission power and carrier sensing using the new optimized values. Otherwise, the nodes are not updated and they continue to use the old parameters $\psi_i^{(n)}$ until the next optimization round.

7.6 Evaluation

In this section, the performance of the proposed learning-based joint adaptation of Physical Carrier Sensing Adaptation (PCSA) and Transmit Power Control (TPC) is eval-

uated through extensive system level simulations.

Table 7.2 – Simulation parameters

Parameter	Value	Description
K	4	Number of nodes in hidden and exposed scenarios
	63	Number of nodes in cellular scenario
HN_{nb}	8	Number of hidden layer neurons in hidden and exposed scenarios
	126	Number of hidden layer neurons in cellular scenario
μ	0.001	Learning rate
η	0.01, 0.001	Optimization update rate
$MaxEpochs_{nb}$	1000	Maximum number of training epochs
MSE_{des}	10^{-6}	Desired mean squares error
FL_{des}	0.4	Desired fail limit ($Mbps$)
FNr_{des}	0.1	Desired fail number ratio
$Offline\ DSe_{nb}$	15	Offline data set entries number
T_{ON}	10 sec	Data collection interval duration
MIN_{PCSA}	$-110\ dBm$	Minimum PCS threshold value
MAX_{PCSA}	$-60\ dBm$	Maximum PCS threshold value
DEF_{PCSA}	$-82\ dBm$	Default PCS threshold value
MAX_{TPC}	15 dBm	Maximum transmit power value
MIN_{TPC}	0 dBm	Minimum transmit power value
DEF_{TPC}	6 dBm	Default transmit power value
$Load$	20 $Mbps$	Traffic load per device in hidden and exposed scenarios
	4 $Mbps$	Traffic load per device in cellular scenario
X_T	20 $Mbps$	Target throughput per device in hidden and exposed scenarios
	4 $Mbps$	Target throughput per device in cellular scenario
NSS	1	Number of spatial streams (antennas)
B	5 GHz	Frequency band
BW	20 MHz	Channel bandwidth
MCS	MCS_7	Modulation and coding scheme (no rate control)

For these simulations, we use the modified WLAN node model of OPNET 17.5 that implements the neural network solution as described earlier in this chapter. The main parameters of the simulation system are shown in Table (7.2). The mentioned values are the initial values at the beginning of a simulation run. The effect of some key parameters on the performance of the proposed solution is discussed and highlighted in this section. Firstly, we evaluate the performance of the proposed solution in mitigating hidden and exposed node problems in two simple scenarios. Then, we consider a more complex scenario that reflects a real world high density deployment and we evaluate our proposal in such challenging circumstances.

7.6.1 Hidden node scenario

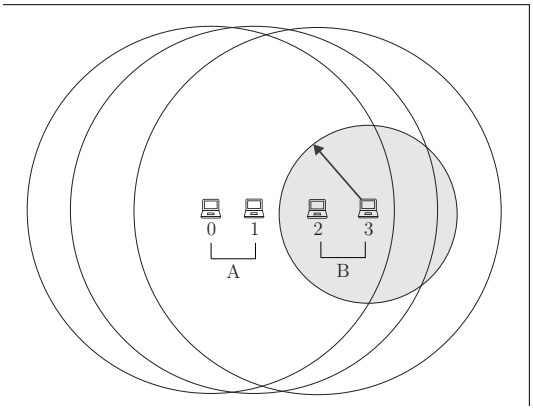

Figure 7.9 – Hidden node scenario, illustration of the protection range at optimization round 0 (initial situation)

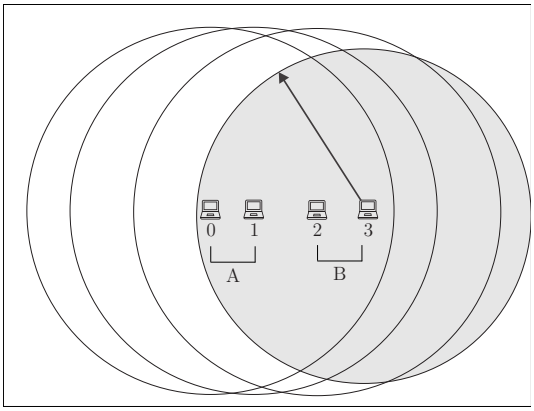

Figure 7.10 – Hidden node scenario, illustration of the protection range at optimization round 5

We talk about a hidden node problem when a node that is not able to sense the signal transmitted by an another neighboring node (the hidden node) operating at the same channel, and hence it assumes that the medium is free and transmits. The simultaneously transmitted signals interfere at the receiving node causing a failure in the reception process. As a solution to this problem, an exchange of Request To Send (RTS) and Clear To Send (CTS) frames is described in the IEEE 802.11 standard. However, as widely highlighted in the literature [23], the RTS/CTS mechanism introduces an important overhead and reduces the capacity of the network in terms of throughput since each node has to transmit the RTS and wait for the CTS response before any transmission. Furthermore, in specific scenarios, this mechanism fails to eliminate hidden nodes [24]. In this study, we experiment the performance of our solution in solving the hidden node problem without using the RTS/CTS.

The topology used for this scenario consists of four nodes (two couples: $couple_A$ includes node 0 and node 1 and couple B includes node 2 and node 3) placed as shown in Figure 7.9. All these nodes are operating at the same frequency channel. Each node generates a saturated constant bit rate (CBR) traffic to the other node of the same couple. In this scenario, in order to reproduce the hidden node problem, the distances between the different nodes are configured in such a way that if two nodes belonging to different couples transmit simultaneously, the both receiving nodes will not be able to receive the signal of interest successfully. This means that couple A and couple B are sharing the total capacity of the network. Basing on a simple simulation of a single transmitter-receiver couple, without any source of co-channel interference, the maximum capacity of a network using the default configurations is around 49 $Mbps$.

Furthermore, by properly configuring the carrier sensing parameters, each node is able to sense the transmissions of all the other nodes except node 3 that is not able to sense the transmissions of the nodes of couple A. Hence, node 3 is a hidden node and its transmissions degrade the performance of the network. In Figure 7.9, we illustrate the initial protection range around each node. At the end of the simulation, the final protection ranges are depicted in Figure 7.10.

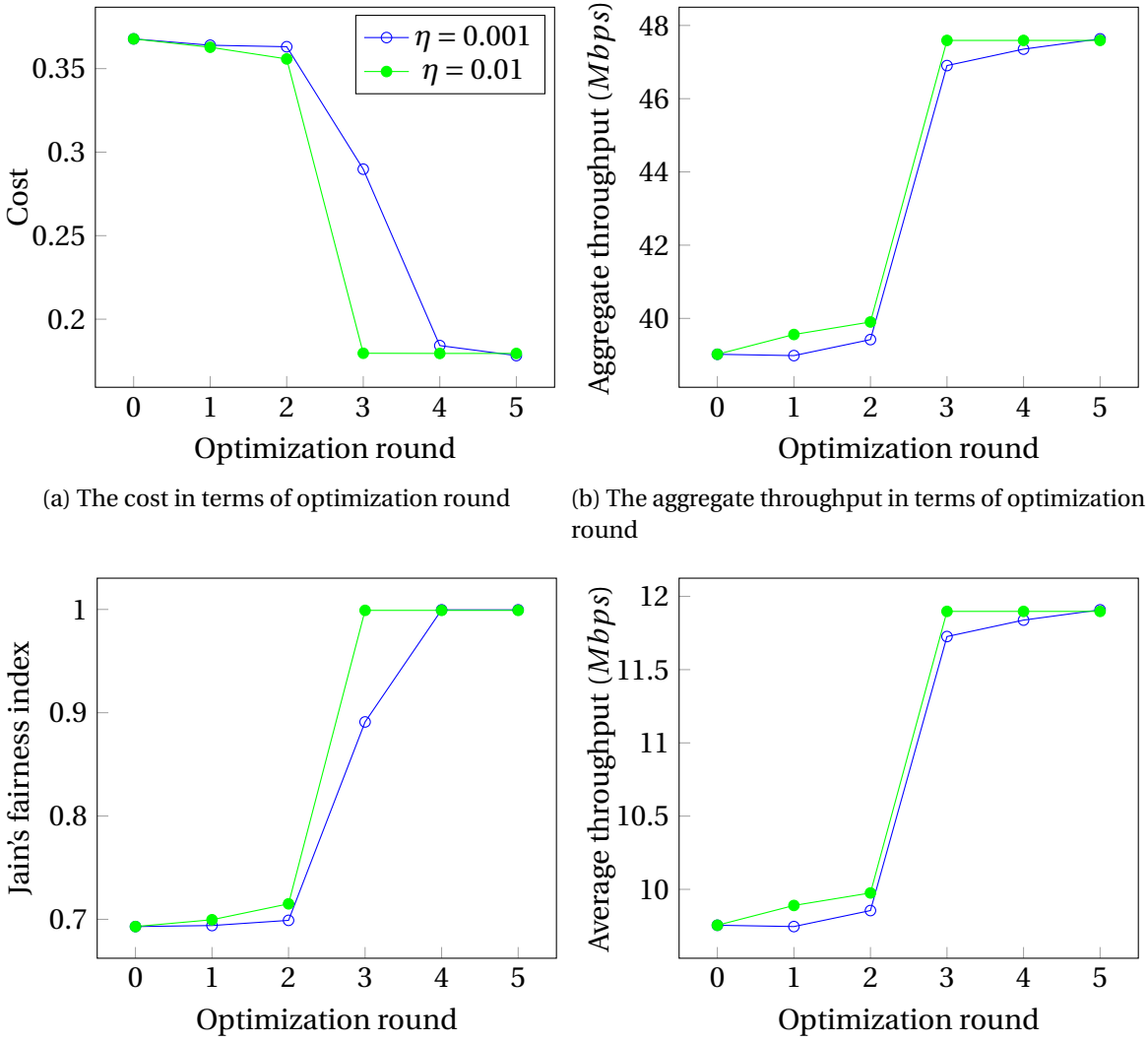

(a) The cost in terms of optimization round

(b) The aggregate throughput in terms of optimization round

(c) The Jain's fairness index in terms of optimization round

(d) The average throughput in terms of optimization round

Figure 7.11 – The performance of the proposed optimization in hidden nodes scenario

All the collected results related to this scenario are plotted in Figure 7.11 in terms of the optimization round number. For this evaluation we consider four metrics: the aggregate throughput (or global throughput), the average throughput (per node), the cost function, and the Jain's fairness index. Each metric is evaluated for two different optimization update rates η: 0.01 and 0.001. Since all the nodes of this scenario are in the same contention domain and the mutual interference between the two couples is destructive in case of

simultaneous communications, the maximum achievable throughput is bounded by the maximum capacity of a single transmitter-receiver couple (i.e., 49 $Mbps$). However, the presence of the hidden node (i.e., node 3 in Figure 7.9) is degrading the performance of the system. As depicted in Figure 7.11b, at the optimization round 0 (initial situation before any optimization), the achieved aggregate throughput is not reaching its optimal level. At the final optimization round, the aggregate throughput is improved by more than 20 % compared to the initial situation. Thanks to the learning-based mechanism, the hidden node problem is completely revealed as illustrated by Figure 7.10. Consequently, the total capacity of the system is fairly shared between the four nodes as shows the Jain's fairness index in Figure 7.11c.

As defined in Equation (7.15), η determines the aggressiveness of the optimization round update. The Figure 7.11a shows that with a higher η, the cost is minimized with less optimization rounds. The same logic applies to the Jain's fairness that reaches its maximum value after the first two optimization rounds for $\eta = 0.01$. It is worth mentioning that the cost function is not minimized to zero since the individual average throughput cannot reach X_T (i.e., the target throughput). In fact, the maximum capacity of the network is attained before the satisfaction of the target throughput.

7.6.2 Exposed node scenario

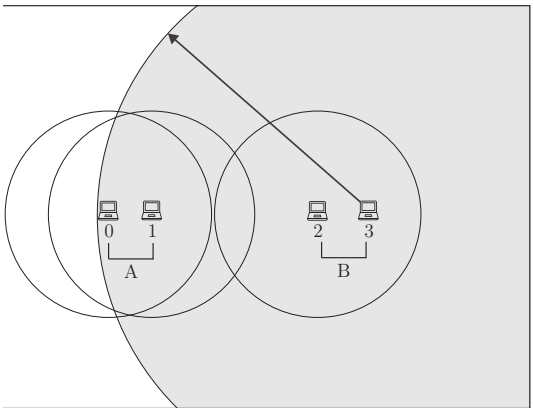

Figure 7.12 – Exposed node scenario, illustration of the protection range at optimization round 0 (initial situation)

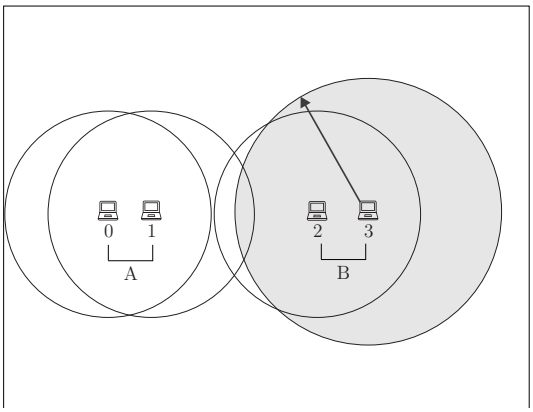

Figure 7.13 – Exposed node scenario, illustration of the protection range at optimization round 5

In this scenario, we examine the ability of the proposed solution to mitigate the exposed node problem. The scenario topology shown in Figure 7.12 consists of the same two couples of nodes used in the previous section but differently configured to reproduce the exposed node problem. Here, the Signal to Interference and Noise Ratio (SINR) values at a receiver node, in presence of a simultaneous transmission with the other couple, always permit the receiver to decode successfully the signal of interest. However, the transmission power and carrier sensing are configured in such a way as to prohibit node 3 from transmitting when one of the nodes of couple A is transmitting. Node 3 that belongs to couple B is exposed here to the transmissions of the nodes of couple A as illustrated in Figure 7.12.

As in the previous scenario, we run the simulation for different η values and we plot the resulting metrics over 5 optimization rounds in Figure 7.14. At the initial situation (i.e., optimization round 0), the Jain's fairness index in Figure 7.14c show clearly the impact of the exposed node problem. $Node\ 3$ is not able to gain access to the medium because it is exposed to the transmissions of the other couple. In this scenario, thanks to the initial configurations of the network topology, the maximum attainable capacity of the network is the aggregation of two transmitter-receiver couples (about 98 $Mbps$). This is due to the fact that relative interfering couples separation is sufficient for successful simultaneous transmissions. However, as clearly depicted in Figure 7.14b, the aggregate throughput at the optimization round 0 is far away from the optimal value because node 3 is not able to initiate transmissions neither responding to the transmissions received from node 2.

Our proposed scheme is able to relieve the exposed node situation by decreasing the protection range around the exposed node (node 3) as illustrated in Figure 7.13. This led, in this particular scenario, to a two-fold increase in the aggregate throughput as shown in

Figure 7.14b at optimization round 5. Since the target throughput X_T can be easily attained by the different nodes before the saturation point of the system, the cost function plotted in Figure 7.14a is minimized to zero at the last optimization round for all the η values.

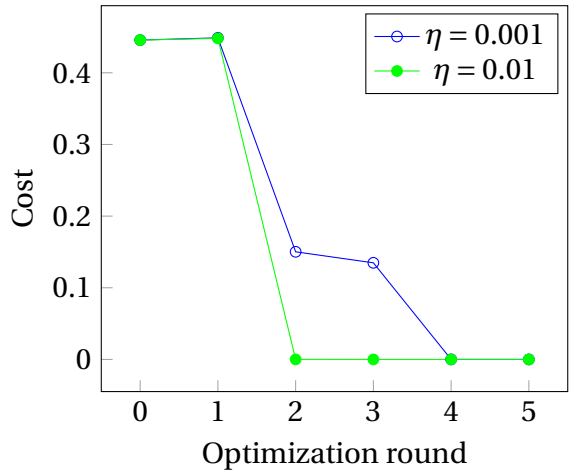

(a) The cost in terms of optimization round

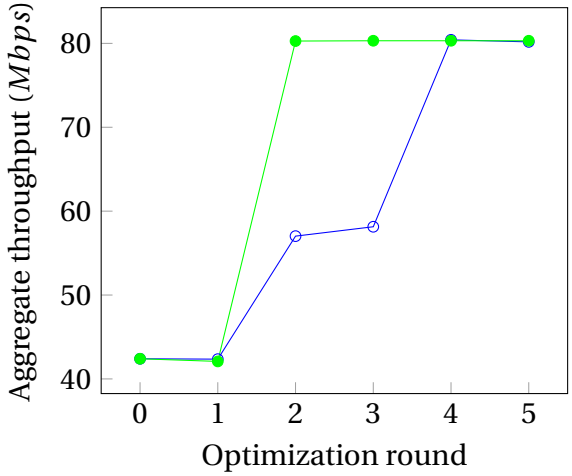

(b) The aggregate throughput in terms of optimization round

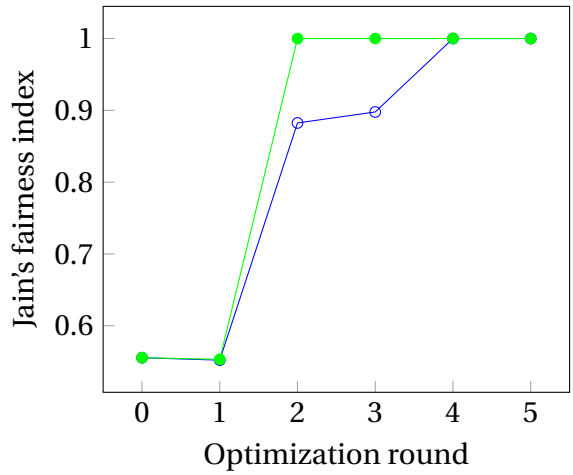

(c) The Jain's fairness index in terms of optimization round

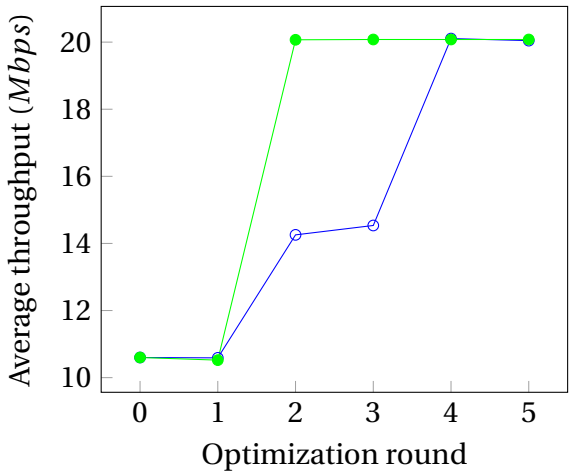

(d) The average throughput in terms of optimization round

Figure 7.14 – The performance of the proposed optimization in exposed nodes scenario

7.6.3 High density cellular deployment scenario

In this scenario, we consider the cellular scenario described in Section 3.2.1. The latter represents a challenging high density deployment. The definition of this scenario is based on the simulation scenarios defined by the IEEE 802.11ax Task Group (TG) [80]. An important real-world use case considered at the standardization TG is deploying Wi-Fi in a stadium which is characterized by very high numbers of APs and STAs [81]. The cellular topology considered for our evaluation is illustrated in Figure 7.15.

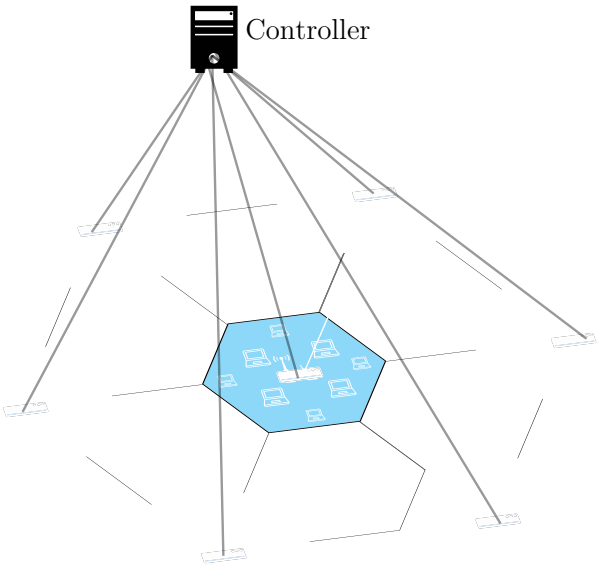

Figure 7.15 – Cellular scenario network topology

The obtained results are presented in Figure 7.16. The first important observation when comparing to the results of the previous scenarios is that the system needs more optimization rounds to converge. This is normal since the scenario is more complex because of the much higher number of devices and hence the ANN has larger number of neurons with 126 inputs and 63 outputs. Another observation is related to the Jain's fairness index curve plotted in Figure 7.16c. Contrary to the previous scenarios, this index does not reach its maximum value in the current scenario, meaning that not all the devices are achieving the same throughput. In fact, this is due to the difference in throughput between uplink and downlink flows. The AP that is transmitting to 8 STAs has almost the opportunity to access the medium as any other ordinary STA.

Since the network is saturated, the share of airtime used by the AP to transmit data to one STA is much lower than that used by a STA to send data to the AP. However, after the convergence of the adaptation, the fairness index is importantly enhanced (from ≈ 0.5 at optimization round 0 to ≈ 0.7 at the final round). This enhancement reflects the ability of the proposed adaptation to solve the exposed node situations and increasing the spatial reuse between all the BSSs. This enhancement in spatial reuse is clearly seen in Figure 7.16b, where the gain in aggregate throughput exceeds 45 %.

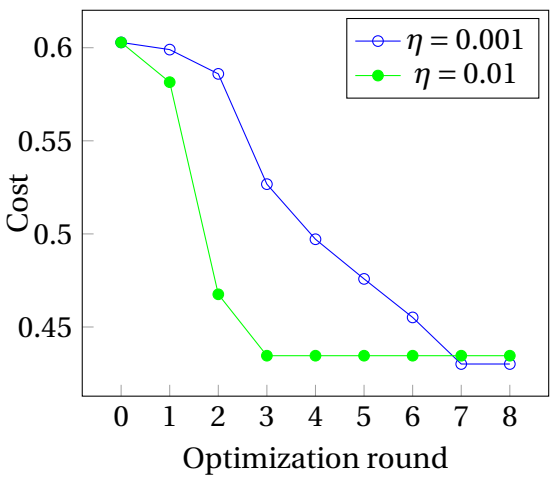

(a) The cost in terms of optimization round

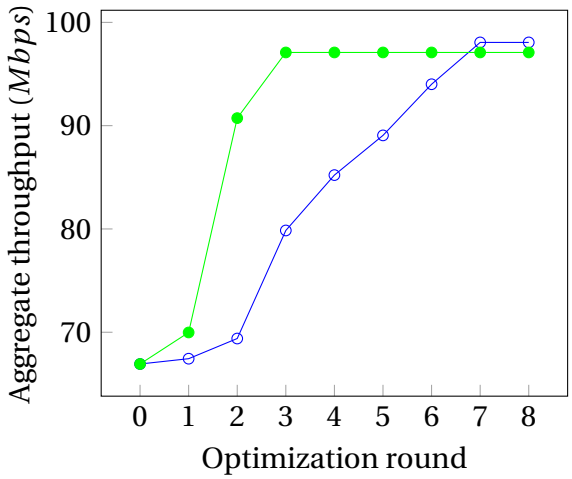

(b) The aggregate throughput in terms of optimization round

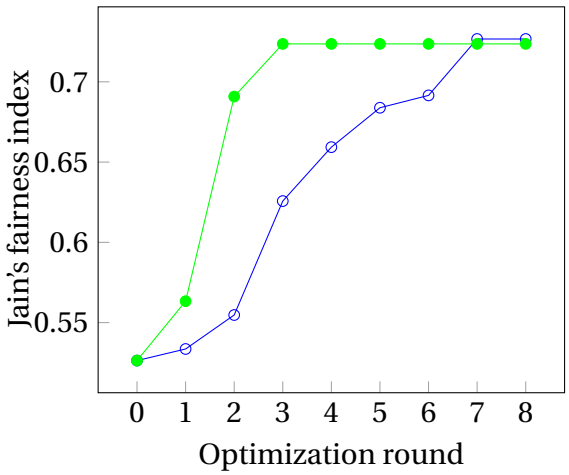

(c) The Jain's fairness index in terms of optimization round

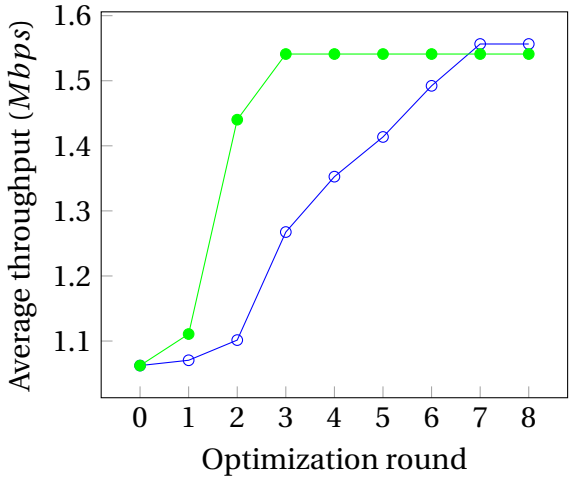

(d) The average throughput in terms of optimization round

Figure 7.16 – The performance of the proposed optimization in cellular scenario

7.7 Summary

To overcome the fairness problem discussed in the previous chapter, we exploit a new solution for jointly optimizing the transmission power and the physical carrier sensing. The main motivation of this joint solution is that the impact of one of these two key parameters on the performance of legacy devices is opposed to the other. While TPC mechanisms favor the legacies, the adaptation of the carrier sensing mechanism disfavors these devices.

In this chapter we proposed a new learning-based mechanism using artificial neural networks that is able to optimally adapt the two mechanisms (TPC and PCSA) in order to increase spatial reuse and preserve fairness in managed WLANs. This approach takes benefit from the capability of artificial neural networks to approximate complex functions

in order to model the throughput performance in terms of MAC layer parameters. This allows an intelligent adaptation of these parameters that enhances the spatial reuse in dense deployments. We showed through extensive simulations that our proposal is capable of resolving hidden and exposed node problems and hence leveraging the aggregate throughput in high density deployments while enhancing the fairness among all the nodes.

Furthermore, this solution could be used to optimize other important parameters in the future IEEE 802.11ax WLANs such as the length of the Transmit Opportunity (TXOP). Future centralized deployments could benefit directly from this new approach to achieve better Quality of Experience (QoE). This would allow the integration of high efficiency WLANs in saturated cellular networks for mobile traffic offloading.

Conclusions and perspectives

Conclusions

To satisfy the growing demand for wireless systems capacity, the industry is dramatically increasing the density of the deployed networks. Like other wireless technologies, Wi-Fi is following this trend, particularly because of its increasing popularity. In parallel, Wi-Fi is being deployed for new use cases that are atypically far from the context of its first introduction as an Ethernet network replacement. In fact, the conventional operation of Wi-Fi networks is not likely to be ready for these super dense environments and new challenging scenarios. For that reason, the High Efficiency WLAN (HEW) Study Group (SG) was formed in May 2013 within the IEEE 802.11 Working Group (WG). The intents are to improve the “real world" Wi-Fi performance especially in dense deployments.

After reviewing thoroughly the challenges facing present and future Wireless Local Area Network (WLAN) systems, we have extracted the possible improvement tracks along with the existing contributions in the state-of-the-art. This has been done with a view to being in accordance with the currently ongoing standardization efforts in the IEEE 802.11ax Task Group (TG), the continuity of the HEW SG, where the preparations for the next WLAN standard are taking place.

In the present work, we have considered increasing the spatial reuse in high density deployments by adapting the Media Access Control Layer (MAC) protocols. While the control of the transmission power (i.e., Transmit Power Control (TPC)) has always been one of the chosen techniques when targeting spatial reuse improvements (traditionally in cellular technologies), we have shown the weakness points of TPC especially in deployments where the compliance of all the wireless devices is not always possible. Consequently, we have proposed a dynamic adaptation of the Physical Carrier Sensing (PCS) mechanism to leverage the spatial reuse. We have showed through extensive simulations that the proposed Physical Carrier Sensing Adaptation (PCSA) outperforms other schemes especially when

legacy devices are present in the network.

While there are many more incentives behind preferring PCSA over TPC, we have highlighted that instead of favoring the legacy devices (as TPC does), PCSA favors the devices applying it (i.e., that we refer to as 802.11ax devices). This behavior alters the throughput fairness level among contending devices.

To enhance the situation, we have proposed the Balanced TPC and PCS Adaptation (BTPA), a novel joint adaptation of the two techniques. The key aim behind BTPA is to preserve fairness while improving spatial reuse in dense WLAN deployments. This distributed solution is applied locally at each device without the need for coordination among Overlapping BSS (OBSS)s.

Although BTPA is applicable in centralized deployments, it is more appropriate to design a fully centralized solution for these deployments. Such an approach could profit from the presence of a central controller to devise closed loop solutions. In this manner, we have used Artificial Neural Network (ANN) to propose a new learning-based optimization of the MAC parameters aiming at leveraging the spatial reuse in high density WLANs. The proposal has been designed, implemented and evaluated in different simulation scenarios. The results have proven the capability of our proposal to resolve hidden and exposed node problems. Moreover, we have shown its effectiveness in improving the spatial reuse in dense WLAN scenarios while preserving high fairness levels in terms of achieved throughputs.

The contributions presented in this thesis are an important step in the direction of specifying future high efficiency WLAN. They have resulted in one patent and publications in 4 international conferences (ICT 2014, NoF 2014, WCNC 2015, ICC 2015). Furthermore, the contribution and the results presented in the last chapter have been submitted to the EURASIP Journal on Wireless Communications and Networking.

Perspectives

This thesis considered the improvement of spatial reuse in dense WLAN deployments. In the following, we describe some relevant points that further studies could investigate to extend the work achieved in this dissertation.

The performance analysis that we made in this thesis is based on system level simulations. Obviously, an implementation in real WLAN interfaces would be the natural next step in evaluating the performance of our proposals. A software implementation of PCSA and BTPA in a real equipment's driver as a part of a future testbed is essential to study their performance in real networks paving the way for their implementation in future IEEE

802.11ax devices.

However, since we are targeting high density deployments, the scalability of such an approach is limited. For that reason, we suggest a hybrid platform mixing simulation and real equipments. Such a platform will benefit from the scalability offered by the simulation tools and will be able to interact with real world devices to evaluate a practical implementation of our proposals.

In Chapter 5, we have studied the impact of the currently widely used rate control schemes on the performance of PCSA and we have shown that the latter performs efficiently without substantial modifications of these schemes. However, a new dynamic mechanism to set the minimum Modulation and Coding Scheme (MCS) allowed by a conventional rate control algorithm is needed. Such a mechanism could be designed as a complement of the rate control schemes currently used in production.

Our work could be extended in other research directions. The continuations of this work, notably by extending them to the minimization of the energy consumption of Wi-Fi, will be even more important as the number of Wi-Fi devices present in home networks increases. In addition, Wi-Fi is now integrated into the majority of small portable devices supplied by batteries, for which the reduction of energy consumption is particularly important. It will therefore be increasingly needed to reduce the energy consumed by Wi-Fi interfaces. Improving TPC seems a natural direction to emphasize in order to reduce energy consumption related to the use of Wi-Fi. Additionally, the solutions that we have proposed in this thesis could be considered from a power efficiency study perspective. We believe that BTPA could be useful in future studies targeting at minimizing power consumption in dense WLANs. In practice, the BTPA's $ratio$ could be adapted according to consumption constraints to minimize the transmission power while enhancing the spatial reuse.

Moreover, concerning the learning-based spatial reuse optimization solution that we have proposed in Chapter 7, relaxing the requirements of offline datasets is an important step to make such a mechanism more practical in real world implementations.

On a slightly different topic, as it has been already revoked in Section 2.6.4, the 802.11ax will provide multi-user uplink transmissions through Orthogonal Frequency Division Multiple Access (OFDMA) or/and Multi-User MIMO (MU-MIMO). For their operation, these techniques need to implement interference management mechanisms. In high density environments, controlling the transmission power of the Station (STA)s is of high importance to prevent interferences between uplink transmissions scheduled by the Access Point (AP). Accordingly, adapting our solutions and studying their performance in the context of such a scheduled system is necessary.

Furthermore, the 3rd Generation Partnership Project (3GPP) activities concerning the oper-

ation of the Long-Term Evolution (LTE) in unlicensed frequency bands are drawing our attention. Even though at the time of writing this thesis it is still under development, the LTE in Unlicensed spectrum (LTE-U) or Licensed-Assisted Access (LAA) poses new challenges to the current and future Wi-Fi networks. LTE-U will operate on the Industrial, Scientific and Medical (ISM) bands already occupied by Wi-Fi, Bluetooth, and other systems. The coexistence between these different technologies without impacting their performance is a real challenge. The Wi-Fi Alliance (WFA) discussions reveal great fears that the use of LTE-U will swamp the unlicensed band causing the Wi-Fi users to suffer from severe performance degradation. Consequently, LTE-U systems must be carefully designed to overcome these issues. One of the main requirements to operate in these bands is to apply a Listen Before Talk (LBT) mechanism before transmitting (e.g., the Clear Channel Assessment (CCA) that is explained in Section 1.3.2). In this context, our contributions in this thesis are of great importance and could be studied to enhance the performance of each of the coexisting technologies especially in when dense deployments are needed.

Bibliography

[1] N. Abramson, "THE ALOHA SYSTEM: Another Alternative for Computer Communications," in *Proceedings of the November 17-19, 1970, Fall Joint Computer Conference*, ser. AFIPS '70 (Fall), pp. 281–285. New York, NY, USA: ACM, November 1970. doi: 10.1145/1478462.1478502

[2] Global Broadband and WLAN (Wi-Fi) Networked Households Forecast 2009-2018. [Online]. Available: http://www.strategyanalytics.com/default.aspx?mod=reportabstractviewer&a0=10232

[3] Total Wi-Fi device shipments to surpass ten billion. [Online]. Available: https://www.abiresearch.com/market-research/product/1021330-wi-fi/

[4] Total Wi-Fi device shipments to surpass ten billion. [Online]. Available: http://www.wi-fi.org/news-events/newsroom/total-wi-fi-device-shipments-to-surpass-ten-billion-this-month

[5] *IEEE Std 802.11-2012 (Revision of IEEE Std 802.11-2007) - IEEE Standard for Information technology–Telecommunications and information exchange between systems Local and metropolitan area networks–Specific requirements Part 11: Wireless LAN Medium Access Control (MAC) and Physical Layer (PHY) Specifications*, IEEE Std., March 2012.

[6] IEEE 802.11 High Efficiency Wireless Local Area Networks (HEW) Study Group. [Online]. Available: http://www.ieee802.org/11/Reports/hew_update.htm

[7] IEEE 802.11ax Task Group for High Efficiency WLAN (HEW). [Online]. Available: http://www.ieee802.org/11/Reports/tgax_update.htm

[8] *IEEE Std 802.11-1997 (Revised by IEEE Std 802.11-1999) - IEEE Standard for Information Technology- Telecommunications and Information Exchange Between Systems-Local and Metropolitan Area Networks-Specific Requirements-Part 11: Wireless LAN*

Medium Access Control (MAC) and Physical Layer (PHY) Specifications, IEEE Std., 1997.

[9] *IEEE Std 802.11b-1999 (Supplement to IEEE Std 802.11-1999) - IEEE Standard for Information Technology- Telecommunications and Information Exchange Between Systems- Local and Metropolitan Area Networks- Specific Requirements- Part 11: Wireless LAN Medium Access Control (MAC) and Physical Layer (PHY) Specifications: Higher-Speed Physical Layer Extension in the 2.4 GHz Band*, IEEE Std., 2000.

[10] *IEEE Std 802.11a-1999 (Supplement to IEEE Std 802.11-1999) - IEEE Standard for Telecommunications and Information Exchange Between Systems - LAN/MAN Specific Requirements - Part 11: Wireless Medium Access Control (MAC) and physical layer (PHY) specifications: High Speed Physical Layer in the 5 GHz band*, IEEE Std., Dec 1999.

[11] *IEEE Std 802.11g-2003 (Amendment to IEEE Std 802.11-1999) - IEEE Standard for Information Technology- Telecommunications and Information Exchange Between Systems- Local and Metropolitan Area Networks- Specific Requirements Part 11: Wireless LAN Medium Access Control (MAC) and Physical Layer (PHY) Specifications*, IEEE Std., 2003.

[12] *IEEE Std 802.11n-2009 (Amendment to IEEE Std 802.11-2007) - IEEE Standard for Information technology– Local and metropolitan area networks– Specific requirements– Part 11: Wireless LAN Medium Access Control (MAC)and Physical Layer (PHY) Specifications Amendment 5: Enhancements for Higher Throughput*, IEEE Std., Oct 2009.

[13] *IEEE Std 802.11ac-2013 (Amendment to IEEE Std 802.11-2012) - IEEE Standard for Information technology– Telecommunications and information exchange between systemsLocal and metropolitan area networks– Specific requirements–Part 11: Wireless LAN Medium Access Control (MAC) and Physical Layer (PHY) Specifications–Amendment 4: Enhancements for Very High Throughput for Operation in Bands below 6 GHz.*, IEEE Std., Dec 2013.

[14] *IEEE Standard for Information technology–Telecommunications and information exchange between systems–Local and metropolitan area networks–Specific requirements-Part 11: Wireless LAN Medium Access Control (MAC) and Physical Layer (PHY) Specifications Amendment 3: Enhancements for Very High Throughput in the 60 GHz Band*, IEEE Std., Dec 2012.

[15] "Ieee standard for information technology - telecommunications and information exchange between systems - local and metropolitan area networks - specific requirements - part 11: Wireless lan medium access control (mac) and physical layer (phy) specifications amendment 5: Television white spaces (tvws) operation,"

IEEE Std 802.11af-2013 (Amendment to IEEE Std 802.11-2012, as amended by IEEE Std 802.11ae-2012, IEEE Std 802.11aa-2012, IEEE Std 802.11ad-2012, and IEEE Std 802.11ac-2013), Feb 2014.

[16] 802.11ah Sub 1 GHz Task Group. [Online]. Available: http://www.ieee802.org/11/Reports/tgah_update.htm

[17] D. Tse and P. Viswanath, *Fundamentals of Wireless Communication*, ser. Wiley series in telecommunications. Cambridge University Press, 2005. ISBN 9780521845274

[18] R. v. Nee and R. Prasad, *OFDM for Wireless Multimedia Communications*, 1st ed. Norwood, MA, USA: Artech House, Inc., 2000. ISBN 0890065306

[19] M. Engels, *Wireless OFDM Systems: How to make them work?*, ser. The Springer International Series in Engineering and Computer Science. Springer US, 2002. ISBN 9781475784596

[20] V. K. N. Lau and Y.-K. Ricky Kwok, *Channel-Adaptive Technologies and Cross-Layer Designs for Wireless Systems with Multiple Antennas*. John Wiley & Sons, Inc., 2006. ISBN 9780471774068

[21] *IEEE Std 802.11e-2005 (Amendment to IEEE Std 802.11-1999) - IEEE Standard for Information technology–Local and metropolitan area networks–Specific requirements–Part 11: Wireless LAN Medium Access Control (MAC) and Physical Layer (PHY) Specifications - Amendment 8: Medium Access Control (MAC) Quality of Service Enhancements*, IEEE Std., Nov 2005.

[22] M. Heusse, F. Rousseau, G. Berger-Sabbatel, and A. Duda, "Performance anomaly of 802.11b," in *Proceedings of the Twenty-Second Annual Joint Conference of the IEEE Computer and Communications*, ser. INFOCOM '03, vol. 2, pp. 836–843, March 2003. doi: 10.1109/INFCOM.2003.1208921. ISSN 0743-166X

[23] J. Sobrinho, R. de Haan, and J. Brazio, "Why RTS-CTS is not your ideal wireless LAN multiple access protocol," in *Proceedings of the IEEE Wireless Communications and Networking Conference*, ser. WCNC '05, vol. 1, pp. 81–87, March 2005. doi: 10.1109/WCNC.2005.1424480. ISSN 1525-3511

[24] K. Xu, M. Gerla, and S. Bae, "How effective is the IEEE 802.11 RTS/CTS handshake in ad hoc networks," in *Proceedings of the IEEE Global Telecommunications Conference*, ser. GLOBECOM '02, vol. 1, pp. 72–76, Nov 2002. doi: 10.1109/GLOCOM.2002.1188044

[25] J. Choi, J. Na, Y. sup Lim, K. Park, and C.-K. Kim, "Collision-aware design of rate adaptation for multi-rate 802.11 WLANs," *IEEE Journal on Selected Areas in Communications*, vol. 26, no. 8, pp. 1366–1375, October 2008. doi: 10.1109/JSAC.2008.081003

[26] K. Leentvaar and J. Flint, "The Capture Effect in FM Receivers," *IEEE Transactions on Communications*, vol. 24, no. 5, pp. 531–539, May 1976. doi: 10.1109/TCOM.1976.1093327

[27] C. Ware, J. Chicharo, and T. Wysocki, "Simulation of capture behaviour in IEEE 802.11 radio modems," in *Proceedings of the 54th IEEE Vehicular Technology Conference*, ser. VTC '01 (Fall), vol. 3, pp. 1393–1397, October 2001. doi: 10.1109/VTC.2001.956425. ISSN 1090-3038

[28] P. S. Sang, *On capture effect of FM demodulators*. M.S. Thesis Naval Postgraduate School, Monterey, CA., March 2006. [Online]. Available: https://archive.org/details/oncaptureeffecto00park

[29] J. del Prado Pavon and S. Choi, "Link adaptation strategy for IEEE 802.11 WLAN via received signal strength measurement," in *Proceedings of the IEEE International Conference on Communications*, ser. ICC '03, vol. 2, pp. 1108–1113 vol.2, May 2003. doi: 10.1109/ICC.2003.1204534

[30] S. Muthuswamy, I. Marsic, and A. Annamalai, "New methods for estimating/forecasting link bandwidths in 802.11b WLANs," in *Proceedings of the 60th IEEE Vehicular Technology Conference*, ser. VTC '04 (Fall), vol. 2, pp. 1163–1168 Vol. 2, Sept 2004. doi: 10.1109/VETECF.2004.1400204. ISSN 1090-3038

[31] A. Kashyap, S. Ganguly, and S. R. Das, "A Measurement-based Approach to Modeling Link Capacity in 802.11-based Wireless Networks," in *Proceedings of the 13th Annual ACM International Conference on Mobile Computing and Networking*, ser. MobiCom '07, pp. 242–253. New York, NY, USA: ACM, 2007. doi: 10.1145/1287853.1287883. ISBN 978-1-59593-681-3

[32] F. Tobagi and L. Kleinrock, "Packet Switching in Radio Channels: Part II–The Hidden Terminal Problem in Carrier Sense Multiple-Access and the Busy-Tone Solution," *IEEE Transactions on Communications*, vol. 23, no. 12, pp. 1417–1433, Dec 1975. doi: 10.1109/TCOM.1975.1092767

[33] S. Roy and H.-Y. Wang, "Performance of CDMA slotted ALOHA multiple access with multiuser detection," in *Proceedings of the IEEE Wireless Communications and Networking Conference*, ser. WCNC 1999, vol. 2, pp. 839–843, 1999. doi: 10.1109/WCNC.1999.796787. ISSN 1525-3511

[34] A. Sheikh, T. Wan, and Z. Alakhdar, "A Unified Approach to Analyze Multiple Access Protocols for Buffered Finite Users," *Journal of Network and Computer Applications*, vol. 27, no. 1, pp. 49–76, January 2004. doi: 10.1016/S1084-8045(03)00029-8

[35] L. Kleinrock and S. Lam, "Packet Switching in a Multiaccess Broadcast Channel: Performance Evaluation," *IEEE Transactions on Communications*, vol. 23, no. 4, pp. 410–423, Apr 1975. doi: 10.1109/TCOM.1975.1092814

[36] G. Bianchi, "IEEE 802.11-saturation throughput analysis," *IEEE Communications Letters*, vol. 2, no. 12, pp. 318–320, Dec 1998. doi: 10.1109/4234.736171

[37] ——, "Performance analysis of the IEEE 802.11 distributed coordination function," *IEEE Journal on Selected Areas in Communications*, vol. 18, no. 3, pp. 535–547, March 2000. doi: 10.1109/49.840210

[38] Y. Xiao, "Performance analysis of priority schemes for IEEE 802.11 and IEEE 802.11e wireless LANs," *IEEE Transactions on Wireless Communications*, vol. 4, no. 4, pp. 1506–1515, July 2005. doi: 10.1109/TWC.2005.850328

[39] J. Robinson and T. Randhawa, "Saturation throughput analysis of IEEE 802.11e enhanced distributed coordination function," *IEEE Journal on Selected Areas in Communications*, vol. 22, no. 5, pp. 917–928, June 2004. doi: 10.1109/JSAC.2004.826929

[40] R. Nelson, *Probability, Stochastic Processes, and Queueing Theory: The Mathematics of Computer Performance Modeling*. New York, NY, USA: Springer-Verlag New York, Inc., 1995. ISBN 0-384-94452-4

[41] X. Ling, K.-H. Liu, Y. Cheng, X. Shen, and J. W. Mark, "A Novel Performance Model for Distributed Prioritized MAC Protocols," in *Proceedings of the IEEE Global Telecommunications Conference*, ser. GLOBECOM '07, pp. 4692–4696, Nov 2007. doi: 10.1109/GLOCOM.2007.890

[42] M. Ergen, B. Dundar, and P. Varaiya, "Throughput analysis of an extended service set in IEEE 802.11," in *Proceedings of the IEEE Global Telecommunications Conference*, ser. GLOBECOM '04, vol. 2, pp. 1040–1045 Vol.2, Nov 2004. doi: 10.1109/GLOCOM.2004.1378116

[43] E. Garcia, E. Lopez-Aguilera, R. Vidal, and J. Paradells, "IEEE Wireless LAN Capacity in Multicell Environments with Rate Adaptation," in *Proceedings IEEE 18th International Symposium on Personal, Indoor and Mobile Radio Communications*, ser. PIMRC '07, pp. 1–6, Sept 2007. doi: 10.1109/PIMRC.2007.4394489

[44] L. Wang, K. Wu, and M. Hamdi, "Combating Hidden and Exposed Terminal Problems in Wireless Networks," *IEEE Transactions on Wireless Communications*, vol. 11, no. 11, pp. 4204–4213, November 2012. doi: 10.1109/TWC.2012.092712.120628

[45] S. Katti, S. Gollakota, and D. Katabi, "Embracing Wireless Interference: Analog Network Coding," in *Proceedings of the 2007 Conference on Applications, Technologies,*

Architectures, and Protocols for Computer Communications, ser. SIGCOMM '07, pp. 397–408. New York, NY, USA: ACM, 2007. doi: 10.1145/1282380.1282425. ISBN 978-1-59593-713-1

[46] K. Wu, H. Tan, H.-L. Ngan, Y. Liu, and L. Ni, "Chip Error Pattern Analysis in IEEE 802.15.4," *IEEE Transactions on Mobile Computing*, vol. 11, no. 4, pp. 543–552, April 2012. doi: 10.1109/TMC.2011.44

[47] J. Bordim, T. Hunziker, and K. Nakano, "Adaptive Carrier Sensing and Packet Sending - An Alternative to Boost the Performance in Directional Communications," in *Proceedings of the Sixth International Conference on Parallel and Distributed Computing, Applications and Technologies*, ser. PDCAT '05, pp. 274–279, Dec 2005. doi: 10.1109/PDCAT.2005.62

[48] Y.-B. Ko, V. Shankarkumar, and N. Vaidya, "Medium access control protocols using directional antennas in ad hoc networks," in *Proceedings of the Nineteenth IEEE Annual Joint Conference of the IEEE Computer and Communications Societies*, ser. INFOCOM '00, vol. 1, pp. 13–21 vol.1, March 2000. doi: 10.1109/INFCOM.2000.832169. ISSN 0743-166X

[49] J. Bordim, T. Ueda, and S. Tanaka, "Delivering the Benefits of Directional Communications for Ad Hoc Networks Through an Efficient Directional MAC Protocol," *Telecommunications and Networking - ICT 2004*, pp. 461–470, 2004. doi: 10.1007/978-3-540-27824-5

[50] R. Choudhury and N. Vaidya, "Deafness: a MAC problem in ad hoc networks when using directional antennas," in *Proceedings of the 12th IEEE International Conference on Network Protocols*, ser. ICNP '04, pp. 283–292, Oct 2004. doi: 10.1109/ICNP.2004.1348118. ISSN 1092-1648

[51] M. Abusubaih, B. Rathke, and A. Wolisz, "A framework for interference mitigation in multi-BSS 802.11 wireless LANs," in *Proceedings of the IEEE International Symposium on a World of Wireless, Mobile and Multimedia Networks Workshops*, ser. WoWMoM '09, pp. 1–11, June 2009. doi: 10.1109/WOWMOM.2009.5282490

[52] *IEEE Standard for Information technology– Local and metropolitan area networks– Specific requirements– Part 15.4: Wireless Medium Access Control (MAC) and Physical Layer (PHY) Specifications for Low Rate Wireless Personal Area Networks (WPANs)*, IEEE Std., Sept 2006.

[53] *IEEE Standard for Telecommunications and Information Exchange Between Systems - LAN/MAN - Specific Requirements - Part 15: Wireless Medium Access Control (MAC) and Physical Layer (PHY) Specifications for Wireless Personal Area Networks (WPANs)*, IEEE Std., June 2002.

[54] K. Medepalli and F. Tobagi, "On Optimization of CSMA/CA based Wireless LANs: Part I - Impact of Exponential Backoff," in *Proceedings of the IEEE International Conference on Communications*, ser. ICC '06, vol. 5, pp. 2089–2094, June 2006. doi: 10.1109/ICC.2006.255078. ISSN 8164-9547

[55] K. Medepalli, F. Tobagi, D. Famolari, and T. Kodama, "On Optimization of CSMA/CA based Wireless LANs: Part II - Mitigating Efficiency Loss," in *Proceedings of the IEEE International Conference on Communications*, ser. ICC '06, vol. 10, pp. 4799–4804, June 2006. doi: 10.1109/ICC.2006.255399. ISSN 8164-9547

[56] X. Sun and L. Dai, "Backoff Design for IEEE 802.11 DCF Networks: Fundamental Tradeoff and Design Criterion," *IEEE/ACM Transactions on Networking*, vol. 23, no. 1, pp. 300–316, Feb 2015. doi: 10.1109/TNET.2013.2295242

[57] C.-H. Ke, C.-C. Wei, T.-Y. Wu, and D.-J. Deng, "A smart exponential-threshold-linear backoff algorithm to enhance the performance of IEEE 802.11 DCF," in *Proceedings of the Fourth International Conference on Communications and Networking in China*, ser. ChinaCOM '09, pp. 1–5, Aug 2009. doi: 10.1109/CHINACOM.2009.5339950

[58] S. Biaz and S. Wu, "Rate adaptation algorithms for IEEE 802.11 networks: A survey and comparison," in *Proceedings of the IEEE Symposium on Computers and Communications*, ser. ISCC '08, pp. 130–136, July 2008. doi: 10.1109/ISCC.2008.4625680. ISSN 1530-1346

[59] G. Bhanage, R. Mahindra, I. Seskar, and D. Raychaudhuri, "Implication of MAC Frame Aggregation on Empirical Wireless Experimentation," in *Proceedings of the IEEE Global Telecommunications Conference*, ser. GLOBECOM '09, pp. 1–7, Nov 2009. doi: 10.1109/GLOCOM.2009.5426069. ISSN 1930-529X

[60] S. Chieochan, E. Hossain, and J. Diamond, "Channel assignment schemes for infrastructure-based 802.11 WLANs: A survey," *IEEE Communications Surveys Tutorials*, vol. 12, no. 1, pp. 124–136, January 2010. doi: 10.1109/SURV.2010.020110.00047

[61] M. Chiang, P. Hande, T. Lan, and C. W. Tan, "Power Control in Wireless Cellular Networks," *Foundations and Trends in Networking*, vol. 2, no. 4, pp. 381–533, April 2008. doi: 10.1561/1300000009

[62] V. Kawadia and P. Kumar, "Principles and protocols for power control in wireless ad hoc networks," *IEEE Journal on Selected Areas in Communications*, vol. 23, no. 1, pp. 76–88, 2005. doi: 10.1109/JSAC.2004.837354(410) 23

[63] V. P. Mhatre and K. Papagiannaki, "Optimal Design of High Density 802.11 WLANs," in *Proceedings of the ACM CoNEXT Conference*, ser. CoNEXT '06, pp. 8:1–8:12. New York, NY, USA: ACM, 2006. doi: 10.1145/1368436.1368448. ISBN 1-59593-456-1

[64] J. Zhu, X. Guo, L. Lily Yang, W. Steven Conner, S. Roy, and M. M. Hazra, "Adapting Physical Carrier Sensing to Maximize Spatial Reuse in 802.11 Mesh Networks: Research Articles," *wireless communications and mobile computing*, vol. 4, no. 8, pp. 933–946, Dec. 2004. doi: 10.1002/wcm.v4:8

[65] R. Liao, B. Bellalta, M. Oliver, and Z. Niu, "MU-MIMO MAC Protocols for Wireless Local Area Networks: A Survey," *IEEE Communications Surveys Tutorials*, vol. PP, no. 99, pp. 1–1, December 2014. doi: 10.1109/COMST.2014.2377373

[66] C. Shepard, H. Yu, N. Anand, E. Li, T. Marzetta, R. Yang, and L. Zhong, "Argos: Practical Many-antenna Base Stations," in *Proceedings of the 18th Annual International Conference on Mobile Computing and Networking*, ser. Mobicom '12, pp. 53–64. New York, NY, USA: ACM, 2012. doi: 10.1145/2348543.2348553. ISBN 978-1-4503-1159-5

[67] X. Zhang, K. Sundaresan, M. A. A. Khojastepour, S. Rangarajan, and K. G. Shin, "NEMOx: Scalable Network MIMO for Wireless Networks," in *Proceedings of the 19th Annual International Conference on Mobile Computing and Networking*, ser. MobiCom '13, pp. 453–464. New York, NY, USA: ACM, 2013. doi: 10.1145/2500423.2500445. ISBN 978-1-4503-1999-7

[68] A. Akella, G. Judd, S. Seshan, and P. Steenkiste, "Self-management in Chaotic Wireless Deployments," in *Proceedings of the 11th Annual International Conference on Mobile Computing and Networking*, ser. MobiCom '05, pp. 185–199. New York, NY, USA: ACM, 2005. doi: 10.1145/1080829.1080849. ISBN 1-59593-020-5

[69] A. LaMarca, Y. Chawathe, S. Consolvo, J. Hightower, I. Smith, J. Scott, T. Sohn, J. Howard, J. Hughes, F. Potter, J. Tabert, P. Powledge, G. Borriello, and B. Schilit, "Place Lab: Device Positioning Using Radio Beacons in the Wild," *Pervasive Computing*, pp. 116–133, 2005. doi: 10.1007/11428572

[70] Y.-C. Cheng, Y. Chawathe, A. LaMarca, and J. Krumm, "Accuracy Characterization for Metropolitan-scale Wi-Fi Localization," in *Proceedings of the 3rd International Conference on Mobile Systems, Applications, and Services*, ser. MobiSys '05, pp. 233–245. New York, NY, USA: ACM, 2005. doi: 10.1145/1067170.1067195. ISBN 1-931971-31-5

[71] N. Ahmed and S. Keshav, "SMARTA: A Self-managing Architecture for Thin Access Points," in *Proceedings of the 2006 ACM CoNEXT Conference*, ser. CoNEXT '06, pp. 9:1–9:12. New York, NY, USA: ACM, 2006. doi: 10.1145/1368436.1368449. ISBN 1-59593-456-1

[72] Aerohive: Controller-less WLAN Architecture. [Online]. Available: http://www.aerohive.com/solutions/technology-behind-solution/controller-less-wlan-architecture

[73] Wireless Geographic Logging Engine (WiGLE). [Online]. Available: https://wigle.net/

[74] IEEE 802.11 Wireless Local Area Networks Working Group. [Online]. Available: http://www.ieee802.org/11/

[75] A. de la Oliva, A. Morelli, V. Mancuso, M. Draexler, T. Hentschel, T. Melia, P. Seite, and C. Cicconetti, "Denser Networks for the Future Internet, the CROWD Approach," *Mobile Networks and Management*, pp. 28–41, 2013. doi: 10.1007/978-3-642-37935-2

[76] N. Jorgensen, I. Rodriguez, J. Elling, and P. Mogensen, "3G Femto or 802.11g WiFi: Which Is the Best Indoor Data Solution Today?" in *Proceedings of the 80th IEEE Vehicular Technology Conference*, ser. VTC '14 (Fall), pp. 1–5, Sept 2014. doi: 10.1109/VTCFall.2014.6965802

[77] S. Dimatteo, P. Hui, B. Han, and V. Li, "Cellular Traffic Offloading through WiFi Networks," in *Proceedings of the 8th IEEE International Conference on Mobile Adhoc and Sensor Systems*, ser. MASS '11, pp. 192–201, Oct 2011. doi: 10.1109/MASS.2011.26. ISSN 2155-6806

[78] Cisco, "Cisco Visual Networking Index: Global Mobile Data Traffic Forecast Update, 2012-2017," *Cisco White Paper*, February 2013.

[79] LTE to Wi-Fi offloading is driving IEEE's 802.11 HEW effort. [Online]. Available: http://www.fiercewireless.com/tech/special-reports/lte-wi-fi-offloading-driving-ieees-80211hew-effort

[80] TGax, "TGax Simulation Scenarios," *IEEE 802.11ax: 802.11-14/0980r14*, July 2015.

[81] L. Cariou, "HEW SG usage models and requirements - Liaison with WFA," *IEEE 802.11 High Efficient WLAN (HEW) Study Group (SG)*, July 2013.

[82] Nokia, "HEW Simulation Methodology," *IEEE 802.11 HEW: 802.11-13/1081r0*, September 2013.

[83] TGax, "TGax Evaluation Methodology," *IEEE 802.11ax: 802.11-14/0571r10*, July 2015.

[84] NS-3 (Network Simulator 3). [Online]. Available: https://www.nsnam.org/

[85] GNU General Public License (GPL). [Online]. Available: http://www.gnu.org/copyleft/gpl.html

[86] Riverbed Modeler, formerly known as OPNET Modeler. [Online]. Available: http://www.riverbed.com/products/performance-management-control/network-performance-management/network-simulation.html

[87] I. E. Publication, "Report ITU-R M.2135-1: Guidelines for evaluation of radio interface technologies for IMT-Advanced," *ITU-R Report, M Series*, December 2009.

[88] 802.11 Modulation Curves - Extension to the OPNET WLAN model. [Online]. Available: https://splash.riverbed.com/docs/DOC-3104

[89] L. E. Miller, "Validation of 802.11a/UWB coexistence simulation," *WCTG white paper*, October 2003.

[90] D. Haccoun and G. Begin, "High-rate punctured convolutional codes for Viterbi and sequential decoding," *IEEE Transactions on Communications*, vol. 37, no. 11, pp. 1113–1125, Nov 1989. doi: 10.1109/26.46505

[91] P. Chevillat, J. Jelitto, A. Barreto, and H. Truong, "A dynamic link adaptation algorithm for IEEE 802.11 a wireless LANs," in *Proceedings of the IEEE International Conference on Communications*, ser. ICC '03, vol. 2, pp. 1141–1145 vol.2, May 2003. doi: 10.1109/ICC.2003.1204543

[92] A. Muqattash and M. Krunz, "POWMAC: a single-channel power-control protocol for throughput enhancement in wireless ad hoc networks," *IEEE Journal on Selected Areas in Communications*, vol. 23, no. 5, pp. 1067–1084, May 2005. doi: 10.1109/JSAC.2005.845422

[93] I. Jamil, L. Cariou, and J.-F. Helard, "Improving the capacity of future IEEE 802.11 high efficiency WLANs," in *Proceedings of the 21st International Conference on Telecommunications*, ser. ICT '14, pp. 303–307, May 2014. doi: 10.1109/ICT.2014.6845128

[94] S. Gollakota and D. Katabi, "Zigzag Decoding: Combating Hidden Terminals in Wireless Networks," *SIGCOMM Computer Communication Review*, vol. 38, no. 4, pp. 159–170, Aug 2008. doi: 10.1145/1402946.1402977

[95] M. Vutukuru, K. Jamieson, and H. Balakrishnan, "Harnessing Exposed Terminals in Wireless Networks," in *Proceedings of the 5th USENIX Symposium on Networked Systems Design and Implementation*, ser. NSDI '08, pp. 59–72. Berkeley, CA, USA: USENIX Association, 2008. ISBN 111-999-5555-22-1

[96] *IEEE Standard for Information Technology - Telecommunications and Information Exchange Between Systems - Local and Metropolitan Networks - Specific Requirements - Part 11: Wireless LAN Medium Access Control (MAC) and Physical Layer (PHY) Specifications - Spectrum and Transmit Power Management Extensions in the 5 GHz Band in Europe*, IEEE Std., 2003.

[97] V. Shah and S. Krishnamurthy, "Handling Asymmetry in Power Heterogeneous Ad Hoc Networks: A Cross Layer Approach," in *Proceedings of the 25th IEEE International*

Conference on Distributed Computing Systems, ser. ICDCS '05, pp. 749–759. IEEE Computer Society, June 2005. doi: 10.1109/ICDCS.2005.41. ISSN 1063-6927

[98] A. Pires, J. Rezende, and C. Cordeiro, "Protecting Transmissions when Using Power Control on 802.11 Ad Hoc Networks," *Challenges in Ad Hoc Networking*, pp. 41–50, 2006.

[99] B. Radunović, R. Chandra, and D. Gunawardena, "Weeble: Enabling Low-power Nodes to Coexist with High-power Nodes in White Space Networks," in *Proceedings of the 8th International Conference on Emerging Networking Experiments and Technologies*, ser. CoNEXT '12, pp. 205–216. ACM, 2012. doi: 10.1145/2413176.2413201. ISBN 978-1-4503-1775-7

[100] E.-S. Jung and N. H. Vaidya, "A power control MAC protocol for ad hoc networks," in *Proceedings of the 8th annual international conference on Mobile computing and networking*, ser. MobiCom '02, pp. 36–47. ACM, 2002. doi: 10.1145/570645.570651. ISBN 1-58113-486-X

[101] F. Ben Abdesslem, L. Iannone, M. Dias de Amorim, K. Kabassanov, and S. Fdida, "On the feasibility of power control in current IEEE 802.11 devices," in *Proceedings of the IEEE International Conference on Pervasive Computing and Communications Workshops*, ser. PERCOMW '06, pp. 468–473, March 2006. doi: 10.1109/PERCOMW.2006.103

[102] X. Yue, C.-F. Wong, and S.-H. Chan, "CACAO: Distributed Client-Assisted Channel Assignment Optimization for Uncoordinated WLANs," *IEEE Transactions on Parallel and Distributed Systems*, vol. 22, no. 9, pp. 1433–1440, Sept 2011. doi: 10.1109/TPDS.2011.59

[103] A. Kamerman and L. Monteban, "WaveLAN-II: A high-performance wireless LAN for the unlicensed band," *Bell Labs Technical Journal*, vol. 2, no. 3, pp. 118–133, April 1997. doi: 10.1002/bltj.2069

[104] J. Kim, S. Kim, S. Choi, and D. Qiao, "CARA: Collision-Aware Rate Adaptation for IEEE 802.11 WLANs," in *Proceeding of the 25th IEEE International Conference on Computer Communications*, ser. INFOCOM '06, pp. 1–11, April 2006. doi: 10.1109/INFOCOM.2006.316. ISSN 0743-166X

[105] J. Choi, J. Na, Y. sup Lim, K. Park, and C.-K. Kim, "Collision-aware design of rate adaptation for multi-rate 802.11 WLANs," *IEEE Journal on Selected Areas in Communications*, vol. 26, no. 8, pp. 1366–1375, October 2008. doi: 10.1109/JSAC.2008.081003

[106] M. Lacage, M. H. Manshaei, and T. Turletti, "IEEE 802.11 Rate Adaptation: A Practical Approach," in *Proceedings of the 7th ACM International Symposium on*

Modeling, Analysis and Simulation of Wireless and Mobile Systems, ser. MSWiM '04, pp. 126–134, New York, NY, USA, 2004. doi: 10.1145/1023663.1023687. ISBN 1-58113-953-5. [Online]. Available: http://doi.acm.org/10.1145/1023663.1023687

[107] Q. Pang, V. Leung, and S. Liew, "A rate adaptation algorithm for IEEE 802.11 WLANs based on MAC-layer loss differentiation," in *Proceedings of the 2nd International Conference on Broadband Networks*, ser. BroadNets '05, pp. 659–667 Vol. 1, Oct 2005. doi: 10.1109/ICBN.2005.1589671

[108] D. Qiao and S. Choi, "Fast-responsive link adaptation for IEEE 802.11 WLANs," in *Proceedings of the IEEE International Conference on Communications*, ser. ICC '05, vol. 5, pp. 3583–3588 Vol. 5, May 2005. doi: 10.1109/ICC.2005.1495085

[109] I. Jamil, L. Cariou, and J.-F. Helard, "Carrier sensing-aware rate control mechanism for future efficient WLANs," in *Proceedings of the International Conference and Workshop on the Network of the Future*, ser. NoF '14, pp. 1–6, Dec 2014. doi: 10.1109/NOF.2014.7119777

[110] ——, "Efficient MAC protocols optimization for future high density WLANS," in *Proceedings of the IEEE Wireless Communications and Networking Conference*, ser. WCNC '15, pp. 1054–1059, March 2015. doi: 10.1109/WCNC.2015.7127615

[111] S. Haykin, *Neural Networks and Learning Machines*, ser. Neural networks and learning machines. Prentice Hall, 2009, no. v. 10. ISBN 9780131471399. [Online]. Available: https://books.google.fr/books?id=K7P36lKzI_QC

[112] M. van der Schaar and S. S. N, "Cross-layer wireless multimedia transmission: challenges, principles, and new paradigms," vol. 12, no. 4, pp. 50–58, Aug 2005. doi: 10.1109/MWC.2005.1497858

[113] "Multilayer feedforward networks are universal approximators," vol. 2, no. 5, pp. 359–366, 1989. doi: 10.1016/0893-6080(89)90020-8

[114] C. Wang, J. Hsu, K. Liang, and T. Tai, "Application of neural networks on rate adaptation in IEEE 802.11 WLAN with multiples nodes," in *Proceedings of the 3rd IEEE International Conference on Computer Science and Information Technology*, ser. ICCSIT '10, vol. 4, pp. 425–430, July 2010.

[115] C.-L. Chen, "IEEE 802.11e EDCA QoS Provisioning with Dynamic Fuzzy Control and Cross-Layer Interface," in *Proceedings of the 16th International Conference on Computer Communications and Networks*, ser. ICCCN '07, pp. 766–771, Aug 2007. doi: 10.1109/ICCCN.2007.4317910. ISSN 1095-2055

[116] H. Zhang and X. Shi, "A new indoor location technology using back propagation neural network to fit the RSSI-d curve," in *Proceedings of the 10th World Congress on Intelligent Control and Automation*, ser. WCICA '12, pp. 80–83, July 2012. doi: 10.1109/WCICA.2012.6357843

[117] P. Gogoi and K. Sarma, "Hybrid channel estimation scheme for IEEE 802.11n-based STBC MIMO system," in *Proceedings of the International Conference on Communications, Devices and Intelligent Systems*, ser. CODIS '12, pp. 49–52, Dec 2012. doi: 10.1109/CODIS.2012.6422133

[118] P. Lin and T. Lin, "Machine-Learning-Based Adaptive Approach for Frame-Size Optimization in Wireless LAN Environments," vol. 58, no. 9, pp. 5060–5073, Nov 2009. doi: 10.1109/TVT.2009.2025133

[119] H. Luo and N. Shankaranarayanan, "A distributed dynamic channel allocation technique for throughput improvement in a dense WLAN environment," in *Proceedings of the IEEE International Conference on Acoustics, Speech, and Signal Processing*, ser. ICASSP '04, vol. 5, pp. V–345–8 vol.5, May 2004. doi: 10.1109/ICASSP.2004.1327118. ISSN 1520-6149

[120] C. Wang, P.-C. Lin, and T. Lin, "A Cross-Layer Adaptation Scheme for Improving IEEE 802.11e QoS by Learning," vol. 17, no. 6, pp. 1661–1665, Nov 2006. doi: 10.1109/TNN.2006.883014

[121] R. Jain, D.-M. Chiu, and W. R. Hawe, *A quantitative measure of fairness and discrimination for resource allocation in shared computer system.* Technical Report, Eastern Research Laboratory, Digital Equipment Corporation Hudson, MA, DEC-TR-301, 1984.

INSA de RENNES
Service des Formations

AVIS DU JURY SUR LA REPRODUCTION DE LA THESE SOUTENUE

Titre de la thèse:
Improving spatial reuse in future dense high efficiency Wireless Local Area Networks

Nom Prénom de l'auteur : JAMIL IMAD

Membres du jury :
- Monsieur SARI Hikmet
- Monsieur CARIOU Laurent
- Monsieur HELARD Jean-François
- Monsieur BEYLOT André-Luc
- Monsieur LE RUYET Didier
- Monsieur PYNDIAH Ramesh

Président du jury : Hikmet SARI

Date de la soutenance : 17 Décembre 2015

Reproduction de la these soutenue

Thèse pouvant être reproduite en l'état
~~Thèse pouvant être reproduite après corrections suggérées~~

Fait à Rennes, le 17 Décembre 2015

Signature du président de jury

Le Directeur,

INSTITUT NATIONAL des SCIENCES APPLIQUÉES RENNES

M'hamed DRISSI

Résumé

Malgré leur réussite remarquable, les premières versions des normes de réseau local sans fil IEEE 802.11, 802.11a/b/g Wireless Local Area Networks (WLAN), sont caractérisées par une efficacité spectrale faible qui est devenue insuffisante pour satisfaire la croissance explosive de la demande de capacité et de couverture. Le standard 802.11n et plus récemment le 802.11ac ont amélioré les débits offerts par la couche physique grâce principalement à l'introduction des techniques multi-antennaires (MIMO, pour Multiple-Input Multiple-Output) et des techniques avancées de modulation et de codage. Aujourd'hui, deux décennies après sa première apparition, le Wi-Fi est présenté comme une technologie WLAN permettant des débits supérieurs à 1 gigabit par seconde. Cependant, dans la plupart des scénarios de déploiement du monde réel, il n'est pas possible d'atteindre la pleine capacité offerte par la couche physique. Avec la croissance rapide de la densité des déploiements des WLANs, l'énorme popularité des équipements Wi-Fi et l'apparition des nouveaux cas d'utilisation (couverture des stades, déchargement des réseaux cellulaire, etc.), la réutilisation spatiale doit être optimisée.

C'est dans ce contexte que s'inscrit l'objectif de cette thèse qui porte sur l'amélioration de l'efficacité des protocoles de la couche MAC des réseaux WLAN de haute densité. Notamment, un des buts de cette thèse est de contribuer à la préparation de la prochaine génération du standard Wi-Fi : IEEE 802.11ax High Efficiency WLAN (HEW). Plutôt que de continuer à cibler l'augmentation des débits maximums théoriques d'un lien unique, nous nous concentrons dans le contexte de HEW sur l'amélioration du débit réel des utilisateurs.

Nous proposons une adaptation dynamique du mécanisme de détection de signal. Comparé au contrôle de la puissance de transmission, le mécanisme proposé est plus incitatif parce que l'utilisateur concerné bénéficie directement de son application. Les résultats de nos simulations montrent des gains importants en termes de débit atteint dans les scénarios de haute densité. Ensuite, nous étudions l'impact de la nouvelle adaptation sur les mécanismes de sélection de débit actuellement utilisés. D'après les résultats obtenus, l'adaptation proposée peut être appliquée sans avoir besoin de modifications substantielles des algorithmes de sélection de débit. Pour améliorer l'équité entre les différents utilisateurs, nous élaborons une nouvelle approche distribuée pour adapter conjointement le mécanisme de détection de signal et le contrôle de la puissance de transmission. Cette approche est évaluée ensuite dans différents scénarios de simulation de haute densité où elle prouve sa capacité à résoudre les problèmes d'équité en particulier en présence de nœuds d'anciennes générations dans le réseau, cela tout en améliorant le débit moyen d'un facteur 4 par rapport à la performance conventionnelle du standard.

Enfin, nous concevons et mettons en œuvre une solution centralisée basée sur l'apprentissage à base de réseaux de neurones. Cette approche repose sur l'adaptation conjointe de puissance de transmission et du mécanisme de détection du signal. Cette nouvelle solution bénéficie de la capacité des réseaux de neurones artificiels à modéliser les fonctions

Abstract

Despite their remarkable success, the first widely spread versions of the IEEE 802.11 Wireless Local Area Networks (WLAN) standard, 802.11a/b/g, featured low spectral efficiencies that are becoming insufficient to satisfy the explosive growth in capacity and coverage demands. The 802.11n and recently the 802.11ac amendments improved the PHY data rates by introducing Multiple-Input Multiple-Output (MIMO) techniques, and higher Modulation and Coding Schemes (MCS), etc. Today, after almost two decades of its first appearance, Wi-Fi is presented as a gigabit wireless technology. However, the full potential of the latest PHY layer advances cannot be enabled in all real world deployment scenarios. With the rapidly increasing density of WLAN deployments and the huge popularity of Wi-Fi enabled devices, spatial reuse must be optimized. On another hand, the new challenging use case environments and the integration of mobile networks mainly for cellular offloading are limiting the opportunity of the current Wi-Fi generations to provide better quality at lower cost.

In this thesis, we contribute to the current standardization efforts aiming to leverage the Wi-Fi efficiency in high density environments. At the time of writing this document, the IEEE 802.11ax Task Group (TG) is developing the specifications for the High Efficiency WLAN (HEW) standard (next Wi-Fi evolution). Rather than continuing to target increased theoretical peak throughputs of a single communication link, we focus in the context of HEW on improving the throughput experienced by users in real life scenarios.

We propose a dynamic adaptation of the carrier sensing mechanism. Compared to controlling the transmission power, the proposed mechanism has more incentives because it benefits directly the concerned user. Extensive simulation results show important throughput gains in dense scenarios. Then, we study the impact of the new adaptation on the current rate control algorithms. We find that our adaptation mechanism operates efficiently without substantially modifying these algorithms that are widely used in today's operating WLANs. Furthermore, after analyzing the fairness performance of the proposed adaptation, we devise a new approach to jointly adapt the carrier sensing and the transmission power in order to preserve higher fairness degrees while improving the spatial reuse. This approach is evaluated in different dense deployment scenarios where it proves its capability to resolve the unfairness issues especially in the presence of legacy nodes in the network, while improving the achieved throughput by 4 times compared to the standard performance.

Finally, we design and implement a centralized learning-based solution that uses also an approach based on joint adaptation of transmission power and carrier sensing. This new solution takes benefit from the capability of artificial neural networks to model complex nonlinear functions to optimize the spatial reuse in dense WLANs while preserving high fairness levels.

INSA RENNES

N° d'ordre : 15ISAR 39 / D15 - 39

Institut National des Sciences Appliquées de Rennes
20, Avenue des Buttes de Coëmes • CS 70839 • F-35708 Rennes Cedex 7
Tel : 02 23 23 82 00 - Fax : 02 23 23 83 96

défi pour tous les systèmes de communication sans fil. Cette combinaison est encore plus difficile à atteindre pour le Wi-Fi car cette technologie n'a pas été conçue pour fonctionner dans de tels cas d'utilisations extrêmes. Depuis son introduction, cette norme n'a pas cessé d'évoluer. En conséquence, une longue liste d'amendements ont été adoptés et plusieurs générations se sont succédées. La dernière version de la norme IEEE 802.11 [5] qui intègre tous les amendements précédents remonte à 2012. Dans toute son histoire d'évolution, la réussite de la technologie Wi-Fi est due à son prix modeste et son opération simple. Aujourd'hui, les réseaux locaux sans fil (i.e., WLAN ou Wi-Fi) basés sur la norme IEEE 802.11 sont à nouveau contraints d'évoluer afin de garder le même rythme imposé par les nouveaux besoins. Bien que le défi est grand, la technologie Wi-Fi doit garder sa simplicité opérationnelle, la clé de son succès, tout en façonnant sa nouvelle génération.

0.2 Panorama de la norme IEEE 802.11

L'élément de base dans un réseau local sans fil IEEE 802.11 est nommé le BSS (pour "Basic Service Set") et formé d'un point d'accès (AP, pour "Access Point") et des stations (STA, pour "Station") associées à l'AP. L'AP est une STA normale à laquelle on ajoute des fonctionnalités permettant la gestion du BSS (contrôle et synchronisation de toutes les transmissions). Généralement, chaque AP est lié à un système de distribution (DS pour "Distribution System") comme montré par la Figure 1. Le DS assure la liaison de l'AP avec le monde extérieur, typiquement l'internet et dans des autres cas des réseaux locaux étendus ou ESS (pour "Extended Service Set").

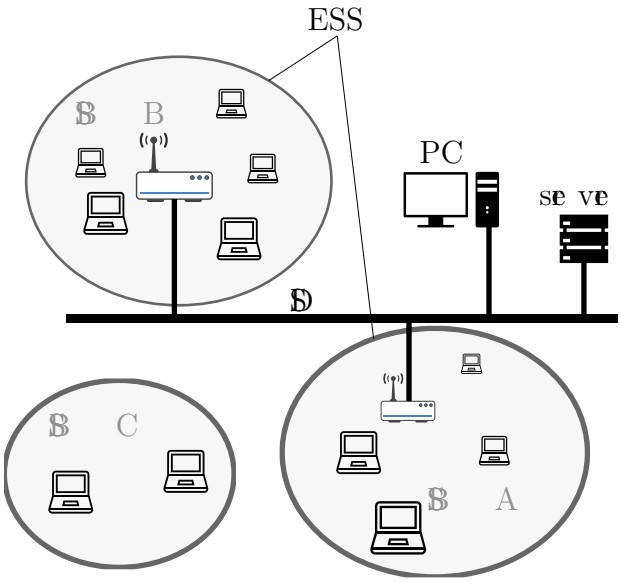

Figure 1 – L'arichecture générale d'un réseau du 802.11

ploiement. La densité croissante des réseaux Wi-Fi en termes du nombre des APs déployés et le nombre des STAs associées à ces APs pose de nouveaux problèmes de performances. En raison de la nature de l'accès multiple concurrent défini par la norme IEEE 802.11, les utilisateurs Wi-Fi fonctionnant sur la même fréquence partagent le temps d'accès au canal. Dans la même zone géographique, le débit moyen de chaque utilisateur Wi-Fi diminue proportionnellement avec l'augmentation du nombre total des utilisateurs co-canaux. Comme nous le montrons à travers cette thèse, le comportement sur-protecteur des protocoles de la couche MAC aggrave la situation. Bien qu'il y ait un besoin d'atténuer les problèmes de sur-protection, l'équité entre les utilisateurs en contention doit être préservée.

0.3 L'adaptation du Physical Carrier Sensing (PCS) dans les environnements denses

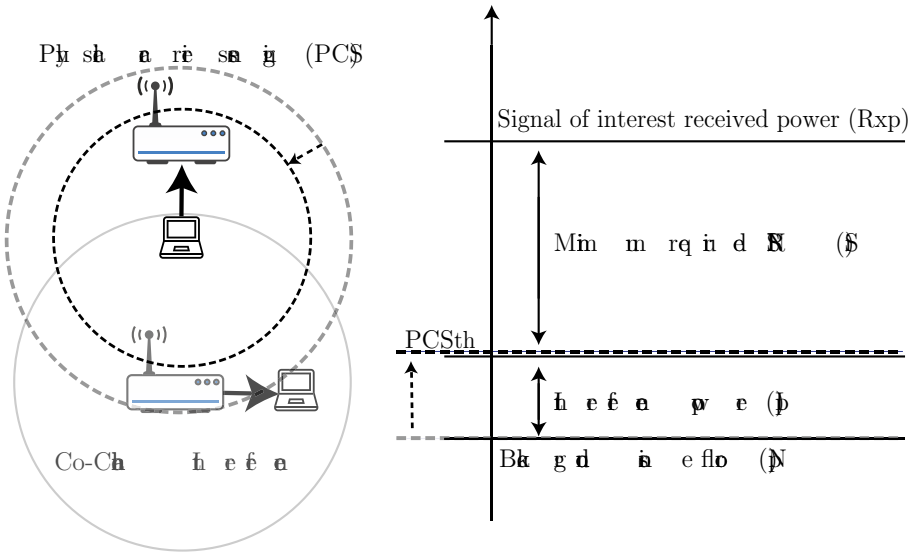

Figure 3 – Physical Carrier Sensing (PCS)

L'adaptation du mécanisme de PCS est proposée comme une solution alternative pour augmenter la réutilisation spatiale sans nuire aux autres utilisateurs. L'augmentation du seuil de PCS, illustrée par la Figure 3, montre un important potentiel afin d'exploiter la capacité offerte par les déploiements denses des réseaux locaux sans fil. Contrairement au contrôle de la puissance de transmission (TPC, pour "Transmit Power Control"), cette solution est plus incitative parce que l'utilisateur concerné bénéficie directement de son application. Pour un scénario de déploiement cellulaire de haute densité, nos résultats de simulation montrent un gain global de 190 % en débit total par rapport à la limite actuelle assumée par la norme 802.11. Cependant, un seuil statique n'est pas la solution la plus appropriée compte tenu du fait que le mécanisme d'accès au canal et la quantité

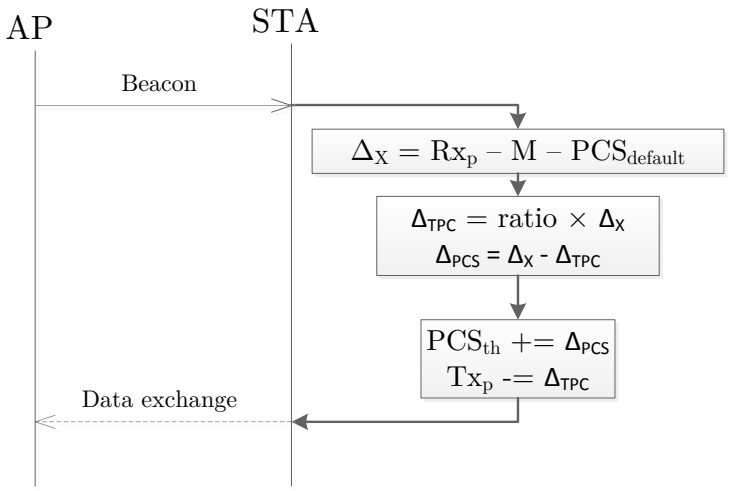

Figure 4 – Un cas de figure d'utilisation du BTPA

$$\Delta_{TPC}[dB] = ratio \times \Delta_X[dB] \tag{3}$$

Pour un simple cas de figure, l'application du BTPA est illustrée par la Figure 4. Dans cet exemple, une nouvelle STA s'associe à un BSS et commence une nouvelle communication avec son AP. A la réception d'une trame de beacon (ou balise) de l'AP, la STA calcule la valeur de Δ_X. Dans une implémentation pratique, il est facile de diffuser la valeur $ratio$ par l'AP dans la trame de beacon. Connaissant le $ratio$, la STA déduit les valeurs de Δ_{PCS} et Δ_{TPC}. La dernière étape consiste à calculer le nouveau seuil de PCS (PCS_{th}) et la puissance de transmission (Tx_p) et à les appliquer avant de procéder à l'échange de données prévu.
Dans un scénario cellulaire de haute densité, on compare la performance des différentes approches en terme de débit moyen atteint par chaque utilisateur. Nous montrons respectivement dans les Figures 5 et 6 les fonctions de répartitions (CDF, pour "Cumulative Distribution Function") de ces débits pour deux cas: (a) sans STAs legacy; (b) en présence des STAs legacy. La pente de la courbe de CDF donne une idée claire sur l'équité entre les différents utilisateurs. On peut remarquer clairement d'après ces courbes que les meilleurs résultats sont obtenus avec le BTPA dans les deux cas. Cette solution améliore le débit moyen ainsi que le niveau de l'équité. On distingue surtout dans le cas (b) (Figure 6) l'inefficacité du TPC en présence des STAs legacy et la capacité du BTPA à maintenir les meilleurs débits moyens avec une pente élevée indiquant une meilleur équité entre les différents utilisateurs.

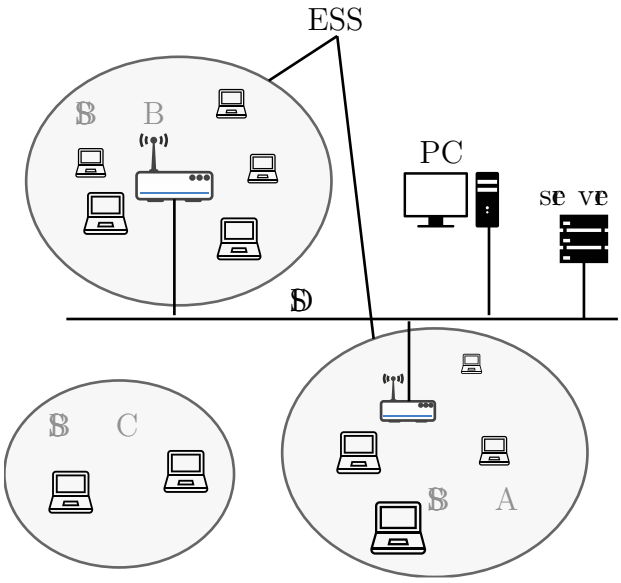

Figure 1.3 – The 802.11 network architecture

communication between Wi-Fi devices without being associated to an AP. This specification is called Wi-Fi Direct and can be seen as a variation of the IBSS. However, Wi-Fi Direct differs from the IBSS in the sense that one of the peers assumes a role similar to that of an AP in an infrastructure BSS. The device assuming this role is called the Group Owner (GO). The other peer devices associate with the GO. However, what differs a Wi-Fi Direct network from an infrastructure BSS is that the GO does not provide the access to a distribution system and it could be a mobile battery powered device.

1.3 Media Access Control Layer (MAC) basics

Among other functionalities, the MAC layer coordinates the access to the shared medium allowing the communication of multiple devices over a common wireless channel. In addition, the MAC layer provides the addressing scheme that permits the identification of these different devices. Mainly, this layer is responsible for resolving the contention between the communicating devices so that the limited radio resources are shared efficiently and fairly. The first version of the 802.11 standard was influenced by the success of the Ethernet which was standardized as 802.3. In fact, in terms of channel access and addressing, 802.11 is similar to Ethernet. For that reason, the 802.11 is often referred to as wireless Ethernet. The 802.3 or Ethernet would not exist without that simple distributed access protocol that is called the Carrier Sense Multiple Access (CSMA). Similarly, the 802.11 MAC adopted the same simple yet efficient contention-based distributed access scheme. Another common aspect between Ethernet and 802.11 is the use of the same 48-bit addressing space. This made these two technologies compatible at the DLL layer.

in Figure 1.7, STA_B fails to correctly decode the frame. As a result, STA_A will not receive an ACK and on that account it will start a new channel access to retransmit the same data frame.

Initially, the CW is set to its minimum value CW_{min}. In case of a retransmission, the CW is doubled until the CW_{max} is reached. After a successful MPDU transmission (i.e., the reception of an ACK), the CW is set again to its initial value CW_{min}. Actually, the device choses randomly a backoff in the range of [0,CW]. The number of retransmission of an MSDU is indeed limited. When the counter of retransmission of a particular MSDU exceeds a configured retry limit, the MSDU is discarded.

1.3.2.3 Request To Send (RTS)/Clear To Send (CTS) handshake

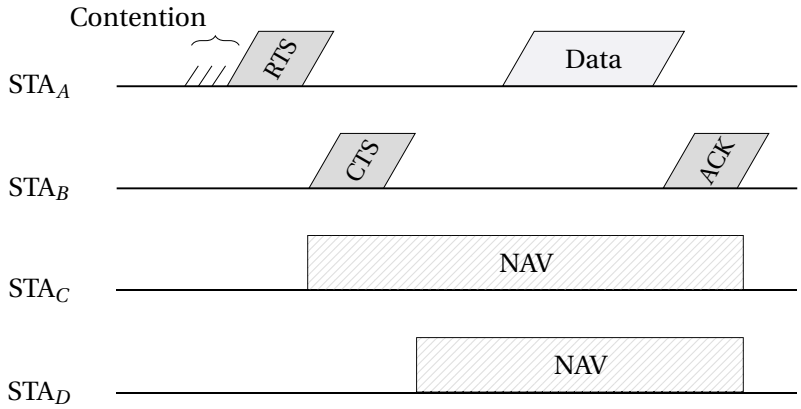

Figure 1.8 – Request To Send (RTS)/Request To Send (RTS) handshaking and Virtual Carrier Sensing (VCS)

Additionally to the previously described basic access method, the 802.11 standard defines an optional four-way handshake. This access method is called Request To Send (RTS)/Clear To Send (CTS) and consists of exchanging two control frames prior to any data frame exchange. After the contention period, the device that gains the access to the medium sends an RTS. After decoding correctly this frame, the destination device waits for SIFS and responds with a CTS. Finally, the transmitter device begins data transmission after a SIFS starting from the reception of the CTS. These control frames include the duration of the data exchange and hence all the devices that are able to successfully decode them update their NAV accordingly. The described access mechanism is illustrated in Figure 1.8 where four STAs are depicted as follows. STA_B and STA_C are in the range of STA_A. STA_D is out of the range of STA_A but in the range of STA_B. A STA is in the range of another STA when they hear the transmissions of each other and defer their own transmissions accordingly. It is worth mentioning that even if the CCA senses the channel as *idle*, the device can't transmit during the time period indexed by the NAV (i.e., the VCS mechanism). The aim of the optional RTS/CTS handshaking is to cope with the hidden node problem where an

3.2.2 Residential scenario

This scenario represents a dense apartment building that was initially proposed in HEW SG by [82]. Indeed, this represents a real world situation that is common in urban areas and crowded cities. The main purpose of such practical scenario is involving interference between APs placed in the different apartment units. As a general rule, residential APs are installed arbitrary without any planning. This leads in chaotic WLAN environments where many BSSs operating on the same channel overlaps creating the OBSS problem (Section 1.6.2). The network topology of the residential scenario is depicted in Figure 3.2.

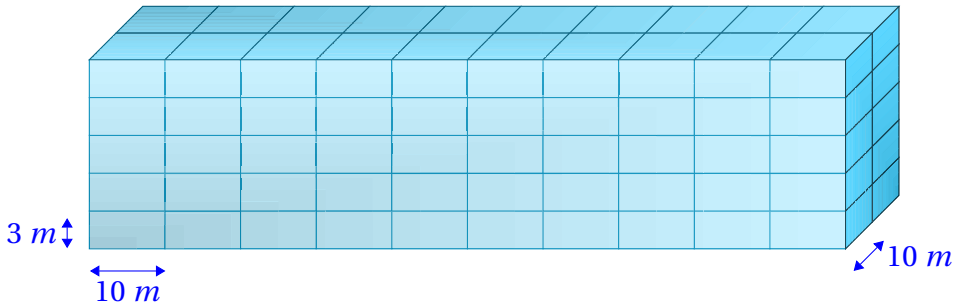

Figure 3.2 – Residential scenario building layout

It consists of a multistory building with story height of 3 m. Each floor is composed of 20 apartment units of 10 m × 10 m. The number of APs in the whole building is N_{AP}. These APs are randomly distributed over the totality of the units following a uniform distribution. By default, an AP is randomly located within its unit. However, there is an option to fix the location of all the APs in the center of their units. Each apartment unit that includes an AP has N_{STA} STAs randomly located (uniform distribution) inside it. By default, all the STAs of the unit X are associated with AP of unit X. The simulation parameters are set conformity with those chosen in the TGax simulation document [80]. The most important of these parameters are listed in Table 3.2 with their default value. Obviously, the main difference when comparing to the cellular scenario is the propagation path loss model. The same traffic parameters are used in both scenarios for the sake of throughput performance comparison.

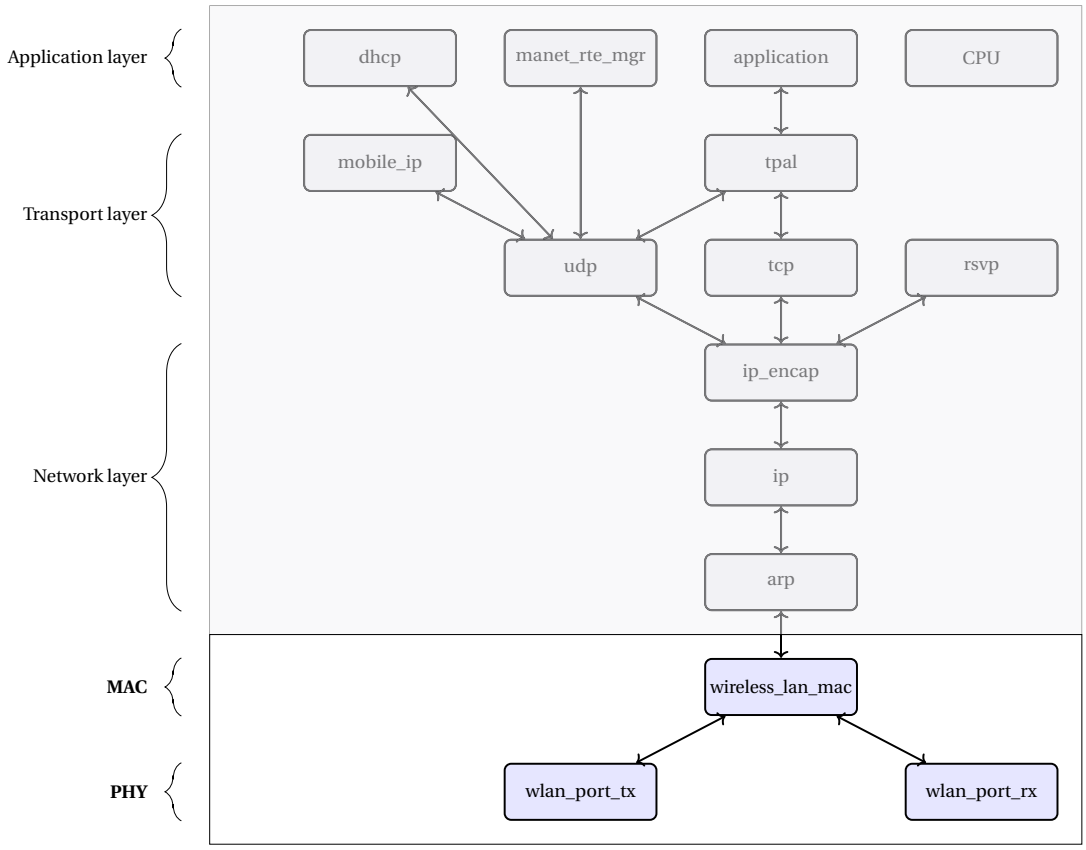

Figure 3.3 – OPNET simulation node model of a WLAN workstation

3.4 Improvements and modifications of the simulation model

Throughout the different phases of the thesis project, many modifications to the standard OPNET model have been made to enhance the simulation model or to add a new functionality.

3.4.1 Propagation channel model

The path loss model is implemented in the "wlan_power" pipeline stage at the radio receiver. The default OPNET 17.5 model implements the standard Friis path loss for wireless propagation with a path loss exponent equal to two. Which is a free space path loss model that in not appropriate for the scenarios described above. Accordingly, we added new models for path loss to the default simulation model. Typically, the International Telecommunication Union (ITU) Urban Micro (UMi) model defined by the ITU-R SG [87] for hexagonal cell layout as follows:

$$PL(d_{TR}) = 22.7 + 36.7\log(d_{TR}) + 26\log(f_c) \tag{3.1}$$

transmission by a WLAN device is static throughout the simulation. However, a part of this thesis studies the implication of the rate control mechanisms on the performance. Accordingly, as we will discuss in details in Chapter 5, the rate control mechanism proposed by [91] has been implemented by modifying the "wireless_lan_mac" process model. By employing only local information, the transmitter determines the quality of the radio link and decides to switch accordingly to higher or lower data rate (i.e., MCS). The advantage such a mechanism is that it does not require any changes to the standard 802.11. Moreover since the radio link quality is determined basing on local information, no overheard is added to the system and the operation is fully distributed. The basic performance of this link adaptation mechanism is discussed in Section 3.5.

3.5 Baseline performance

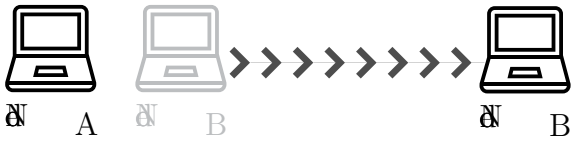

Figure 3.4 – Baseline performance simulation scenario

In this section we study the baseline performance of the modified simulation model. This serves as a point of reference for all the simulations conducted in the rest of this thesis. For the sake of this analysis, we consider a simple network scenario consisting of a single link that is illustrated in Figure 3.4.

Table 3.4 – Baseline performance scenario parameters

Parameter	**Value**
Standard version	802.11n
Radio band	5 GHz
Bandwidth	20 MHz
Path loss	Path loss model in Equation (3.2)
Background noise	-130 dBm
Number of antennas for each device	1
Maximum number of retransmissions	7
Transmission power	15 dBm
Physical carrier sensing threshold	-82 dBm
Traffic	Full buffer
Simulation run duration	5 min

This scenario consists of two WLAN devices (two OPNET WLAN node models), $Node_A$ that represents the transmitter node and $Node_B$ representing the receiver node. The default

neighboring nodes to do so. While TPC fails if not all the adjacent WLANs apply it, CCA adaptation doesn't need their compliance.

4.3 Hidden and exposed node regions

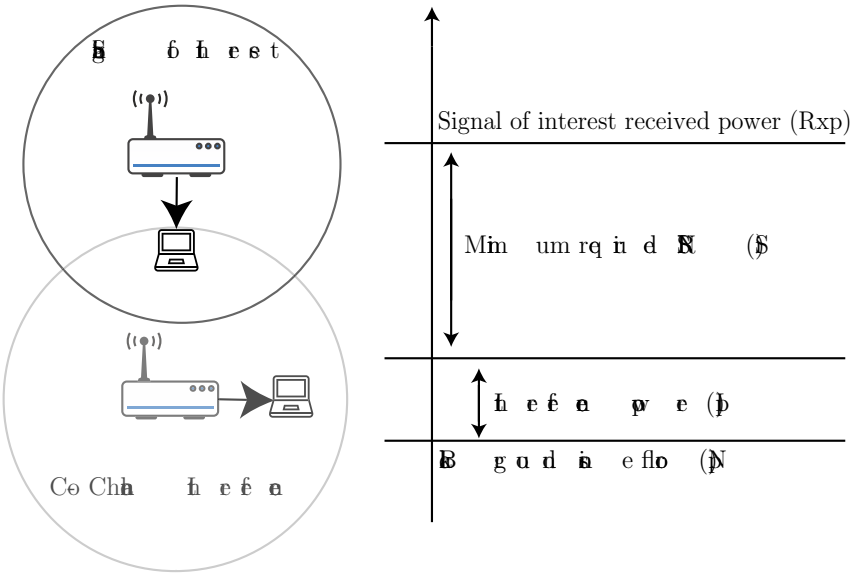

Figure 4.1 – Signal to Interference and Noise Ratio (SINR)

Depending on the data rate used to transmit, a communication is sustained only if the corresponding Signal to Interference and Noise Ratio (SINR) at the receiver exceeds certain mandatory minimum value. As represented in Figure 4.1, S_i is the minimum required SINR for a Modulation and Coding Scheme (MCS) of index i, namely MCS_i. This is translated by the following expression.

$$SINR \geq S_i \tag{4.1}$$

Where the SINR is defined by

$$SINR = \frac{Rx_p}{N_P + I_P} \tag{4.2}$$

where Rx_p is the power of the signal of interest at the receiver, N_P is the background noise level and I_P is the interference power at the receiver's close vicinity. Notably, CCI is one of the greatest challenges threatening wireless communications. This challenge is more pronounced in dense WLAN environments since co-channel Basic Service Set (BSS)s are deployed closer to each other. Basing on the illustration of Figure 4.1, the interference region is defined as the region around the receiver where any co-channel transmission (considered as CCI) can decrease the SINR of the signal of interest below the acceptable threshold S_i. The region around a node in which any occurring transmission is detected,

thanks to the carrier sensing mechanism, is termed the detection region of that node.

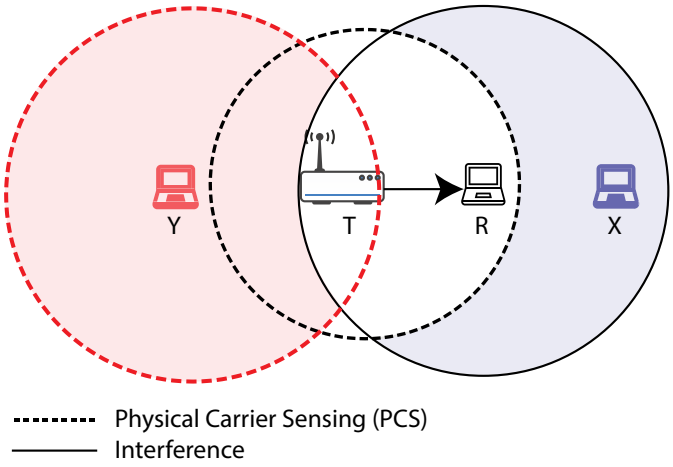

Figure 4.2 – Hidden and exposed node regions

In the literature, two main problems are identified to be detrimental to WLAN performance. Namely, the hidden and exposed node problems caused by the distributed nature of the channel access in IEEE 802.11 WLANs [94] [95]. To explain these problems, we consider the scenario shown in Figure 4.2. When a potential interferer X is outside the detection range of a transmitter T, X is defined as a hidden node with respect to T. Note that, in order to threaten the transmission of T, X must be in the interference region of R, the intended receiver of X. In this case, it is impossible to achieve successful transmissions by X and T simultaneously because X transmissions will corrupt the reception at R. Otherwise, if X is outside the interference region of R, it can transmit at the same time as T without any problem.

In another situation, T may be in the detection region of node Y. Thus any transmission initiated by T will be detected by Y and, as a consequence, the medium is inferred to be busy. Although, as shown in Figure 4.2, Y is outside the interference region of the intended receiver of T (i.e., R) and therefore its transmission will not interfere with the ongoing transmission of T. In that way, Y is banned unfairly from transmitting and is termed an exposed node. This loss of possible transmission opportunities decreases the overall performance of the network. This decrease is more significant when the deployments become more and more dense.

To cope with the hidden and exposed node problems, one can think about identifying all the possibly hidden and/or exposed nodes and trying to avoid them in a per-communication basis. However, any similar approach is highly cost-ineffective in terms of complexity and overhead. In practice, a node may be considered as 'hidden' with respect to a specific transmitter-receiver communicating pair but not with respect to another pair. Additionally, a reception may be corrupted due to the superposition of two or more signals

transmitted simultaneously by two or more devices that are not considered as hidden nodes if they are transmitting individually. Moreover, any mechanism aiming at identifying hidden and/or exposed nodes cannot be designed without adding more overhead burden to the network (e.g., exchanging statistics and new management frames, etc.).

4.4 Transmit Power Control (TPC)

As mentioned before, TPC is the traditional intuitive way to manage interferences and increase the spatial reuse in wireless networks. As shown in Figure 4.3, decreasing the transmission power of the possible interferers helps to fulfill the required SINR (S_i) at the neighboring receivers. In that way, the transmission ranges in the neighboring networks are shrunk and hence more reuse is permitted.

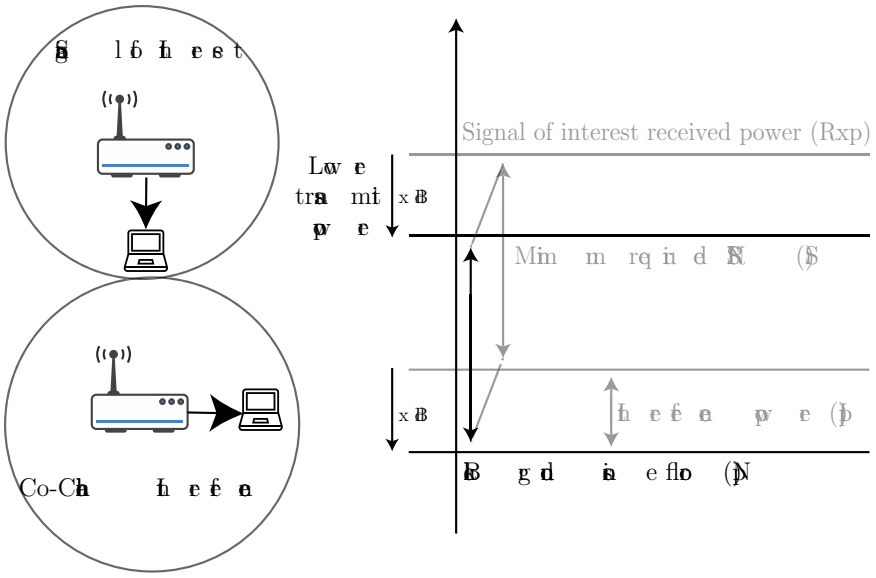

Figure 4.3 – Transmit Power Control (TPC)

4.4.1 Transmit Power Control (TPC) in cellular networks

In cellular networks, a frequency division multiplex is possible inside the same cell. Thus, the transmission power is controlled by the base station individually for each user apart from others. This kind of power control is used in almost all the mobile communication technology (e.g;, Code Division Multiple Access (CDMA), Wideband Code Division Multiple Access (WCDMA), Long-Term Evolution (LTE), etc.). Such closed loop scheme is possible thanks to the centralized hierarchy present in cellular networks and the adopted Frequency Division Multiple Access (FDMA) scheme. Unfortunately, in WLANs, all the nodes of the same BSS share the same frequency and we can't always assume a centralized deployment.

4.5 Physical Carrier Sensing (PCS)

Recalling that the Distributed Coordination Function (DCF) function described by the IEEE 802.11 standard [5] is based on a well known medium access scheme, the Carrier Sense Multiple Access with Collision Avoidance (CSMA/CA). The multiple access to the communication medium is defined by CSMA/CA to be contention-based. In that way, all the nodes in the same physical area compete to transmit on the half-duplex medium of a single frequency. This physical area is termed "contention domain". While one node is transmitting, all other nodes of the same contention domain must wait until it finishes. The decision whether a node is in the same contention domain of a transmitter is based on the value of the Physical Carrier Sensing (PCS) threshold that is part of the CCA mechanism (see Section 1.3.2 for more details about CCA). Briefly, if the in-band signal energy crosses this threshold, CCA is held busy until the medium energy is below the threshold again.

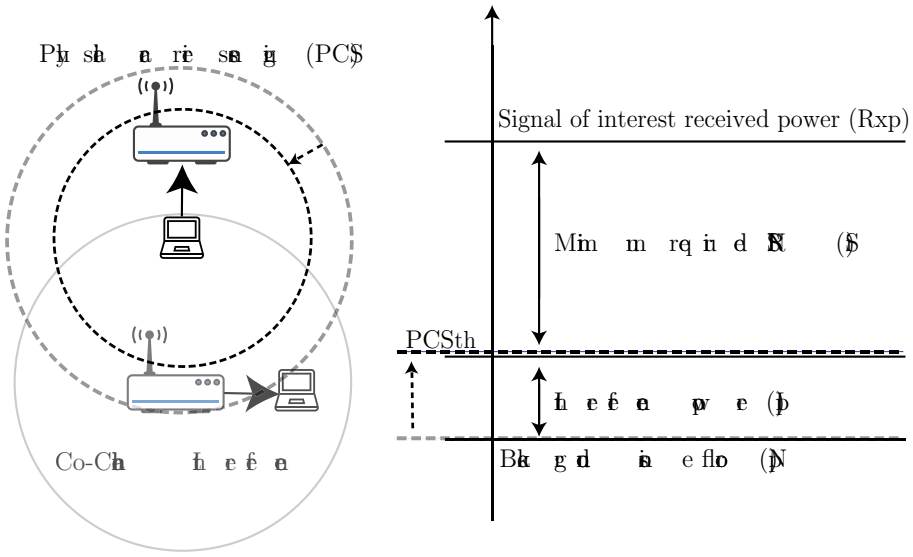

Figure 4.4 – Physical Carrier Sensing (PCS)

Due to the direct role of the carrier sensing mechanism in accessing the shared medium, specifically the PCS, its adaptation is indeed effective in managing interferences and leveraging the spatial reuse in WLANs. Interestingly enough, the adaptation of the PCS is one of the solutions currently discussed in the newly created IEEE 802.11ax TG. As will be shown in the sequel, this promising solution is highly efficient in dense environments. The most important feature of this approach is that there is an incentive to adopt it in production. Contrary to TPC, the node applying PCS adaptation will benefit directly from its application.

The current carrier sensing mechanism is over conservative in today's dense environments. An important number of nodes in these dense networks are exposed to the transmissions

of the neighboring co-channel networks. Thus, the available spectrum is not efficiently exploited and the system is loosing a great amount of possible spatial reuse. In carrier sensing adaptation, instead of decreasing its transmission power, a node will decrease its sensitivity in detecting signals in its environment. In Figure 4.4, the PCS threshold is increased so that tolerable interferences are prohibited from triggering busy channel assessments. Consequently, in situations where the signal of interest is received with a power sufficiently higher than the interference power, the reuse between neighboring networks will be possible.

Let us take a simple example from real world deployment scenarios to explain the effect of modifying the PCS threshold. This example includes two neighboring BSSs depicted in Figure 4.5. For a PCS threshold equal to T_{1a}, the PCS range of AP_1 (equal to R_{1a}) covers the STA_{2x} that's associated to AP_2 of the neighboring WLAN. The previous statement means that AP_1 is not able to transmit at the same time as STA_{2x}. This fact is very harmful for the BSS_1, since AP_1 is obliged to stay silent when STA_{2x} is transmitting. Add to this the fact that, in almost all WLANs, the most important amount of data is directed from the AP towards its STAs. Clearly, the PCS range R_{1a} is reducing the aggregated capacity of this network by restricting possible concurrent transmissions. Now let's consider T_{1b} (given $T_{1b} > T_{1a}$) as the PCS threshold of AP_1. Here, in contrast to the previous case, the PCS range has been shrunk sufficiently (R_{1b}) to let simultaneous transmission for both AP_1 and STA_{2x} and thus increasing the spatial reuse.

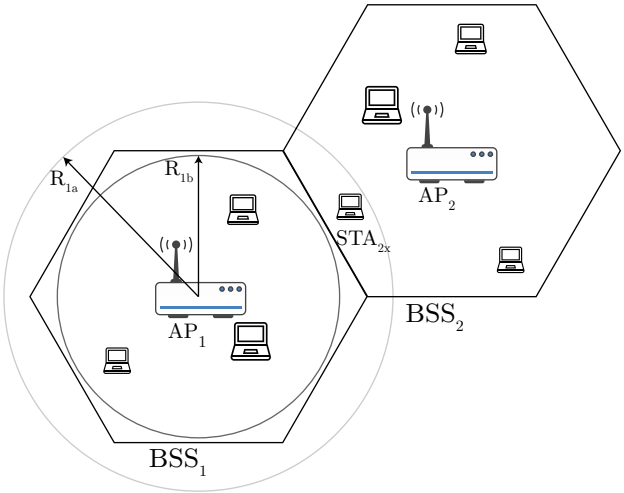

Figure 4.5 – Increasing spatial reuse with Physical Carrier Sensing (PCS) – an example

It's worth pointing out that simultaneous transmissions of STA_{2x} are still received by AP_1, but the latter ignores them because their received power is below the new PCS threshold T_{1b}. However, these transmissions are treated by AP_1 as interferences. So, if STA_{2x} is highly loaded and there are other devices belonging to neighboring BSSs and having the same effect on AP_1, one can imagine a drop in the achieved SINR at AP_1. This fact brings

to light the necessity of establishing a trade-off between spatial reuse and interference level. Furthermore, the results' analysis reveals that in dense environments, thanks to short distances, the SINR values stay high enough assuring successful transmissions.

As shown in the previous example, if the carrier sensing threshold is increased, more concurrent transmissions are permitted. Additionally, by decreasing the carrier sensing (protection) region, the number of contending devices decreases and hence the probability of synchronous collisions is reduced. However, generally speaking, this behavior may involve more interference because the communication range of the node will decrease and it becomes less aware of other concurrent transmissions. Interestingly enough, the simulations prove that in dense environments this behavior is of minor importance due to short distances between transmitter-receiver nodes in dense environments and the capture effect discussed in Section 1.6.2.2.

4.5.1 Increasing the PCS threshold in high density deployment scenario

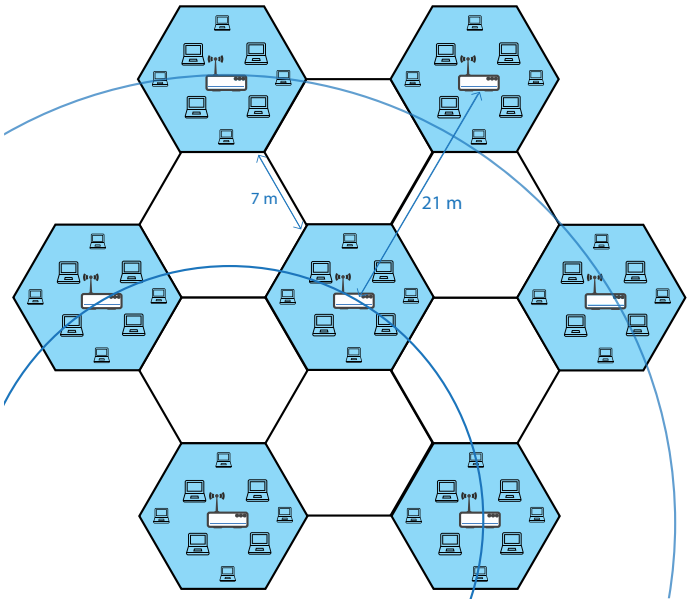

Figure 4.6 – Cellular scenario network topology

In this section, we consider the cellular scenario previously described in Section 3.2.1. The cellular topology illustrated in Figure 4.6 consists of 6 BSSs forming the first tier around a central BSS. If we consider the south east corner BSS, then the central BSS is in the first tier and the BSS of the north west corner of the topology belongs to the second tier. The default settings depicted in Table 3.1 are used for the simulation setup. However, for these simulations, to be as close as possible to a current real world deployed network, the TPC is only applied on the AP. For that purpose, the APs are transmitting at 6 dBm and the STAs at 15 dBm. Additionally, all the traffic is generated by the APs towards their STAs (i.e., only downlink). Since all the traffic is in downlink, the transmission power configuration will

Figure 6.1 – Balanced Transmit power control (TPC) and Physical carrier sensing (PCS) Adaptation (BTPA) – the $ratio$

According to the PCSA, the PCS_{th} is increased by Δ_X to adapt the carrier sensing mechanism. Instead of that, in the BTPA, Δ_X is used to adapt both the carrier sensing and the transmission power. Accordingly, the PCS_{th} will be increased by Δ_{PCS} dB and the transmission power will be decreased by Δ_{TPC} dB. The following equations show how the values of Δ_{PCS} and Δ_{TPC} are calculated using the $ratio$.

$$\Delta_X[dB] = \Delta_{PCS}[dB] + \Delta_{TPC}[dB] \tag{6.9}$$

$$\Delta_{TPC}[dB] = ratio \times \Delta_X[dB] \tag{6.10}$$

As depicted in Figure 6.1, a $ratio$ equal to 0 means no TPC, i.e., the PCS is increased by Δ_X. Increasing the $ratio$ means introducing more and more TPC. If the $ratio$ is set to 1, the Δ_{TPC} value would be equal to Δ_X and the node performs only a TPC without PCSA. This rule is proposed in order that each mechanism (PCSA and TPC) counteracts the unfairness of the other mechanism.

For a simple scenario, the application of BTPA is illustrated in Figure 6.2. In this example, a new STA associates to an existing BSS and starts a new communication with its Access Point (AP). Upon the reception of a beacon frame from the AP, the STA calculates Δ_X value. From an implementation point of view, it is simple to broadcast the $ratio$ value in the beacon frame itself. Knowing the $ratio$, the STA deduces the values of Δ_{PCS} and Δ_{TPC}. The last step is to calculate the new carrier sensing threshold (PCS_{th}) and transmission power (Tx_p) parameters and apply them before proceeding to the intended data exchange.

6.5 Evaluation

To study the fairness problem and evaluate the proposed solution, we consider first the cellular scenario described in Section 3.2.1.

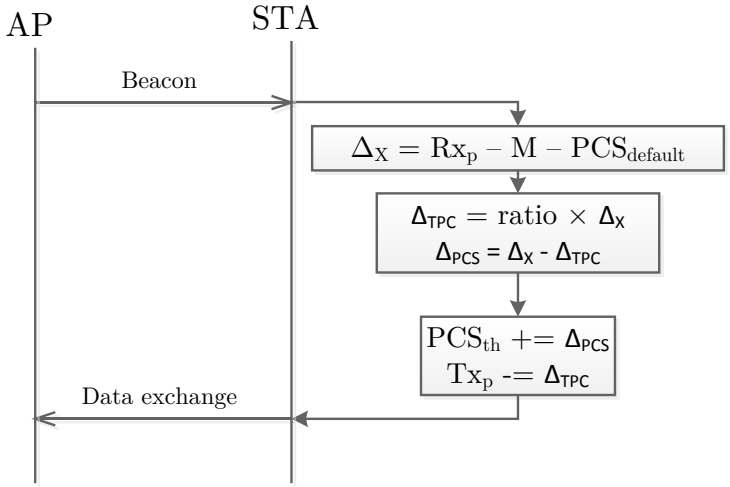

Figure 6.2 – Balanced Transmit power control (TPC) and Physical carrier sensing (PCS) Adaptation (BTPA) – an example

This scenario consists of a high density cellular deployment as depicted in Figure 3.1. Table 3.1 presents a summary of the main simulation system parameters. All the simulated nodes implement the IEEE 802.11n Media Access Control Layer (MAC) and Physical Layer (PHY), operate in 20 MHz band and have only one spatial stream (i.e., one antenna). A User Datagram Protocol (UDP) full buffer traffic generator is configured on all nodes. The default transmission power is 15 dBm and the default PCS threshold is as defined by the standard for 20 MHz bandwidth, -82 dBm. For each of the adaptation mechanisms we chose the $margin$ value achieving the best performance in terms of aggregate throughput. As shown in Chapter 4, for PCSA, M = 20 dB achieves the best performance in terms of aggregate throughput. However, for TPC, the best performance is obtained using M = 30 dB. For BTPA, the best aggregate throughput performance is obtained when M = 20 dB. Furthermore, the rate control algorithm approach described in Chapter 5 is activated with the best MCS configuration (i.e., *"MCS 4-7"*).

6.5.1 Performance comparison

In this section, we compare the performance in terms of throughput fairness of five different modes: no adaptation (applying default settings), the best fixed PCS threshold, PCSA, TPC, and the proposed BTPA. The first mode serves as a reference and reflects the conventional Wi-Fi deployments today. For BTPA, we consider a $ratio$ of 0.5 to carry out this comparison. Later in this chapter, we study the optimal value of the $ratio$ in terms of the number of legacy nodes present in the network. After running the same simulation scenario for the different adaptation mechanisms, the Cumulative Distribution

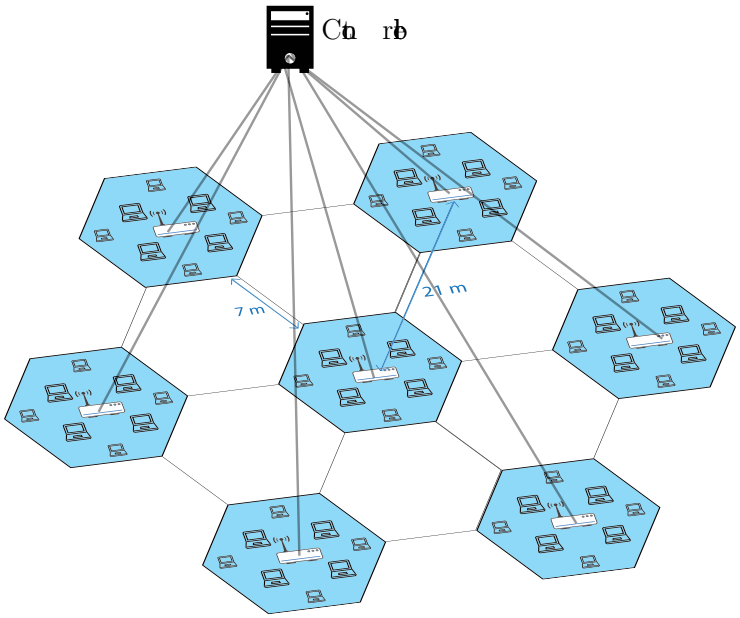

Figure 7.15 – Cellular scenario network topology

The obtained results are presented in Figure 7.16. The first important observation when comparing to the results of the previous scenarios is that the system needs more optimization rounds to converge. This is normal since the scenario is more complex because of the much higher number of devices and hence the ANN has larger number of neurons with 126 inputs and 63 outputs. Another observation is related to the Jain's fairness index curve plotted in Figure 7.16c. Contrary to the previous scenarios, this index does not reach its maximum value in the current scenario, meaning that not all the devices are achieving the same throughput. In fact, this is due to the difference in throughput between uplink and downlink flows. The AP that is transmitting to 8 STAs has almost the opportunity to access the medium as any other ordinary STA.

Since the network is saturated, the share of airtime used by the AP to transmit data to one STA is much lower than that used by a STA to send data to the AP. However, after the convergence of the adaptation, the fairness index is importantly enhanced (from ≈ 0.5 at optimization round 0 to ≈ 0.7 at the final round). This enhancement reflects the ability of the proposed adaptation to solve the exposed node situations and increasing the spatial reuse between all the BSSs. This enhancement in spatial reuse is clearly seen in Figure 7.16b, where the gain in aggregate throughput exceeds 45 %.

Résumé

Malgré leur réussite remarquable, les premières versions des normes de réseau local sans fil IEEE 802.11, 802.11a/b/g Wireless Local Area Networks (WLAN), sont caractérisées par une efficacité spectrale faible qui est devenue insuffisante pour satisfaire la croissance explosive de la demande de capacité et de couverture. Le standard 802.11n et plus récemment le 802.11ac ont amélioré les débits offerts par la couche physique grâce principalement à l'introduction des techniques multi-antennaires (MIMO, pour Multiple-Input Multiple-Output) et des techniques avancées de modulation et de codage. Aujourd'hui, deux décennies après sa première apparition, le Wi-Fi est présenté comme une technologie WLAN permettant des débits supérieurs à 1 gigabit par seconde. Cependant, dans la plupart des scénarios de déploiement du monde réel, il n'est pas possible d'atteindre la pleine capacité offerte par la couche physique. Avec la croissance rapide de la densité des déploiements des WLANs, l'énorme popularité des équipements Wi-Fi et l'apparition des nouveaux cas d'utilisation (couverture des stades, déchargement des réseaux cellulaire, etc.), la réutilisation spatiale doit être optimisée.

C'est dans ce contexte que s'inscrit l'objectif de cette thèse qui porte sur l'amélioration de l'efficacité des protocoles de la couche MAC des réseaux WLAN de haute densité. Notamment, un des buts de cette thèse est de contribuer à la préparation de la prochaine génération du standard Wi-Fi : IEEE 802.11ax High Efficiency WLAN (HEW). Plutôt que de continuer à cibler l'augmentation des débits maximums théoriques d'un lien unique, nous nous concentrons dans le contexte de HEW sur l'amélioration du débit réel des utilisateurs.

Nous proposons une adaptation dynamique du mécanisme de détection de signal. Comparé au contrôle de la puissance de transmission, le mécanisme proposé est plus incitatif parce que l'utilisateur concerné bénéficie directement de son application. Les résultats de nos simulations montrent des gains importants en termes de débit atteint dans les scénarios de haute densité. Ensuite, nous étudions l'impact de la nouvelle adaptation sur les mécanismes de sélection de débit actuellement utilisés. D'après les résultats obtenus, l'adaptation proposée peut être appliquée sans avoir besoin de modifications substantielles des algorithmes de sélection de débit. Pour améliorer l'équité entre les différents utilisateurs, nous élaborons une nouvelle approche distribuée pour adapter conjointement le mécanisme de détection de signal et le contrôle de la puissance de transmission. Cette approche est évaluée ensuite dans différents scénarios de simulation de haute densité où elle prouve sa capacité à résoudre les problèmes d'équité en particulier en présence de nœuds d'anciennes générations dans le réseau, cela tout en améliorant le débit moyen d'un facteur 4 par rapport à la performance conventionnelle du standard.

Enfin, nous concevons et mettons en œuvre une solution centralisée basée sur l'apprentissage à base de réseaux de neurones. Cette approche repose sur l'adaptation conjointe de puissance de transmission et du mécanisme de détection du signal. Cette nouvelle solution bénéficie de la capacité des réseaux de neurones artificiels à modéliser les fonctions

Abstract

Despite their remarkable success, the first widely spread versions of the IEEE 802.11 Wireless Local Area Networks (WLAN) standard, 802.11a/b/g, featured low spectral efficiencies that are becoming insufficient to satisfy the explosive growth in capacity and coverage demands. The 802.11n and recently the 802.11ac amendments improved the PHY data rates by introducing Multiple-Input Multiple-Output (MIMO) techniques, and higher Modulation and Coding Schemes (MCS), etc. Today, after almost two decades of its first appearance, Wi-Fi is presented as a gigabit wireless technology. However, the full potential of the latest PHY layer advances cannot be enabled in all real world deployment scenarios. With the rapidly increasing density of WLAN deployments and the huge popularity of Wi-Fi enabled devices, spatial reuse must be optimized. On another hand, the new challenging use case environments and the integration of mobile networks mainly for cellular offloading are limiting the opportunity of the current Wi-Fi generations to provide better quality at lower cost.

In this thesis, we contribute to the current standardization efforts aiming to leverage the Wi-Fi efficiency in high density environments. At the time of writing this document, the IEEE 802.11ax Task Group (TG) is developing the specifications for the High Efficiency WLAN (HEW) standard (next Wi-Fi evolution). Rather than continuing to target increased theoretical peak throughputs of a single communication link, we focus in the context of HEW on improving the throughput experienced by users in real life scenarios.

We propose a dynamic adaptation of the carrier sensing mechanism. Compared to controlling the transmission power, the proposed mechanism has more incentives because it benefits directly the concerned user. Extensive simulation results show important throughput gains in dense scenarios. Then, we study the impact of the new adaptation on the current rate control algorithms. We find that our adaptation mechanism operates efficiently without substantially modifying these algorithms that are widely used in today's operating WLANs. Furthermore, after analyzing the fairness performance of the proposed adaptation, we devise a new approach to jointly adapt the carrier sensing and the transmission power in order to preserve higher fairness degrees while improving the spatial reuse. This approach is evaluated in different dense deployment scenarios where it proves its capability to resolve the unfairness issues especially in the presence of legacy nodes in the network, while improving the achieved throughput by 4 times compared to the standard performance.

Finally, we design and implement a centralized learning-based solution that uses also an approach based on joint adaptation of transmission power and carrier sensing. This new solution takes benefit from the capability of artificial neural networks to model complex nonlinear functions to optimize the spatial reuse in dense WLANs while preserving high fairness levels.

INSA RENNES

N° d'ordre : 15ISAR 39 / D15 - 39

Institut National des Sciences Appliquées de Rennes
20, Avenue des Buttes de Coëmes • CS 70839 • F-35708 Rennes Cedex 7
Tel : 02 23 23 82 00 - Fax : 02 23 23 83 96